Molekularbiologische Studien neu entdeckter Biosynthesewege in den Cyanobakterien *Anabaena* und *Synechocystis* und ihre Bedeutung für die Bildung zellulärer Reservestoffe und autotrophe Lebensweise

Dissertation

der Mathematisch-Naturwissenschaftlichen Fakultät
der Eberhard Karls Universität Tübingen
zur Erlangung des Grades eines
Doktors der Naturwissenschaften
(Dr. rer. nat.)

vorgelegt von
Friederike Christine Klemke
aus Berlin

Tübingen
2018

Gedruckt mit Genehmigung der Mathematisch-Naturwissenschaftlichen Fakultät der Eberhard Karls Universität Tübingen.

Tag der mündlichen Qualifikation:	28.03.2019
Dekan:	Prof. Dr. Wolfgang Rosenstiel
1. Berichterstatter:	PD Dr. Iris Maldener
2. Berichterstatter:	Prof. Dr. Karl Forchhammer

Inhaltsverzeichnis

I. Abkürzungen

3PGA	3-Phosphoglycerat
ABC	*ATP- binding casette*
ATCC	*American Type Culture Collection*
ATP	Adenosintriphosphat
β-Asp-Arg	β-Aspartyl-Arginin
CphA	Cyanophycin Synthetase
CphB	Cyanophycinase
DAPI	4', 6'-Diamidin- 2 phenylindol
E. coli	*Escherichia coli*
GFP	grün fluoreszierendes Protein
GOGAT	Glutamin Oxoglutarat Aminotransferase
GS	Glutamin Synthase
GST	Glutathion-S-Transferase
kDa	kilo Dalton
Mbp	Mega Basenpaare
NtcA	*nitrogen transcription control*
ORF	*open reading frame*
PALP	Pyridoxal-5´-Phosphat
PCC	*pasteur culture collection*
PGDH	Phosphoglycerat Dehydrogenase
PolyP	Polyphosphat
PPGK	Polyphosphatglukokinase
PPK	Polyphosphatkinase
PSTA	Phosphoserin Transaminase
PSP	Phosphoserin Phosphatase

PTA	Isoaspartyl-Dipeptidase
RubisCO	Ribulose-1,5-Bisphosphat-Carboxylase/Oxygenase
SDS-Page	*sodium dodecyl sulfate polyacrylamide gel electrophoresis*
SEM	*standard error of the mean*
WT	Wildtyp

II. Zusammenfassung

Das Enzym CphA2, kodiert durch den ORF *ava_0335* von *Anabaena variabilis* ATCC 29413, wurde als eine Cyanophycin Synthetase eines neuen, bisher unbekannten Typus charakterisiert. CphA2 katalysiert die Synthese des stickstoffreichen Reservepolymers Cyanophycin durch Verknüpfung von β-Aspartyl-Arginin-Einheiten unter Einsatz eines Moleküls ATP. Durch die Verwendung von β-Aspartyl-Arginin, einem Produkt des Cyanophycin-hydrolysierenden Enzyms Cyanophycinase, kann CphA2 als wichtiges Recyclingenzym fungieren. Im Gegensatz zum Hauptenzym für die Cyanophycin-Biosynthese CphA1, welches unter Verwendung von jeweils einem ATP die Aminosäuren Arginin und Aspartat verknüpft, ist CphA2 eine verkürzte Enzymvariante und besitzt nur eine ATP-Bindestelle. Homologe von CphA2 konnten in einzelligen und filamentösen, stickstofffixierenden Cyanobakterien identifiziert werden, die auch eine CphA1 besaßen. Die Analysen zu CphA2 komplettieren den bereits gut untersuchten Cyanophycin-Metabolismus in Heterozysten-bildenden Cyanobakterien und weisen auf eine Regulationsfunktion des Enzyms innerhalb dieses Stoffwechselwegs hin.

Neben einem lichtabhängigen Serin-Biosyntheseweg existiert in vielen Cyanobakterien ein lichtunabhängiger Weg für die Synthese von Serin, der Phosphoserin-Biosyntheseweg. Die Gene, die die relevanten Enzyme PGDH, PSTA und die PSP aus *Synechocystis* sp. PCC 6803 kodieren, wurden identifiziert und die Proteine umfassend biochemisch *in vitro* charakterisiert. Es konnte durch Kombination aller drei Enzyme mit den Substraten 3PGA (3-Phosphoglycerat), NAD^+ und Glutamat gezeigt werden, dass der Phosphoserin-Biosyntheseweg *in vitro* rekonstituiert werden kann. Untersuchungen an Mutanten weisen darauf hin, dass dieser Stoffwechselweg essentiell in *Synechocystis* sp. PCC 6803 und *Synechococcus elongatus* sp. PCC 7942 sein könnte. Der Phosphoserin-Weg scheint einen wesentlichen Beitrag zur gesamten Serin-Biosynthese im cyanobakteriellen Stoffwechsel zu leisten.

Das Enzym All1371 aus *Anabaena* sp. PCC 7120 ist die erste strikt PolyP-abhängige Glukokinase, die in Cyanobakterien charakterisiert wurde. Das

Enzym phosphoryliert ausschließlich mit Hilfe von PolyP die Substrate Glukose oder Mannose zu Glukose-6-Phosphat bzw. Mannose-6-Phosphat. Die PolyP-abhängige Glukomannokinase besitzt eine Wechselzahl von 48,2 s^{-1} und Michaelis-Konstanten von 1,76 µM für PolyP, 0,118 mM für Glukose und 24,3 mM für Mannose (pH 7,5; 28 °C). Das Enzym katalysiert eine Zwei-Substrat Reaktion, die einem bi-bi-ping-pong Mechanismus folgt. Physiologische Untersuchungen an einer *all1371* defizienten Mutante, GFP Promotorstudien und bioinformatische Analysen deuten darauf hin, dass das Enzym besonders in Heterozysten-bildenden Cyanobakterien unter Stickstoff-mangelbedingungen eine besondere Rolle spielt.

III. Summary

The enzyme CphA2, encoded by ORF *ava_0335*, of *Anabaena variabilis* ATCC 29413 was characterized as a cyanophycin synthetase of a new, previously unknown type. CphA2 catalyzes the synthesis of the nitrogen-rich reserve polymer cyanophycin by linking β-aspartyl-arginine units consuming one molecule of ATP. By using β-aspartyl-arginine, a product of the cyanophycin-hydrolyzing enzyme cyanophycinase, CphA2 can act as an important recycling enzyme. In contrast to the main enzyme for the cyanophycin biosynthesis CphA1, which combines the amino acids arginine and aspartate using ATP, CphA2 is a truncated enzyme variant and has only one ATP binding site. Homologues of CphA2 could be identified in unicellular and filamentous, nitrogen-fixing cyanobacteria that also has CphA1. The CphA2 analysis completes the already well-studied cyanophycin metabolism in heterocyst-producing cyanobacteria and points to a regulatory function of the enzyme within this metabolic pathway.

In addition to a light-dependent serine biosynthetic pathway, in many cyanobacteria a light-independent metabolic pathway exists for the synthesis of serine, the phosphoserine biosynthetic pathway. The genes responsible for the relevant enzymes PGDH, PSTA and PSP from *Synechocystis* sp. PCC 6803 were identified and the proteins biochemically characterized *in vitro*. By combining all three enzymes with the substrates 3PGA, NAD^+ and glutamate, it was shown that the phosphoserine biosynthesis pathway can be reconstituted *in vitro.* Studies on mutants indicate that this metabolic pathway could be essential in *Synechocystis* sp. PCC 6803 and *Synechococcus elongatus* sp. PCC 7942, where the phosphoserine pathway seems to significantly contribute to the overall serine biosynthesis in the cyanobacterial metabolism.

The enzyme All1371 from *Anabaena* sp. PCC 7120 is the first strictly PolyP-dependent glucokinase that has been characterized in cyanobacteria. The enzyme exclusively phosphorylates the substrates glucose or mannose with the aid of PolyP to form glucose 6-phosphate or mannose 6-phosphate. The PolyP-dependent glucomannokinase has a turnover number of 48.2 s^{-1} and

Michaelis constants of 1.76 µM for PolyP, 0.118 mM for glucose and 24.3 mM for mannose (pH 7.5, 28 °C). The enzyme catalyzes a two-substrate reaction that follows a bi-bi-ping pong mechanism. Physiological studies on an all1371 deficient mutant, GFP promoter studies and bioinformatic analyses indicate that the enzyme plays a special role in heterocyst-producing cyanobacteria under conditions of nitrogen deficiency.

IV. Publikationsliste der kumulativen Dissertation

Klemke*, F., D. J. Nürnberg*, K. Ziegler*, G. Beyer, U. Kahmann, W. Lockau and T. Volkmer (2016). "CphA2 is a novel type of cyanophycin synthetase in N_2-fixing cyanobacteria." Microbiology **162**(3): 526-536.

Klemke, F., A. Baier, H. Knoop, R. Kern, J. Jablonsky, G. Beyer, T. Volkmer, R. Steuer, W. Lockau and M. Hagemann (2015). "Identification of the light-independent phosphoserine pathway as an additional source of serine in the cyanobacterium *Synechocystis* sp. PCC 6803." Microbiology **161**(Pt 5): 1050-1060.

Klemke, F., G. Beyer, L. Sawade, A. Saitov, T. Korte, I. Maldener, W. Lockau, D. J. Nürnberg and T. Volkmer (2014). "All1371 is a polyphosphate-dependent glucokinase in *Anabaena* sp. PCC 7120." Microbiology **160**(Pt 12): 2807-2819.

*geteilte Erstautorenschaft

V. Eigenanteil an den Publikationen

Die hier aufgeführten Arbeiten wurden unter der Leitung von Prof. W. Lockau in der Arbeitsgruppe Biochemie der Pflanzen an der Humboldt Universität zu Berlin durchgeführt. Hier wurde auch die Vorgehensweise für die Durchführung der Experimente diskutiert. Die Resultate wurden im Team und mit den Kooperationspartnern erörtert und interpretiert.

CphA2- eine Cyanophycin Synthetase neuen Typs

Der Expressionsvektor mit CphA2 aus *Anabaena variabilis* wurde von Karl Ziegler erstellt, der auch das Substrat und damit die Funktion des Enzyms entdeckte. Er etablierte zudem die enzymatischen Aktivitätstests für CphA2 und führte auch die Insertionsmutagenese durch. Die quantitativen und qualitativen Analysen des Polymers Cyanophycin, bzw. dessen Abbau durch die rekombinanten Enzyme Cyanophycinase und Isoaspartyl-Dipeptidase wurden von mir durchgeführt. Diese Enzyme wurden dafür aus *E. coli* isoliert. In Zusammenarbeit mit Dr. Gabriele Beyer präparierte ich das Substrat β-Asp-Arg und erstellte die kinetischen Analysen an vorher isoliertem CphA2. Ich ermittelte die native molekulare Masse des Enzyms mittels Gelfiltration. Zudem führte ich den Wachstumstest mit WT und Mutanten durch und wählte die Kulturen für die elektronenmikroskopische Untersuchung aus, die von Uwe Kahmann ausgeführt wurde. Weiterhin isolierte ich CphA1 und CphA2 für die Antikörperherstellung, testete die Seren und stellte diese für immuno-zytologische Untersuchungen Uwe Kahmann zur Verfügung. Die Anti-CphA1- und Anti-CphA2-Antiseren verwendete ich weiter für Expressionsanalysen (Western Blot). Die Sequenzanalyse wurde in Zusammenarbeit mit Dennis Nürnberg angefertigt. Schließlich beteiligte ich mich an der Anfertigung der Publikation sowie an der Erstellung der Bilder und Grafiken.

Identifizierung des Phosphoserin-Stoffwechselwegs in *Synechocystis*

In diesem Projekt erfolgte eine enge Zusammenarbeit mit der Arbeitsgruppe von Martin Hagemann (Universität Rostock). Dort wurden die bioinformatischen Analysen sowie die Sequenzanalysen erstellt, der Expressionsvektor für die PGDH kloniert und die Substratanalyse für dieses

Enzym durchgeführt. Die drei Expressionsvektoren für die beiden putativen PSTA‘s und die PSP wurden durch mich erstellt. Ich isolierte die Proteine mittels Affinitätschromatographie und etablierte die *in vitro* Enzymtests für die drei Enzyme, inklusive der kinetischen Analysen. Außerdem führte ich die Experimente zur Rekonstitution des Phosphoserin-Weges durch und ermittelte die native molekulare Masse der Enzyme. Zudem konstruierte ich die Plasmide für die Ausschaltung der Gene. In Zusammenarbeit mit Antje Beier führte ich Experimente durch, um homologe Klone zu erhalten. Ich beteiligte mich an der Veröffentlichung der Ergebnisse. Eine schriftliche Zusammenfassung der Ergebnisse mit Literaturrecherche sowie Grafiken und Tabellen für die Publikation wurden von mir erstellt.

All1371- eine Polyphosphat-abhängige Glukomannokinase

Der Expressionsvektor für das Enzym All1371 wurde von mir erstellt. Ebenso führte ich die Genexpression, die Enzymisolierung sowie *in vitro*-Analysen und Substratanalysen durch. In Zusammenarbeit mit Dr. Gabriele Beyer wurden die enzymkinetischen Untersuchungen durchgeführt. Die Analyse zur Verteilung der PPGK‘s in Cyanobakterien wurde von Dennis Nürnberg angefertigt. In Zusammenarbeit mit ihm wurden multiple Sequenz-Alignments erstellt und spezielle Domänen der PPGK All1371 identifiziert. Ich plante und konstruierte zudem die Plasmide für die Knockout-Mutante und für die Promotorfusion, führte Konjugation und die Wachstumsanalysen durch. In Zusammenarbeit mit Thomas Korte (Humboldt-Universität zu Berlin) wurde die GFP-Promotorstudie analysiert. An der Erstellung der Publikation beteiligte ich mich zu einem großen Anteil. Ich erstellte zudem alle Grafiken und Tabellen bis auf das Alignment, welches Dennis Nürnberg beitrug.

1 Einleitung

1.1 Cyanobakterien

1.1.1 Vorkommen, Morphologie und ökologische Bedeutung

Cyanobakterien sind gramnegative Prokaryoten, die wie eukaryontische Algen und Pflanzen eine oxygene Photosynthese betreiben und als Vorläufer von Chloroplasten angesehen werden (Deusch *et al.* 2008). Vor rund 2,5 Milliarden Jahren gaben Cyanobakterien den ersten molekularen Sauerstoff in die Atmosphäre ab (Olson & Blankenship 2004). Im Gegensatz zu höheren Pflanzen besitzen Cyanobakterien meist kein Chlorophyll *b*, sondern Chlorophyll *a*, in einigen speziellen Arten wurde aber auch Chlorophyll *d* und *f* gefunden (Larkum & Kühl 2005, Gan *et al.* 2014). Die blaugrüne Farbe der Cyanobakterien wird durch Chlorophyll und durch zusätzliche Pigmente, die Phycobiliproteine verursacht. Zudem enthalten Cyanobakterien auch Carotinoide, die als akzessorische Pigmente dienen. Cyanobakterien können sich so besonders gut an verändernde Umweltbedingungen in Bezug auf Lichtverhältnisse und Nährstoffangebot anpassen und sind daher weit verbreitet. Sie kommen sowohl terrestrisch als auch in Süß- und Meerwasser vor und können teilweise auch extreme Umweltbedingungen tolerieren (Miller & Castenholz 2000). Dazu tragen verschiedene Mechanismen, wie die Fähigkeit einiger Cyanobakterien zur Reduzierung von molekularem Stickstoff und die Bildung von Speichersubstanzen z.B. für Glukose, Stickstoff und Phosphat bei. Unter suboptimalen Wachstumsbedingungen können diese für die Aufrechterhaltung der physiologischen Prozesse Verwendung finden.

Entsprechend ihrer Morphologie werden Cyanobakterien in fünf Abteilungen untergliedert (Rippka *et al.* 1979). Einzellige Formen gehören zu den Abteilungen I (Ordnung Chroococcales) und II (Ordnung Pleurocapsales). Cyanobakterien der Abteilung III (Ordnung Oscillatoriales) und IV (Ordnung Nostocales) bilden Filamente aus vegetativen Zellen. Cyanobakterien der Abteilung V (Ordnung Stigenomatales) sind filamentös, verzweigt und besitzen ein hohes Maß an Komplexität. Nostocales sowie filamentös-verzweigte Arten

der Abteilung V sind zusätzlich in der Lage spezialisierte Zellen, Heterozysten, auszubilden (siehe Abbildung 1). Heterozysten sind auf die Stickstofffixierung spezialisierte Zellen, sie enthalten das sauerstoffempfindliche Enzym Nitrogenase, welches molekularen Stickstoff zu Ammonium reduziert (Wolk *et al.* 1994, Kumar *et al.* 2010). Stickstofffixierende Cyanobakterien werden diazotroph genannt und sind sowohl unter einzelligen als auch in filamentösen Formen zu finden (Rippka *et al.* 1979, Fredriksson & Bergman 1997, Bandyopadhyay *et al.* 2013). Die Fähigkeit zur Stickstofffixierung verschafft diesen phototrophen Bakterien Vorteile beim Konkurrenzkampf um Habitate und Nahrungsressourcen.

Cyanobakterien sind durch ihre Fähigkeit nur mit Hilfe von Wasser, Kohlenstoffdioxid und Lichtenergie reduzierte Kohlenstoffverbindungen zu synthetisieren, sehr interessante Untersuchungsobjekte für die biotechnologische Forschung. So werden Cyanobakterien z.B. verwendet, um regenerative Biokraftstoffe wie Ethanol oder Metabolite wie biologisch abbaubare Polymere zu erzeugen und damit konventionelle, begrenzte Ressourcen, die auf Erdöl basieren zu ersetzen (Abed *et al.* 2009, Dexter *et al.* 2015, Pade *et al.* 2016). Das Reservepolymer Cyanophycin wird z.B. bereits in gentechnisch veränderten Pflanzen, Bakterien oder Hefen produziert (Frey *et al.* 2002, Neumann *et al.* 2005, Steinle *et al.* 2009, Schmidt *et al.* 2017). Durch eine gezielte Punktmutation an einem Regulatorprotein konnten Synechocystis-Zellen so im Argininstoffwechsel verändert werden, dass sie bis zu 57 % der Zelltrockenmasse dieses Reservepolymers akkumulieren können (Watzer *et al.* 2015).

Eine genaue und umfassende Untersuchung der cyanobakteriellen Stoffwechselwege stellt daher eine unerlässliche Grundlage dar, um Cyanobakterien für diverse biotechnische Anwendungen gezielt gentechnisch manipulieren zu können und diese somit für die Biotechnologie nutzbar zu machen.

1.1.2 Der Modellorganismus *Anabaena*

Für die vorliegende Arbeit wurde mit den beiden diazotrophen, filamentösen und Heterozysten-bildenden Cyanobakterien *Anabaena* sp. PCC 7120 (*Nostoc* sp. PCC 7120, im Folgenden *Anabaena* genannt) und *Anabaena variabilis* ATCC 29413 (im Folgenden *A. variabilis* genannt) aus der Abteilung IV gearbeitet. *Anabaena* ist obligat photoautotroph wohingegen *A. variabilis* auch heterotroph mit Fruktose als Kohlenstoffquelle wachsen kann. *Anabaena* ist ein beliebter und gut untersuchter Modellorganismus mit vollständig sequenziertem Genom (Kaneko *et al.* 2001). Dieses besteht aus einem zirkulären Chromosom (6,4 Mbp) und sechs Plasmiden. Das gesamte Genom hat eine Größe von 7,2 Mbp, kodiert 6223 Gene und jede einzelne Zelle besitzt 10 bis 12 Kopien des Chromosoms (Nakao *et al.* 2010). Steht nicht genügend gebundener Stickstoff wie Ammonium oder Nitrat zum Wachstum zur Verfügung, differenzieren 5-10 % der vegetativen Zellen von *Anabaena* zu Heterozysten (Wolk *et al.* 1994). Von Vorteil ist, dass *Anabaena* leicht zu kultivieren ist und sich durch triparentale Konjugation gut genetisch manipulieren lässt (Elhai & Wolk 1988).

1.1.3 Der Modellorganismus *Synechocystis*

Synechocystis sp. PCC 6803 (im Folgenden *Synechocystis*), ist ein einzelliges, nicht diazotrophes Cyanobakterium der Abteilung I, welches durch die oxygene Photosynthese sowohl phototroph, als auch ohne Licht mittels Glykolyse heterotroph wachsen kann. Dadurch besitzt *Synechocystis* eine sehr hohe Anpassungsfähigkeit. Bereits im Jahr 1968 wurde es aus Frischwasser isoliert. Das Genom ist vollständig sequenziert, es besteht aus einem zirkulären Chromosom sowie sieben Plasmiden und besitzt eine Größe von 3,9 Mbp. *Synechocystis* wird durch seine Fähigkeit zu heterotrophem Wachstum unter anderem für Untersuchungen an der Photosynthese verwendet. Zudem ist *Synechocystis* natürlich kompetent, leicht transformierbar und ist somit ein beliebter Organismus für diverse molekularbiologische Analysen (Shestakov & Khyen 1970, Grigorieva & Shestakov 1982).

1.2 Der Grundstoffwechsel in Cyanobakterien

1.2.1 Kohlenstoff- und Stickstoffmetabolismus

Cyanobakterien sind photoautotrophe Prokaryoten, die eine oxygene Photosynthese betreiben, bei der aus Kohlenstoffdioxid und Wasser (Elektronendonator) unter Nutzung von Lichtenergie organische Verbindungen synthetisiert werden (Rippka *et al.* 1979). Das wichtigste cyanobakterielle Pigment ist Chlorophyll *a*, daneben existieren in Cyanobakterien akzessorische Antennenpigmente, die Phycobiline, die in Phycobilisomen organisiert sind (Mullineaux & Emlyn-Jones 2005). Cyanobakterien sind durch das photoautotrophe Wachstum nur auf ein Minimum an Nährstoffen angewiesen und daher sehr robust. Die oxygene Photosynthese liefert Energie in Form von ATP und Reduktionsäquivalenten, die in anschließenden Schritten der Kohlenstoffdioxidfixierung Verwendung finden. Hier wird CO_2 unter Verbrauch dieser Energie zu Kohlenhydraten reduziert. Dieser Prozess wird als Calvin-Benson-Zyklus oder reduktiver Pentosephosphat-Zyklus bezeichnet und findet im Zytoplasma statt, bei filamentösen, diazotrophen Cyanobakterien nur in den vegetativen Zellen. In den Carboxysomen ist Kohlenstoffdioxid angereichert, dies minimiert die Oxygenasereaktion der RubisCO erheblich aber inhibiert diese nicht komplett (Kaneko *et al.* 2006, Kerfeld & Melnicki 2016). Die im Calvin-Benson-Zyklus entstandenen Triosephosphate können diverse Stoffwechselwege durchlaufen. Zwei Moleküle Glycerinaldehyd-3-phosphat können so beispielsweise über die Glukoneogenese Glukose bilden, welche dann als Kohlenstoffreservemolekül Glykogen (Allen 1984) gespeichert werden kann. Im Citrat-Zyklus werden über Acetyl-CoA zahlreiche für Biosynthesen relevante Vorstufen wie 2-Oxoglutarat gebildet. 2-Oxoglutarat nimmt eine wichtige Stellung im gesamten cyanobakteriellen Stoffwechsel ein, da es als Bindeglied zwischen Kohlenstoff- und Stickstoffstoffwechsel fungiert (Muro-Pastor *et al.* 2001, Luque & Forchhammer 2008, Lüddecke *et al.* 2017).

Cyanobakterien können diverse anorganische und organische Stickstoffquellen, wie Nitrat, Ammonium, Harnstoff oder Aminosäuren für

Wachstum und Entwicklung nutzen. Die bevorzugte Stickstoffquelle ist Ammonium, das direkt über den Glutamin-Synthetase/Glutamin-Oxoglutarat-Aminotransferase-Weg (GS/GOGAT) zu Glutamat umgesetzt wird (Flores & Herrero 2004, Luque & Forchhammer 2008). Nitrat und Nitrit werden über ein ABC-Transportsystem aufgenommen, der aktive Transport des Nitrats in die Zelle ist allerdings inhibiert, wenn Ammonium-Ionen in der Umgebung vorhanden sind (Flores *et al.* 1980). Durch das Schlüsselenzym der Arginin-Biosynthese, der N-Acetylglutamat-Kinase (Maheswaran *et al.* 2006), kann Glutamat weiter zur stickstoffreichen Aminosäure Arginin umgesetzt werden. Als zellulärer Stickstoffspeicher dient das Reservepolymer Cyanophycin, welches aus den beiden Aminosäuren Arginin und Aspartat aufgebaut ist (Kapitel 1.3). Die zelluläre Stickstoffassimilation durch den GS/GOGAT-Zyklus unterliegt einer strengen Regulation, die vor allem von der Stickstoff-Kohlenstoff-Balance der Zelle abhängig ist. Die Kohlenstoffverbindung 2-Oxoglutarat zeigt hierbei den Stickstoff-Kohlenstoff-Status der Zelle an (Li *et al.* 2003). Der interne Mangel an reduzierten Stickstoffverbindungen bzw. eine dadurch erhöhte 2-Oxoglutarat-Konzentration induziert z.B. die Differenzierung der Heterozysten aus den vegetativen Zellen.

Zwei Regulatorproteine, NtcA und PII sind für die zelluläre Stickstoff-Kohlenstoff-Balance von großer Bedeutung. Der globale Stickstoffregulator und Transkriptionsfaktor NtcA (*nitrogen transcription control*) wirkt als positiver Regulator auf Gene der Stickstoffassimilation (Luque *et al.* 1994, Herrero *et al.* 2001), z.B. gebunden mit 2-Oxoglutarat als Aktivator für Gene, die die Heterozysten-Differenzierung in den vegetativen Zellen einleiten (Vazquez-Bermudez *et al.* 2002). Das cyanobakterielle Signalprotein PII regelt Enzymaktivitäten in Abhängigkeit von der Kohlenstoff-, Stickstoff- und Energie-Balance der Zelle (Forchhammer & Lüddecke 2016). PII kann den Energiestatus der Zelle durch Bindung von ADP oder ATP anzeigen (Zeth *et al.* 2014) und so mit unterschiedlichen Zielproteinen interagieren (*energy sensing model*) (Lüddecke & Forchhammer 2015). Das Regulatorprotein nimmt zudem die unterschiedlichen Zustände der Zelle im Kohlenstoff- und Stickstoffhaushalt wahr. P II bindet so Liganden wie z.B. 2-Oxoglutarat.

Die Transkription heterozystenspezifischer Gene wird unter anderem durch das DNA-Bindeprotein HetR reguliert (Buikema & Haselkorn 1991, Kumar *et al.* 2010). HetR ist ein Hauptregulator für die Heterozysten-Differenzierung. Es wurden verschiedene Gene als Ziele von HetR identifiziert, nur einem geringen Teil dieser Gene konnte allerdings eine Funktion bei der Heterozysten-Differenzierung zugeordnet werden (Flaherty *et al.* 2014).

1.2.2 Stickstofffixierung und oxygene Photosynthese

Neben der Verwendung von gebundenem Stickstoff wie Nitrat und Nitrit können diazotrophe Cyanobakterien molekularen Luftstickstoff (N_2) zu Ammonium reduzieren. Die Fixierung von molekularem Stickstoff ist ein sehr energieaufwändiger Prozess. Das Schlüsselenzym der Stickstofffixierung ist die Nitrogenase, die unter Verwendung von Reduktionsäquivalenten und ATP die Umsetzung von molekularem Stickstoff zu Ammonium-Ionen katalysiert. Für die Spaltung eines Moleküls molekularen Luftstickstoffs werden 16 Moleküle ATP und 8 Elektronen benötigt (Hill *et al.* 1981, Kneip *et al.* 2007). In Cyanobakterien wird die hierfür benötigte Energie vor allem durch die oxygene Photosynthese bereitgestellt. Der Nitrogenasekomplex wird durch *nif*HDK Gene kodiert (Golden *et al.* 1985). Der Nitrogenase-Enzymkomplex ist extrem sauerstoffempfindlich (Gallon 1981) und wird durch Sauerstoff irreversibel inaktiviert (Hill *et al.* 1981, Golden *et al.* 1985, Fay 1992).

Stickstofffixierung und oxygene Photosynthese sind daher zwei konträre, inkompatible Prozesse, zumindest wenn sie zeitgleich in einer Zelle ablaufen. In diazotrophen Cyanobakterien entwickelten sich verschiedene Mechanismen, um den Nitrogenase-Komplex trotz oxygener Photosynthese in eine sauerstoffarme Umgebung zu versetzen und dadurch seine Aktivität zu gewährleisten (Wolk *et al* 1994, Gallon 1992).

Einige einzellige Formen nutzen die Möglichkeit der zeitlichen Trennung. Die Sauerstoff-produzierende Photosynthese erfolgt am Tag, während erst in der Dunkelheit die Stickstofffixierung durch die Nitrogenase abläuft (Gallon 1981). Der Sauerstoffpartialdruck ist hier in der Zelle durch die ablaufende Respiration abgesenkt (Mitsui 1986, Toepel *et al.* 2008). Filamentöse

Cyanobakterien der Abteilung IV und V differenzieren unter Stickstoffmangelbedingungen Heterozysten, um in der mikro-oxischen Umgebung dieser spezialisierten Zellen, die Nitrogenaseaktivität zu ermöglichen (Adams & Carr 1981). Diese Arten haben somit die Möglichkeit einer räumlichen Trennung der Prozesse entwickelt. Die Stickstofffixierung läuft ausschließlich in differenzierten Zellen, den Heterozysten ab (Kumar *et al.* 2010, Maldener & Muro-Pastor 2010), wohingegen die oxygene Photosynthese nur in den vegetativen Zellen stattfindet. Eine elektronenmikroskopische Aufnahme von *Anabaena* Zellen, die unter Mangel an gebundenem Stickstoff kultiviert wurden, ist in Abbildung 1 gezeigt.

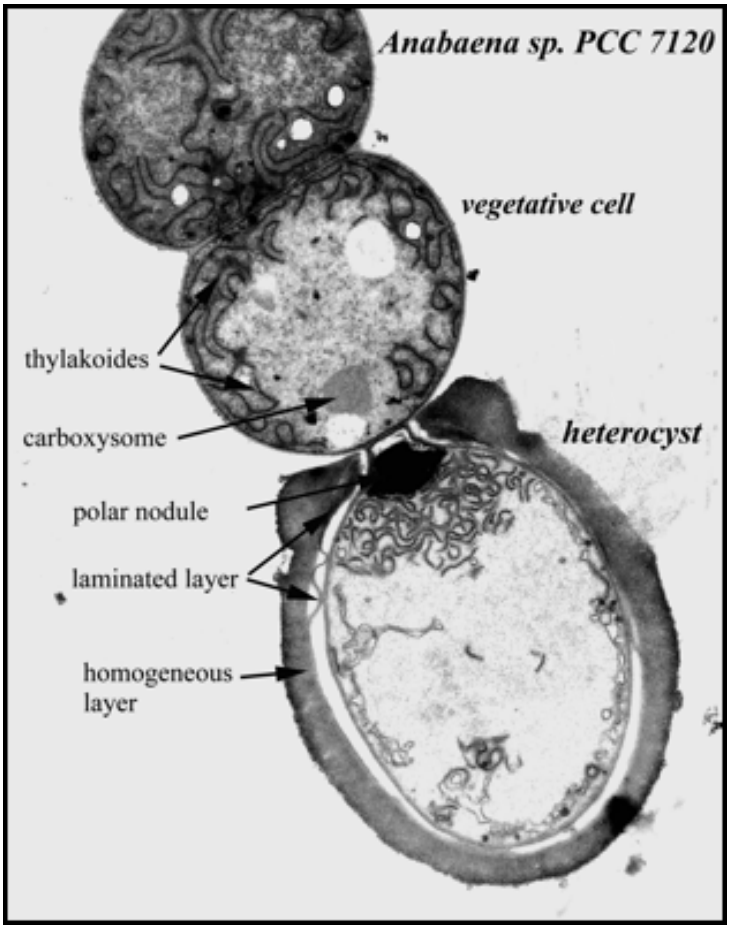

Abbildung 1: Elektronenmikroskopische Aufnahme von Anabaena.
Terminale Heterozyste und vegetative Zellen mit Thylakoidmembranen, Carboxysomen, Cyanophycin (*polar nodule*), heterozystenspezifische *Layer*, (Aufnahme von Iris Maldener, Universität Tübingen, mit freundlicher Genehmigung, unveröffentlicht)

Zahlreiche morphologische und metabolische Veränderungen basieren auf zellspezifischer Genexpression und finden sich in den ausdifferenzierten Heterozysten (Wolk *et al.* 1994, Golden & Yoon 1998, Maldener *et al.* 2014, Flores *et al.* 2018). Die Nitrogenase ist zellspezifisch und ausschließlich in fertig ausgebildeten Heterozysten aktiv (Fay 1992). In Bezug auf den Photosynthese-Apparat zeigen Heterozysten deutliche Unterschiede zu den vegetativen Zellen. Das sauerstoffproduzierende Photosystem II ist in den stickstofffixierenden Zellen inaktiv (Magnuson & Cardona 2016), Phycobilisomen sind weitgehend abgebaut. In den Heterozysten sind ebenso Thylakoidmembranen vorhanden, an denen aber hauptsächlich ein zyklischer Elektronentransport über das Photosystem I abläuft, der benötigtes ATP liefert (Wolk *et al.* 1994). Außerdem findet in den Heterozysten im Licht eine erhöhte Atmung statt, bei der vorhandener molekularer Sauerstoff zu Wasser reduziert wird (Wolk 1996). Reduktionsäquivalente in Form von NADPH werden allerdings nicht durch den zyklischen Elektronentransport produziert. Statt des reduktiven Pentosephosphat-Wegs (Calvin-Benson-Zyklus) findet in den Heterozysten der oxidative Pentosephosphat-Zyklus statt, über welchen NADPH gebildet wird (Wolk *et al.* 1994, Summers *et al.* 1995). Heterozysten besitzen zudem eine spezifische, verstärkte Zellwand aus Polysaccharid- und Glykolipidlayern (Abbildung 1 und 2), die die Diffusion von molekularem Sauerstoff in die spezialisierte Zelle minimiert (Walsby 2007, Nicolaisen *et al.* 2009). Sogenannte „Polar Plaques“ sind spezifische Strukturen aus dem Reservepolymer Cyanophycin, die an den Zellpolen zu den angrenzenden vegetativen Zellen sichtbar sind (Sherman *et al.* 2000).

Durch die Arbeitsteilung zwischen Heterozysten (N_2-Fixierung) und vegetativen Zellen (oxygene Photosynthese und Calvin-Benson-Zyklus) in ein und demselben Filament, ist ein Austausch von Metaboliten und Signalen und damit eine Kommunikation zwischen den Zellen und beiden Zellarten im Filament erforderlich (Wolk 1968, Wolk *et al.* 1974). Ein Modell der räumlichen Trennung und Arbeitsteilung in Heterozystenbildnern ist in Abbildung 2 gezeigt.

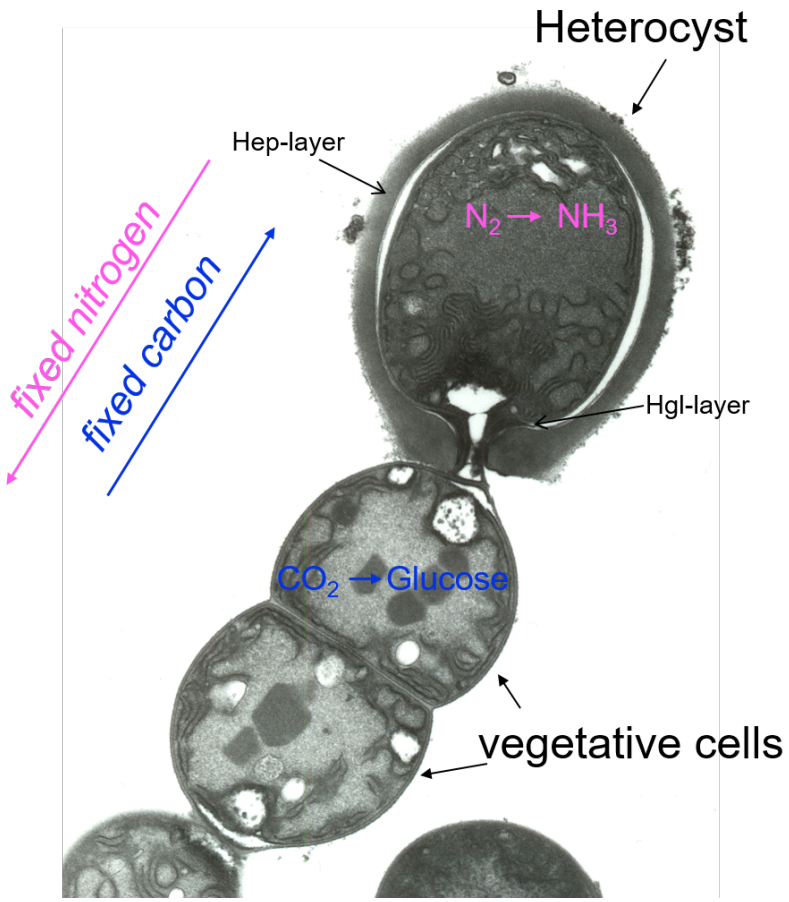

Abbildung 2: Modell der räumlichen Trennung der Photosynthese und der Stickstofffixierung.
Terminale Heterozyste und vegetative Zellen von *Anabaena*, die Heterozysten erhalten fixierten Kohlenstoff (Disaccharide) durch die vegetativen Zellen, diese erhalten fixierten Stickstoff (β-Aspartyl-Arginin) (Bild mit freundlicher Genehmigung von Iris Maldener, Universität Tübingen, unveröffentlicht)

Die Kommunikation zwischen den Zellen kann dabei sowohl extrazellulär durch ein kontinuierliches Periplasma (Flores *et al.* 2006, Mariscal *et al.* 2007, Wilk *et al.* 2011) als auch - für kleinere Moleküle - intrazellulär durch sogenannte „Septal Junctions“, früher auch Mikroplasmodesmata genannt erfolgen (Maldener & Muro-Pastor 2010, Flores *et al.* 2016). An Heterozysten angrenzende vegetative Zellen werden mit reduziertem Stickstoff wie Glutamin oder dem Dipeptid β-Aspartyl-Arginin versorgt (Thomas *et al.* 1977, Burnat *et al.* 2014), wohingegen die vegetativen Zellen Glutamat und reduzierte Kohlenhydrate wie z.B. das chemisch inerte Disaccharid Saccharose (Curatti *et al.* 2002, Vargas *et al.* 2011) an die Heterozysten liefern (Nürnberg *et al.* 2015).

1.3 Der Cyanophycinstoffwechsel in Cyanobakterien

Cyanophycin (Multi-L-Arginyl-poly-L-Aspartat) ist neben Poly (ε-L-Lysin) und Poly (γ-Glutamat) eine von drei natürlich vorkommenden Poly-Aminosäuren. Für die biotechnologische Forschung und Anwendung sind Poly-Aminosäuren als biologisch abbaubare Polymere und als Ausgangsbasis für die Herstellung von Polyamiden von Interesse (Frommeyer *et al.* 2014). Cyanophycin ist ein stickstoffreiches Reservepolymer, welches aus den beiden Aminosäuren Aspartat und Arginin aufgebaut ist. Das Polymer besteht aus einem Poly-Aspartat-Rückgrat, an dessen β-Carboxylgruppen durch Iso-Peptidbindungen Arginin gebunden ist (Simon 1971, Simon & Weathers 1976). Cyanophycin kann so unter anderem als natürliche Quelle für Aminosäuren wie Arginin und Aspartat dienen, das Poly-Aspartat-Rückgrat dieses Polymers könnte zudem als biologisch abbaubarer Ersatzstoff für Poly-Acrylate Verwendung finden. Cyanophycin besitzt eine molekulare Masse zwischen 25 bis 100 kDa (Simon 1971) und es hat ungewöhnliche Löslichkeitseigenschaften. Es ist bei physiologischem pH-Wert unlöslich, im Sauren und Basischen aber löslich. Das Polymer fungiert in der Zelle als reversibles Reservemolekül für Stickstoff, Kohlenstoff und Energie (Carr 1988, Herrero & Burnat 2014, Watzer & Forchhammer 2018). Cyanophycin kommt in den meisten diazotrophen und nicht-diazotrophen Cyanobakterien und einigen heterotrophen Bakterien als membranlose Granula im Zytoplasma vor (Simon 1971, Simon & Weathers 1976, Allen & Weathers 1980, Allen 1984, Allen 1988, Krehenbrink *et al.* 2002, Ziegler *et al.* 2002, Füser & Steinbüchel 2007). Bei Heterozystenbildnern kommt das Reservepolymer Cyanophycin sowohl in den vegetativen Zellen als auch in den Heterozysten vor, hier besonders an den Zellpolen als „Polar Plaques“ (Ziegler *et al.* 2001) (Abbildung 1). Die nicht-ribosomale Biosynthese von Cyanophycin durch das Enzym Cyanophycin Synthetase (CphA1) erfolgt, sofern der Zelle genügend Stickstoff und Energie zur Verfügung steht, vor allem in der stationären Wachstumsphase. Die Masse an Cyanophycin pro Zelltrockengewicht hängt stark von den vorherrschenden Wachstums-bedingungen ab. In der exponentiellen Wachstumsphase kann das Polymer bis zu 1 % der Trockenmasse ausmachen, in der stationären Phase und in Phasen von ungünstigen Wachstumsbedingungen wie Nährstoff- oder

Lichtstress (Simon 1973) wurden bis zu 18 % des Zelltrockengewichtes an Cyanophycin bestimmt. Das einzellige Cyanobakterium *Synechocystis* sp PCC 6803 wurde durch gentechnische Veränderungen dazu gebracht mehr als das 10-fache der Aminosäure Arginin zu synthetisieren (Watzer *et al.* 2015). Der Stamm *Synechocystis* BW86, bei dem durch Punktmutation im PII Signalprotein die Aminosäure Isoleucin 86 gegen Asparagin ausgetauscht wurde, akkumulierte durch den hohen Gehalt an Arginin bis zu 57 % Cyanophycin pro Zelltrockenmasse.

Die Synthese des Polymers Cyanophycin erfolgt enzymatisch durch CphA1, wobei die Aminosäuren Aspartat und Arginin in zwei Schritten unter ATP-Verbrauch kondensieren (Ziegler *et al.* 1998, Berg *et al.* 2000, Berg 2003). CphA1 besitzt zwei aktive Zentren, welche N-terminal und C-terminal lokalisiert sind. Am N-terminalen aktiven Zentrum wird unter ATP-Hydrolyse die Peptidbindung mit einem Aspartat-Rest geknüpft und somit die Aspartat-Kette verlängert. Das aktive Zentrum am C-terminalen Teil des Enzyms bildet hingegen, unter ATP-Hydrolyse, die Iso-Peptidbindung zwischen der β-Carboxylgruppe des Aspartats und der α-Aminogruppe des Arginins. Durch diese Zwei-Schritt-Reaktion entsteht ein stickstoffreiches Polymer, welches aus hunderten β-Asp-Arg-Einheiten aufgebaut ist (Carr 1988, Aboulmagd *et al.* 2001, Obst & Steinbüchel 2006) und als interner Stickstoffspeicher bei Bedarf genutzt werden kann. Im Vergleich mit einer CphA-defizienten Mutante in *Synechocystis* konnte gezeigt werden, dass die Synthese von Cyanophycin durch CphA der Zelle einen Wachstumsvorteil bietet (Watzer & Forchhammer 2018). Besonders unter wechselnden Bedingungen der Lichtverhältnisse (Tag-Nacht-Rhythmus) und der verfügbaren Stickstoffquellen war dieser Effekt zu beobachten. Das Polymer trägt so dazu bei, eine kontinuierliche Stickstoffassimilation auch unter Stickstoffmangelbedingungen zu gewährleisten.

Der Cyanophycin-Abbau wird mittels enzymatischer Hydrolyse durch ein spezielles Enzym, die Cyanophycinase, durchgeführt (Richter *et al.* 1999). Dabei entstehen Dipeptide aus β-Asp-Arg-Einheiten, die weiter durch das Enzym Isoaspartyl-Dipeptidase (PTA) in die einzelnen Aminosäuren gespalten werden (Hejazi *et al.* 2002). Die beiden Enzyme CphA und Cyanophycinase

(CphB) sind in *Anabaena* in allen Zellen, vorwiegend aber in den Heterozysten, die Isoaspartyl-Dipeptidase dagegen in den vegetativen Zellen zu finden (Burnat *et al.* 2014). Die Synthese der Isoaspartyl-Dipeptidase ist zudem unter Stickstoffmangelbedingungen induziert (Flaherty *et al.* 2011). Das in den Heterozysten zum Dipeptid β-Asp-Arg abgebaute Cyanophycin könnte so neben anderen Molekülen wie Glutamin als mobile Stickstoffreserve für die vegetativen Zellen dienen (Burnat *et al.* 2014).

In einigen Cyanobakterien kommt zusätzlich zum Hauptsyntheseenzym CphA1 ein zweites Enzym vor, welches als CphA2 bezeichnet wird (Picossi *et al.* 2004). Es stellt eine verkürzte Enzymversion von CphA1 dar (Picossi *et al.* 2004). CphA2 zeigt eine hohe Übereinstimmung in der Aminosäuresequenz nur im N-terminalen Teil der CphA1 (ORF *ava_1814*), nicht hingegen zum C-terminalen Teil. CphA2, als verkürzte Enzymvariante, besitzt somit nur eine ATP-Bindestelle mit B- und J-*Loop*, der P-*Loop* (Walker A-Motiv) ist nicht vorhanden (Berg 2003). Die spezielle Funktion von CphA2 blieb bisher unbekannt, obwohl bereits Untersuchungen an einer Knockout-Mutante durchgeführt wurden (Picossi *et al.* 2004). Die Mutante wies eine geringere Menge an Cyanophycin als der WT auf, dies deutet auf eine Funktion von CphA2 für die Cyanophycin Synthese hin.

In dieser Arbeit wurde CphA2 aus *A. variabilis* als neuer Typus einer Cyanophycin Synthetase charakterisiert. Zudem wurden mögliche Funktionen von CphA2 im Stoffwechsel von diazotrophen Cyanobakterien aufgezeigt.

1.4 Die Aminosäure L-Serin: Bedeutung und Biosynthese

Die Aminosäure L-Serin stellt ein Schlüsselintermediat im Kohlenstoff- und Stickstoffhaushalt von cyanobakteriellen Zellen dar. L-Serin ist eine hydrophile, proteinogene Aminosäure, die als Baustein von Proteinen in allen Organismen ebenso eine Rolle spielt wie in diversen Stoffwechselwegen. So ist Serin Ausgangsmolekül für Aminosäuren wie Glycin und Cystein und für andere Verbindungen, wie Phosphatidylcholin, einer Komponente der Zellmembran. Serin ist an der Biosynthese von Nukleinbasen beteiligt und somit ein Baustein der Erbinformation (DNA) und des Energieträgers ATP

(Walton & Woolhouse 1986). Es ist zudem häufig in aktiven Zentren von Enzymen anzutreffen, wie innerhalb der katalytischen Triade von Serinproteasen. Serin kann auch zur Regulation von Enzymaktivitäten beitragen, da es an seiner Hydroxygruppe phosphoryliert werden kann (Forchhammer 2004). Auch als metabolisches Signal für die transkriptionale Genregulation von photorespiratorischen Genen scheint Serin in *Arabidopsis thaliana* (im Folgenden *A. thaliana*) zu fungieren (Timm *et al.* 2013).

In photosynthetischen Organismen wie Pflanzen, Cyanobakterien und Algen existiert ein Serin-Biosynthese-Stoffwechselweg, der lichtabhängig ist und 2-Phosphoglycolat als Ausgangsmolekül verwendet. In Pflanzen stellt dieser gut untersuchte Weg den Hauptbiosyntheseweg sowohl für die Aminosäure Glycin als auch für Serin dar (Eisenhut *et al.* 2006, Bauwe 2010, Ros *et al.* 2014). Der Stoffwechselweg wird als C2-Zyklus oder photorespiratorischer Serin-Biosyntheseweg bezeichnet, da er während der Photorespiration abläuft (Tolbert 1997). Die Photorespiration ist ein Rückgewinnungsprozess für Kohlenstoff, da das aus der Oxygenase-Reaktion der RubisCO im Calvin-Benson-Zyklus hervorgegangene 2-Phosphoglycolat verstoffwechselt werden muss (Husic & Tolbert 1987, Norman & Colman 1991). Die Photorespiration ist in Pflanzen essentiell (Somerville 2001). Auch Cyanobakterien besitzen einen photorespiratorischen Stoffwechselweg, obwohl sie auch einen CO_2-anreichernden Mechanismus entwickelt haben, um die Oxygenasereaktion der RubisCO zu minimieren. Die Photorespiration tritt zeitgleich mit der CO_2-Fixierung im Calvin-Benson-Zyklus auf, da die RubisCO sowohl CO_2 als auch O_2 als Substrat umsetzen kann. Bei der Photorespiration wird durch die RubisCO Sauerstoff verbraucht und es entsteht 2-Phosphoglycolat, welches aus dem Stoffwechsel entfernt werden muss, da es toxisch wirkt und für den Calvin-Benson-Zyklus nicht nutzbar ist. Im C2-Zyklus konvertieren zwei Moleküle 2-Phosphoglycolat zu einem Molekül 3-Phosphoglycerat (3PGA) (Bauwe 2010). Hierbei werden die beiden Aminosäuren Glycin und Serin synthetisiert. Eine schematische Übersicht ist in Abbildung 4 gezeigt. Zuerst wird 2-Phosphoglycolat enzymatisch dephosphoryliert, dabei entsteht Glycolat, welches dann zu Glyoxylat oxidiert wird. Mit Hilfe von Glutamat und einer Aminotransferase entsteht durch

Aminierung Glycin, welches wiederum durch eine PALP-abhängige Serinhydroxymethyl-Transferase zu Serin umgesetzt wird. Der Zyklus wird geschlossen, indem Serin zu Hydroxypyruvat konvertiert, dieses zu Glycerat oxidiert wird und dieses wiederum mit Hilfe von ATP und der Glycerat Kinase zu 3PGA regeneriert wird. In dem Cyanobakterium *Synechocystis* ist dieser lichtabhängige photorespiratorische Serin-Biosyntheseweg bereits ausführlich untersucht worden (Eisenhut *et al.* 2008, Bauwe 2010).

Alternativ wurde in Pflanzen ein zweiter Serin-Biosyntheseweg beschrieben, der unabhängig von Licht verläuft (Ho & Saito 2001, Muñoz-Bertomeu *et al.* 2013, Ros *et al.* 2014). Dieser als Phosphoserin-Weg bezeichnete Metabolismus kommt auch in tierischen Organismen sowie in heterotrophen Bakterien vor und verläuft ebenfalls über das Molekül 3-PGA, welches während der Glykolyse und der Glukoneogenese entsteht (Greenberg & Ichihara 1957, Umbarger *et al.* 1963). L-Serin geht hierbei aus Phosphoserin als Stoffwechselintermediat hervor. Der Phosphoserin-Biosyntheseweg besteht aus drei nacheinander geschalteten enzymatischen Reaktionen. Das Enzym PGDH (EC 1.1.1.95) katalysiert mit Hilfe des Coenzyms NAD^+/$NADP^+$ die Oxidation von 3PGA zu 3-Phosphohydroxypyruvat. Dabei entsteht NADH bzw. NADPH. Das zweite Enzym, die PSTA (EC 2.6.1.52), ist ein PALP-abhängiges Enzym, welches mit Glutamat die Konversion von 3-Phosphohydroxypyruvat zu 3-Phosphoserin katalysiert. Schließlich wird 3-Phosphoserin durch das Enzym PSP (EC 3.1.3.3) zu Serin hydrolysiert (Greenberg & Ichihara 1957).

Bisher war der vom Licht unabhängige Phosphoserin-Biosyntheseweg in Cyanobakterien allerdings nicht nachgewiesen worden (Colman & Norman 1997, Huege *et al.* 2011, Young *et al.* 2011). In *Synechocystis* galt bisher der lichtabhängige photorespiratorische Stoffwechselweg als Haupt-Biosyntheseweg für Serin (Knoop *et al.* 2010). Zudem waren nicht alle Gene für die drei Enzyme des lichtunabhängigen Wegs im Genom von *Synechocystis* oder anderen Cyanobakterien bekannt. Nur das Gen von *Synechocystis*, welches für die PGDH kodiert, ist korrekt in der Datenbank annotiert (CyanoBase). Es existierten aber Hinweise auf das Vorhandensein des Phoshoserin-Biosynthesewegs in Cyanobakterien. So wurden in

cyanobakteriellen Zellextrakten Enzymaktivitäten des Phosphoserin-Stoffwechselwegs detektiert (Colman & Norman 1997). Ein zweiter Anhaltspunkt ergab sich aus Mutationsstudien an *Synechocystis* (Eisenhut *et al.* 2008). In der Photorespiration inhibierte Mutanten benötigten hohe CO_2-Konzentrationen, konnten aber ohne zusätzliche Serin-Zugabe wachsen. Insgesamt lag die Vermutung nahe, dass auch in Cyanobakterien dieser lichtunabhängige Weg der Serin-Biosynthese existiert.

In dieser Arbeit wurden daher bioinformatische, biochemische und genetische Daten erhoben, um die Existenz des Phosphoserin-Stoffwechselwegs neben dem photorespiratorischen Stoffwechselweg in *Synechocystis* zu belegen.

1.5 Der Polyphosphatstoffwechsel

1.5.1 Anorganisches Polyphosphat: Aufbau und Funktionen

Anorganisches Polyphosphat (PolyP) ist eines der ältesten Biopolymere und wahrscheinlich präbiotischen Ursprungs (Yamagata *et al.* 1991). Es ist aus bis zu hunderten Orthophosphat-Resten aufgebaut, die durch energiereiche Phosphorsäureanhydrid-Bindungen miteinander zu einem linearen Molekül verbunden sind. In der biotechnologischen Forschung findet PolyP eine breite Anwendung, da es über eine sehr hohe pH- und Thermo-Stabilität verfügt (Andexer & Richter 2015). PolyP ist ein ubiquitäres, in allen Organismen vorkommendes Reservemolekül. Das Polymer ist in Bakterien und Archaea hauptsächlich im Zytoplasma lokalisiert und findet sich in pflanzlichen und tierischen Zellen als membranlose PolyP-Granula (Rao *et al.* 2009, Achbergerova & Nahalka 2011). In dem fakultativ chemolithoautotrophen Bakterium *Ralstonia eutropha* wurden an PolyP co-lokalisierte Proteine identifiziert und es konnte eine räumliche Nähe zu Polyhydroxybutyraten (PHB) festgestellt werden (Tumlirsch *et al.* 2015). Auch bei der Aufbereitung von Wasser wird die Beziehung zwischen PolyP und PHB bereits genutzt (Yuan *et al.* 2012).

Durch eine Speicherung von anorganischem Phosphat als Polyphosphatgranula können Cyanobakterien langandauernde Phosphatmangelbedingungen gut überbrücken. Durch PolyP und dessen Hydrolyse wird in der Zelle ein gleichbleibender Phosphat-Spiegel gewährleistet, der essentiell für Wachstum und Metabolismus ist. In Abbildung 3 ist eine fluoreszenzmikroskopische Aufnahme eines *Anabaena*-Filaments zu sehen, welches zum Nachweis von PolyP und DNA mit dem Fluoreszenzfarbstoff DAPI behandelt wurde. Aufgrund der Strukturähnlichkeiten interagiert DAPI sowohl mit DNA als auch mit PolyP (Gomes *et al.* 2013). Die Interaktion von DAPI mit Polyphosphat verschiebt das Emissionsmaximum bei einer Anregung von 360 nm bis 405 nm von 450 nm (blau) auf bis zu 526 nm (gelbgrün) (Aschar-Sobbi *et al.* 2008).

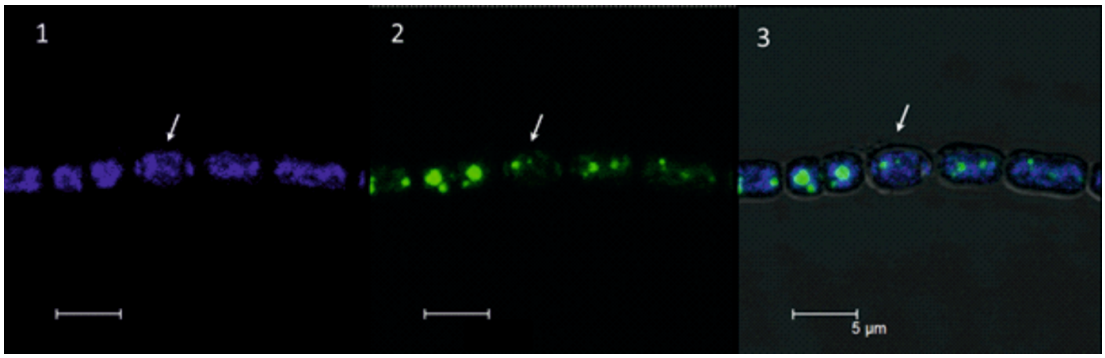

Abbildung 3: Nachweis von anorganischem PolyP in Anabaena-Filamenten, kultiviert unter Stickstoffmangelbedingungen.
1) DAPI-DNA-Interaktionen sind als blaue Fluoreszenz erkennbar. 2) DAPI-PolyP-Komplexe fluoreszieren gelbgrün. 3) Die Überlagerung der Bilder 1 und 2 mit der lichtmikroskopischen Aufnahme zeigt die Lokalisation von DNA und anorganischem PolyP. Die Anregung erfolgte bei 405 nm. Die Heterozyste ist durch einen Pfeil gekennzeichnet.

Als energiereiches Speichermolekül übernimmt PolyP eine Vielzahl an unterschiedlichen Funktionen in der Zelle. Anorganisches PolyP fungiert vor allem als ein dynamischer Phosphat- und Energiespeicher (Kornberg *et al.* 1956, Harold 1966). Die Hydrolyse einer energiereichen Phosphorsäureanhydridbindung im PolyP-Molekül bewirkt die Freisetzung von Energie, thermodynamisch ähnlich zu der Freien Energie, die bei der Hydrolyse einer gemischten Säureanhydridbindung z.B. eines ATP-Moleküls freigesetzt wird.

Anorganisches PolyP kann das organische ATP-Molekül, welches als universelle Energiewährung der Zelle betrachtet werden kann (Resnick & Zehnder 2000), teilweise in der Funktion des Energieträgers substituieren. Durch seinen präbiotischen Ursprung gilt anorganisches PolyP als Vorläufer des ATP-Moleküls (Kornberg 1995). PolyP hat darüber hinaus weitere vielfältige Funktionen in der Zelle (Albi & Serrano 2016). Es ist ein Molekül mit hoher negativer Ladung und somit als Polyanion ein effektiver Kationenkomplexbildner. Eine Bindung von Kalzium-Ionen, Kalium-, Magnesium- oder Mangan-Ionen, aber auch von Schwermetall-Ionen, wie die des Cadmiums, ist nachgewiesen (Kulaev & Kulakovskaya 2000). Durch Komplexierung mit Mangan- und Eisen-Ionen schützt PolyP die Zelle vor oxidativem Stress durch Superoxidanion-Radikale (O_2^-) und die Fenton-Reaktion (Gray & Jakob 2015, Soto *et al.* 2018). Weiterhin kann PolyP Proteine vor Aggregation und Entfaltung schützen (Gray *et al*. 2014). PolyP kann schließlich als Substrat für diverse enzymatische Reaktionen wie für Phosphorylierungen von Glukose oder NAD/NADH durch Kinasen dienen (Kornberg *et al.* 1999). Tatsächlich wurden PolyP-abhängige NAD^+-Kinasen oder Glukokinasen bisher aber nur in Prokaryonten nachgewiesen. PolyP-abhängige Glukokinasen waren in Cyanobakterien bisher nicht untersucht.

1.5.2 Enzyme des Polyphosphat-Metabolismus in Prokaryonten

Enzyme, die an der Synthese und der Umsetzung von PolyP beteiligt sind, wie z.B. PolyP-Kinasen oder ATP- und PolyP-abhängige Glukokinasen, sind in Bakterien der Ordnung Actinomycetales bereits biochemisch gut charakterisiert. Das Hauptenzym für die Synthese von PolyP ist die Polyphosphat-Kinase 1 (PPK1, EC 2.7.4.1), welche zuerst in *E. coli* entdeckt wurde (Kornberg *et al.* 1956). Das Enzym katalysiert die reversible Übertragung des γ-Phosphates von ATP oder GTP auf PolyP (Kornberg 1995). Zusätzlich besitzt die PPK1 weitere Enzymaktivitäten, eine ATP-Synthese mittels PolyP, eine Nukleosiddiphosphat-Kinase-Aktivität und eine Autophosphorylierung. Homologe *ppk1*-Gene wurden in mehr als 354 prokaryontischen Genomen festgestellt (Tzeng & Kornberg 1998). In *Ralstonia eutropha* wurden 7 Gene für Polyphosphat-Kinasen identifiziert, die

jeweils einen Beitrag zur Polyphosphat-Biosynthese leisten. Eine Co-Lokalisation dieser Polyphosphat-Kinasen an PolyP-Granula konnte zudem durch eYFP-Fusionsproteine gezeigt werden (Tumlirsch *et al.* 2015). In *Synechococcus elongatus* sp. PCC 7942 wurde das Gen für die Polyphosphat-Kinase gezielt ausgeschaltet. Elektronenmikroskopisch waren hier keine PolyP-Granula mehr nachweisbar (Vaillancourt *et al.* 1978). In Pflanzen und in Tieren wurden dagegen keine PPK1-Homologe gefunden. Neben der PPK des Typ 1 existiert ein alternatives Enzym, die PPK2. Dieses katalysiert aber primär die GTP- oder ATP-Bildung durch den Transfer von Phosphat-Resten von PolyP auf ADP und damit einen PolyP-Abbau (Zhang *et al.* 2002). Gene, die für eine PPK1 und PPK2 kodieren sind auch in cyanobakteriellen Genomen, wie im Genom von *Synechocystis* und *Anabaena* zu finden (Zhang *et al.* 2002). Der ORF *alr3593* kodiert für eine PPK1 in *Anabaena* (Nakao *et al.* 2010).

Von Bedeutung für den enzymatischen Abbau von PolyP in Mikroorganismen sind vor allem Phosphatasen. Exopolyphosphatasen (PPX, EC 3.6.1.11) hydrolysieren die terminalen Reste des PolyP und setzen so Orthophosphat frei (Akiyama *et al.* 1993, Kornberg *et al.* 1999). In *Anabaena* kodiert der ORF *all3552* eine Exopolyphosphatase, eine biochemische Charakterisierung des Enzyms steht noch aus (Nakao *et al.* 2010). Endophosphatasen dagegen hydrolysieren interne Phosphorsäureanhydridbindungen und verkürzen so die PolyP-Kette ohne Bildung von Orthophosphat (Sethuraman *et al.* 2001, Lichko *et al.* 2010). Aufgrund seiner energiereichen Phosphorsäureanhydrid-bindungen kann PolyP neben ATP oder GTP als Phosphorylgruppendonator für verschiedene enzymatische Reaktionen dienen. NAD^+/NADH-Kinasen können mit Hilfe von ATP oder PolyP NAD^+/NADH zu $NADP^+$/NADPH umsetzen.

Die Polyphosphatglukomannokinase (PPGK, EC 2.7.1.63), ein Enzym der Repressor-ORF-Kinase-Familie (Pfam PF00480), katalysiert die Phosphory-lierung von Monosacchariden wie Glukose, Mannose oder Fruktose durch ATP bzw. GTP oder PolyP. Bei dieser Reaktion entstehen als Reaktionsprodukte phosphorylierte Zucker, wie Glukose-6-phosphat und um einen Phosphatrest verkürztes PolyP, bzw. ADP oder GDP. Die erste ATP- und PolyP-abhängige

PPGK wurde in *Mycobacterium phlei* entdeckt (Szymona & Ostrowski 1964). Später wurde in den unterschiedlichsten Bakterien eine PPGK-Aktivität beschrieben, darunter in zahlreichen Pathogenen (Szymona & Ostrowski 1964, Szymona & Widomski 1974, Pepin & Wood 1986, Lindner *et al.* 2010, Koide *et al.* 2013). PPGK wurden bisher nur in Bakterien und nicht in Archaea, Pflanzen, Pilzen oder Tieren gefunden. Phylogenetische Untersuchungen belegen, dass die meisten bakteriellen Enzyme wie die Glukomannokinase sowohl ATP als auch PolyP als Substrat verwenden können, dass jedoch die Präferenz der Glukokinasen für PolyP bei phylogenetisch höherentwickelten Organismen abnimmt (Albi & Serrano 2015). Eine Ausnahme von der Bifunktionalität wurde in der PPGK von *Microlunatus phosphovorus*, einem grampositiven Bakterium, gefunden, welches PolyP in großen Mengen speichern kann. Das hochspezifische Enzym phosphoryliert Glukose ATP-unabhängig ausschließlich mit PolyP (Tanaka *et al.* 2003). Glukose-6-Phosphat ist ein zentrales Molekül, welches Grundlage für verschiedene biotechnologisch relevante Chemikalien, wie Fructose 1,6-bisphasphat oder Myo-inositol sein kann. Kürzlich wurde durch ein *Screening* eine hochaktive und thermostabile PPGK aus *Thermobifida fusca* identifiziert, die zur Herstellung von Glukose-6-Phosphat mit Hilfe von PolyP Anwendung finden soll (Zhou *et al.* 2018).

In *Anabaena* kodiert der ORF *alr2973* eine typische ATP-abhängige Glukokinase. Zusätzlich ist im Genom von *Anabaena* der ORF *all1371* als mögliches Gen für eine PPGK annotiert (Nakao *et al.* 2010). Durch die globale Analyse des Transkriptoms mittels Gesamt-RNA-Sequenzierung wurde der Transkriptionsstartpunkt für *all1371* und somit eine mögliche Promotorstelle identifiziert (Mitschke *et al.* 2011).

In dieser Arbeit wurde das Genprodukt von *all1371* untersucht und damit erstmals eine cyanobakterielle Polyphosphat-abhängige Glukokinase charakterisiert. Die Bedeutung für den Stoffwechsel in *Anabaena* wurde herausgearbeitet.

2 Ziele der Arbeit

Diese Arbeit gliedert sich in drei Teilfragestellungen.

a) Zunächst sollte das Enzym CphA2 aus *A. variabilis* biochemisch charakterisiert werden und in einen funktionellen Zusammenhang zum gut untersuchten Cyanophycin-Metabolismus von Heterozysten-bildenden Cyanobakterien gestellt werden. Da bis dahin wenig über CphA2 bekannt war, aber schon einige Erkenntnisse zu CphA1 aus *A. variabilis* vorlagen, sollten die Untersuchungen an den beiden diazotrophen Cyanobakterien *A. variabilis* und *Cyanothece* sp. PCC 7425 durchgeführt werden. Es sollten eine umfassende Charakterisierung *in vitro* und eine Einordnung der physiologischen Rolle des Enzyms erfolgen. *In vivo* Untersuchungen an genetisch veränderten Cyanobakterien sollten die Ergebnisse vervollständigen und eventuelle Zusammenhänge zwischen Cyanophycin-Stoffwechsel und Stickstoffmetabolismus zeigen.

b) Ferner sollte experimentell untersucht werden, ob ein lichtunabhängiger Serin-Biosyntheseweg, der in Pflanzen vorhanden ist, auch in Cyanobakterien existiert. Dieser Phosphoserin-Stoffwechselweg sollte in *Synechocystis* durch *in vitro* Analysen nachgewiesen werden. Durch gezielte Mutagenesen sollte die Bedeutung dieses Stoffwechselwegs für Cyanobakterien aufgeklärt werden.

c) Das dritte Teilziel bestand darin, einen tieferen Einblick in den Polyphosphatmetabolismus des Heterozysten-bildenden Cyanobakteriums *Anabaena* sp. PCC 7120 zu erlangen. Konkret sollten hierzu *in vitro* und *in vivo* Studien zu All1371 von *Anabaena* vorgenommen werden. Der ORF *all1371*, der für eine putative PPGK kodiert, sollte analysiert und das gereinigte Enzym biochemisch charakterisiert werden. Parallel dazu sollten *in silico* Analysen durchgeführt werden, um die Verteilung von PPGK‘s innerhalb der Cyanobakterien aufzuklären. Hieraus sollten Anhaltspunkte für *in vivo* Experimente abgeleitet und ein so möglicher Zusammenhang zwischen dem Vorkommen einer PPGK und einem diazotrophen Wachstum beleuchtet werden.

3 Ergebnisse und Diskussion

3.1 CphA2- eine Cyanophycin Synthetase neuen Typs

3.1.1 CphA2 kommt vorwiegend in diazotrophen Cyanobakterien vor

Um einen allgemeinen Überblick zu erhalten in welchen Abteilungen der Cyanobakterien das Gen *cphA2* grundsätzlich vorkommt, wurde eine Sequenzanalyse vergleichend zum Vorkommen von *cphA1* durchgeführt. Dieses Vorgehen hatte außerdem zum Ziel Hinweise auf mögliche Funktionen des Enzyms CphA2 im Cyanophycin-Metabolismus zu erkennen.

Eine Überprüfung von 155 sequenzierten Cyanobakterien-Genomen ergab, dass ein zweites Cyanophycin Synthetase-Gen, *cphA2,* ausschließlich in Cyanobakterien vorkommt, die auch das Gen für CphA1 besitzen. Während *cphA1* in 72,9 % aller Cyanobakterien vorkommt (113 von 155), haben dagegen nur 28,4 % der untersuchten Genome ein *cphA2*-Gen (44 von 155). Das Gen für das Hauptsyntheseenzym CphA1 ist in 100 % der Heterozystenbildner (Abteilung IV und V), in 97 % der Filamentösen (Abteilung III) und nur in 11 % der sequenzierten Genome der einzelligen Cyanobakterien der Abteilungen I und II zu finden. Insgesamt besitzen 39 % der cyanobakteriellen Genome, die das Gen für CphA1 aufweisen auch das Gen für CphA2 (44 von 113). Vorwiegend wurde *cphA2* dabei in filamentösen Spezies der Abteilungen III, IV und V identifiziert (77 %). In Heterozystenbildnern der Abteilung IV wurde in 71 % und in der Abteilung V in 82 % der Cyanobakterien, die eine CphA1 besaßen zusätzlich das *cphA2*-Gen gefunden. In den sequenzierten Cyanobakterien-Genomen der Abteilung III wiesen nur ca. 30 % ein *cphA2*-Gen auf, innerhalb dieser Gruppe, in der die Bakterien keine Heterozysten ausbilden, befinden sich allerdings Spezies, die molekularen Stickstoff fixieren können wie *Oscillatoria sp*. (Stal & Heyer 1987). In nur 23 % der einzelligen Formen (Abteilungen I und II) wurde das *cphA2*-Gen identifiziert. Darunter befanden sich einzellige Cyanobakterien der Spezies *Cyanothece* und *Gloeocapsa*, welche im Dunkeln unter mikroaeroben Bedingungen diazotroph wachsen können, wie beispielsweise

Cyanothece sp. PCC 7425 (Millineaux *et al.* 1981, Bandyopadhyay *et al.* 2013). Insgesamt lassen diese Ergebnisse einen potenziellen Zusammenhang zu diazotrophem Wachstum vermuten.

3.1.2 *In vitro* Charakterisierung von CphA2 als Cyanophycin Synthetase

Durch biochemische Untersuchung mit zwei rekombinanten, aus *E. coli* isolierten CphA2-Enzymen aus dem Heterozystenbildener *A. variabilis* (Abteilung IV) und dem einzelligen Cyanobakterium *Cyanothece* sp. PCC 7425 aus der Abteilung I konnte gezeigt werden, dass CphA2 unter Verbrauch von je einem Molekül ATP-spezifisch β-Asp-Arg-Einheiten verknüpft und so einen neuen Typus einer Cyanophycin Synthetase darstellt. Mit diversen anderen getesteten Dipeptiden wie β-Aspartyl-Lysin oder β-Aspartyl-Alanin und unter Einsatz der einzelnen Aminosäuren Aspartat und Arginin zeigte sich dagegen keine Enzymaktivität. Für die *in vitro* Reaktion waren zudem Kalium-Ionen essentiell. Diese ließen sich nicht durch Natriumionen ersetzen. Durch einen spezifischen, hydrolytischen Abbau des Reaktionsproduktes mittels Cyanophycinase (Richter *et al.* 1999), welche heterolog in *E. coli* exprimiert und dann isoliert wurde, konnte das Produkt, mit einer Größe von ca. 20-30 kDa eindeutig als das Polymer Cyanophycin identifiziert werden. Es ist anzunehmen, dass der Reaktionsmechanismus, wie auch beim Hauptsyntheseenzym CphA1, über Acyl-Phosphat-Intermediate verläuft (Ziegler *et al.* 1998) und so die Peptidbindung zwischen den Aminosäureresten der Aspartate der Dipeptide geknüpft wird.

Kinetische Analysen ergaben eine sigmoide Sättigungskurve für β-Asp-Arg mit einem relativ hohen $K_{0,5}$-Wert von 76 mM. Der K_M-Wert für ATP lag bei 3,5 mM. Der relativ hohe $K_{0,5}$-Wert für für β-Asp-Arg, der *in vitro* bestimmt wurde, korrespondiert aber nicht unbedingt mit den Verhältnissen in der Zelle, wo das Enzym direkt an Cyanophycin gebunden vorkommt (siehe Kapitel 3.1.3). Die Wechselzahl des Enzyms wurde mit 1,1 s^{-1} (pH 8,0 und 30 °C) bestimmt. Die molekulare Masse der beiden rekombinanten CphA2 Enzyme aus *A. variabilis* wurde mittels Gelfiltration bestimmt. Das isolierte Enzym His10_CphA2 (Monomer: 75 kDa) wies eine molekulare Masse von 273 +/- 2,4 kDa auf. Das isolierte Protein CphA2 (ohne *Tag*, 73 kDa) wies eine Masse

von 265 +/- 0,6 kDa auf. Demnach kommt CphA2 in nativen Zustand entweder als Homotrimer oder Homotetramer.

Insgesamt zeigen die *in vitro* Ergebnisse deutlich, dass das Enzym CphA2 eine bisher dahin unbekannte Funktion als Cyanophycin Synthetase besitzt.

3.1.3 Untersuchungen zur Funktion von CphA2 *in vivo*

Die Rolle von CphA2 im cyanobakteriellen Stoffwechsel wurde durch Insertionsmutagenese in *A. variabilis* näher untersucht. Dabei zeigte sich, dass die *cphA2*-Mutante etwa 10-15 % weniger Cyanophycin enthält, als der WT. Auch eine ∆*cphA2*-Mutante *in Anabaena* enthielt 20 % weniger des Reservemoleküls als der WT (Picossi *et al.* 2004). Die molekulare Masse des Cyanophycins lag im Bereich von 30-130 kDa (Ziegler *et al.* 2001). Durch Immunogold-Markierung konnte das verbliebene Cyanophycin in der Mutante, genau wie im WT, an den Zellpolen der Heterozysten und als Granula in den vegetativen Zellen lokalisiert werden. Wachstumsanalysen unter verschiedenen Licht- und Stickstoffbedingungen zeigten zudem, dass die ∆*cphA2*-Mutante von *A. variabilis* besonders bei starkem Licht und stickstofffixierenden Bedingungen einen Wachstumsnachteil gegenüber dem WT hatte. Ähnliche Ergebnisse wurden bereits für eine ∆*cphA1*-Mutante in *A. variabilis* gezeigt (Ziegler *et al.* 1998) sowie für eine *cphA1* defiziente Mutante von *Synechocystis* (Watzer & Forchhammer 2018).

Durch Elektronenmikroskopie und Einsatz eines CphA2-Antikörpers konnte nachgewiesen werden, dass das Enzym direkt am Polymer lokalisiert ist. Eine zellspezifische Verteilung des Enzyms wurde nicht festgestellt. Auch für das Hauptsyntheseenzym CphA1 in *A. variabilis* wurde eine Lokalisation direkt am Cyanophycin nachgewiesen. Kürzlich konnte zudem gezeigt werden, dass eine aktive Cyanophycin Synthase in *Synechocystis* ebenfalls am Polymer lokalisiert ist, wohingegen sie in inaktiver Form im Cytoplasma vorliegt (Watzer & Forchhammer 2018). Das Resultat für CphA2 wird durch Transkript-Analysen gestützt, die keine zellspezifische Expression von *cphA2* zeigten (Park *et al.* 2013). Es konnte zudem nachgewiesen werden, dass die Transkriptmenge von CphA2 in *A. variabilis* relativ konstant blieb, auch 48 h

nach Entzug von gebundenem Stickstoff aus dem Medium. Im Gegensatz dazu stieg das Expressionsniveau von CphA1 nach Stickstoffentzug in *A. variabilis* an. Dieser Effekt fand sich noch verstärkt in der Δ*cphA2*-Mutante. Diese Ergebnisse entsprachen den Transkript-Daten aus *Anabaena* (Picossi *et al.* 2004, Flaherty *et al.* 2011).

3.1.4 Zusammenfassung und Ausblick zur CphA2

Das Gen für das Enzym CphA2 wurde vorwiegend in diazotroph wachsenden Cyanobakterien, die auch das Gen für CphA1 besitzen, identifiziert. *In vitro* Analysen mit zwei rekombinanten CphA2-Enzymen ergaben eindeutig, dass das Enzym eine Funktion als Cyanophycin Synthetase eines neuen Typus besitzt: durch Verknüpfung des Dipeptids β-Asp-Arg und ATP-Hydrolyse wird Cyanophycin synthetisiert. *In vivo* zeigte eine Δ*cphA2*-Mutante eine Wachstumsverzögerung unter Stressbedingungen wie Starklicht und Stickstoffmangel. Als Recyclingenzym für das Reservepolymer Cyanophycin schließt das Enzym CphA2 den dynamischen Kreislauf für Synthese und Abbau dieses Polymers. CphA2 scheint zusammen mit dem Abbauenzym Cyanophycinase für eine kontinuierliche Umverteilung des Dipeptids β-Asp-Arg im Filament zu sorgen. Cyanophycin kann so bei Bedarf, direkt aus β-Asp-Arg polymerisiert werden, wobei nur ein Molekül ATP hydrolysiert wird. Gerade in Heterozystenbildnern könnte dies ein Vorteil sein, da β-Asp-Arg hier als Haupttransportform für Stickstoffverbindungen zur Versorgung der vegetativen Zellen fungiert (Burnat *et al.* 2014). Daneben lassen sich aber noch weitere bisher unbekannt gebliebene Funktionen von CphA2 vermuten, die in einem Zusammenhang mit der Stickstofffixierung stehen, da das Enzym auch in einzelligen Diazotrophen zu finden ist. CphA2 könnte z.B. den zellulären β-Asp-Arg-Pool beschränken und damit einen Abbau des Dipeptids durch die Isoaspartyl Dipeptidase in die Aminosäuren Arginin und Aspartat regulieren (Forchhammer & Watzer 2016). Ob die Enzyme CphA1 und CphA2 aus *A. variabilis in vivo* in direkten Kontakt treten, bleibt weiter Gegenstand der Untersuchungen.

3.2 Identifizierung des Phosphoserin-Biosynthesewegs in Synechocystis

3.2.1 Die Gene des Phosphoserin-Synthesewegs

Der Phosphoserin-Syntheseweg ist ein Serin-Biosyntheseweg, der unabhängig von Licht verläuft. Er kommt sowohl in Pflanzen als auch in tierischen Organismen sowie in heterotrophen Bakterien vor und wurde in Cyanobakterien bisher nur angenommen. Die Ergebnisse zum Nachweis dieses Syntheseweges in *Synechocystis* sind hier gezeigt.

Drei Enzyme sind notwendig, um aus 3PGA über den Phosphoserin-Biosyntheseweg die Aminosäure Serin zu synthetisieren: PGDH, PSTA und PSP. Zuerst wurden Kandidaten der Gene dieser drei Enzyme im Genom von *Synechocystis* durch bioinformatische Methoden identifiziert. In der Datenbank CyanoBase war das Gen *sll1908* bereits als *serA* annotiert und ist somit ein möglicher Kandidat für das Enzym PGDH (SLL1908).

Dagegen wurden zwei Gene identifiziert, die für eine PSTA in *Synechocystis* kodieren könnten: *sll1559* und *slr5022*. Die Übersetzung in die Aminosäuresequenz zeigte im Vergleich mit bekannten PSTA‘s aus *E. coli* (Duncan & Coggins 1986), *A. thaliana* (Ho *et al.* 1998) und *Bacillus circulans* (Battchikova *et al.* 1996) eine hohe Übereinstimmung zu Aminotransferasen der Klasse V, die PALP als Kofaktor benötigen (Ouzounis & Sander 1993). Außerdem wurden konservierte Motive, inklusive einer speziellen Signatursequenz für PSTA‘s, mit einem Lysin im katalytischen Zentrum identifiziert (Belhumeur *et al.* 1994).

Zur Identifizierung der PSP wurden Zellextrakte von *Synechocystis* durch klassische chromatographische Methoden aufgearbeitet und auf eine PSP-Aktivität hin überprüft. Es konnten so Proteine angereichert werden, die eine ca. 500-fach erhöhte PSP-Aktivität aufwiesen. Diese wurden mittels SDS-Page und Massenspektrometrie überprüft. Auch das Enzym Slr1124 wurde hierbei als Kandidat für eine PSP identifiziert. Das Gen *slr1124* war aber in CyanoBase als eine Phosphoglyceratmutase annotiert. Es wurde aber gezeigt, dass eine Phosphoglyceratmutase in dem Bakterium

Hydrogenobacter thermophilus ausschließlich eine PSP-Aktivität besitzt (Chiba *et al.* 2012). Ein Sequenz-Vergleich zeigte eine große Übereinstimmung mit Slr1124, welches damit als Kandidat für eine PSP in *Synechocystis* galt.

3.2.2 Biochemische Charakterisierung der PGDH, PSTA und PSP *in vitro*

Die Gene *sll1908*, *all1559*, *slr5022* und *slr1124* wurden in Expressionsvektoren eingebracht und in *E. coli* exprimiert. Die rekombinanten Enzyme wurden mittels Affinitätschromatografie isoliert und in enzymatische Tests eingesetzt, um eine Funktion als PGDH, PSTA oder PSP festzustellen. Außerdem wurden die kinetischen Parameter der Enzyme ermittelt.

3.2.2.1 Sll1908 besitzt eine PGDH-Aktivität

Das Enzym Sll1908 wurde als lösliches His-*Tag*-Fusionsprotein mit einer molekularen Masse von 58 kDa isoliert. Als Kofaktor wurde NAD^+ eingesetzt, um zu überprüfen, ob das Enzym das Substrat 3PGA zu Phosphohydroxypyruvat und NADH oxidiert. Absorptionsmessungen bei 340 nm zeigten, dass Sll1908 eine deutliche PGDH-Aktivität besitzt. Sll1908 wies eine spezifische Aktivität von 2,3 U/mg und eine Wechselzahl von 2,25 s^{-1} bei einem optimalen pH-Wert von 9,0 auf. Bei einem pH-Wert von 7,5 zeigte sich ein Verlust der Enzymaktivität von ca. 67 %. Wurde anstelle von NAD^+ das Substrat $NADP^+$ als Kofaktor eingesetzt, fiel die Aktivität von Sll1908 auf 5 % vom Maximalwert. Eine Zugabe von 0,1 mM NADH zum Ansatz bewirkte eine Endprodukthemmung, das Enzym zeigte nur noch 16 % seiner ursprünglichen Aktivität. Michaelis-Konstanten von 0,63 mM für das Substrat 3PGA und von 0,13 mM für NAD^+ wurden ermittelt. Ein ähnlich hoher K_M-Wert für 3PGA wurde mit 1,19 mM für eine rekombinante PGDH aus *A. thaliana* bei pH 9,0 gefunden, der K_M-Wert für NAD^+ war dagegen mit 0,01 mM deutlich geringer (Ho *et al.* 1999). Durch Gelfiltration wurde die molekulare Masse des nativen Proteins mit ca. 234 kDa bestimmt. Dieses Ergebnis zeigt, dass Sll1908 in seiner nativen Form als Homotetramer vorkommt, wie auch PGDH‘s aus *Corynebacterium glutamicum* und *A. thaliana* (Ho & Saito 2001).

3.2.2.2 Sll1559 besitzt eine PSTA-Aktivität

Die Proteine Sll1559 und Slr5022 wurden als rekombinante Enzyme isoliert und der vorhandene GST-*Tag* nach Affinitätschromatographie durch Einsatz einer Protease entfernt. Das Enzym Sll1559, mit einer molekularen Masse von 41 kDa, zeigte *in vitro* eine PSTA-Aktivität, Slr5022 dagegen nicht. Somit wurde Slr5022 als Kandidat für eine PSTA ausgeschlossen. Sll1559 katalysiert *in vitro* den Aminogruppentransfer der α-Aminogruppe des Glutamats auf die α-Ketosäure 3-Phosphohydroxypyruvat. Diese PSTA-Reaktion wurde mit der PGDH-Reaktion gekoppelt, um die Bildung von 3-Phosphoserin indirekt über die Entstehung von NADH bei 340 nm verfolgen zu können. Durch eine Produkthemmung des Enzyms PGDH durch 3-Phosphohydroxypyruvat, welche in *A. thaliana* gezeigt wurde (Ho & Saito 2001), konnte *in vitro* ein Start der PSTA-Reaktion und damit ein Verbrauch des Produktes der PGDH-Reaktion herbeigeführt werden. Sll1559 wies eine spezifische Aktivität von 3,64 U/mg und eine Wechselzahl von 2,49 s^{-1} bei pH 9,0 auf. Kinetische Messungen ergaben eine Michaelis-Konstante von 1,03 mM für die Aminosäure Glutamat. Für eine rekombinante PSTA aus *A. thaliana* wurden bisher verschiedene K_M-Werte für Glutamat ermittelt: 70 µM (Ho *et al.* 1998) und 5.05 mM (Ali & Nozaki 2006). Durch Gelfiltration wurde die molekulare Masse des nativen Enzyms mit 84 kDa bestimmt. Dies spricht für ein Vorkommen als homodimeres Enzym in *Synechocystis*. Eine Homodimere Struktur wurde ebenso für die PSTA aus *Bacillus circulans* bestimmt (Battchikova *et al.* 1996).

3.2.2.3 Slr1124 ist eine PSP

Das isolierte rekombinante Protein Slr1124, mit einer molekularen Masse von 49,8 kDa wurde in einen kolorimetrischen Test eingesetzt, um die Aktivität des Enzyms zu bestimmen. Das Enzym katalysiert hierbei die Hydrolyse des Substrats 3-Phosphoserin zu Serin und Orthophosphat. Slr1124 wies mit 36,2 U/mg eine deutliche und sehr spezifische PSP-Aktivität bei pH 7,5 (28 °C) auf. Die Wechselzahl des Enzyms betrug 30,2 s^{-1}. Eine Michaelis-Konstante für das Substrat 3-Phosphoserine von 0,42 mM wurde für das Enzym aus

Synechocystis bestimmt, wohingegen in *A. thaliana* ein höherer K_M-Wert von 3,5 mM bei pH 7,5 ermittelt wurde (Ho & Saito 2001). Die Aktivität von Slr1124 wurde ebenso bei pH 9,0 bestimmt und verringerte sich hier um ca. 44 % im Vergleich zur Aktivität bei pH 7,5. Das Enzym wurde zudem durch Zugabe von 5 mM und 10 mM Serin *in vitro* gehemmt. Slr1124 wies in der Gelfiltration eine native molekulare Masse von 50 kDa auf, was dem Monomer entspricht.

3.2.3 Die Rekonstitution des Phosphoserin-Wegs

Durch Kombination der drei Enzymtestansätze wurde eine Rekonstitution des Phosphoserin-Wegs *in vitro* erreicht. Neben den rekombinanten Enzymen Sll1908, Sll1559 und Slr1124 wurden in einen Ansatz nur die Substrate NAD^+, 3PGA und Glutamat eingesetzt. Die Aktivität wurde bei 340 nm über die Entstehung von NADH sowie über die Orthophosphat-Freisetzung ermittelt. Nach 10 min Inkubation wurden 8,8 µmol Phosphat / mg und (über die Verfolgung der Extinktionsänderung bei 340 nm) 8,9 µmol NADH / mg detektiert. Wurde nur das Enzym PSP durch Hitze inaktiviert und dann in den vollständigen Test eingesetzt, ließ sich zwar eine NADH-Bildung aber keine Freisetzung von Phosphat feststellen. *In vitro* konnte so gezeigt werden, dass die Kombination der Aktivitätstests aller drei Enzyme zur Rekonstitution des Phosphoserin-Wegs führt. Es wurde somit bewiesen, dass die Serin-Biosynthese in *Synechocystis*, neben dem lichtabhängigen Syntheseweg auch durch den lichtunabhängigen Phosphoserin-Stoffwechselweg stattfinden kann.

3.2.4 Der Phosphoserin-Syntheseweg ist in Cyanobakterien von Bedeutung

Um die physiologische Rolle des lichtunabhängigen Phosphoserin-Wegs zu untersuchen, sollten die Gene, die für die Phosphoserin-Phosphatasen in *Synechocystis* und dem obligat phototrophen Cyanobakterium *Synechococcus elongatus* PCC 7942 kodieren (im Folgenden *Synechococcus*), inaktiviert werden. Die Gene *slr1124* und *Synpcc7942_0485* wurden durch eine Kanamycin-Resistenzkassette ersetzt und durch Transformation eines Vektors in die Cyanobakterien eingebracht. Die erhaltenen Klone wurden stets auf Kanamycin-haltigen Platten unter

verschiedensten Lichtbedingungen und Serin-Konzentrationen kultiviert. Es konnten aber in keinem Fall vollständig segregierte Mutanten erzeugt werden. Diese Resultate deuten darauf hin, dass die Gene für die Phosphoserin-Phosphatasen essentiell für *Synechocystis* und *Synechococcus* sind. Auch eine vollständige Ausschaltung des Gens der PSTA aus Synechocystis (*sll1559)* war in einer früheren Studie nicht möglich; es konnten ebenso keine homozygoten Klone erzeugt werden (Eisenhut *et al.* 2006). Auch scheint in *A. thaliana* sowohl die PSP als auch die PGDH essentiell zu sein (Benstein *et al.* 2013, Muñoz-Bertomeu *et al.* 2013). In Pflanzen ist der Phosphoserin-Weg neben der Biosynthese von Serin auch für andere Prozesse, wie der Variationen von Signalstoffwechselwegen oder Protein- und Lipidphosphorylierungen verantwortlich. Ob diese Funktionen so auch für Cyanobakterien angenommen werden können, werden weitere Untersuchungen zeigen.

3.2.5 Zusammenfassung und Ausblick zum Phosphoserin-Biosyntheseweg

Ein bisher nur vermuteter lichtunabhängiger Serin-Biosyntheseweg wurde für *Synechocystis* nachgewiesen. Die Gene, die für die Enzyme dieses Phosphoserin-Biosynthesewege kodieren wurden identifiziert und die drei Proteine biochemisch *in vitro* charakterisiert. Durch Kombination der Enzyme mit den Substraten 3PGA, NAD^+ und Glutamat wurde gezeigt, dass der Phosphoserin-Biosyntheseweg *in vitro* rekonstituiert werden kann. Untersuchungen an Mutanten lassen vermuten, dass dieser Stoffwechselweg essentiell in *Synechocystis* und *Synechococcus* ist. Insgesamt scheint der Phosphoserin-Biosyntheseweg zudem einen wesentlichen Beitrag zur gesamten Serin-Biosynthese im cyanobakteriellen Stoffwechsel zu leisten.

Obwohl Cyanobakterien über einen universellen, lichtabhängigen Weg Serin synthetisieren (Hagemann *et al.* 2013), kommen in den meisten sequenzierten Stämmen Homologe zu allen drei benötigten Enzymen des lichtunabhängigen Phosphoserin-Wegs vor. Es kann daraus die Schlussfolgerung gezogen werden, dass der Phosphoserin-Biosyntheseweg in den meisten Cyanobakterien vorkommt und somit eine bedeutendere Rolle spielt, als bisher angenommen.

3.3 All1371 - eine strikt Polyphosphat-abhängige Glukokinase

3.3.1 All1371 ist eine PolyP-abhängige Glukomannokinase

Eine cyanobakterielle Polyphosphat-abhängige Glukokinase sollte hier erstmals umfassend biochemisch charakterisiert und die Bedeutung für den Stoffwechsel in *Anabaena* aufgezeigt werden. Im Genom von *Anabaena* ist der ORF *all1371* als mögliches Gen für eine PPGK (EC 2.7.1.63) annotiert (Nakao *et al.* 2010). Ein Sequenzvergleich von All1371 mit gut charakterisierten PPGK‘s von Actinomycales zeigte eindeutig sieben teilweise hoch konservierte Sequenzmotive als funktionelle und strukturelle Domänen. Diese Protein-Domänen sind in Interaktionen mit den Substraten Glukose, Mannose, ATP und PolyP involviert (Mukai *et al.* 2003, Liao *et al.* 2012, Koide *et al.* 2013). Die Präsenz der konservierten Motive weist somit auf eine Funktion des All1371-Proteins als PPGK hin. Der Nachweis dazu wurde an einer rekombinanten Enzymvariante *in vitro* geführt. Hierzu wurde ein Expressionskonstrukt erstellt und in *E. coli* eingebracht. All1371 konnte durch Affinitätschromatographie als aktives Enzym isoliert werden. *In vitro* Tests zeigten, dass All1371 ausschließlich PolyP als Substrat nutzt, um Glukose und Mannose zu Glukose-6-phosphat bzw. Mannose-6-phosphat zu phosphorylieren. Eine spezifische Aktivität von 107 U/mg und eine Wechselzahl von 48,2 ± 6,9 pro Sekunde wurden ermittelt. Mit anderen Phosphorylgruppendonatoren wie ATP, ADP, AMP, GTP, UTP, CTP und Pyrophosphat, die in verschiedenen Konzentrationen eingesetzt wurden, war dagegen keine Aktivität nachweisbar. Diese Substratspezifität für PolyP ist eine bemerkenswerte Eigenschaft der PPGK aus *Anabaena*. All1371 unterscheidet sich darin von anderen bisher charakterisierten bakteriellen PPGK‘s, die bifunktional sind, d.h. ATP oder GTP als alternativen Phosphorylgruppendonator zu PolyP verwenden können. Dazu gehören die PPGK‘s *aus Mycobacterium tuberculosis* (Hsieh *et al.* 1996b), *Propionibacterium shermanii* (Phillips *et al.* 1993) und *Corynebacterium glutamicum* (Lindner *et al.* 2010). Die ausschließliche PolyP-Abhängigkeit, die neben der hohen Substratspezifität eine kennzeichnende Eigenschaft von All1371 ist, wurde nahezu parallel zur Publikation dieser Ergebnisse bestätigt

und auch für eine PPGK von *Nostoc punctiforme* PCC 73102 gezeigt (Albi & Serrano 2015). Ohne Zugabe von $MgCl_2$ konnte mit All1371 *in vitro* keine enzymatische Aktivität nachgewiesen werden. $MgCl_2$ konnte aber vollständig durch $MnCl_2$ ersetzt werden. Dieses Resultat spricht für die Abhängigkeit von All1371 von divalenten Kationen als Kofaktoren, wie sie auch an bakteriellen PPGK's z.B. von *Microlunatus phosphorus* (Tanaka *et al.* 2003), *Mycobacterium phlei* (Szymona & Ostrowski 1964) und *Thermobifida fusca* festgestellt wurde.

Kinetische Messungen mit Glukose und PolyP ergaben eine typische Michaelis-Menten-Kinetik. Ein relativ geringer K_M-Wert für PolyP von 1,76 µM spricht für eine hohe Affinität zum Substrat PolyP. Die K_M-Werte für PolyP35 für die ATP/PolyP-abhängigen PPGK's von *Propionibacterium shermanii* und *Mycobacterium tuberculosis* wurden in einem ähnlichen Bereich mit 1,2 µM und 4,6 µM bestimmt (Phillips *et al.* 1993, Phillips *et al.* 1999). Das Bakterium *Microlunatus phosphorus*, dessen PPGK ausschließlich PolyP als Phosphorylgruppendonator verwendet, weist dagegen einen K_M-Wert für PolyP30 von 3,8 mM auf (Tanaka *et al.* 2003). Dieser im Vergleich relativ hohe K_M-Wert für PolyP lässt sich mit den PolyP-akkumulierenden Eigenschaften des Bakteriums erklären. Hier ergibt sich aus der geringeren Affinität kein Nachteil für den Organismus. Neben der Funktion Glukose zu phosphorylieren, ist All1371 ebenso in der Lage Mannose als Substrat zu nutzen. Der ermittelte $K_{0,5}$-Wert für D-Mannose beträgt 24,3 mM und ist damit etwa 200-fach höher als der K_M-Wert für Glukose von 0,118 mM. Dieses Ergebnis zeigt, dass Glukose das deutlich favorisierte Substrat von All1371 ist. Freie Glukose kann in der Zelle einerseits während des Abbaus von Gykogen entstehen, zum anderen aber auch während einer Saccharose-Metabolisierung in den Heterozysten (Cumino *et al.* 2007, Kolman *et al.* 2015). D-Mannose, als Epimer der D-Glukose, besitzt die gleiche Summenformel und unterscheidet sich nur in der räumlichen Anordnung der Hydroxylgruppe am C2-Atom von Glukose. In *Anabaena* existiert ein ausgeprägter Fruktose/Mannose-Metabolismus, der bisher nicht vollständig aufgeklärt ist (Kanehisa & Goto 2000). Mannose ist ein wichtiger Bestandteil von zellulären Glykoproteinen und Polysacchariden z.B. der Zellwand. Mannose als

zusätzliches Substrat für All1371 zu nutzen erscheint also sinnvoll. Das Produkt dieser Reaktion Mannose-6-phosphat kann durch eine Mannose-6-phosphat Isomerase (kodiert durch die ORFs *all4342* und *all4538*) zu Fruktose-6-Phosphat umgesetzt werden. Fruktose-6-Phosphat könnte daraufhin auch durch eine Glukose-6-phosphat-Isomerase (ORF *alr1050*) weiter zu Glukose-6-phosphat isomerisiert werden. Fruktose-6-Phosphat könnte aber auch, da es ein Zwischenprodukt des Calvin-Benson-Zyklus und des oxidativen Zweiges des Pentosephosphat-Zyklus ist, dort weiter Verwendung finden. Die Ergebnisse der kinetischen Untersuchungen zeigen zudem, dass All1371 mit seiner Zweisubstratreaktion einem [bi-bi ping-pong] - Mechanismus folgt (Cleland 1963). Das hier aufgestellte Modell der Katalyse lässt sich wie folgt beschreiben: in einem ersten Schritt bindet PolyP kovalent an All1371. Das Enzym wird durch PolyP phosphoryliert und das erste Reaktionsprodukt, ein um ein Phosphat reduziertes PolyP, diffundiert ab. Nachdem Glukose als zweites Substrat an das nun phosphorylierte Enzym gebunden hat, kann die Phosphorylierung von Glukose erfolgen und das zweite Reaktionsprodukt Glukose-6-phosphat wird entlassen. Das Enzym geht nach diesem Schritt wieder in den Grundzustand über. Die kinetischen Mechanismen der ATP/PolyP-abhängigen Glukokinasen von *Mycobacterium tuberculosis* (Hsieh *et al.* 1996a) und *Streptomyces coelicolor* (Imriskova *et al.* 2005) wurden bereits untersucht. Beide Enzyme zeigen einen [bi-bi sequenziellen] - Mechanismus. Ob es tatsächlich einen Unterschied zwischen ATP/PolyP-anhängigen Glukokinasen und strikt PolyP-abhängigen Glukokinasen im Hinblick auf den Reaktionsmechanismus geben könnte, lässt sich bisher nur vermuten und muss durch weitere Analysen geprüft werden.

3.3.2 PPGK‘s kommen in diazotrophen Cyanobakterien vor

Eine mit der Aminosäuresequenz von All1371 durchgeführte BlastP-Suche (Altschul *et al.* 1997) verdeutlichte die Präsenz des Enzyms PPGK innerhalb der zurzeit sequenzierten Genome der Cyanobakterien. Insgesamt wurde bei 34 % der Cyanobakterien eine putative PPGK gefunden, und zwar in allen fünf Abteilungen. In Abteilung IV wurde mit 85 % aller sequenzierten

Cyanobakterien die höchste Rate an putativen PPGK's gefunden. Dies könnte ein Hinweis darauf sein, dass die PPGK eine besondere Rolle in Heterozysten-bildenden Cyanobakterien bzw. beim Wachstum unter Stickstoffmangel spielt. In Cyanobakterien der Abteilung V besitzen 54.5 % Sequenzen mit hoher Ähnlichkeit zur PPGK von *Anabaena*. 53 % der filamentbildenden Cyanobakterien ohne Zelldifferenzierung (Abteilung III) besitzen nach dieser Analyse das Gen für eine putative PPGK. In der Abteilung II ist für 50 % der einzelligen Cyanobakterien eine PPGK vorhergesagt. Dazu gehören *Pleurocapsa* sp. PCC 7319 sowie *Stanieria cyanosphaera*, die beide das Enzym Dinitrogenase und somit die Fähigkeit zur Stickstofffixierung besitzen (Rippka & Waterbury 1977, Markowitz *et al.* 2012) und das Cyanobakterium *Chroococcidiopsis* sp. PCC 6712, welches bekannt ist für seine Fähigkeit der Stickstofffixierung unter anaeroben Bedingungen (Rippka *et al.* 1979) und seiner engen verwandtschaftlichen Verbindung zu Heterozystenbildnern (Fewer *et al.* 2002). Innerhalb der Abteilung I besitzen dagegen nur 5,7 % der einzelligen Cyanobakterien Sequenzen mit hoher Ähnlichkeit zu All1371. Dazu gehören *Synechococcus* sp. PCC 7335 und *Synechococcus* sp. PCC 7502, die verwandtschaftlich eher zu den Filamentösen der Abteilung III gehören (Robertson *et al.* 2001, Shih *et al.* 2013). *Acaryochloris marina* MBIC11017 und *Acaryochloris* sp. CCMEE 5410 bilden einen separaten Zweig im phylogenetischen Stammbaum und sind mit dem diazotrophen Cyanobakterium *Acaryochloris* sp. HICR111A verwandt (Loughlin *et al.* 2013, Shih *et al.* 2013). Die Ergebnisse dieser Analyse weisen auf eine Korrelation zwischen dem Vorhandensein einer PPGK und der Möglichkeit molekularen Stickstoff unter anoxischen oder micro-oxischen Bedingungen zu fixieren hin.

3.3.3 Die Funktion von All1371 im Stoffwechsel von *Anabaena*

Der direkte Nachweis einer PPGK-Aktivität erfolgte in Zellextrakten von drei filamentösen, diazotrophen Cyanobakterien, die sowohl mit als auch ohne gebundenem Stickstoff im Medium kultiviert wurden. Zellextrakte von *Anabaena* wiesen eine spezifische PPGK-Aktivität von 4,3 nmol/min*mg beim Wachstum auf Nitrat bzw. eine um 35 % erhöhte Aktivität von 5,8 nmol/min*mg nach vier Tagen Wachstum unter Stickstoffmangelbedingungen auf.

Unerwartet war, dass die PPGK-Aktivität in Extrakten von *Mastigocladus laminosus* und *Fisherella musicola* (Abteilung V) insgesamt drei bis vierfach gegenüber der Aktivität in *Anabaena* erhöht war und hier keine stickstoffmangelbedingte Erhöhung der PPGK-Aktivität messbar war.

Um die physiologische Funktion von All1371 im Stoffwechsel von *Anabaena in vivo* zu untersuchen wurde eine *all1371*-Deletionsmutante von *Anabaena* erzeugt und phänotypisch charakterisiert. In zellfreien Extrakten dieser Mutante war keine PPGK-Aktivität nachweisbar. Dieses Ergebnis zeigt, dass *all1371* in *Anabaena* unter den gewählten Bedingungen nicht essentiell ist. Insgesamt konnten bei der phänotypischen Charakterisierung der Mutante keine morphologischen Unterschiede zum Wildtyp von *Anabaena* festgestellt werden. Die Überlebensfähigkeit von Δ*all1371* im Vergleich zum WT wurde unter verschiedenen Licht- und Stickstoffbedingungen analysiert. Ein deutlicher Wachstumsnachteil von Δ*all1371* war nur unter stickstofffixierenden Bedingungen im Vergleich zum WT feststellbar. Dieser Effekt trat noch verstärkt unter Tag-Nacht-Bedingungen auf, welche die natürlichen Bedingungen von *Anabaena* repräsentieren. Das deutlich verzögerte Wachstum der Δ*all1371*-Mutante unter diazotrophen Bedingungen deutet auf eine spezielle Funktion des Enzyms bei der N_2-Fixierung hin. Möglich wäre es, dass All1371 in *Anabaena* besonders unter diesen Mangel-Bedingungen eine ATP-abhängige Glukokinase unterstützt und zusätzliches Glukose-6-phosphat zur Verfügung stellt. ATP würde so für die energieaufwändige Fixierung von molekularem Stickstoff gespart werden. Experimentell gestützt wird diese Annahme durch die Beobachtung, dass die All1371-Aktivität in zellfreien Extrakten unter Stickstoffmangelbedingungen um 35 % erhöht war. Insgesamt können die Ergebnisse so interpretiert werden, dass All1371 unter diazotrophen Wachstumsbedingungen, unter denen viel ATP für die Stickstofffixierung aufgewendet werden muss, eine Strategie darstellt, um ATP bei der Phosphorylierung von Glukose einzusparen. All1371 stellt so in *Anabaena* eine Alternative zur ATP abhängigen Glukokinase, kodiert durch den ORF *alr2973* dar.

In der Promotorregion von *all1371* konnte ein DIF^+-ähnliches Motiv (Mitschke *et al.* 2011) in der Nähe der -35 Box identifiziert werden. Das

Vorkommen dieses Motives lässt vermuten, dass der Promotor von *all1371* heterozysten-spezifisch und HetR-abhängig ist. Tatsächlich zeigte die hergestellte GFP-Promotorfusionsmutante eine GFP-Fluoreszenz in den Heterozysten und somit eine erhöhte *all1371*-Promotoraktivität. Damit wird ein direkter Zusammenhang zum Prozess der Stickstofffixierung bestätigt. Diese Ergebnisse gehen einher mit *Deep Sequencing* Analysen in *Anabaena*, welche nach 21 Stunden Stickstoffentzug eine Steigerung des Transkriptionsniveaus von *all1371* um das 4,8-fache zeigen (Flaherty *et al.* 2011). Zusammenfassend lässt sich somit eine heterozystenspezifische Promotoraktivität des Gens *all1371* feststellen. Die Ergebnisse legen den Schluss nahe, dass stickstofffixierende Zellen eine erhöhte PPGK-Aktivität besitzen.

3.3.4 Zusammenfassung und Ausblick zur PPGK in *Anabaena*

All1371 wurde als strikt Polyphosphat-abhängige Glukomannokinase aus *Anabaena* identifiziert und ist damit die erste cyanobakterielle Glukokinase, welche diese ganz spezielle Substratspezifität aufweist. Die Verwendung von PolyP anstelle von ATP für die Glukose-Phosphorylierung durch die PPGK, scheint für Heterozystenbildner wie *Anabaena* von Vorteil zu sein. Heterozysten, die Orte der Stickstofffixierung, sind selbst nicht in der Lage Kohlenstoffdioxid über den Calvin-Benson-Zyklus zu fixieren. Reduzierter Kohlenstoff wird ihnen z.B. in Form von Saccharose zur Verfügung gestellt, welches über die vegetativen Zellen importiert wird. Das Photosystem II mit seinem sauerstoffproduzierenden Komplex ist in den spezialisierten Zellen inaktiv, um die Nitrogenase vor Sauerstoff zu schützen. Ein zyklischer Elektronentransport über das Photosystem I zur ATP-Produktion findet aber auch in den Heterozysten statt. Reduktionsäquivalente in Form von NADPH, die für Biosyntheseprozesse benötigt werden, werden in den Heterozysten selbst über den oxidativen Pentosephosphat-Zyklus generiert (Maldener & Muro-Pastor 2010). Hierbei wird in einem ersten enzymatischen Schritt Glukose zu Glukose-6-Phosphat umgesetzt. Eine PPGK wie All1371 kann hierzu spezifisch PolyP anstelle von ATP als Phosphorylgruppendonator verwenden. Glukose-6-phosphat ist das Substrat für das Schlüsselenzym des

oxidativen Pentosephosphat-Wegs, der Glukose-6-phosphat-Dehydrogenase. Unter diesen Umständen ist eine Funktion von All1371 offensichtlich von Vorteil für die Zelle, die ohne direkt ATP zu verbrauchen Glukose zu Glukose-6-phosphat umsetzen kann. Auf der anderen Seite ist das Gen für eine PPGK auch in Cyanobakterien zu finden, die keine Heterozysten ausbilden. Hier scheint das Enzym ebenso als alternatives Protein zu einer ATP-abhängigen Glukokinase zu fungieren. Ob die PPGK auch in anderen Cyanobakterien eine ausschließliche Substratspezifität zu PolyP zeigt, oder ob das Enzym auch andere Phosphorylgruppendonatoren wie ATP nutzt und damit wie die meisten bakteriellen PPGK‘s bifunktional ist, bleibt zu untersuchen.

3.4 Zusammenfassung

In dieser Arbeit wurden durch molekularbiologische Studien in drei Teilprojekten neue Biosynthesewege in den Cyanobakterien *Anabaena* und *Synechocystis* beschrieben und ihre Bedeutung für den cyanobakteriellen Stoffwechsel herausgestellt. Eine modellhafte Übersicht über den Grundstoffwechsel (Kohlenstoff- und Stickstoffmetabolismus) in Cyanobakterien sowie der Ergebnisse, der in dieser Arbeit untersuchten speziellen Stoffwechselwege zur Serin-Biosynthese, zum Cyanophycin-Stoffwechsel und zur Phosphorylierung von Glukose über eine strikt PolyP-abhängige PPGK und ihre Zusammenhänge sind in Abbildung 4 dargestellt.

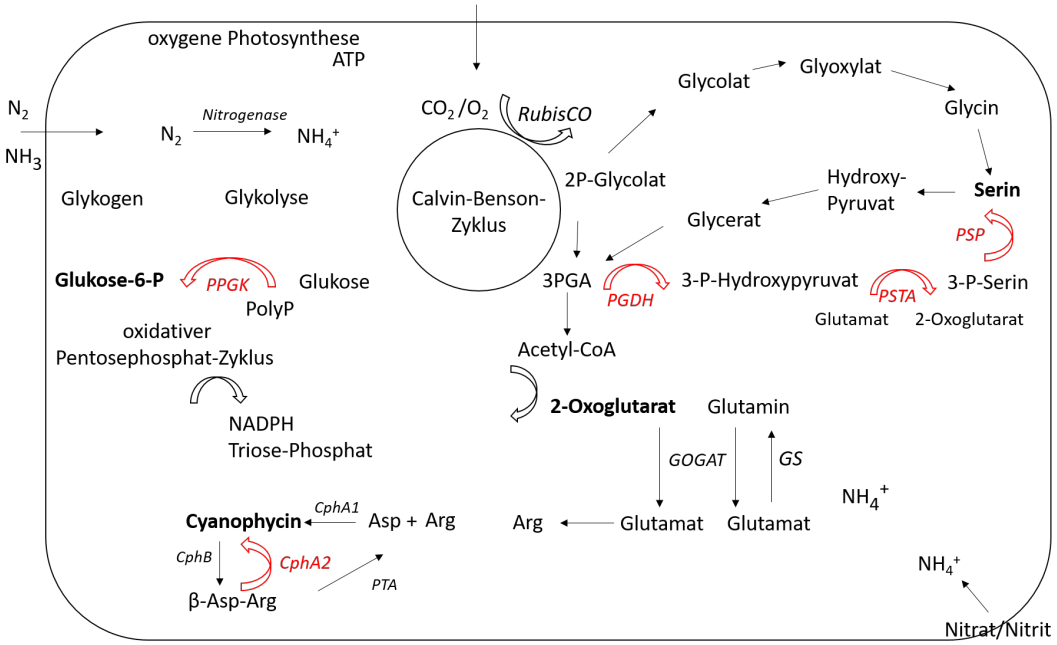

Abbildung 4: Schema zum Stoffwechsel in Cyanobakterien.
Übersicht über die Zusammenhänge zwischen Kohlenstoff- und Stickstoff-metabolismus in Cyanobakterien, sowie dem Cyanophycin-Metabolismus, der Serin-Biosynthese und der Phosphorylierung von Glukose durch eine PPGK. Rot gekennzeichnet sind die in dieser Arbeit untersuchten Enzyme.

Die hier gezeigten Resultate machen den Weg frei, für weiterführende Studien und Experimente im Bereich des Stoffwechsels von Cyanobakterien, dessen grundlegende Erforschung von Interesse ist, um die biotechnologische Anwendbarkeit von Cyanobakterien weiter auszubauen.

4 Literatur

Abed, R. M., Dobretsov, S. & Sudesh, K. (2009). Applications of cyanobacteria in biotechnology. *J Appl Microbiol* 106: 1-12

Aboulmagd, E., Oppermann-Sanio, F. B. & Steinbüchel, A. (2001). Purification of *Synechocystis* sp. strain PCC 6308 cyanophycin synthetase and its characterization with respect to substrate and primer specificity. *Appl Environ Microbiol* 67: 2176-2182

Achbergerova, L. & Nahalka, J. (2011). Polyphosphate-an ancient energy source and active metabolic regulator. *Microb Cell Fact* 10: 63

Adams, D. G. & Carr, N. G. (1981). The developmental biology of heterocyst and akinete formation in cyanobacteria. *Crit Rev Microbiol* 9: 45-100

Akiyama, M., Crooke, E. & Kornberg, A. (1993). An exopolyphosphatase of *Escherichia coli.* The enzyme and its *ppx* gene in a polyphosphate operon. *J Biol Chem* 268: 633-639

Albi, T. & Serrano, A. (2015). Two strictly polyphosphate-dependent gluco(manno)kinases from diazotrophic cyanobacteria with potential to phosphorylate hexoses from polyphosphates. *Appl Microbiol Biotechnol* 99: 3887-3900

Albi, T. & Serrano, A. (2016). Inorganic polyphosphate in the microbial world. Emerging roles for a multifaceted biopolymer. *World J Microbiol Biotechnol* 32: 27

Ali, V. & Nozaki, T. (2006). Biochemical and functional characterization of phosphoserine aminotransferase from *Entamoeba histolytica*, which possesses both phosphorylated and non-phosphorylated serine metabolic pathways. *Mol Biochem Parasitol* 145: 71-83

Allen, M. M. (1984). Cyanobacterial cell inclusions. *Annu Rev Microbiol* 38: 1-25

Allen, M. M. (1988). Inclusions: Cyanophycin. *Cyanobacteria*. *Academic Press* 207-213. L. Packer & A. N. Glaser. Methods Enzymol.

Allen, M. M. & Weathers, P. J. (1980). Structure and composition of cyanophycin granules in the cyanobacterium *Aphanocapsa* 6308. *J Bacteriol* 141: 959-962

Altschul, S. F., Madden, T. L., Schaffer, A. A., Zhang, J., Zhang, Z., Miller, W. & Lipman, D. J. (1997). Gapped BLAST and PSI-BLAST: a new generation of protein database search programs. *Nucleic Acids Res* 25: 3389-3402

Andexer, J. N. & Richter, M. (2015). Emerging enzymes for ATP regeneration in biocatalytic processes. *Chembiochem* 16: 380-386

Aschar-Sobbi, R., Abramov, A. Y., Diao, C., Kargacin, M. E., Kargacin, G. J., French, R. J. & Pavlov, E. (2008). High sensitivity, quantitative measurements of polyphosphate using a new DAPI-based approach. *J Fluoresc* 18: 859-866

Bandyopadhyay, A., Elvitigala, T., Liberton, M. & Pakrasi, H. B. (2013). Variations in the rhythms of respiration and nitrogen fixation in members of the unicellular diazotrophic cyanobacterial genus *Cyanothece*. *Plant Physiol* 161: 1334-1346

Battchikova, N., Himanen, J. P., Ahjolahti, M. & Korpela, T. (1996). Phosphoserine aminotransferase from *Bacillus circulans* subsp. *alkalophilus*: purification, gene cloning and sequencing. *Biochim Biophys Acta* 1295: 187-194

Bauwe, H. (2010). Recent developments in photorespiration research. *Biochem Soc Trans* 38: 677-682

Belhumeur, P., Fortin, N. & Clark, M. W. (1994). A gene from *Saccharomyces cerevisiae* which codes for a protein with significant homology to the bacterial 3-phosphoserine aminotransferase. *Yeast* 10: 385-389

Benstein, R. M., Ludewig, K., Wulfert, S., Wittek, S., Gigolashvili, T., Frerigmann, H., Gierth, M., Flügge, U. I. & Krueger, S. (2013). Arabidopsis phosphoglycerate dehydrogenase1 of the phosphoserine pathway is essential for development and required for ammonium assimilation and tryptophan biosynthesis. *Plant Cell* 25: 5011-5029

Berg, H. (2003). Untersuchungen zur Funktion und Struktur der Cyanophycin-Synthetase von Anabaena variabilis ATCC 29413. Doctoral Thesis, Humboldt-Universität zu Berlin

Berg, H., Ziegler, K., Piotukh, K., Baier, K., Lockau, W. & Volkmer-Engert, R. (2000). Biosynthesis of the cyanobacterial reserve polymer multi-L-arginyl-poly-L-aspartic acid (cyanophycin). *Eur J Biochem* 267: 5561-5570

Buikema, W. J. & Haselkorn, R. (1991). Characterization of a gene controlling heterocyst differentiation in the cyanobacterium *Anabaena* 7120. *Genes Dev* 5: 321-330

Burnat, M., Herrero, A. & Flores, E. (2014). Compartmentalized cyanophycin metabolism in the diazotrophic filaments of a heterocyst-forming cyanobacterium. *Proc Natl Acad Sci USA* 111: 3823-3828

Carr, N. (1988). Nitrogen reserves and dynamic reservoirs in cyanobacteria. *Biochemistry of Algae and Cyanobacteria*. *Phytochem Lett* 13-21. J. R. Gallon & L. J. Rogers. Oxford, Clarendon Press.

Chiba, Y., Oshima, K., Arai, H., Ishii, M. & Igarashi, Y. (2012). Discovery and analysis of cofactor-dependent phosphoglycerate mutase homologs as novel phosphoserine phosphatases in *Hydrogenobacter thermophilus*. *J Biol Chem* 287: 11934-11941

Cleland, W. W. (1963). The kinetics of enzyme-catalyzed reactions with two or more substrates or products. I. Nomenclature and rate equations. *Biochim Biophys Acta* 67: 104-137

Colman, B. & Norman, E. G. (1997). Serine synthesis in cyanobacteria by a nonphotorespiratory pathway. *Physiol Plant* 100: 133-136

Cumino, A. C., Marcozzi, C., Barreiro, R. & Salerno, G. L. (2007). Carbon cycling in *Anabaena* sp. PCC 7120. Sucrose synthesis in the heterocysts and possible role in nitrogen fixation. *Plant Physiol* 143: 1385-1397

Curatti, L., Flores, E. & Salerno, G. (2002). Sucrose is involved in the diazotrophic metabolism of the heterocyst-forming cyanobacterium *Anabaena* sp. *FEBS Lett* 513: 175-178

Deusch, O., Landan, G., Roettger, M., Gruenheit, N., Kowallik, K. V., Allen, J. F., Martin, W. & Dagan, T. (2008). Genes of cyanobacterial origin in plant nuclear genomes point to a heterocyst-forming plastid ancestor. *Mol Biol Evol* 25: 748-761

Dexter, J., Armshaw, P., Sheahan, C. & Pembroke, J. T. (2015). The state of autotrophic ethanol production in cyanobacteria. *J Appl Microbiol* 119: 11-24

Duncan, K. & Coggins, J. R. (1986). The serC-aro A operon of *Escherichia coli*. A mixed function operon encoding enzymes from two different amino acid biosynthetic pathways. *Biochem J* 234: 49-57

Eisenhut, M., Kahlon, S., Hasse, D., Ewald, R., Lieman-Hurwitz, J., Ogawa, T., Ruth, W., Bauwe, H., Kaplan, A. & Hagemann, M. (2006). The plant-like C2 glycolate cycle and the bacterial-like glycerate pathway cooperate in phosphoglycolate metabolism in cyanobacteria. *Plant Physiol* 142: 333-342

Eisenhut, M., Ruth, W., Haimovich, M., Bauwe, H., Kaplan, A. & Hagemann, M. (2008). The photorespiratory glycolate metabolism is essential for cyanobacteria and might have been conveyed endosymbiontically to plants. *Proc Natl Acad Sci U S A* 105: 17199-17204

Elhai, J. & Wolk, C. P. (1988). Conjugal transfer of DNA to cyanobacteria. *Methods Enzymol* 167: 747-754

Fay, P. (1992). Oxygen relations of nitrogen fixation in cyanobacteria. *Microbiol Rev* 56: 340-373

Fewer, D., Friedl, T. & Budel, B. (2002). *Chroococcidiopsis* and heterocyst-differentiating cyanobacteria are each other's closest living relatives. *Molecular Phylogenetics and Evolution* 23: 82-90

Flaherty, B. L., Johnson, D. B. & Golden, J. W. (2014). Deep sequencing of HetR-bound DNA reveals novel HetR targets in *Anabaena* sp. strain PCC 7120. *BMC Microbiol* 14: 255

Flaherty, B. L., Van Nieuwerburgh, F., Head, S. R. & Golden, J. W. (2011). Directional RNA deep sequencing sheds new light on the transcriptional response of *Anabaena* sp strain PCC 7120 to combined-nitrogen deprivation. *BMC Genomics* 12

Flores, E., Guerrero, M. G. & Losada, M. (1980). Short-term ammonium inhibition of nitrate utilization by *Anacystis nidulans* and other cyanobacteria. *Arch Microbiol* 128: 137-144

Flores, E. & Herrero, A. (2004). Assimilatory nitrogen metabolism and its regulation. *The Molecular Biology of Cyanobacteria*. *Kluwer Academic Publishers* 487-517. D. A. Bryant. Dordrecht.

Flores, E., Herrero, A., Forchhammer, K. & Maldener, I. (2016). Septal junctions in filamentous heterocyst-forming cyanobacteria. *Trends Microbiol* 24: 79-82

Flores, E., Herrero, A., Wolk, C. P. & Maldener, I. (2006). Is the periplasm continuous in filamentous multicellular cyanobacteria? *Trends Microbiol* 14: 439-443

Flores, E., Picossi, S., Valladares, A. & Herrero, A. (2018). Transcriptional regulation of development in heterocyst-forming cyanobacteria. *Biochim Biophys Acta Gene Regul Mech*

Forchhammer, K. (2004). Global carbon/nitrogen control by PII signal transduction in cyanobacteria: from signals to targets. *Fems Microbiology Reviews* 28: 319-333

Forchhammer, K. & Lüddecke, J. (2016). Sensory properties of the PII signalling protein family. *FEBS J* 283: 425-437

Forchhammer, K. & Watzer, B. (2016). Closing a gap in cyanophycin metabolism. *Microbiology* 162: 727-729

Fredriksson, C. & Bergman, B. (1997). Ultrastructural characterisation of cells specialised for nitrogen fixation in a non-heterocystous cyanobacterium,*Trichodesmium* spp. *Protoplasma* 197: 76-85

Frey, K. M., Oppermann-Sanio, F. B., Schmidt, H. & Steinbüchel, A. (2002). Technical-scale production of cyanophycin with recombinant strains of *Escherichia coli*. *Appl Environ Microbiol* 68: 3377-3384

Frommeyer, M., Wiefel, L. & Steinbüchel, A. (2014). Features of the biotechnologically relevant polyamide family "cyanophycins" and their biosynthesis in prokaryotes and eukaryotes. *Crit Rev Biotechnol*: 1-12

Füser, G. & Steinbüchel, A. (2007). Analysis of genome sequences for genes of cyanophycin metabolism: Identifying putative cyanophycin metabolizing prokaryotes. *Macromol Biosci* 7: 278-296

Gallon, J. R. (1981). The oxygen sensitivity of nitrogenase: a problem for biochemists and micro-organisms. *Trends Biochem Sci* 6: 19-23

Gallon, J. R. (1992). Reconciling the incompatible: N_2 fixation and O_2. *New Phytol* 122: 571-609

Gan, F., Zhang, S., Rockwell, N. C., Martin, S. S., Lagarias, J. C. & Bryant, D. A. (2014). Extensive remodeling of a cyanobacterial photosynthetic apparatus in far-red light. *Science* 345: 1312-1317

Golden, J. W., Robinson, S. J. & Haselkorn, R. (1985). Rearrangement of nitrogen fixation genes during heterocyst differentiation in the cyanobacterium *Anabaena*. *Nature* 314: 419-423

Golden, J. W. & Yoon, H. S. (1998). Heterocyst formation in *Anabaena*. *Curr Opin Microbiol* 1: 623-629

Gomes, F. M., Ramos, I. B., Wendt, C., Girard-Dias, W., De Souza, W., Machado, E. A. & Miranda, K. (2013). New insights into the in situ microscopic visualization and quantification of inorganic polyphosphate stores by 4',6-diamidino-2-phenylindole (DAPI)-staining. *Eur J Histochem* 57: 34

Gray, M. J., Wholey, W., Wagner, N. O., Cremers, C. M., Müller-Schickert, A., Hock, N. T., Krieger, A. G., Smith, E. M., Bender, R. A., Bardwell, J. C. A., Jakob, U. (2014). Polyphosphate is a primordial Chaperone. *Mol Cell* 53: 689-699

Gray, M. J. & Jakob, U. (2015). Oxidative stress protection by polyphosphate--new roles for an old player. *Curr Opin Microbiol* 24: 1-6

Greenberg, D. M. & Ichihara, A. (1957). Further studies on the pathway of serine formation from carbohydrate. *J Biol Chem* 224: 331-340

Grigorieva, G. & Shestakov, S. (1982). Transformation in the cyanobacterium *Synechocystis* sp. 6803. *FEMS Microbiol Lett* 13: 367-370

Hagemann, M., Fernie, A. R., Espie, G. S., Kern, R., Eisenhut, M., Reumann, S., Bauwe, H. & Weber, A. P. (2013). Evolution of the biochemistry of the photorespiratory C2 cycle. *Plant Biol (Stuttg)* 15: 639-647

Harold, F. M. (1966). Inorganic polyphosphates in biology: structure, metabolism, and function. *Bacteriol Rev* 30: 772-794

Hejazi, M., Piotukh, K., Mattow, J., Deutzmann, R., Volkmer-Engert, R., Lockau, W. (2002). Isoaspartyl dipeptidase activity of plant-typ asparaginases. *Biochem J* 364: 129-136

Herrero, A. & Burnat, M. (2014). Cyanophycin: a cellular nitrogen reserve material. *The Cell Biology of Cyanobacteria*. *Caister Academic Press* 308. E. Flores & A. Herrero. U.K.

Herrero, A., Muro-Pastor, A. M. & Flores, E. (2001). Nitrogen control in cyanobacteria. *J Bacteriol* 183: 411-425

Hill, S., Kennedy, C., Kavanagh, E., Goldberg, R. B. & Hanau, R. (1981). Nitrogen-fixation gene (Nifl) involved in oxygen regulation of nitrogenase synthesis in *K. pneumoniae*. *Nature* 290: 424-426

Ho, C.-L., Noji, M., Saito, M., Yamazaki, M. & Saito, K. (1998). Molecular characterization of plastidic phosphoserine aminotransferase in serine biosynthesis from *Arabidopsis*. *Plant J* 16: 443-452

Ho, C. L., Noji, M., Saito, M. & Saito, K. (1999). Regulation of serine biosynthesis in *Arabidopsis*. Crucial role of plastidic 3-phosphoglycerate dehydrogenase in non-photosynthetic tissues. *J Biol Chem* 274: 397-402

Ho, C. L. & Saito, K. (2001). Molecular biology of the plastidic phosphorylated serine biosynthetic pathway in *Arabidopsis thaliana*. *Amino Acids* 20: 243-259

Hsieh, P. C., Kowalczyk, T. H. & Phillips, N. F. (1996a). Kinetic mechanisms of polyphosphate glucokinase from *Mycobacterium tuberculosis*. *Biochemistry* 35: 9772-9781

Hsieh, P. C., Shenoy, B. C., Samols, D. & Phillips, N. F. (1996b). Cloning, expression, and characterization of polyphosphate glucokinase from *Mycobacterium tuberculosis*. *J Biol Chem* 271: 4909-4915

Huege, J., Goetze, J., Schwarz, D., Bauwe, H., Hagemann, M. & Kopka, J. (2011). Modulation of the major paths of carbon in photorespiratory mutants of *Synechocystis*. *PLoS One* 6: e16278

Husic, D. W. & Tolbert, N. E. (1987). Inhibition of glycolate and D-lactate metabolism in a *Chlamydomonas reinhardtii* mutant deficient in mitochondrial respiration. *Proc Natl Acad Sci U S A* 84: 1555-1559

Imriskova, I., Arreguin-Espinosa, R., Guzman, S., Rodriguez-Sanoja, R., Langley, E. & Sanchez, S. (2005). Biochemical characterization of the glucose kinase from *Streptomyces coelicolor* compared to *Streptomyces peucetius var. caesius*. *Res Microbiol* 156: 361-366

Kanehisa, M. & Goto, S. (2000). KEGG: Kyoto Encyclopedia of Genes and Genomes. *Nucleic Acids Research* 28: 27-30

Kaneko, T., Nakamura, Y., Wolk, C. P., Kuritz, T., Sasamoto, S., Watanabe, A., Iriguchi, M., Ishikawa, A., Kawashima, K., Kimura, T., Kishida, Y., Kohara, M., Matsumoto, M., Matsuno, A., Muraki, A., Nakazaki, N., Shimpo, S., Sugimoto, M., Takazawa, M., Yamada, M., Yasuda, M. & Tabata, S. (2001). Complete genomic sequence of the filamentous nitrogen-fixing cyanobacterium *Anabaena* sp. strain PCC 7120. *DNA Res* 8: 205-213; 227-253

Kaneko, Y., Danev, R., Nagayama, K. & Nakamoto, H. (2006). Intact carboxysomes in a cyanobacterial cell visualized by hilbert differential contrast transmission electron microscopy. *J Bacteriol* 188: 805-808

Kerfeld, C. A. & Melnicki, M. R. (2016). Assembly, function and evolution of cyanobacterial carboxysomes. *Curr Opin Plant Biol* 31: 66-75

Kneip, C., Lockhart, P., Voss, C. & Maier, U. G. (2007). Nitrogen fixation in eukaryotes-new models for symbiosis. *BMC Evol Biol* 7: 55

Knoop, H., Zilliges, Y., Lockau, W. & Steuer, R. (2010). The metabolic network of *Synechocystis* sp. PCC 6803: systemic properties of autotrophic growth. *Plant Physiol* 154: 410-422

Koide, M., Miyanaga, A., Kudo, F. & Eguchi, T. (2013). Characterization of polyphosphate glucokinase SCO5059 from *Streptomyces coelicolor* A3(2). *Biosci Biotechnol Biochem* 77: 2322-2324

Kolman, M. A., Nishi, C. N., Perez-Cenci, M. & Salerno, G. L. (2015). Sucrose in cyanobacteria: from a salt-response molecule to play a key role in nitrogen fixation. *Life* 5: 102-126

Kornberg, A. (1995). Inorganic polyphosphate - toward making a forgotten polymer unforgettable. *Journal of Bacteriology* 177: 491-496

Kornberg, A., Kornberg, S. R. & Simms, E. S. (1956). Metaphosphate synthesis by an enzyme from *Escherichia coli*. *Biochim Biophys Acta* 20: 215-227

Kornberg, A., Rao, N. N. & Ault-Riche, D. (1999). Inorganic polyphosphate: a molecule of many functions. *Annu Rev Biochem* 68: 89-125

Krehenbrink, M., Oppermann-Sanio, F.-B. & Steinbüchel, A. (2002). Evaluation of non-cyanobacterial genome sequences for occurrence of genes encoding proteins homologous to cyanophycin synthetase and cloning of an active cyanophycin synthetase from *Acinetobacter* sp. strain DSM 587. *Arch Microbiol* 177: 371-380

Kulaev, I. & Kulakovskaya, T. (2000). Polyphosphate and phosphate pump. *Annu Rev Microbiol* 54: 709-734

Kumar, K., Mella-Herrera, R. A. & Golden, J. W. (2010). Cyanobacterial heterocysts. *Cold Spring Harb Perspect Biol* 2: 1-15

Larkum, A. W. & Kühl, M. (2005). Chlorophyll d: the puzzle resolved. *Trends Plant Sci* 10: 355-357

Li, J. H., Laurent, S., Konde, V., Bedu, S. & Zhang, C. C. (2003). An increase in the level of 2-oxoglutarate promotes heterocyst development in the cyanobacterium *Anabaena* sp. strain PCC 7120. *Microbiology* 149: 3257-3263

Liao, H., Myung, S. & Zhang, Y. H. (2012). One-step purification and immobilization of thermophilic polyphosphate glucokinase from *Thermobifida fusca* YX: glucose-6-phosphate generation without ATP. *Appl Microbiol Biotechnol* 93: 1109-1117

Lichko, L. P., Kulakovskaya, T. V. & Kulaev, I. S. (2010). Properties of partially purified endopolyphosphatase of the yeast *Saccharomyces cerevisiae*. *Biochemistry (Mosc)* 75: 1404-1407

Lindner, S. N., Knebel, S., Pallerla, S. R., Schoberth, S. M. & Wendisch, V. F. (2010). Cg2091 encodes a polyphosphate/ATP-dependent glucokinase of *Corynebacterium glutamicum*. *Appl Microbiol Biotechnol* 87: 703-713

Loughlin, P., Lin, Y. & Chen, M. (2013). Chlorophyll d and *Acaryochloris marina*: current status. *Photosynth Res*

Lüddecke, J. & Forchhammer, K. (2015). Energy sensing versus 2-oxoglutarate dependent ATPase switch in the control of *Synechococcus* PII interaction with its targets NAGK and PipX. *PLoS One* 10: e0137114

Lüddecke, J., Francois, L., Spat, P., Watzer, B., Chilczuk, T., Poschet, G., Hell, R., Radlwimmer, B. & Forchhammer, K. (2017). PII protein-derived FRET sensors for quantification and live-cell imaging of 2-Oxoglutarate. *Sci Rep* 7: 1437

Luque, I., Flores, E. & Herrero, A. (1994). Molecular mechanism for the operation of nitrogen control in cyanobacteria. *EMBO J* 13: 5794

Luque, I. & Forchhammer, K. (2008). Nitrogen Assimilation and C/N Balance Sensing. *The Cyanobacteria: Molecular Biology, Genomics and Evolution Caister Academic Press* 335-382. A. Herrero & E. Flores. Norfolk, U.K.

Magnuson, A. & Cardona, T. (2016). Thylakoid membrane function in heterocysts. *Biochim Biophys Acta* 1857: 309-319

Maheswaran, M., Ziegler, K., Lockau, W., Hagemann, M. & Forchhammer, K. (2006). PII-regulated arginine synthesis controls accumulation of cyanophycin in *Synechocystis* sp. strain PCC 6803. *J Bacteriol* 188: 2730-2734

Maldener, I. & Muro-Pastor (2010). Cyanobacterial Heterocysts. *eLS*. *John Wiley & Sons, Ltd*.

Maldener, I., Summers, M. L. & Sukenik, A. (2014). Cellular differentiation in filamentous cyanobacteria. *The Cell Biology of Cyanobacteria*. *Caister Academic Press* 263-291. E. Flores & A. Herrero. Norfolk, UK.

Mariscal, V., Herrero, A. & Flores, E. (2007). Continuous periplasm in a filamentous, heterocyst-forming cyanobacterium. *Mol Microbiol* 65: 1139-1145

Markowitz, V. M., Chen, I. M., Palaniappan, K., Chu, K., Szeto, E., Grechkin, Y., Ratner, A., Jacob, B., Huang, J., Williams, P., Huntemann, M., Anderson, I., Mavromatis, K., Ivanova, N. N. & Kyrpides, N. C. (2012). IMG: the Integrated Microbial Genomes database and comparative analysis system. *Nucleic Acids Res* 40: D115-122

Miller, S. R. & Castenholz, R. W. (2000). Evolution of thermotolerance in hot spring cyanobacteria of the genus *Synechococcus*. *Appl Environ Microbiol* 66: 4222-4229

Millineaux, P. M., Gallon, J. R. & Chaplin, A. E. (1981). Acetylene reduction (nitrogen fixation) by cyanobacteria grown under alternating light-dark cycles. *FEMS Microbiol Lett* 10: 245-247

Mitschke, J., Vioque, A., Haas, F., Hess, W. R. & Muro-Pastor, A. M. (2011). Dynamics of transcriptional start site selection during nitrogen stress-induced cell differentiation in *Anabaena* sp. PCC7120. *Proc Natl Acad Sci U S A* 108: 20130-20135

Mitsui, A. (1986). Strategy by which nitrogen-fixing unicellular cyanobacteria grow photoautotrophically. *Nature* 323: 720-722

Mukai, T., Kawai, S., Matsukawa, H., Matuo, Y. & Murata, K. (2003). Characterization and molecular cloning of a novel enzyme, inorganic polyphosphate/ATP-glucomannokinase, of *Arthrobacter* sp. strain KM. *Appl Environ Microbiol* 69: 3849-3857

Mullineaux, C. W. & Emlyn-Jones, D. (2005). State transitions: an example of acclimation to low-light stress. *J Exp Bot* 56: 389-393

Muñoz-Bertomeu, J., Anoman, A. D., Flores-Tornero, M., Toujani, W., Rosa-Téllez, S., Fernie, A. R., Roje, S., Segura, J. & Ros, R. (2013). The essential role of the phosphorylated pathway of serine biosynthesis in Arabidopsis. *Plant Signal Behav* 8: e27104

Muro-Pastor, M. I., Reyes, J. C. & Florencio, F. J. (2001). Cyanobacteria perceive nitrogen status by sensing intracellular 2-oxoglutarate levels. *J Biol Chem* 276: 38320-38328

Nakao, M., Okamoto, S., Kohara, M., Fujishiro, T., Fujisawa, T., Sato, S., Tabata, S., Kaneko, T. & Nakamura, Y. (2010). CyanoBase: the cyanobacteria genome database update 2010. *Nucleic Acids Res* 38: D379-381

Neumann, K., Stephan, D. P., Ziegler, K., Hühns, M., Broer, I., Lockau, W. & Pistorius, E. K. (2005). Production of cyanophycin, a suitable source for the biodegradable polymer polyaspartate, in transgenic plants. *Plant Biotechnol J* 3: 249-258

Nicolaisen, K., Mariscal, V., Bredemeier, R., Pernil, R., Moslavac, S., Lopez-Igual, R., Maldener, I., Herrero, A., Schleiff, E. & Flores, E. (2009). The outer membrane of a heterocyst-forming cyanobacterium is a permeability barrier for uptake of metabolites that are exchanged between cells. *Mol Microbiol* 74: 58-70

Norman, E. G. & Colman, B. (1991). Purification and Characterization of Phosphoglycolate Phosphatase from the Cyanobacterium *Coccochloris peniocystis*. *Plant Physiol* 95: 693-698

Nürnberg, D. J., Mariscal, V., Bornikoel, J., Nieves-Morion, M., Krauss, N., Herrero, A., Maldener, I., Flores, E. & Mullineaux, C. W. (2015). Intercellular diffusion of a fluorescent sucrose analog via the septal junctions in a filamentous cyanobacterium. *MBio* 6: e02109

Obst, M. & Steinbüchel, A. (2006). Cyanophycin—an ideal bacterial nitrogen storage material with unique chemical properties *Inclusions in Prokaryotes.* 167-193. J. Shively. Springer Berlin / Heidelberg.

Olson, J. M. & Blankenship, R. E. (2004). Thinking about the evolution of photosynthesis. *Photosynth Res* 80: 373-386

Ouzounis, C. & Sander, C. (1993). Homology of the NifS family of proteins to a new class of pyridoxal phosphate-dependent enzymes. *FEBS Lett* 322: 159-164

Pade, N., Erdmann, S., Enke, H., Dethloff, F., Duhring, U., Georg, J., Wambutt, J., Kopka, J., Hess, W. R., Zimmermann, R., Kramer, D. & Hagemann, M. (2016). Insights into isoprene production using the cyanobacterium *Synechocystis* sp. PCC 6803. *Biotechnol Biofuels* 9: 89

Park, J.-J., Lechno-Yossef, S., Wolk, C. & Vieille, C. (2013). Cell-specific gene expression in *Anabaena variabilis* grown phototrophically, mixotrophically, and heterotrophically. *BMC Genomics* 14: 759

Pepin, C. A. & Wood, H. G. (1986). Polyphosphate glucokinase from *Propionibacterium shermanii.* Kinetics and demonstration that the mechanism involves both processive and nonprocessive type reactions. *J Biol Chem* 261: 4476-4480

Phillips, N. F., Horn, P. J. & Wood, H. G. (1993). The polyphosphate- and ATP-dependent glucokinase from *Propionibacterium shermanii:* both activities are catalyzed by the same protein. *Arch Biochem Biophys* 300: 309-319

Phillips, N. F., Hsieh, P. C. & Kowalczyk, T. H. (1999). Polyphosphate glucokinase. *Prog Mol Subcell Biol* 23: 101-125

Picossi, S., Valladares, A., Flores, E. & Herrero, A. (2004). Nitrogen-regulated genes for the metabolism of cyanophycin, a bacterial nitrogen reserve polymer: expression and mutational analysis of two cyanophycin synthetase and cyanophycinase gene clusters in heterocyst-forming cyanobacterium *Anabaena* sp. PCC 7120. *J Biol Chem* 279: 11582-11592

Rao, N. N., Gomez-Garcia, M. R. & Kornberg, A. (2009). Inorganic polyphosphate: essential for growth and survival. *Annu Rev Biochem* 78: 605-647

Resnick, S. M. & Zehnder, A. J. (2000). *In vitro* ATP regeneration from polyphosphate and AMP by polyphosphate:AMP phosphotransferase and adenylate kinase from *Acinetobacter johnsonii* 210A. *Appl Environ Microbiol* 66: 2045-2051

Richter, R., Hejazi, M., Kraft, R., Ziegler, K. & Lockau, W. (1999). Cyanophycinase, a peptidase degrading the cyanobacterial reserve material multi-L-arginyl-poly-L-aspartic acid (cyanophycin). *Eur J Biochem* 263: 163-169

Rippka, R., Deruelles, J., Waterbury, J. B., Herdman, M. & Stanier, R. Y. (1979). Generic assignments, strain histories and properties of pure cultures of cyanobacteria. *Journal of General Microbiology* 111: 1-61

Rippka, R. & Waterbury, J. B. (1977). Synthesis of nitrogenase by non-heterocystous cyanobacteria. *FEMS Microbiology Letters* 2: 83-86

Robertson, B. R., Tezuka, N. & Watanabe, M. M. (2001). Phylogenetic analyses of *Synechococcus* strains (cyanobacteria) using sequences of 16S rDNA and part of the phycocyanin operon reveal multiple evolutionary lines and reflect phycobilin content. *Int J Syst Evol Microbiol* 51: 861-871

Ros, R., Muñoz-Bertomeu, J. & Krueger, S. (2014). Serine in plants: biosynthesis, metabolism, and functions. *Trends Plant Sci* 19: 564-569

Schmidt, K., Schmidtke, J., Mast, Y., Waldvogel, E., Wohlleben, W., Klemke, F., Lockau, W., Hausmann, T., Hühns, M. & Broer, I. (2017). Comparative statistical component analysis of transgenic, cyanophycin-producing potatoes in greenhouse and field trials. *Transgenic Res* 26: 529-539

Sethuraman, A., Rao, N. N. & Kornberg, A. (2001). The endopolyphosphatase gene: essential in *Saccharomyces cerevisiae*. *Proc Natl Acad Sci U S A* 98: 8542-8547

Sherman, D. M., Tucker, D. & Sherman, L. A. (2000). Heterocyst development and localization of cyanophycin in N_2-fixing cultures of *Anabaena* sp. PCC 7120 (Cyanobacteria). *J Phycol* 36: 932-941

Shestakov, S. V. & Khyen, N. T. (1970). Evidence for genetic transformation in blue-green alga *Anacystis nidulans*. *Mol Gen Genet* 107: 372-375

Shih, P. M., Wu, D., Latifi, A., Axen, S. D., Fewer, D. P., Talla, E., Calteau, A., Cai, F., Tandeau de Marsac, N., Rippka, R., Herdman, M., Sivonen, K., Coursin, T., Laurent, T., Goodwin, L., Nolan, M., Davenport, K. W., Han, C. S., Rubin, E. M., Eisen, J. A., Woyke, T., Gugger, M. & Kerfeld, C. A. (2013). Improving the coverage of the cyanobacterial phylum using diversity-driven genome sequencing. *Proc Natl Acad Sci U S A* 110: 1053-1058

Simon, R. D. (1971). Cyanophycin granules from the blue-green alga *Anabaena cylindrica*: A reserve material consisting of copolymers of aspartic acid and arginine. *Proc Natl Acad Sci U S A* 68: 265-267

Simon, R. D. (1973). Measurement of the cyanophycin granule polypeptide contained in the blue-green alga *Anabaena cylindrica*. *J Bacteriol* 114: 1213-1216

Simon, R. D. & Weathers, P. (1976). Determination of the structure of the novel polypeptide containing aspartic acid and arginine which is found in cyanobacteria. *Biochim Biophys Acta - Protein Structure* 420: 165-176

Somerville, C. R. (2001). An early *Arabidopsis* demonstration. Resolving a few issues concerning photorespiration. *Plant Physiol* 125: 20-24

Soto, D. F., Recalde, A., Orell, A., Albers, S. V., Paradela, A., Navarro, C. A. & Jerez, C. A. (2018). Global effect of the lack of inorganic polyphosphate in the extremophilic archaeon *Sulfolobus solfataricus*: A proteomic approach. *J Proteomics*

Stal, L. J. & Heyer, H. (1987). Dark anaerobic nitrogen fixation (acetylene reduction) in the cyanobacterium *Oscillatoria* sp. *FEMS Microbiol Lett* 45: 227-232

Steinle, A., Bergander, K. & Steinbüchel, A. (2009). Metabolic engineering of *Saccharomyces cerevisiae* for production of novel cyanophycins with an extended range of constituent amino acids. *Appl Environ Microbiol* 75: 3437-3446

Summers, M. L., Wallis, J. G., Campbell, E. L. & Meeks, J. C. (1995). Genetic evidence of a major role for glucose-6-phosphate dehydrogenase in nitrogen fixation and dark growth of the cyanobacterium *Nostoc* sp. strain ATCC 29133. *J Bacteriol* 177: 6184-6194

Szymona, M. & Ostrowski, W. (1964). Inorganic polyphosphate glucokinase of *Mycobacterium phlei*. *Biochim Biophys Acta* 85: 283-295

Szymona, M. & Widomski, J. (1974). Kinetic study on inorganic polyphosphate glucokinase from *Mycobacterium tuberculosis* H37ra. *Physiological Chemistry and Physics* 6: 393-404

Tanaka, S., Lee, S. O., Hamaoka, K., Kato, J., Takiguchi, N., Nakamura, K., Ohtake, H. & Kuroda, A. (2003). Strictly polyphosphate-dependent glucokinase in a polyphosphate-accumulating bacterium, *Microlunatus phosphovorus*. *J Bacteriol* 185: 5654-5656

Thomas, J., Meeks, J. C., Wolk, C. P., Shaffer, P. W. & Austin, S. M. (1977). Formation of glutamine from [^{13}N]ammonia, [^{13}N]dinitrogen, and [^{14}C]glutamate by heterocysts isolated from *Anabaena cylindrica*. *J Bacteriol* 129: 1545-1555

Timm, S., Florian, A., Wittmiss, M., Jahnke, K., Hagemann, M., Fernie, A. R. & Bauwe, H. (2013). Serine acts as a metabolic signal for the transcriptional control of photorespiration-related genes in *Arabidopsis*. *Plant Physiol* 162: 379-389

Toepel, J., Welsh, E., Summerfield, T. C., Pakrasi, H. B. & Sherman, L. A. (2008). Differential transcriptional analysis of the cyanobacterium *Cyanothece* sp. strain ATCC 51142 during light-dark and continuous-light growth. *J Bacteriol* 190: 3904-3913

Tolbert, N. E. (1997). The C2 oxidative photosynthetic carbon cycle. *Annu Rev Plant Physiol Plant Mol Biol* 48: 1-25

Tumlirsch, T., Sznajder, A. & Jendrossek, D. (2015). Formation of polyphosphate by polyphosphate kinases and its relationship to poly(3-hydroxybutyrate) accumulation in *Ralstonia eutropha* strain H16. *Appl Environ Microbiol* 81: 8277-8293

Tzeng, C. M. & Kornberg, A. (1998). Polyphosphate kinase is highly conserved in many bacterial pathogens. *Mol Microbiol* 29: 381-382

Umbarger, H. E., Umbarger, M. A. & Siu, P. M. (1963). Biosynthesis of serine in *Escherichia coli* and *Salmonella typhimurium*. *J Bacteriol* 85: 1431-1439

Vaillancourt, S., Beuchemin-Newhouse, N. & Cedergren, R. J. (1978). Polyphosphate-deficient mutants of *Anacystis nidulans*. *Can J Microbiol* 24: 112-116

Vargas, W. A., Nishi, C. N., Giarrocco, L. E. & Salerno, G. L. (2011). Differential roles of alkaline/neutral invertases in *Nostoc* sp. PCC 7120: Inv-B isoform is essential for diazotrophic growth. *Planta* 233: 153-162

Vazquez-Bermudez, M. F., Herrero, A. & Flores, E. (2002). 2-Oxoglutarate increases the binding affinity of the NtcA (nitrogen control) transcription factor for the *Synechococcus* glnA promoter. *FEBS Lett* 512: 71-74

Walsby, A. E. (2007). Cyanobacterial heterocysts: terminal pores proposed as sites of gas exchange. *Trends Microbiol* 15: 340-349

Walton, N. J. & Woolhouse, H. W. (1986). Enzymes of serine and glycine metabolism in leaves and nonphotosynthetic tissues of *Pisum-sativum-L*. *Planta* 167: 119-128

Watzer, B., Engelbrecht, A., Hauf, W., Stahl, M., Maldener, I. & Forchhammer, K. (2015). Metabolic pathway engineering using the central signal processor PII. *Microb Cell Fact* 14: 192-204

Watzer, B. & Forchhammer, K. (2018). Cyanophycin synthesis optimizes nitrogen utilization in the unicellular cyanobacterium *Synechocystis* sp. PCC 6803. *Appl Environ Microbiol*

Wilk, L., Strauss, M., Rudolf, M., Nicolaisen, K., Flores, E., Kuhlbrandt, W. & Schleiff, E. (2011). Outer membrane continuity and septosome formation between vegetative cells in the filaments of *Anabaena* sp. PCC 7120. *Cell Microbiol* 13: 1744-1754

Wolk, C. P. (1968). Movement of carbon from vegetative cells to heterocysts in *Anabaena cylindrica*. *J Bacteriol* 96: 2138-2143

Wolk, C. P. (1996). Heterocyst formation. *Annu Rev Genet* 30: 59-78

Wolk, C. P., Austin, S. M., Bortins, J. & Galonsky, A. (1974). Autoradiographic localization of ^{13}N after fixation of ^{13}N-labeled nitrogen gas by a heterocyst-forming blue-green alga. *J Cell Biol* 61: 440-453

Wolk, C. P., Ernst, A. & Elhai, J. (1994). Heterocyst metabolism and development. *The Molecular biology of cyanobacteria.* . *Kluwer Academic Publishers* 769-823. D. A. Bryant. Dordrecht, The Netherlands.

Yamagata, Y., Watanabe, H., Saitoh, M. & Namba, T. (1991). Volcanic production of polyphosphates and its relevance to prebiotic evolution. *Nature* 352: 516-519

Young, J. D., Shastri, A. A., Stephanopoulos, G. & Morgan, J. A. (2011). Mapping photoautotrophic metabolism with isotopically nonstationary $^{(13)}C$ flux analysis. *Metab Eng* 13: 656-665

Yuan, Z., Pratt, S. & Batstone, D. J. (2012). Phosphorus recovery from wastewater through microbial processes. *Curr Opin Biotechnol* 23: 878-883

Zeth, K., Fokina, O. & Forchhammer, K. (2014). Structural basis and target-specific modulation of ADP sensing by the *Synechococcus elongatus* PII signaling protein. *J Biol Chem* 289: 8960-8972

Zhang, H., Ishige, K. & Kornberg, A. (2002). A polyphosphate kinase (PPK2) widely conserved in bacteria. *Proc Natl Acad Sci U S A* 99: 16678-16683

Zhou, W., Huang, R., Zhu, Z. & Zhang, Y. P. J. (2018). Coevolution of both thermostability and activity of polyphosphate glucokinase from *Thermobifida fusca* YX. *Appl Environ Microbiol*

Ziegler, K., Deutzmann, R. & Lockau, W. (2002). Cyanophycin synthetase-like enzymes of non-cyanobacterial eubacteria: characterization of a polymer produced by a recombinant synthetase of *Desulfitobacterium hafniense*. *Z Naturforsch C* 57: 522-529

Ziegler, K., Diener, A., Herpin, C., Richter, R., Deutzmann, R. & Lockau, W. (1998). Molecular characterization of cyanophycin synthetase, the enzyme catalyzing the biosynthesis of the cyanobacterial reserve material multi-L-arginyl-poly-L-aspartate (cyanophycin). *Eur J Biochem* 254: 154-159

Ziegler, K., Stephan, D. P., Pistorius, E. K., Ruppel, H. G. & Lockau, W. (2001). A mutant of the cyanobacterium *Anabaena variabilis* ATCC 29413 lacking cyanophycin synthetase: growth properties and ultrastructural aspects. *FEMS Microbiol Lett* 196: 13-18

5 Danksagung

Die vorliegende Arbeit entstand mit Unterstützung der nachgenannten Personen.

Bedanken möchte ich mich besonders bei Prof. Dr. Wolfgang Lockau für die Bereitstellung der interessanten Forschungsthemen, für das in mich gesetzte Vertrauen und für seine allumfassende freundliche Unterstützung meiner Arbeit. Dank gilt der gesamten Arbeitsgruppe von Prof. Dr. Lockau an der Humboldt-Universität zu Berlin, die mir stets durch zahlreiche Diskussionen, hilfreiche Hinweise und tatkräftige Unterstützung zur Seite gestanden hat. Danke auch für die angenehme und aufgeschlossene Arbeitsatmosphäre! Ein besonderer Dank gilt hier Dr. Karl Ziegler und Dr. Thomas Volkmer, die mich bei der Planung und Auswertung meiner Daten stets sachkundig und geduldig unterstützten. Sabine Nicklisch und Dr. Gabriele Beyer waren mir eine sehr wertvolle und fachkundige Hilfe im Labor, besonders bei der Erfassung der kinetischen Daten sowie bei der Proteinisolation und Enzymanalyse. Zudem danke ich Dr. Dennis Nürnberg für die Erstellung der Verteilungsanalysen und für die anregenden Diskussionen zu den Themen CphA2 und PolyP-Glukokinase.

Meinen Kooperationspartnern Prof. Dr. Martin Hagemann (Universität Rostock), Dr. Thomas Korte (Humboldt-Universität zu Berlin) und Dr. Uwe Kahmann (Universität Bielefeld) möchte ich zudem für die erfolgreiche und sehr effiziente Zusammenarbeit danken. Dr. Iris Maldener und Prof. Dr. Karl Forchhammer (Universität Tübingen) bin ich sehr verbunden, dass sie mir bei der Zusammenfassung meiner Arbeit fachkundig und hilfsbereit zur Seite standen.

Zuletzt möchte ich meiner Familie danken, die mich in jeder Hinsicht und uneingeschränkt unterstützt hat.

Diese Arbeit widme ich meiner Großmutter Gertrud und meinen Kindern Anna, Jonas und Marlene.

6 Anhang mit Publikationen

Microbiology (2016), **162**, 526–536 DOI 10.1099/mic.0.000241

CphA2 is a novel type of cyanophycin synthetase in N_2-fixing cyanobacteria

Friederike Klemke,[1]† Dennis J. Nürnberg,[1,2]† Karl Ziegler,[1]† Gabriele Beyer,[1] Uwe Kahmann,[3] Wolfgang Lockau[1] and Thomas Volkmer[1]

Correspondence
Thomas Volkmer
thomas.volkmer@rub.de

[1]Institut für Biologie, Humboldt-Universität zu Berlin, Chausseestraße 117, 10115 Berlin, Germany
[2]Department of Life Sciences, Imperial College London, London SW7 2AZ, UK
[3]Zentrum für Ultrastrukturelle Diagnostik im IIT, Universitätsstraße 25, 33615 Bielefeld, Germany

Received 21 July 2015
Revised 8 January 2016
Accepted 12 January 2016

Most cyanobacteria use a single type of cyanophycin synthetase, CphA1, to synthesize the nitrogen-rich polymer cyanophycin. The genomes of many N_2-fixing cyanobacteria contain an additional gene that encodes a second type of cyanophycin synthetase, CphA2. The potential function of this enzyme has been debated due to its reduced size and the lack of one of the two ATP-binding sites that are present in CphA1. Here, we analysed CphA2 from *Anabaena variabilis* ATCC 29413 and *Cyanothece* sp. PCC 7425. We found that CphA2 polymerized the dipeptide β-aspartyl-arginine to form cyanophycin. Thus, CphA2 represents a novel type of cyanophycin synthetase. A *cphA2* disruption mutant of *A. variabilis* was generated. Growth of this mutant was impaired under high-light conditions and nitrogen deprivation, suggesting that CphA2 plays an important role in nitrogen metabolism under N_2-fixing conditions. Electron micrographs revealed that the mutant had fewer cyanophycin granules, but no alteration in the distribution of granules in its cells was observed. Localization of CphA2 by immunogold electron microscopy demonstrated that the enzyme is attached to cyanophycin granules. Expression of CphA1 and CphA2 was examined in *Anabaena* WT and *cphA* mutant cells. Whilst the CphA1 level increased upon nitrogen deprivation, the CphA2 level remained nearly constant.

INTRODUCTION

Cyanophycin [multi-(L-arginyl-poly-L-aspartic acid) (Simon, 1971; Simon & Weathers, 1976), also referred to as cyanophycin granule polypeptide, is a branched, nitrogen-rich polymer found in most cyanobacteria and in some heterotrophic bacteria (Füser & Steinbüchel, 2007). The compound consists of a poly-α-aspartic acid backbone, with arginine residues linked to the β-carboxyl groups of the aspartate units by isopeptide bonds (Simon & Weathers, 1976). Cyanophycin is thought to serve as a dynamic reservoir of nitrogen, carbon and energy in cyanobacteria (Carr, 1988), and has attracted biotechnological attention as a precursor molecule for polyaspartate – a completely biodegradable substitute for polyacrylate (Erickson *et al.*, 2001). The key enzyme in cyanophycin synthesis is cyanophycin synthetase CphA1 (Ziegler *et al.*, 1998). CphA1 synthesizes cyanophycin from its constituent amino acids, aspartate and arginine, in two consecutive, ATP-dependent reactions at its two predicted active sites (Berg, 2003; Berg *et al.*, 2000; Ziegler *et al.*, 1998). The N-terminal active site phosphorylates the α-carboxyl group at the C terminus of the poly-L-aspartate backbone, followed by substitution of the phosphoryl group with aspartic acid [cyanophycin : L-aspartate ligase (ADP-forming; EC 6.3.2.29)]. By the same mechanism, the C-terminal active site connects the β-carboxyl group of the C-terminal aspartic acid residue to the α-amino group of arginine, thereby forming an isopeptide bond [cyanophycin : L-arginine ligase (ADP-forming; EC 6.3.2.30)] (Berg, 2003; Berg *et al.*, 2000). In accordance with the proposed mechanism, two ATP per β-aspartyl-arginine, the formal building block of cyanophycin, are converted to ADP and phosphate (Aboulmagd *et al.*, 2001). Genes for CphA1 are present in the genomes of most cyanobacterial species and some heterotrophic bacteria (Füser & Steinbüchel, 2007). Activity for some of these proteins has been shown by heterologous expression in bacteria, yeasts and plants (Frommeyer *et al.*, 2016). In addition, some cyanobacteria possess a second gene named *cphA*2 (Picossi *et al.*, 2004). In a CphA2-lacking mutant strain of the filamentous, heterocyst-forming cyanobacterium

†These authors contributed equally to this paper.

Abbreviation: SEC, size exclusion chromatography.

Six supplementary figures and three supplementary tables are available with the online Supplementary Material.

000241 © 2016 The Authors *Printed in Great Britain*

Anabaena sp. PCC 7120, a lower cyanophycin content was observed than in the WT, suggesting a role of CphA2 in cyanophycin synthesis. However, *cphA2* encodes what appears to be a shortened version of CphA1. An alignment of the amino acid sequences of CphA1 and CphA2 from the closely related cyanobacterium *Anabaena variabilis* ATCC 29413 is shown in Fig. 1. CphA2 possesses a region with high sequence similarity to the N-terminal cyanophycin : L-aspartate ligase active site of CphA1 with the potential ATP-binding sites in the B- and J-loop (Berg *et al.*, 2000), but is missing the one in the P-loop of the C-terminal cyanophycin : L-arginine ligase site. The biochemical function of CphA2 has remained unknown. Here, we report on the catalytic properties of CphA2 from the N_2-fixing cyanobacteria *A. variabilis* and *Cyanothece* sp. PCC 7425. Our biochemical data show the functionality of CphA2 as a novel type of cyanophycin synthetase that polymerizes β-aspartyl-arginine to cyanophycin. Furthermore, the localization and physiological role of CphA2 in the context of N_2 fixation is discussed. A CphA2-lacking mutant of *A. variabilis* was found to have a reduced viability when deprived of combined nitrogen in high light.

METHODS

Recombinant DNA techniques. Standard methods (Sambrook *et al.*, 1989) or minor modifications thereof were used. DNA modification enzymes were purchased from New England Biolabs and Fermentas Thermo Scientific. Purification of plasmids, and isolation of DNA fragments after electrophoresis was performed with commercial kits (Macherey-Nagel).

Construction of *cphA2* expression vectors. Two different expression vectors were generated for the expression of *cphA2* (ava_0335) from *A. variabilis*: pETcphA2, a pET19b (Novagen) derivative containing a gene coding for a CphA2 fusion protein including an N-terminal His_{10}-tag (H_{10}-CphA2), and pGEXava_0335, a pGEX-6-P derivative (GE Healthcare) containing a gene coding for a fusion protein that consisted of an N-terminal GST-tag and CphA2 (GST-CphA2) linked by a PreScission protease recognition and cleavage site. Oligonucleotides used as primers to amplify the genes are listed in Table S1 (available in the online Supplementary Material).

A pET19b-based expression vector containing Cyan7425_4446 was constructed using primer pair D.1/D.2, providing a His_{10}-tagged CphA2 from *Cyanothece* sp. PCC 7425. The generated expression vectors were verified by restriction analyses and DNA sequencing.

Production and isolation of H_{10}-CphA2. An overnight culture of BL21(DE3)[pETcphA2] was used to inoculate lysogeny broth (LB) medium containing 100 μg ampicillin ml^{-1} and 1 % (w/v) glucose to a cell density corresponding to OD_{600} 0.05. The culture was grown for 3 h at 37 °C and 200 r.p.m. Cells were harvested by centrifugation (15 min; 3800 ***g***, 4 °C), transferred to fresh LB medium supplemented with 250 μg ampicillin ml^{-1} and incubated under vigorous shaking at 18 °C for 18 h. Cells were harvested by centrifugation (15 min; 3800 ***g***, 4 °C), resuspended in buffer A (50 mM Tris/HCl, pH 8.1, 300 mM NaCl, 50 mM KCl) supplemented with 10 mM imidazole and disrupted by sonication. Cell debris was removed by centrifugation (15 min; 20 000 ***g***) and the supernatant loaded onto a His-trap-column (Qiagen; 1 ml volume) equilibrated with buffer A. After washing with 30 matrix volumes of buffer A containing (i) 20 mM imidazole and (ii) 30 mM imidazole, bound proteins were eluted with 250 mM imidazole in buffer A. Buffer A was exchanged on PD-10 desalting columns (GE Healthcare Life Science) against 50 mM Tris/HCl, pH 8.1, 20 mM KCl and 1 mM DTT. The purity of the enzyme was checked by SDS-PAGE.

Preparation of untagged CphA2. An overnight culture of BL21[pGEXava_0335] was used to inoculate LB medium supplemented with 100 μg ampicillin ml^{-1} to an initial cell density of OD 0.05. The culture was grown in Erlenmeyer flasks at 37 °C under shaking at 200 r.p.m. After inducing expression with 1 mM IPTG at OD_{600} 0.6–0.8, the culture was grown at 18 °C for 18 h. Harvested cells were resuspended in 50 mM Tris/HCl buffer, pH 8.5 containing 300 mM NaCl and 50 mM KCl. This buffer was used for all subsequent purification steps. Cells were treated as described for the purification of H_{10}-CphA2. The GST-CphA2 fusion protein was enriched by affinity chromatography on glutathione agarose in a batch procedure. The supernatant was added to Protino glutathione agarose 4B (Macherey-Nagel) which was equilibrated with the same buffer, and the suspension was inverted at 10 r.p.m. for 30 min at ambient temperature. The sedimented matrix was washed with 30 matrix volumes of buffer and resuspended in 1 matrix volume of buffer. To elute CphA2, 200 U PreScission protease (GE Healthcare Life Science) was added per 1 ml matrix volume. The matrix was inverted for 14 h at 10 r.p.m., and the eluate was collected by centrifugation for 10–30 s at 4 °C and the lowest adjustment. The CphA2-containing supernatant was collected and the purity checked by SDS-PAGE.

Disruption of cphA2 in *A. variabilis*. The *cphA2* (ava_0335) gene was interrupted in *A. variabilis* by insertional mutagenesis. The gene was amplified in two steps. Primer sequences are given in Table S1. One PCR was performed with the primer pair C.1/C.2 and a second PCR with C.3/C.4. A *Xba*I restriction site was introduced in ava_0335. In a second step, the 5′ and 3′ parts of the gene were ligated by PCR using the PCR products as template and C.1/C.3 as primers. The resulting PCR product was cloned into vector pRL271 (Black *et al.*, 1993) via *Pst*I and *Spe*I sites (see Physiological role of CphA2). The kanamycin resistance cassette C.K3 from plasmid pRL448 (Elhai & Wolk, 1988a) was inserted into the generated *Xba*I site. *Escherichia coli* DH5α cells were transformed by the resulting pRL derivatives, and the transformants checked by PCR and restriction analysis. Two derivatives with resistance cassettes in opposite orientations were isolated, transferred to *A. variabilis* by conjugation according to published procedures (Elhai & Wolk, 1988b) and double recombinants identified by PCR analysis.

Preparation of β-aspartyl-arginine. Cyanophycin was synthesized by heterologous expression of *cphA1* from *A. variabilis* in *E. coli* and isolated from the cells as described by Ziegler *et al.*, (1998). Cyanophycin was resuspended in 50 mM Tris/HCl, pH 7.5 and enzymically depolymerized to β-aspartyl-arginine using cyanophycinase (CphB) from *Thermosynechococcus elongatus* BP-1 (Hejazi, 2002). After centrifugation at 10 000 ***g*** for 20 min, the enzyme was removed by passing the supernatant through a protein concentrator (Vivaspin 4, cut-off 5 kDa; Sartorius). The flow-through was concentrated by vacuum concentration centrifugation at 80 °C and β-aspartyl-arginine was purified by chromatography on P2 columns (Bio-Rad; 1 × 18 cm, 0.1 M acetic acid, flow rate 0.4 ml min^{-1}). Ninhydrin-positive fractions were pooled and concentrated at 80 °C as described earlier. The β-aspartyl-arginine was quantified as described by Hejazi *et al.* (2002). Purity of the substrate was checked by gel filtration on a Superdex Peptide 10/300 GL column (GE Healthcare) with 50 mM Tris/HCl, pH 8.0 as running buffer. The result was verified by MALDI-TOF MS analysis (Oliver Brödel, Technische Hochschule Wildau, Wildau, Germany).

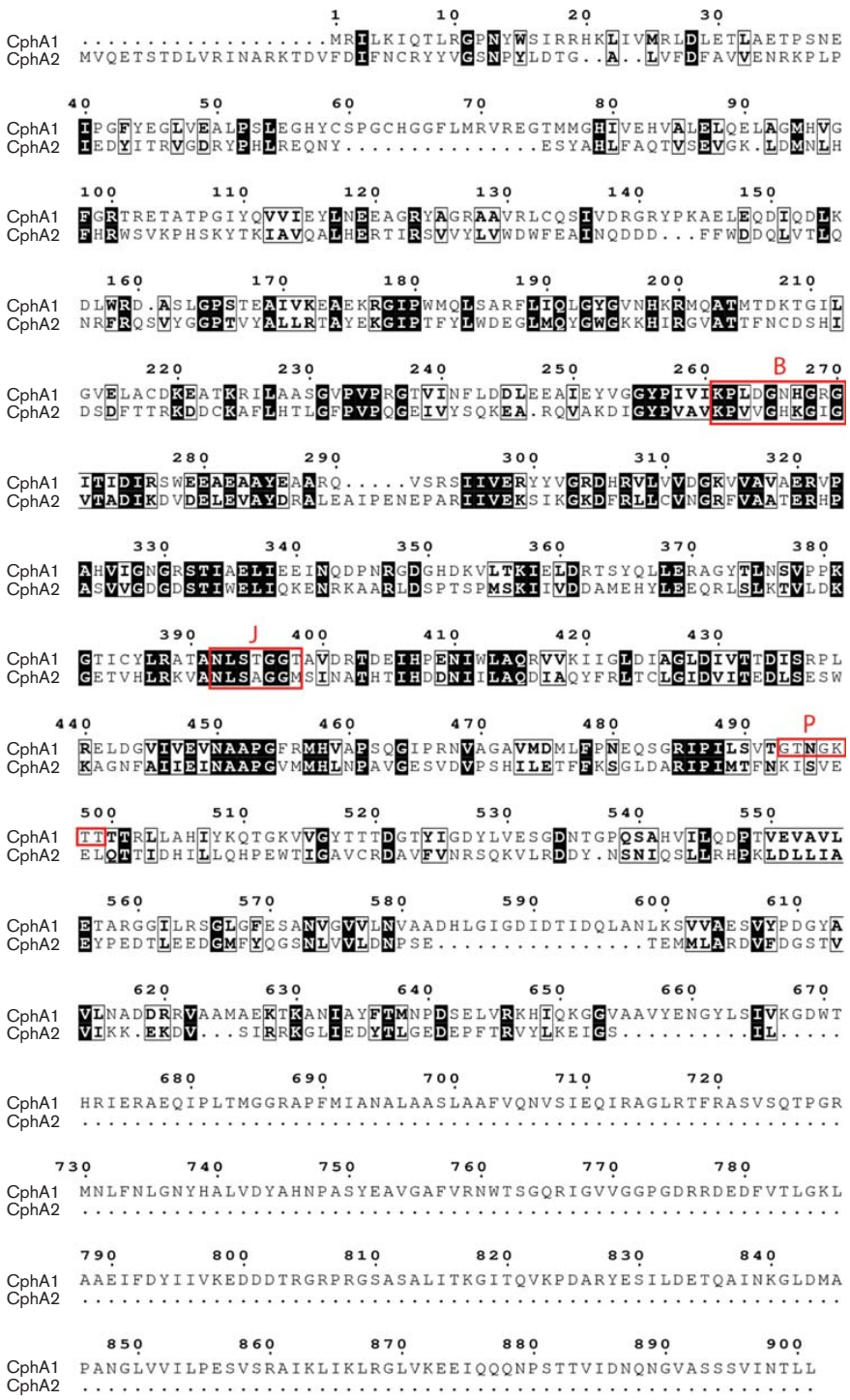

Fig. 1. Comparison of CphA1 and CphA2 amino acid sequences and potential ATP-binding sites. Alignment of the amino acid sequences of CphA1 (Ava_1814) and CphA2 (Ava_0335) from *A. variabilis* ATCC 29413. Strictly conserved residues are shaded in black; similar residues are framed in black. The loop regions predicted to be involved in ATP binding (Berg *et al.*, 2000) are framed in red and are labelled with the corresponding motif name above the sequence.

***In vitro* synthesis of cyanophycin and CphA2 activity assay.** The standard reaction mixture for *in vitro* synthesis of cyanophycin contained 50 mM Tris/HCl, pH 8.0, 20 mM $MgCl_2$, 50 mM KCl, 2 mM DTT, 10 mM ATP (disodium salt), 100 mM β-aspartyl-arginine (substrate) and 0.3 mg H_{10}-CphA2 ml^{-1}. After incubation at 30 °C for defined times, aliquots were withdrawn to determine ATP hydrolysis (phosphate release) and polymer production on SDS-PAGE. Kinetic analysis of CphA2 was performed with (i) 170 mM β-aspartyl-arginine and ATP concentrations ranging from 0.5 to 10 mM, and (ii) 10 mM ATP and β-aspartyl-arginine concentrations ranging from 15 to 210 mM. The kinetic data were analysed with Enzyme Kinetics module 1.3 for SigmaPlot 10 software (Systat). To determine the substrate specificity of CphA2, a range of dipeptides (Bachem) was individually added to the reaction mixture from stock solutions (adjusted to pH 8.0 with 1 M NaOH) to give a final dipeptide concentration of 100 mM. Aliquots of 2.0 or 20 µl were withdrawn at different time points during incubation at 30 °C, and the extent of ATP hydrolysis followed as release of phosphate measured with the malachite green assay (Lanzetta *et al.*, 1979).

Cyanophycin and protein analysis. Cyanophycin was isolated from *A. variabilis* WT and *cphA2* mutant (Ziegler *et al.*, 1998). The cyanophycin was quantified as aspartate release after total enzymic digestion of cyanophycin (Hejazi, 2002). Protein concentrations were determined using the Lowry assay (Lowry *et al.*, 1951). SDS-PAGE of proteins and of cyanophycin was performed on 15 % polyacrylamide (acrylamide/bisacrylamide, 29 : 1, v/v). To analyse the size and purity of *in vitro*-synthesized cyanophycin, 1 µl aliquots of the reaction mixtures were subjected to SDS-PAGE analysis.

Molecular mass of CphA2. The molecular mass of both H_{10}-CphA2 and CphA2 was determined by size exclusion chromatography (SEC) on a calibrated column of Superdex 200 10/300 GL (GE Healthcare) using 50 mM Tris/HCl, pH 8.0, 100 mM KCl and 1 mM DTT as running buffer at a flow rate of 0.5 ml min^{-1}. A gel filtration standard from Serva, ranging from 12.4 to 450 kDa, was used for calibration.

Sequence data analysis. A BLASTP search (Altschul *et al.*, 1997) was performed against all cyanobacterial sequences available from the Integrated Microbial Genomes database (Markowitz *et al.*, 2012) and GenBank (Benson *et al.*, 2011), and against the recently published sequences of Section V cyanobacteria by Dagan *et al.* (2013). The amino acid sequences of CphA1 (Ava_1814) and of CphA2 (Ava_0335) from *A. variabilis* were used as queries. Sequence alignment analysis and illustration preparation were performed with CLUSTAL W (Larkin *et al.*, 2007) and ESPript 3.0 (http://espript.ibcp.fr/ESPript/ESPript/; Robert & Gouet, 2014), respectively.

Strains and culture conditions. Liquid cultures of *A. variabilis* ATCC 29413 strain FD (Currier & Wolk, 1979) and the *cphA2* disruption strain were grown at 30 °C in fourfold-diluted AA medium (Allen & Arnon, 1955) with or without 5 mM KNO_3 in airlift flasks aerated with air enriched with 2 % CO_2. When necessary, the medium was supplemented with 50 µg kanamycin ml^{-1}. Cultures were grown under constant illumination with white light of 50 (low light) or 280 µmol photons m^{-2} s^{-1} (high light), respectively.

Growth tests. Growth of *A. variabilis cphA2* and *cphA1* mutants was assayed on solidified AA medium (Allen & Arnon, 1955) supplemented, as indicated, with 5 mM KNO_3 as nitrogen source. Three different dilutions of cells were spotted on agar plates, corresponding to 12.5, 25 and 50 ng chlorophyll *a*. Plates were incubated as stated earlier and photographed after 4 days of constant illumination.

Ultrastructural and immunocytochemical investigations. Ultrastructural and immunocytochemical analyses were carried out (Fuhrmann *et al.*, 2009). An anti-CphA2 antiserum against H_{10}-CphA2 and an antiserum against His-tagged CphA1 from *A. variabilis* were generated in rabbits by a commercial supplier (Pineda Antikörper Service). The dilutions of the anti-CphA1 and antiserum were 1 : 100. The secondary antiserum, a gold-coupled anti-rabbit IgG, was used at 1 : 30 dilution. The anti-cyanophycin antiserum was used as described previously (Ziegler *et al.*, 2001).

Expression analysis of *cphA2*. Samples of liquid cultures of *A. variabilis* WT and *cphA2* mutant were grown under low-light conditions, and cells were collected at 0, 24 and 48 h after nitrogen step-down. Cell-free extracts were prepared as described previously (Ziegler *et al.*, 1998). The concentration of chlorophyll *a* was determined according to de Marsac & Houmard (1988) for normalization. Cell-free extracts corresponding to 1 or 2 µg chlorophyll *a* were separated by SDS-PAGE and transferred electrophoretically to nitrocellulose membranes. The antisera against CphA2 and CphA1 were used in a dilution of 1 : 10 000. Antigen–antibody complexes were visualized with peroxidase-labelled anti-rabbit IgG (Sigma-Aldrich) and an ECL Detection kit (Merck Millipore). After the blot was digitized, the amounts of protein were determined by measuring the signal density using Quantity One software (Bio-Rad).

RESULTS

Distribution of cyanophycin synthetases amongst cyanobacteria

To gain new insights into the distribution of cyanophycin synthetases amongst cyanobacteria, we performed a BLASTP search (Altschul *et al.*, 1997) against all recently sequenced cyanobacterial genomes (155 genomes). The search included species of the five taxonomic sections defined according to their morphology (Rippka *et al.*, 1979): unicellular forms (Sections I and II), filamentous forms (Section III), filamentous heterocyst-forming forms (Section IV) and filamentous heterocyst-forming branching forms (Section V). The results are summarized in Fig. 2 and Table S2 and S3. A cyanophycin synthetase of type 1 (CphA1) was present in 72.9 % of all sequenced cyanobacteria, whilst only 28.4 % possessed a second cyanophycin synthetase of type 2 (CphA2). CphA2-like proteins were only present when species possess a CphA1. The lowest percentage of CphA1-like proteins was observed for cyanobacteria of Section I at only 50.6 %, whereas almost all of the other cyanobacteria possessed a CphA1-like protein. In filamentous, N_2-fixing cyanobacteria of Sections IV and V the percentage of CphA2-like proteins was high, at 71.4 and 81.8 %, respectively. In comparison, only 8.4 % of Section I cyanobacteria possessed an additional CphA2-like protein, including three *Cyanothece* and one *Gloeocapsa* species that grow diazotrophically (Bandyopadhyay *et al.*, 2013; Millineaux *et al.*, 1981). CphA-coding ORFs of the sequenced species are summarized in Table S3. In Section II, half of the sequenced cyanobacteria possessed a CphA2-like protein; all these species contained *nifH* genes encoding a subunit of the nitrogenase – a marker gene widely used to study the ecology and evolution of nitrogen-fixing bacteria (Raymond *et al.*, 2004). The presence of CphA2-like proteins in species of Section III was relatively low at 29.4 %, but some of these species have been reported to fix nitrogen (Stal & Heyer, 1987).

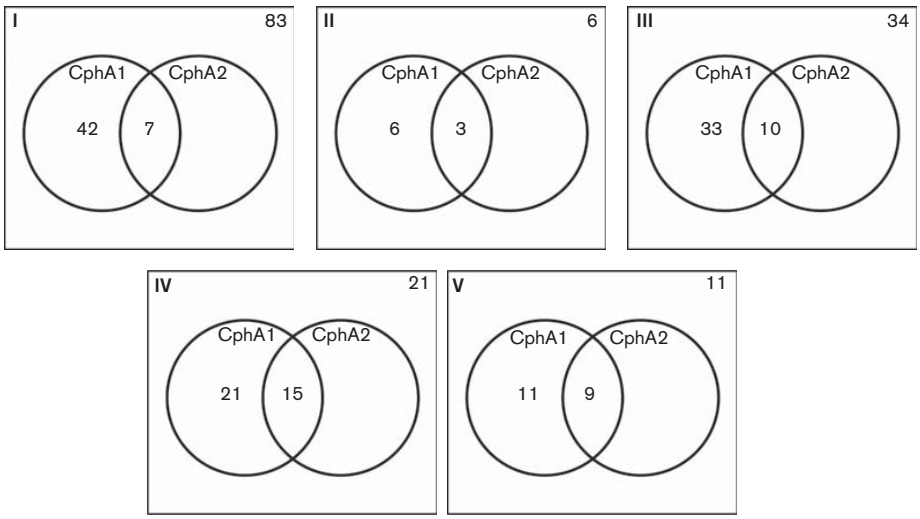

Fig. 2. Distribution of CphA1 and CphA2 in cyanobacteria. CphA1 and CphA2 within the five sections (indicated by Roman numerals, left corner) of cyanobacteria referring to the cyanobacterial genomes summarized in Table S2 and S3. The number of all sequenced species within the section is shown in the right corner.

CphA2 forms cyanophycin from β-aspartyl-arginine

Preparation and SEC of CphA2. The His_{10}-CphA2 fusion protein from *A. variabilis* (H_{10}-CphA2) was purified from crude extracts of recombinant *E. coli*. The protein was visible as a single band on SDS-PAGE gels with an apparent molecular mass of ~75 kDa (Fig. 3a, lane 2). The size corresponded well to the predicted monomeric mass of 75 kDa calculated for H_{10}-CphA2 using the ProtParam tool (Gasteiger *et al.*, 2005). The molecular mass of the native enzyme was determined by SEC. The His_{10}-CphA2 was eluted as a symmetrical peak corresponding to a molecular mass of 273 ± 2.4 kDa ($n=2$). Additionally, a recombinant GST-CphA2 variant from *A. variabilis* was purified and cleaved by PreScission protease. SEC was performed with the resulting CphA2. We obtained a mass of 265 ± 0.6 kDa for the untagged complex ($n=3$). The molecular mass determined for the tagged and untagged CphA2 corresponded to 3.6 momomer masses (75 and 73 kDa, respectively), suggesting that the native protein was either a trimer or a tetramer.

***In vitro* activity of CphA2.** We used H_{10}-CphA2 from *A. variabilis* to identify potential substrates *in vitro*. Enzymic activity was measured as ATP consumption (phosphate release) (mg protein)$^{-1}$. A range of dipeptides was tested as potential substrates in the presence of Mg-ATP (Table 1). The only tested dipeptide found to cause a substantial release of phosphate was β-aspartyl-arginine. The low activity found with α-aspartyl-arginine might have been due to minor β-aspartyl-arginine impurities. In contrast to CphA1, the isolated enzyme did not synthesize cyanophycin from the substrates aspartate, arginine and Mg-ATP (Table 1). SDS-PAGE analyses of the synthesized product over time revealed that CphA2 formed a product with a molecular mass of ~20–30 kDa in a single reaction (Fig. 3b, lanes 1–8). Specific digestion with cyanophycinase CphB (Richter *et al.*, 1999) was used to identify the product as cyanophycin (Fig. 3c, lanes 8 and 9). The amount of cyanophycin was determined based on the amount of aspartate released after treatment of cyanophycin with CphB and isopeptidase, as described previously (Hejazi, 2002; Neumann *et al.*, 2005). The ATP consumption required to form the peptide bond between β-aspartyl-arginine units was determined by comparing the amount of released phosphate to the yield of cyanophycin. To incorporate 1 mol β-aspartyl-arginine into cyanophycin, the hydrolysis of ~1 mol ATP was required (1.15 ± 0.10 mol ATP per 1 mol mol β-aspartyl-arginine; $n=5$).

The presence of potassium ions was essential for enzymic activity, as their replacement with sodium ions abrogated the observed phosphate release. Reactions run without β-aspartyl-arginine or ATP also failed to release phosphate, as did reactions in which ATP was replaced with polyphosphate ($polyP_{45}$; sodium phosphate glass type 45; Sigma-Aldrich). Notably, CphA1 from *A. variabilis* was not able to use β-aspartyl-arginine as substrate, failing to release phosphate or form cyanophycin under our experimental conditions *in vitro*. As a side note, CphA2 activity was enhanced *in vitro* by adding water-soluble cyanophycin from *Desulfitobacterium hafniense* (Otterbach, 2010; Ziegler *et al.*, 2002) as an artificial primer (Fig. S1).

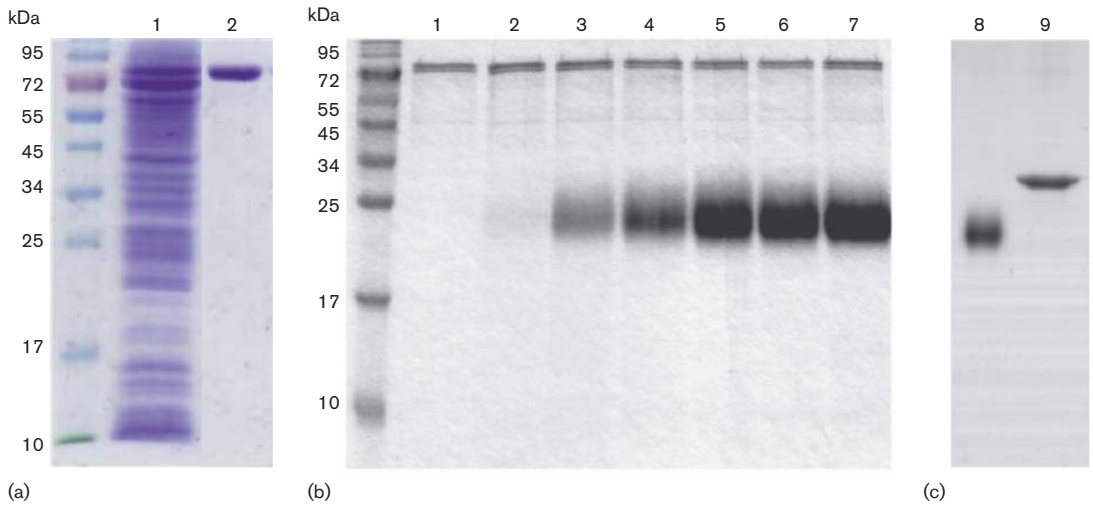

Fig. 3. Cyanophycin synthesis by pure H_{10}-CphA2 from *A. variabilis*. (a) Purification of recombinant H_{10}-CphA2: SDS-PAGE analysis of *E. coli* extracts and purified H_{10}-CphA2. Lane 1, crude protein extract (28 μg); lane 2, H_{10}-CphA2 (1 μg) purified by nickel-affinity chromatography followed by application to a PD-10 desalting column. The positions of standard markers (PageRuler Prestained; Thermo Scientific) are indicated on the left. (b) *In vitro* synthesis of cyanophycin over 60 min. Lanes 1–8, 1 μl standard reaction mixture was loaded per lane at time point (lane 1, t=0 min; lane 2, t=5 min; lane 3, t=10 min; lane 4, t=15 min; lane 5, t=20 min; lane 6, t=30 min; lane 7, t=60 min). The position of standard markers (PageRuler Prestained; Thermo Scientific) are indicated on the left. (c) Degradation of cyanophycin by cyanophycinase. Lane 8, 1 μl standard reaction assay, t=60 min (cyanophycin, ~ 25 kDa). Lane 9, hydrolysis of cyanophycin by cyanophycinase (CphB, 30 kDa). Proteins and cyanophycin analysed on a 15 % acrylamide/bisacrylamide (29 : 1) were stained with Coomassie brilliant blue R-250.

Kinetics. The phosphate release kinetics were determined for both β-aspartyl-arginine and ATP substrates. As shown for β-aspartyl-arginine as an example (Fig. S2), complex sigmoid kinetics were recorded for cyanophycin synthesis.

Table 1. Substrate specificity of CphA2: phosphate release by CphA2 in the presence of various substrates after 120 min (n=2)

Substrate*	Phosphate release [μmol (mg protein)$^{-1}$]
β-Aspartyl-lysine	ND
α-Aspartyl-glycine	ND
β-Aspartyl-glycine	ND
α-Aspartyl-leucine	ND
β-Aspartyl-leucine	ND
α-Aspartyl-arginine	0.7
β-Aspartyl-alanine	ND
β-Aspartyl-phenylalanine	ND
α-Glutamyl-leucine	ND
α-Alanyl-glycine	ND
β-Aspartyl-arginine	31
Without dipeptide	ND
Aspartate + arginine	ND

ND, Not detectable [≤0.25 μmol (mg protein)$^{-1}$].
*Either 100 mM dipeptide or 100 mM aspartate and arginine each.

The $K_{0.5}$ for β-aspartyl-arginine was 76 ± 10.69 mM (n=6). The $K_{0.5}$ for ATP was 3.5 ± 0.45 mM (n=6). The *in vitro* turnover number for one monomer of CphA2 was 1.1 Hz at substrate saturation. Hill coefficients of 3.1 and 2 were determined for β-aspartyl-arginine and ATP, respectively, indicating positive cooperativity.

CphA2 from *Cyanothece* sp. PCC 7425. To confirm our BLASTP results and show the enzymic activity of CphA2 in diazotrophic cyanobacteria, *cphA2* of the unicellular cyanobacterium *Cyanothece* sp. PCC 7425 (Section I) was heterologously expressed in *E. coli*, purified and characterized. Cyanophycin formation from the dipeptide β-aspartyl-arginine was observed *in vitro* (Fig. S3). Samples of the reaction batch were taken at different time points and analysed by SDS-PAGE (Fig. S3). The formed cyanophycin was identified by specific CphB degradation (not shown). CphA2 from *Cyanothece* sp. PCC 7425 showed a lower activity than CphA2 from *A. variabilis* under *in vitro* conditions. A ~25 kDa band representing the final mass of cyanophycin appeared later (Fig. S3). A 17 kDa band representing a soluble cyanophycin fraction was found at the initial stages of cyanophycin synthesis (Fig. S3).

Physiological role of CphA2

To further examine the physiological role of CphA2, we generated a *cphA2* disruption mutant of *A. variabilis* by

insertional mutagenesis (Fig. S4). Cyanophycin isolated from WT and *cphA2* mutant cells ranged from 30 to 130 kDa (data not shown). We observed 10–15 % less cyanophycin per chlorophyll *a* in the mutant during its stationary growth phase under low-light conditions than in the WT. Electron micrographs of cells in which cyanophycin granules were immunocytochemically identified with an anti-cyanophycin antiserum confirmed a similar localization of cyanophycin in the WT and mutant cells. Whilst cyanophycin was localized to polar nodules in the neck region of the cell in heterocysts (Fig. 4), cyanophycin granules were visible in various positions of vegetative cells (Fig. S5 and S6). To further ascertain the distribution of CphA2, we analysed its localization in *A. variabilis* WT cells by immunogold labelling with an anti-CphA2 antiserum. In WT filaments, CphA2, like cyanophycin, was located at the polar nodules of heterocysts and at the cyanophycin granules of vegetative cells. We found no evidence of cell-specific distribution of CphA2 (Figs 4 and S6). CphA2 mutant cells did not show any specific labelling of cyanophycin granules (Fig. 4). Our CphA2 antiserum showed no cross-reaction with CphA1, which is also associated with cyanophycin (Fig. 5). To further examine CphA1 and CphA2 expression at the protein level, samples from *A. variabilis* WT and mutant cells were taken at different time points after nitrogen step-down. Crude extracts were separated by SDS-PAGE and subjected to Western blot analysis using antisera raised against CphA1 and CphA2. The results were quantified by densitometric analysis. Mutants lacking CphA1 (Ziegler *et al.*, 2001) and CphA2 were used as controls. As shown in Fig. 5 (lane 1), the expression level of CphA2 in WT cells was relatively consistent for 48 h after nitrogen step-down (100 ± 16 %). In contrast, the expression level of CphA1 in WT cells increased to 148 ± 27 (Fig. 5, lane 2) and to 304 ± 64 % in *cphA2* mutant cells following nitrogen step-down (Fig. 5, lane 3). Growth profiles of WT, *cphA1* and *cphA2* mutants of *A. variabilis* were examined under different light and nitrogen conditions (Fig. 6). Under low-light conditions (Fig. 6a), no significant difference in growth was observed in the presence and absence of nitrate amongst WT, *cphA1* and *cphA2* mutant cells. In contrast, the *cphA2* mutant was impaired in growth under high-light conditions (Fig. 6b). In the absence of combined nitrogen, the mutant showed pronounced bleaching after 4 days of high-light exposure. The altered phenotype under high-light conditions and nitrogen deprivation was confirmed by growth experiments in liquid medium. Whilst the doubling time for the WT and *cphA2* mutant was similar in the presence of nitrate ($\sim$20 h), it was significantly reduced under nitrogen deprivation (53 versus 28 h for WT).

DISCUSSION

CphA2 presence strongly corresponds to N_2 fixation

The distribution analysis of CphA1 and CphA2 proteins amongst cyanobacteria revealed that the appearance of CphA2 is strictly dependent on the presence of CphA1. CphA2 is predominantly found in filamentous growing species of Section IV and V that are able to fix N_2 in heterocysts (Fig. 2, Tables S2 and S3). CphA2 genes were also found in unicellular cyanobacteria of Section I that are known to fix N_2 in diurnal rhythms in the absence of photosynthesis. The function of CphA2 in one of these strains, i.e. *Cyanothece* sp. PCC 7425, was verified *in vitro*. The presence of CphA2 in species of Section II and III correlates with the presence of both CphA1 and nitrogenase, indicating their capacities for N_2 fixation. We conclude that the presence of CphA2 strongly corresponds to the ability of a cyanobacterium to fix N_2.

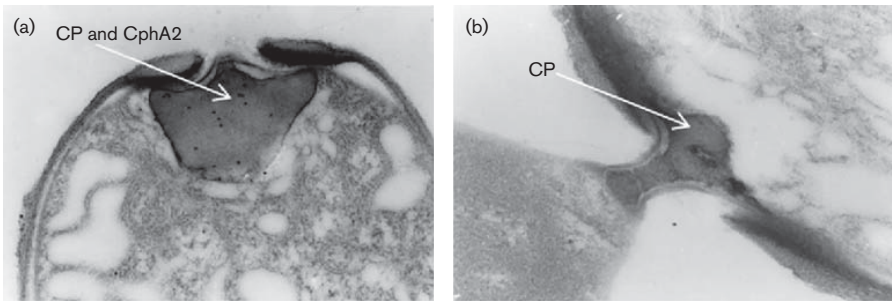

Fig. 4. Localization of CphA2. Electron micrographs of *A. variabilis* WT and *cphA2* mutant cells grown under N_2-fixing conditions. Ultrastructural investigations were performed using electron microscopy following the immunocytochemical visualization of CphA2 with antisera raised against CphA2 and a gold-coupled anti-rabbit IgG antibody in *Anabaena* cultures. (a) *A. variabilis* WT heterocyst with cyanophycin (CP) in polar nodules, treated with anti-CphA2 antisera (1 : 100), magnification $\times$48 000. (b) Heterocyst of *cphA2* mutant cells containing cyanophycin (CP) in polar nodules, treated with anti-CphA2 antisera (1 : 100), magnification $\times$64 000.

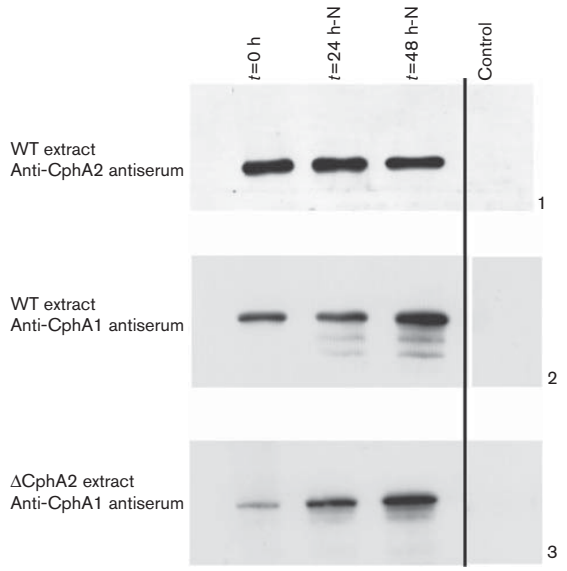

Fig. 5. Expression of *cphA1* and *cphA2* in *A. variabilis* WT and its *cphA2* disruption mutant. Immunoblot analysis of *A. variabilis* cell-free extracts is shown. Samples were taken at 0, 24 and 48 h after a nitrogen step-down ('-N'). Cell-free extracts corresponding to 1 μg chlorophyll *a* were loaded per lane. The enzymes were detected with antisera raised against CphA2 and CphA1 (extracts and antisera are indicate on the left). As negative controls, cell-free extracts were used. 1, *cphA2* mutant; 2, *cphA1* mutant; 3, *cphA1* mutant.

CphA2 acts as cyanophycin synthetase

Although previous studies based on *cphA1* deletion mutants in *A. variabilis* and *Anabaena* sp. PCC 7120 suggested that CphA2 cannot synthesize cyanophycin *de novo* (Picossi *et al.*, 2004; Ziegler *et al.*, 2001), the catalytic activity of CphA2 has remained unknown. Here, we demonstrated substrate consumption as well as product synthesis of CphA2 *in vitro*. The isolated enzyme did not show the canonical activity of CphA1, but was found to be specific for the dipeptide β-aspartyl-arginine and ATP as substrates. Potassium ions were essential for the *in vitro* reaction. SDS-PAGE analyses and specific CphB digestion of the synthesized product revealed that cyanophycin was formed. The ATP : β-aspartyl-arginine ratio of ~1 to incorporate 1 mol β-aspartyl-arginine into cyanophycin suggests that the reaction mechanism involved may be similar to that described for CphA1, which forms cyanophycin via acyl-phosphate intermediates (Ziegler *et al.*, 1998).

The $K_{0.5}$ values obtained *in vitro* are quite high, at 76 ± 10.69 mM for β-aspartyl-arginine and 3.5 ± 0.45 mM for ATP, and probably do not reflect the *in vivo* situation where CphA2 is attached to the insoluble cyanophycin (Fig. 4a). We expect further cofactors, not yet identified, as well as ambient conditions to influence the *in vivo* activity of CphA2. However, these results collectively show that CphA2 is an active cyanophycin synthetase that ligates two β-aspartyl-arginine units by catalysing the formation of a peptide bond between their aspartate residues. As CphA1 was not able to use β-aspartyl-arginine as substrate, we assume that the two enzymes may play different roles in the nitrogen metabolism of *A. variabilis* – whilst CphA1 forms cyanophycin by ligating aspartate and arginine, CphA2 rebuilds cyanophycin from β-aspartyl-arginine. Reactions that affect the cyanophycin/β-aspartyl-arginine pool are presented in Fig. 7. Considering that β-aspartyl-arginine is transferred as the main nitrogen carrier between heterocysts and vegetative cells in *Anabaena* sp. PCC 7120 (Burnat *et al.*, 2014), CphA2 provides the option to form cyanophycin as a storage compound when degradation to the single amino acids is not required. This would be beneficial for the cell due to the lower cost of ATP.

CphA2 and its function

The lack of CphA2 did not affect the molecular mass of cyanophycin in *A. variabilis*, as cyanophycin isolated from CphA2-lacking cells ranged from 30 to 130 kDa, as previously reported for *A. variabilis* WT (Ziegler *et al.*, 2001). However, the mutant produced only 85–90 % of cyanophycin per chlorophyll *a* in comparison with the WT level during its stationary growth phase under low-light conditions. This is consistent with the results of Picossi *et al.* (2004), who found that the cyanophycin content of a *ΔcphA2* mutant from *Anabaena* sp. PCC 7120 was ~20 % lower than that of the WT. The role of CphA2 remained unclear at that time. Based on our findings, we conclude that cells lacking CphA2 possess a lower overall cyanophycin synthesis capacity and need to consume more ATP per cyanophycin unit. The reduced cyanophycin amount observed in *cphA2* mutant cells compared with WT cells might reflect in part the lack of CphA2 activity. We further suggest that nitrogen storage and mobilization in *Anabaena* species are highly dynamic processes that involve cyanophycin/β-aspartyl-arginine pools as reservoirs. In WT and *cphA2* mutant cells, cyanophycin was localized to polar nodules in the neck regions of heterocysts and in the granules of vegetative cells. In WT filaments, CphA2 and cyanophycin were co-located at the polar nodules of heterocysts and in the cyanophycin granules of vegetative cells. We did not observe any evidence of cell-specific distribution along the filaments. These results are supported by recently published transcriptional data (Park *et al.*, 2013) showing no cell-specific *cphA2* expression. The spatial proximity of CphA1 and CphA2 signals with cyanophycin prompted us to speculate that CphA1 and CphA2 co-localize, and are both predominantly attached to cyanophycin granules. Although no indications for a CphA1/CphA2 assembly were observed *in vitro* (Nürnberg, 2008), we would not exclude a direct interaction of CphA1 and CphA2. Both cyanophycin

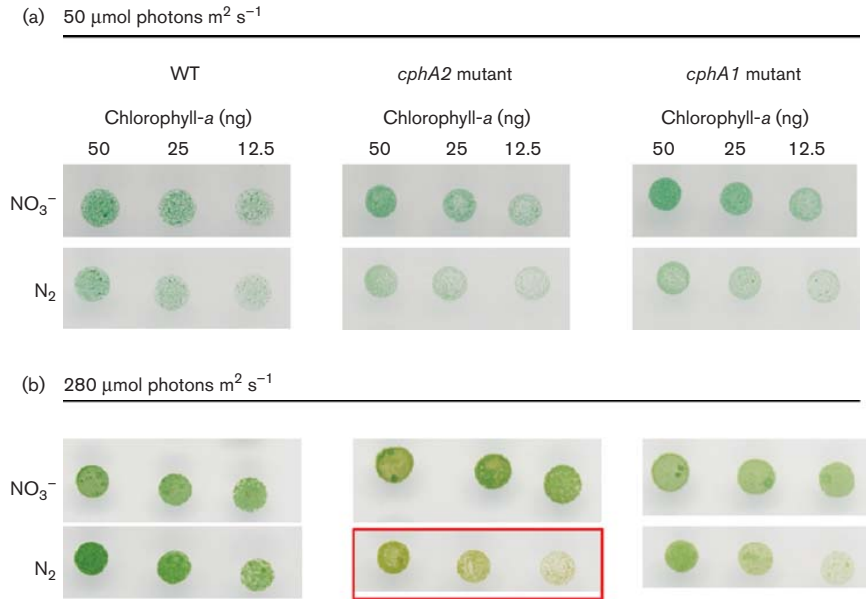

Fig. 6. Growth of *A. variabilis* WT and mutant cells lacking CphA2 and CphA1 cells using nitrate or N_2 as the nitrogen source. *A. variabilis* WT and mutant cells without CphA2 and without CphA1 were grown on solid AA medium using nitrate or N_2 as a nitrogen source. Cells were exposed to (a) low or (b) high light. Each dot represents cells with a chlorophyll-*a* content of 12.5–50 ng. Images were taken 4 days after cultivation. The condition with the highest impact on growth is framed in red.

synthetases might support each other *in vivo*. The nitrogen-dependent expression of *cphA1* and *cphA2* in *Anabaena* sp. PCC 7120 as mono- and polycistronic transcripts was reported previously (Picossi *et al.*, 2004). Here, we analysed the CphA1 and CphA2 protein levels in *A. variabilis* mutants at different time points after nitrogen step-down. As shown in Fig. 5, the CphA2 level remained nearly unchanged when the culture was transferred from the presence of nitrate to the absence of nitrate. This result was consistent with that reported previously at the transcript level in *Anabaena* PCC 7120 subjected to nitrogen step-down (Picossi *et al.*, 2004). Therefore, the expression of CphA2 does not appear to be affected by the supplied nitrogen source. The increased CphA1 level in WT cells following nitrogen step-down is consistent with a previous report that CphA1 mRNA expression was increased under combined nitrogen starvation in *Anabaena* PCC 7120 (Flaherty *et al.*, 2011; Picossi *et al.*, 2004). In the mutant lacking CphA2, the CphA1 level increased at a higher rate than in WT cells following nitrogen step-down (Fig. 5, lane 3). The enhanced increase of CphA1 in the *cphA2* disruption mutant compared with the WT suggests that CphA1 might substitute for CphA2 in the 'rebuilding' of cyanophycin (Fig. 7). Although the *cphA2* mutant was found to express *cphA1* at a higher level than that seen in the WT, this did not fully restore the WT level of cyanophycin.

In the absence of combined nitrogen, the CphA2-lacking mutant strain showed pronounced bleaching after 4 days of high-light exposure (Fig. 6b). Thus, although CphA2 activity was not generally required for growth, it appeared to be essential for the survival of cells in the absence of combined nitrogen under high-light conditions. A similar effect was observed in a CphA1-lacking mutant of *A. variabilis* (a cyanophycin-free mutant) (Ziegler *et al.*, 2001). Whether other stress conditions, such as phosphate and sulphate limitations, that increase the level of cyanophycin (Allen *et al.*, 1980) lead to a similar phenotype remains to be investigated.

In *Anabaena* sp. PCC 7120 and *A. variabilis*, the expression levels of the cyanophycin-degrading enzymes isoaspartyl dipeptidase and cyanophycinase were increased under N_2-fixing conditions (Flaherty *et al.*, 2011; Park *et al.*, 2013; Picossi *et al.*, 2004). A basal, nitrogen-independent CphA2 activity might therefore act as an additional control element at the protein level that is involved in the fine tuning of aspartate and arginine release from cyanophycin. The additional *β*-aspartyl-arginine in CphA2-lacking mutants might lead to an increase of arginine and aspartate in the cell, and a subsequent imbalance in nitrogen metabolism.

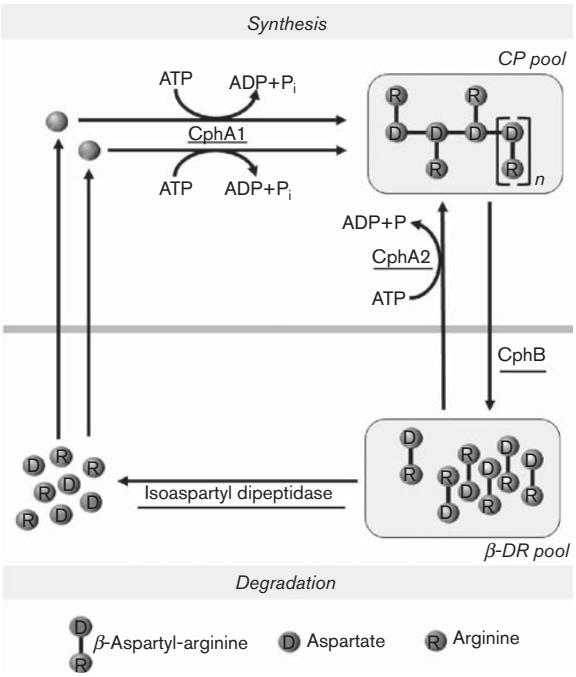

Fig. 7. Storage and mobilization of aspartate and arginine. Illustration of cyanophycin (CP) synthesis by CphA1 and CphA2 (upper panel) and degradation by CphB and isoaspartyl dipeptidase (lower panel) in N_2-fixing cyanobacteria.

CONCLUSIONS

Here, we show that CphA2 is a novel type of cyanophycin synthetase using ATP and β-aspartyl-arginine as substrates to form cyanophycin. As recently published by Burnat *et al.* (2014), β-aspartyl-arginine seems to be the main transport unit for combined nitrogen between heterocysts and vegetative cells in *Anabaena* sp. PCC 7120. In our opinion, CphA2 contributes to a continuous relocation process that shifts combined nitrogen within the filaments of cyanobacteria. However, given that CphA2-like proteins are also found in diazotrophically growing unicellular cyanobacteria such as *Cyanothece* sp. PCC 7425, the CphA2 activity should be considered in the context of N_2 fixation and nitrogen mobilization in addition to nitrogen transfer.

ACKNOWLEDGEMENTS

We dedicate this work to our colleague Karl Ziegler, who died during the preparation of this paper. We would like to thank Oliver Brödel (Technische Hochschule Wildau, Wildau, Germany) for performing the MS measurements. We are also grateful to Sabine Nicklisch for excellent technical support.

REFERENCES

Aboulmagd, E., Oppermann-Sanio, F. B. & Steinbüchel, A. (2001). Purification of *Synechocystis* sp. strain PCC6308 cyanophycin synthetase and its characterization with respect to substrate and primer specificity. *Appl Environ Microbiol* **67**, 2176–2182.

Allen, M. B. & Arnon, D. I. (1955). Studies on nitrogen-fixing blue-green algae. I. Growth and nitrogen fixation by *Anabaena cylindrica Lemm. Plant Physiol* **30**, 366–372.

Allen, M. M., Hutchison, F. & Weathers, P. J. (1980). Cyanophycin granule polypeptide formation and degradation in the cyanobacterium *Aphanocapsa* 6308. *J Bacteriol* **141**, 687–693.

Altschul, S. F., Madden, T. L., Schäffer, A. A., Zhang, J., Zhang, Z., Miller, W. & Lipman, D. J. (1997). Gapped blast and psi-blast: a new generation of protein database search programs. *Nucleic Acids Res* **25**, 3389–3402.

Bandyopadhyay, A., Elvitigala, T., Liberton, M. & Pakrasi, H. B. (2013). Variations in the rhythms of respiration and nitrogen fixation in members of the unicellular diazotrophic cyanobacterial genus *Cyanothece. Plant Physiol* **161**, 1334–1346.

Benson, D. A., Karsch-Mizrachi, I., Lipman, D. J., Ostell, J. & Sayers, E. W. (2011). GenBank. *Nucleic Acids Res* **39**, D32–D37.

Berg, H. (2003). *Untersuchungen zur Funktion und Struktur der Cyanophycin-Synthetase von Anabaena variabilis ATCC 29413 [Studies on the function and structure of cyanophycin synthetase of* Anabaena variabilis *ATCC 29413]*. Dissertation, Institut für Biologie, Humboldt-Universität zu Berlin, Berlin, Germany (in German).

Berg, H., Ziegler, K., Piotukh, K., Baier, K., Lockau, W. & Volkmer-Engert, R. (2000). Biosynthesis of the cyanobacterial reserve polymer multi-l-arginyl-poly-l-aspartic acid (cyanophycin): mechanism of the cyanophycin synthetase reaction studied with synthetic primers. *Eur J Biochem* **267**, 5561–5570.

Black, T. A., Cai, Y. & Wolk, C. P. (1993). Spatial expression and autoregulation of hetR, a gene involved in the control of heterocyst development in *Anabaena. Mol Microbiol* **9**, 77–84.

Burnat, M., Herrero, A. & Flores, E. (2014). Compartmentalized cyanophycin metabolism in the diazotrophic filaments of a heterocyst-forming cyanobacterium. *Proc Natl Acad Sci U S A* **111**, 3823–3828.

Carr, N. G. (1988). Nitrogen reserves and dynamic reservoirs in cyanobacteria. In *Biochemistry of Algae and Cyanobacteria*, pp. 13–21. Edited by L. J. Rogers & J. R. Gallon. Oxford: Clarendon Press.

Currier, T. C. & Wolk, C. P. (1979). Characteristics of *Anabaena variabilis* influencing plaque formation by cyanophage N-1. *J Bacteriol* **139**, 88–92.

Dagan, T., Roettger, M., Stucken, K., Landan, G., Koch, R., Major, P., Gould, S. B., Goremykin, V. V., Rippka, R. & other authors (2013). Genomes of Stigonematalean cyanobacteria (subsection V) and the evolution of oxygenic photosynthesis from prokaryotes to plastids. *Genome Biol Evol* **5**, 31–44.

de Marsac, N. T. & Houmard, J. (1988). Complementary chromatic adaptation: Physiological conditions and action spectra. *Methods Enzymol* **167**, 318–328.

Elhai, J. & Wolk, C. P. (1988a). Conjugal transfer of DNA to cyanobacteria. *Methods Enzymol* **167**, 747–754.

Elhai, J. & Wolk, C. P. (1988b). A versatile class of positive-selection vectors based on the nonviability of palindrome-containing plasmids that allows cloning into long polylinkers. *Gene* **68**, 119–138.

Erickson, N. A., Kolodny, N. H. & Allen, M. M. (2001). A rapid and sensitive method for the analysis of cyanophycin. *Biochim Biophys Acta* **1526**, 5–9.

Flaherty, B. L., Van Nieuwerburgh, F., Head, S. R. & Golden, J. W. (2011). Directional RNA deep sequencing sheds new light on the transcriptional response of *Anabaena sp.* strain PCC 7120 to combined-nitrogen deprivation. *BMC Genomics* **12**, 332.

Frommeyer, M., Wiefel, L. & Steinbüchel, A. (2014). Features of the biotechnologically relevant polyamide family "cyanophycins" and their biosynthesis in prokaryotes and eukaryotes. *Crit Rev Biotechnol* **36**, 153–164.

Fuhrmann, E., Bultema, J. B., Kahmann, U., Rupprecht, E., Boekema, E. J. & Schneider, D. (2009). The vesicle-inducing protein 1 from *Synechocystis* sp. *PCC 6803 organizes into diverse higher-ordered ring structures. Mol Biol Cell* **20**, 4620–4628.

Füser, G. & Steinbüchel, A. (2007). Analysis of genome sequences for genes of cyanophycin metabolism: identifying putative cyanophycin metabolizing prokaryotes. *Macromol Biosci* **7**, 278–296.

Gasteiger, E., Hoogland, C., Gattiker, A., Duvaud, S., Wilkins, M. R., Appel, R. D. & Bairoch, A. (2005). Protein identification and analysis tools on the ExPASy server. In *The Proteomics Protocols Handbook*, pp. 571–607. Edited by J. M. Walker. Totowa, NJ: Humana Press.

Hejazi, M. (2002). *Cyanophycin-Degradation in Cyanobakterien: biochemische und molekularbiologische Charakterisierung der Cyanophycinase und einer Isoaspartyl-Dipeptidase [Cyanophycin degradation in cyanobacteria: biochemical and molecular biological characterization of cyanophycinase and a isoaspartyl dipeptidase*]. Dissertation, Institut für Biologie, Humboldt-Universität zu Berlin, Berlin, Germany (in German).

Hejazi, M., Piotukh, K., Mattow, J., Deutzmann, R., Volkmer-Engert, R. & Lockau, W. (2002). Isoaspartyl dipeptidase activity of plant-type asparaginases. *Biochem J* **364**, 129–136.

Lanzetta, P. A., Alvarez, L. J., Reinach, P. S. & Candia, O. A. (1979). An improved assay for nanomole amounts of inorganic phosphate. *Anal Biochem* **100**, 95–97.

Larkin, M. A., Blackshields, G., Brown, N. P., Chenna, R., McGettigan, P. A., McWilliam, H., Valentin, F., Wallace, I. M., Wilm, A. & other authors (2007). Clustal W and Clustal X version 2.0. *Bioinformatics* **23**, 2947–2948.

Lowry, O. H., Rosebrough, N. J., Farr, A. L. & Randall, R. J. (1951). Protein measurement with the Folin phenol reagent. *J Biol Chem* **193**, 265–275.

Markowitz, V. M., Chen, I. M., Palaniappan, K., Chu, K., Szeto, E., Grechkin, Y., Ratner, A., Jacob, B., Huang, J. & other authors (2012). IMG: the Integrated Microbial Genomes database and comparative analysis system. *Nucleic Acids Res* **40**, D115–D122.

Millineaux, P. M., Gallon, J. R. & Chaplin, A. E. (1981). Acetylene reduction (nitrogen fixation) by cyanobacteria grown under alternating light-dark cycles. *FEMS Microbiol Lett* **10**, 245–247.

Neumann, K., Stephan, D. P., Ziegler, K., Hühns, M., Broer, I., Lockau, W. & Pistorius, E. K. (2005). Production of cyanophycin, a suitable source for the biodegradable polymer polyaspartate, in transgenic plants. *Plant Biotechnol J* **3**, 249–258.

Nürnberg, D. J. (2008). *Expression, purification and* in vitro *analysis of cyanobacterial cyanophycin synthetases.* Dissertation, Institut für Biologie, Humboldt-Universität zu Berlin, Berlin, Germany.

Otterbach, S. (2010). *Vergleichende Untersuchung der in vitro Aktivität der Cyanophycin-Synthetasen aus Desulfitobacterium hafniense und verschiedenen Cyanobakterien [Comparative study of the* in vitro *activity of cyanophycin synthetases from* Desulfitobacterium hafniense *and various cyanobacteria].* Life Science and Technology Department, Beuth University for Applied Science Berlin, Berlin, Germany (in German).

Park, J.-J., Lechno-Yossef, S., Wolk, C. P. & Vieille, C. (2013). Cell-specific gene expression in *Anabaena variabilis* grown phototrophically, mixotrophically, and heterotrophically. *BMC Genomics* **14**, 759.

Picossi, S., Valladares, A., Flores, E. & Herrero, A. (2004). Nitrogen-regulated genes for the metabolism of cyanophycin, a bacterial nitrogen reserve polymer: expression and mutational analysis of two cyanophycin synthetase and cyanophycinase gene clusters in heterocyst-forming cyanobacterium *Anabaena* sp., PCC 7120. *J Biol Chem* **279**, 11582–11592.

Raymond, J., Siefert, J. L., Staples, C. R. & Blankenship, R. E. (2004). The natural history of nitrogen fixation. *Mol Biol Evol* **21**, 541–554.

Richter, R., Hejazi, M., Kraft, R., Ziegler, K. & Lockau, W. (1999). Cyanophycinase, a peptidase degrading the cyanobacterial reserve material multi-l-arginyl-poly-l-aspartic acid (cyanophycin): molecular cloning of the gene of *Synechocystis* sp., PCC 6803, expression in Escherichia coli, and biochemical characterization of the purified enzyme. *Eur J Biochem* **263**, 163–169.

Rippka, R., Deruelles, J., Waterbury, J. B., Herdman, M. & Stanier, R. Y. (1979). Generic assignments, strain histories and properties of pure cultures of cyanobacteria. *J Gen Microbiol* **111**, 1–61.

Robert, X. & Gouet, P. (2014). Deciphering key features in protein structures with the new ENDscript server. *Nucleic Acids Res* **42**, W320–W324.

Sambrook, J., Fritsch, E. F. & Maniatis, T. (1989). *Molecular Cloning: A Laboratory Manual*, 2nd edn. Cold Sping Harbor, NY: Cold Spring Harbor Laboratory.

Simon, R. D. (1971). Cyanophycin granules from the blue-green alga *Anabaena cylindrica*: a reserve material consisting of copolymers of aspartic acid and arginine. *Proc Natl Acad Sci U S A* **68**, 265–267.

Simon, R. D. & Weathers, P. (1976). Determination of the structure of the novel polypeptide containing aspartic acid and arginine which is found in cyanobacteria. *Biochim Biophys Acta* **420**, 165–176.

Stal, L. J. & Heyer, H. (1987). Dark anaerobic nitrogen fixation (acetylene reduction) in the cyanobacterium *Oscillatoria* sp. *FEMS Microbiol Lett* **45**, 227–232.

Ziegler, K., Diener, A., Herpin, C., Richter, R., Deutzmann, R. & Lockau, W. (1998). Molecular characterization of cyanophycin synthetase, the enzyme catalyzing the biosynthesis of the cyanobacterial reserve material multi-l-arginyl-poly-l-aspartate (cyanophycin). *Eur J Biochem* **254**, 154–159.

Ziegler, K., Stephan, D. P., Pistorius, E. K., Ruppel, H. G. & Lockau, W. (2001). A mutant of the cyanobacterium *Anabaena variabilis* ATCC 29413 lacking cyanophycin synthetase: growth properties and ultrastructural aspects. *FEMS Microbiol Lett* **196**, 13–18.

Ziegler, K., Deutzmann, R. & Lockau, W. (2002). Cyanophycin synthetase-like enzymes of non-cyanobacterial eubacteria: characterization of the polymer produced by a recombinant synthetase of *Desulfitobacterium hafniense. Z Naturforsch C* **57**, 522–529.

Edited by: E. Flores

CphA2 is a novel type of cyanophycin synthetase in N_2-fixing cyanobacteria

Supplemental Tables and Figures

Friederike Klemke[1], Dennis J. Nürnberg[1,2], Karl Ziegler[1], Gabriele Beyer[1], Uwe Kahmann[3], Wolfgang Lockau[1] and Thomas Volkmer[1]

[1]Institut für Biologie, Humboldt-Universität zu Berlin, Chausseestraße 117, 10115 Berlin, Germany
[2]Department of Life Sciences, Imperial College London, London SW7 2AZ, United Kingdom
[3]Zentrum für Ultrastrukturelle Diagnostik im IIT, Universitätsstraße 25, 33615 Bielefeld, Germany

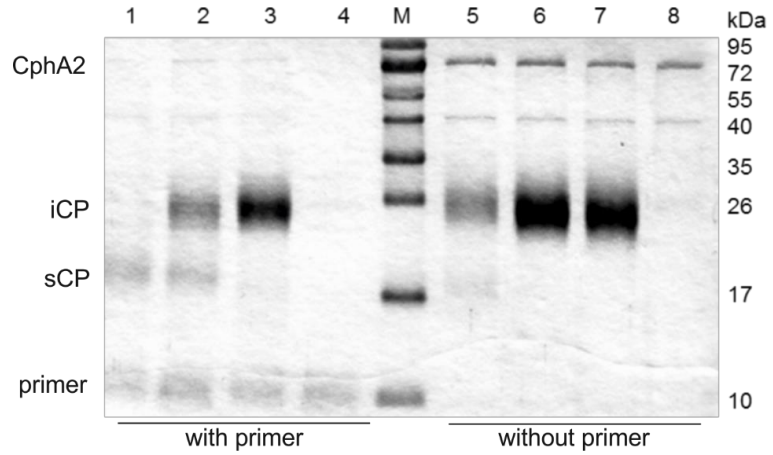

Reaction time (min)	2	4	10	10	10	20	30	30
ATP	+	+	+	-	+	+	+	-

FIGURE S1: Enhanced *in vitro* activity of CphA2 with water soluble cyanophycin from *Desulfitobacterium hafniense*. SDS-PAGE analysis of *in vitro* cyanophycin synthesis with H_{10}-CphA2 from *A. variabilis*. Samples (1 µL) of reaction mixtures were taken at different time points and analyzed on a 15% acrylamide/bisacrylamide (29:1) gel. After staining proteins and cyanophycin with Coomassie Brilliant Blue R-250 the gel was dried on filter paper. The enzyme reactions were performed with 1/3 of H_{10}-CphA2 in presence of 1 mg ml^{-1} water soluble cyanophycin (sCP) from *D. hafniense* (Otterbach, 2010; Ziegler, 2002) as primer (lane 1-4) and under standard conditions (lane 5-8). Lane 1, t = 2 min; lane 2, t = 4 min; lane 3, t = 10 min; lane 4, t = 10 min, without ATP (negative control); lane 5, t = 10 min, lane 6, t = 20 min; lane 7, t = 30 min; lane 8, t = 30 min without ATP (negative control). Please, note the deviating enzyme concentrations and reaction times. Indicated at the left: CphA2 band at 72 kDa; water insoluble cyanophycin (iCP) between 20 and 28 kDa; an intermediate product of sCPat around 17 kDa, appearing only in the initial stages of synthesis; the primer, visible as a diffuse 10 kDa band (lanes 1-4) (Otterbach, 2010). PageRuler™ Prestained (Thermo Scientific) was applied in lane M, the positions of standard markers are indicated on the right.

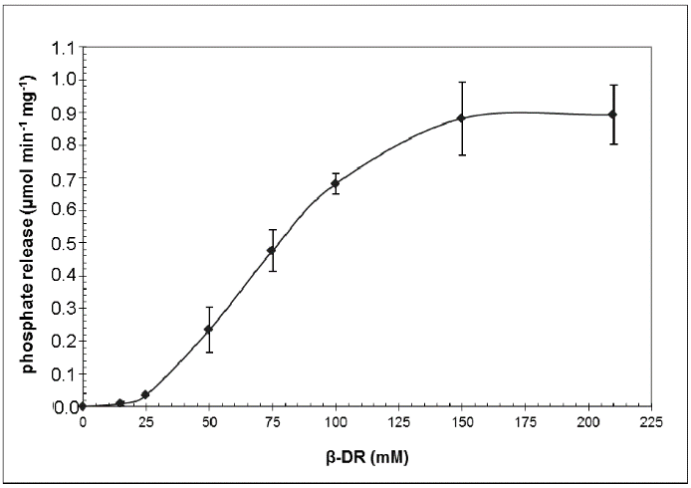

FIGURE S2: *In vitro* kinetics of H_{10}-CphA2 from *A. variabilis*. *In vitro* phosphate release after 15 min at different β-aspartyl-arginine (β-DR) concentrations (n=6).

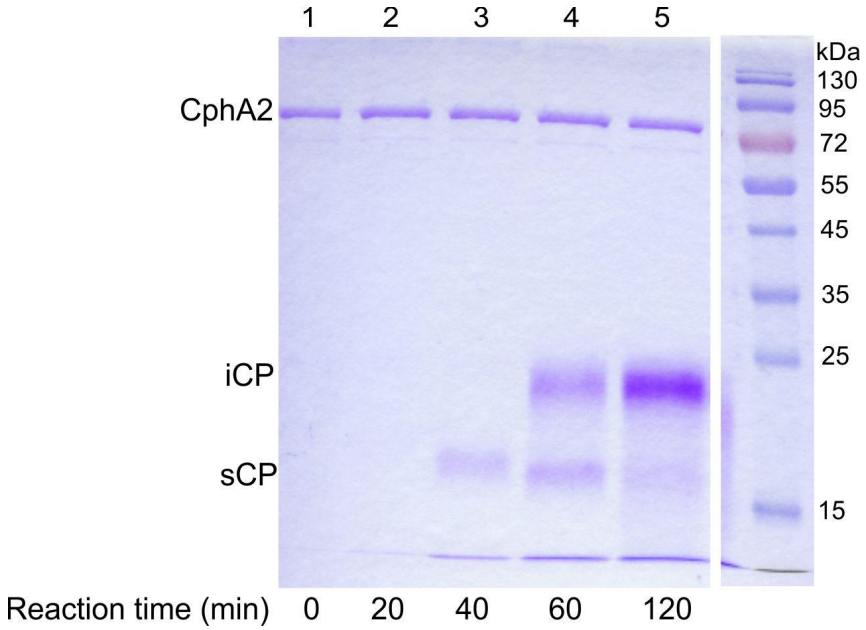

FIGURE S3: Cyanophycin synthesis by pure H_{10}-CphA2 from *Cyanothece* sp. PCC 7425.
Recombinant H_{10}-CphA2 from *Cyanothece* was applied in an *in vitro* standard assay.
In vitro synthesis of CP over 2 hours: in lanes 1-5, 2 µl standard reaction mixture was loaded per lane at time point: lane 1, t=0 min; lane 2, t=20 min; lane 3, t=40 min; lane 4, t=60 min; lane 5, t=120 min. Proteins and cyanophycin analyzed on a 15% acrylamide/bisacrylamide (29:1) gel were stained with Coomassie Brilliant Blue R-250. H_{10}-CphA2 appeared at 74 kDa, water insoluble cyanophycin (iCP) between 20 and 25 kDa. Water soluble cyanophycin (sCP) appeared as intermediate in the early stages of synthesis. The positions of standard markers (PageRuler™ Prestained; Thermo Scientific) are indicated on the right.

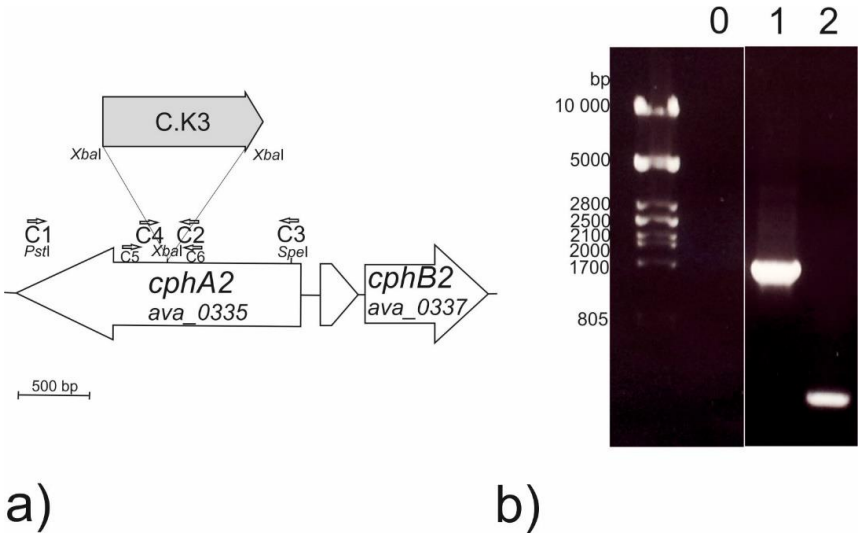

FIGURE S4: Generation and characterization of *cphA2* mutant in *A. variabilis*. a) Schematic of the genomic region surrounding *ava_0335* and the gene inactivation strategy by insertional mutagenesis. Inactivation of *ava_0335* was done by inserting the C.K3 cassette via *Xba*I. Positions of PCR primers are indicated (see Table S1). b) PCR analysis of *cphA2* mutant with primer C5 and C6.Lane 0: negative control without DNA; lane 1: DNA of *cphA2* mutant (including C.K3;1810 bp); lane 2: wild type-DNA (720 bp).

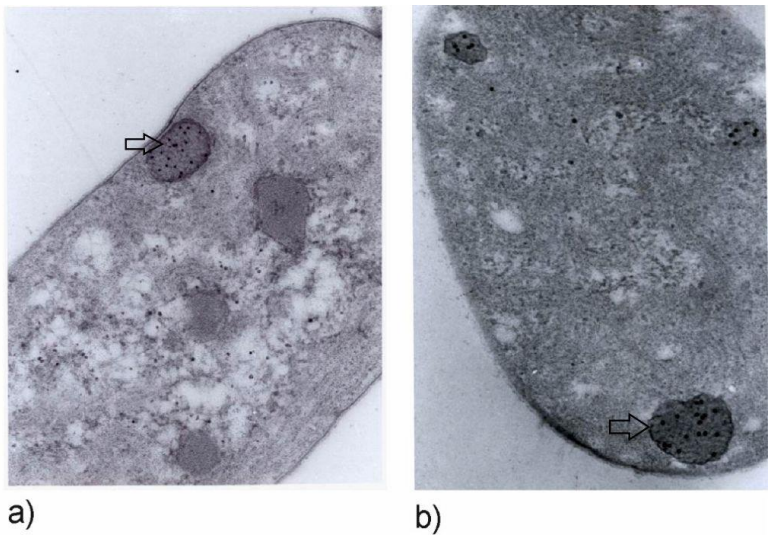

FIGURE S5: Localization of cyanophycin. Electron micrographs of *A. variabilis* wt and CphA2 lacking mutant cells. Ultrastructural investigations were performed using electron microscopy following the immunocytochemical visualization of cyanophycin with antisera raised against cyanophycin and a gold coupled anti-rabbit immunoglobulin G antibody in *Anabaena* cultures. a) *A. variabilis* wt vegetative cell with cyanophycin granules (arrow), treated with anti- cyanophycin antisera (1:20; magnification 44,000 x). b) Vegetative cell of *cphA2* disruption mutant containing cyanophycin granules (arrow), treated with anti-cyanophycin antisera (1:20; 60,000 x).

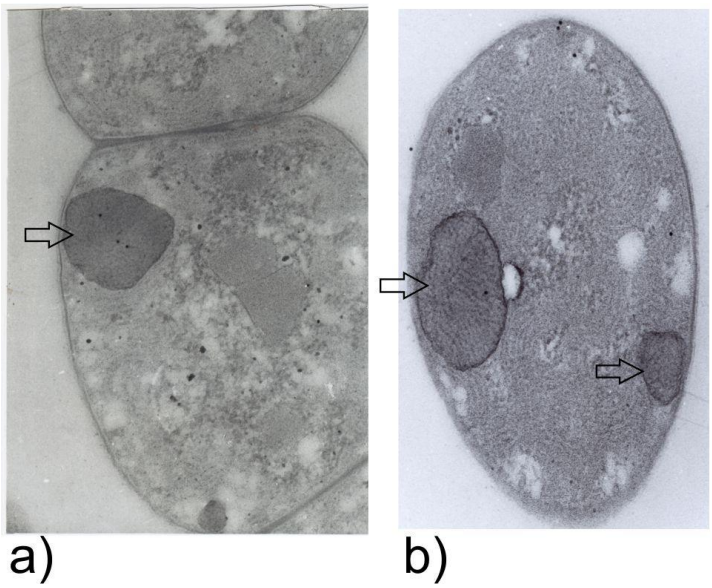

FIGURE S6: Localization of CphA2 in vegetative cells. Electron micrographs of *A*. *variabilis* wt and *cphA2* mutant cells grown under N_2-fixing conditions. Ultrastructural investigations were performed using electron microscopy following the immunocytochemical visualization of CphA2 with antisera raised against CphA2 and a gold coupled anti-rabbit immunoglobulin G antibody in *Anabaena* cultures. a) *A*. *variabilis* wt vegetative cell containing cyanophycin granules (arrow), treated with anti-CphA2 antisera (1:100; magnification 45,500 x). b) Vegetative cell of *cphA2* mutant containing cyanophycin granules (arrows), treated with anti-CphA2 antisera as control (1:100; 48,000 x).

TABLE S1: Oligodeoxynucleotide primers used in this study.

Objectives	Primer	Sequence (5'→3')
H_{10}-CphA2 CphA	A.1	CCAGAGGTTTAGCACATATGGTTCAGG
(ava_0335)	A.2	GTTGCAATGCAACGTCTCGAGGGTG
GST-CphA2	B.1	GCGGATCCATGGTTCAGGAAACAAGCACCG
(ava_0335)	B.2	GCGCGGCCGCTTAGAGGATGGAGCCAATTTC
mutagenesis	C.1	GGTTCATCTGCAGCTAATGTGTAG
	C.2	GTAGCCGCTCTAGAACGTCATCCTGC
	C.3	GGTTCAAATCCCTAACTAGTTACAGG
	C.4	GCAGGATGACGTTCTAGAGCGG
	C.5	CCAAGATTCAGAAAGGTCTT
	C.6	CCACCTTTAATTGCGACAGCC
H_{10}-CphA2	D.1	TATCATATGGTTCTGGATCACG
(Cyan7425_4446)	D.2	AATCTCGAGTTATAAGATCGTCG

TABLE S2: Distribution of cyanophycin synthetases among cyanobacteria. The counts of CphA1 and CphA2 within the five section of cyanobacteria referring to the cyanobacterial genomes summarized in Table S3.

Section	**I**	**II**	**III**	**IV**	**V**	**I-V**
number with CphA1	42	6	33	21	11	113
number with CphA2	7	3	10	15	9	44
number with CphA1 and CphA2	7	3	10	15	9	44
number of sequenced cyanobacteria	83	6	34	21	11	155
percentage with CphA1	50.6	100.0	97.1	100.0	100.0	72.9
percentage with CphA2	8.4	50.0	29.4	71.4	81.8	28.4
percentage with CphA1 and CphA2	8.4	50.0	29.4	71.4	81.8	28.4

References

Otterbach, S. (2010).Vergleichende Untersuchung der *in vitro* Aktivität der Cyanophycin-Synthetasen aus *Desulfitobacterium hafniense* und verschiedenen Cyanobakterien. Berlin: Beuth University for Applied Sciences Berlin - Life Science and Technology Department.

Ziegler, K., Deutzmann, R., Lockau, W. (2002). Cyanophycin Synthetase-like Enzymes of non-cyanobacterial Eubacteria: Characterization of a Polymer produced by a recombinant Synthetase of *Desulfitobacterium hafniense*. *Z Naturforsch C: J Biosci* **57**, 522-529.

Table S3: Distribution of *cphA1* and *cphA2* in cyanobacteria.

organism	section	*cphA1*	*cphA2*
Acaryochloris marina MBIC11017^{T}	I		
Acaryochloris sp CCMEE 5410	I		
Chamaesiphon minutus PCC 6605	I	YP_007098979.1	
Crocosphaera watsonii WH 0003	I	WP_007311023.1	
Crocosphaera watsonii WH 8501	I	WP_007308444.1	
Cyanobacterium stanieri PCC 7202^{T}	I	YP_007165250.1	
Cyanobacterium aponimum PCC 10605^{T}	I	YP_007162985.1	
Cyanobium gracile PCC 6307^{T}	I		
Cyanobium sp. PCC 7001	I		
Cyanothece sp. ATCC 51142	I	YP_001803653.1	
Cyanothece sp. ATCC 51472	I	Cy51472_3251	
Cyanothece sp. CCY 0110	I	WP_008275037.1	WP_008278271.1
Cyanothece sp. PCC 7424	I	YP_002376197.1	YP_002375941.1
Cyanothece sp. PCC 7425	I	YP_002485516.1	YP_002485117.1
Cyanothece sp. PCC 7822	I	YP_003888052.1	YP_003887952.1
Cyanothece sp. PCC 8801	I	YP_002371193.1	
Cyanothece sp. PCC 8802	I	YP_003136756.1	
Dactylococcopsis salina PCC 8305	I		
Geminocystis herdmanii PCC 6308^{T}	I	WP_017295073.1	
Gloeobacter violaceus PCC 7421^{T}	I	NP_927272.1	
Gloeocapsa sp. PCC 73106	I	WP_006530902.1	
Gloeocapsa sp. PCC 7428	I	YP_007126970.1	YP_007127176.1
Halothece sp. PCC 7418	I		
Microcystis sp. T1-4	I	WP_008206266.1	
Microcystis aeruginosa DIANCHI905	I	WP_002746167.1	
Microcystis aeruginosa NIES-843	I	YP_001657760.1	

organism	**section**	***cphA1***	***cphA2***
Microcystis aeruginosa PCC 7806	I		
Microcystis aeruginosa PCC 7941	I	WP_002774131.1	
Microcystis aeruginosa PCC 9432	I	WP_002754721.1	
Microcystis aeruginosa PCC 9443	I	WP_002766570.1	
Microcystis aeruginosa PCC 9701	I	WP_002804175.1	
Microcystis aeruginosa PCC 9717	I	WP_004266767.1	
Microcystis aeruginosa PCC 9806	I	WP_002798889.1	
Microcystis aeruginosa PCC 9807	I	WP_002789032.1	
Microcystis aeruginosa PCC 9808	I	WP_002794881.1	
Microcystis aeruginosa PCC 9809	I	WP_004160447.1	
Microcystis aeruginosa SPC777	I	WP_016517123.1	
Microcystis aeruginosa TAIHU 98	I	WP_002736719.1	
Prochlorococcus marinus AS 9601	I		
Prochlorococcus marinus MIT 9202	I		
Prochlorococcus marinus MIT 9211	I		
Prochlorococcus marinus MIT 9215	I		
Prochlorococcus marinus MIT 9301	I		
Prochlorococcus marinus MIT 9303	I		
Prochlorococcus marinus MIT 9312	I		
Prochlorococcus marinus MIT 9313	I		
Prochlorococcus marinus MIT 9515	I		
Prochlorococcus marinus NATL 1A	I		
Prochlorococcus marinus NATL 2A	I		
Prochlorococcus marinus, subsp. marinus CCMP 1375^{T}	I		
Prochlorococcus marinus, subsp. pastoris CCMP 1986	I		
Prochloron didemni^{T} P1	I		
Synechococcus elongatus PCC 6301	I		
Synechococcus elongatus PCC 7942	I		

organism	**section**	***cphA1***	***cphA2***
Synechococcus sp. BL 107	I		
Synechococcus sp. CB 0101	I		
Synechococcus sp. CB 0205	I		
Synechococcus sp. CC 9311	I		
Synechococcus sp. CC 9605	I		
Synechococcus sp. CC 9902	I		
Synechococcus sp. JA-2-3B	I	YP_477153.1	YP_479091.1
Synechococcus sp. JA-3-3Ab	I		
Synechococcus sp. PCC 6312	I	YP_007061011.1	
Synechococcus sp. PCC 7002	I	YP_001735638.1	
Synechococcus sp. PCC 7335	I	WP_006453792.1	
Synechococcus sp. PCC 7336	I		
Synechococcus sp. PCC 7502	I	YP_007104567.1	
Synechococcus sp. RCC307	I		
Synechococcus sp. RS 9916	I		
Synechococcus sp. RS 9917	I		
Synechococcus sp. WH 5701	I		
Synechococcus sp. WH 7803	I		
Synechococcus sp. WH 7805	I		
Synechococcus sp. WH 8016	I		
Synechococcus sp. WH 8102	I		
Synechococcus sp. WH 8109	I		
Synechocystis sp. GT-S, PCC 6803	I	NP_441210.1	
Synechocystis sp. PCC 6803	I	NP_441210.1	
Synechocystis sp. PCC 6803, GT-I	I	NP_441210.1	
Synechocystis sp. PCC 6803, PCC-N	I	NP_441210.1	
Synechocystis sp. PCC 7509	I	WP_009632376.1	WP_009633965.1
Thermosynechococcus elongatus BP-1	I	NP_682960.1	

organism	**section**	***cphA1***	***cphA2***
unidentified cyanobacterium UCYN-A	I		
Chroococcidiopsis sp. PCC 6712	II	Chr6712_2537	Chr6712_4677
Chroococcidiopsis thermalis PCC 7203	II	YP_007092687.1/ YP_007094526.1/ YP_007089464.1	YP_007090465.1
Pleurocapsa sp. PCC 7319	II	WP_019505758.1	
Pleurocapsa sp. PCC 7327	II	YP_007081042.1	
Stanieria cyanosphaera PCC 7437	II	YP_007131141.1	YP_007133330.1
Xenococcus sp. PCC 7305	II	WP_006511630.1	
Arthrospira maxima CS-328	III	WP_006669096.1	
Arthrospira platensis C1	III	WP_006621431.1	
Arthrospira platensis NIES-39	III	YP_005068483.1	
Arthrospira platensis Paraca	III	WP_006618920.1	
Arthrospira sp. PCC 8005	III	WP_006621431.1	
Crinalium epipsammum PCC 9333	III	YP_007142649.1	YP_007141742.1
Cyanobacterium sp. ESFC-1	III	WP_018398240.1	
Geitlerinema sp. PCC 7105	III	WP_017663676.1	
Geitlerinema sp. PCC 7407	III	YP_007108407.1	
Leptolyngbya boryana PCC 6306	III	WP_017289742.1	WP_017291321.1
Leptolyngbya sp. PCC 6406	III		
Leptolyngbya sp. PCC 7375	III	WP_006516067.1	
Leptolyngbya sp. PCC 7376	III	YP_007071352.1	
Lyngbya sp. PCC 8106	III	WP_009782401.1	
Microcoleus chthonoplastes PCC 7420	III	WP_006105197.1	
Microcoleus sp. PCC 7113	III	YP_007120383.1	YP_007124800.1
Microcoleus vaginatus PCC 9802	III	Mvag_PCC9802_DRAFT2_00007800	Mvag_PCC9802_DRAFT2_00037790
Microcoleus vaginatus FGP-2	III	WP_006635871.1	WP_006632735.1
Moorea producta 3L^{T}	III	WP_009149562.1	

organism	**section**	***cphA1***	***cphA2***
Nodosilinea nodulosa PCC 7104	III	WP_017296720.1	
Oscillatoria acuminata PCC 6304	III	YP_007088828.1	
Oscillatoria formosa PCC 6407	III	WP_019487504.1	Oscil6407DRAFT_00050400
Oscillatoria nigro-viridis PCC 7112	III	YP_007117420.1	YP_007114462.1
Oscillatoria sp. PCC 10802	III	WP_017719728.1	WP_017720384.1
Oscillatoria sp. PCC 6506	III	WP_007353380.1	WP_007353926.1
Oscillatoriales sp. JSC-1	III	CYJSC1_DRAFT_39170	CYJSC1_DRAFT_33300
Oscillatoriales sp. JSC-12	III	WP_009768706.1	
Prochlorothrix hollandica PCC 9006	III	WP_017712275.1	
Pseudanabaena sp. PCC 6802	III	WP_019501513.1	
Pseudanabaena sp. PCC 7367	III	YP_007101627.1	
Pseudanabaena sp. PCC 7429	III	WP_009625973.1	
Spirulina major PCC 6313	III	Spi6313_2188	
Spirulina subsalsa PCC 9445	III	WP_017306758.1	
Trichodesmium erythraeum IMS101	III	YP_721690.1	
Anabaena sp. 90	IV	YP_006996498.1	
Anabaena cylindrica PCC 7122	IV	YP_007156998.1	YP_007158843.1/ YP_007158603.1
Anabaena sp. PCC 7108	IV	WP_016950701.1	
Anabaena variabilis ATCC 29413	IV	YP_322331.1	YP_320856.1
Calothrix desertica PCC 7102	IV	Cal7102DRAFT_09819	
Calothrix sp. PCC 6303	IV	YP_007140001.1	
Calothrix sp. PCC 7103	IV	WP_019494322.1	WP_019490070.1
Calothrix sp. PCC 7507	IV	YP_007064146.1	YP_007068318.1
Cylindrospermopsis raciborskii CS-505	IV	WP_006276546.1	WP_006277172.1
Cylindrospermum stagnale PCC 7417	IV	YP_007149845.1	YP_007148177.1
Microchaete sp. PCC 7126	IV	WP_017652039.1	WP_017652597.1
Nodularia spumigena CCY9414	IV	WP_006198319.1	WP_006195032.1

organism	**section**	***cphA1***	***cphA2***
Nostoc azollae 0708	IV	YP_003720623.1	Aazo_4352
Nostoc punctiforme PCC 73102	IV	YP_001869064.1	YP_001865424.1
Nostoc sp. PCC 7107	IV	YP_007051706.1	YP_007052728.1
Nostoc sp. PCC 7120	IV	NP_487919.1	NP_484617.1
Nostoc sp. PCC 7524	IV	YP_007078177.1	YP_007073872.1
Raphidiopsis brookii D9	IV	WP_009342408.1	
Rivularia sp. PCC 7116	IV	YP_007053936.1	
Scytonema hofmanni PCC 7110	IV	WP_017742891.1	WP_017744393.1
Scytonema hofmanni UTEX 2349	IV	Tol9009DRAFT_00042590	Tol9009DRAFT_00023600
Chlorogloeopsis fritschii PCC 6912	V	UYC_07438	UYC_06945
Chlorogloeopsis fritschii PCC 9212	V	WP_016875500.1	WP_016875098.1
Fischerella muscicola PCC 73103	V	WP_016860063.1	WP_016863096.1
Fischerella muscicola PCC 7414	V	WP_016870213.1	WP_016866890.1
Fischerella sp. JSC-11	V	WP_009456001.1	
Fischerella sp. PCC 9339	V	WP_017309080.1	WP_017311862.1
Fischerella sp. PCC 9431	V	Fis9431DRAFT_0672	Fis9431DRAFT_4081
Fischerella sp. PCC 9605	V	FIS9605DRAFT_06463	FIS9605DRAFT_03416
Fischerella thermalis PCC 7521	V	WP_016871305.1	
Mastigocladopsis repens PCC 10914	V	WP_017316633.1	WP_017318533.1
unidentified cyanobacterium PCC 7702	V	WP_017322792.1	WP_017319496.1

Microbiology (2015), **161**, 1050–1060 DOI 10.1099/mic.0.000055

Identification of the light-independent phosphoserine pathway as an additional source of serine in the cyanobacterium *Synechocystis* sp. PCC 6803

Friederike Klemke,[1] Antje Baier,[1] Henning Knoop,[2] Ramona Kern,[3] Jiri Jablonsky,[4] Gabriele Beyer,[1] Thomas Volkmer,[1] Ralf Steuer,[2] Wolfgang Lockau[1] and Martin Hagemann[3]

Correspondence
Martin Hagemann
martin.hagemann@uni-rostock.de

[1]Plant Biochemistry, Humboldt University Berlin, Germany

[2]Institute of Theoretical Biology, Humboldt University Berlin, Germany

[3]Department of Plant Physiology, University of Rostock, Germany

[4]Laboratory of Experimental Complex Systems, FFPW, University of South Bohemia, Czech Republic

L-Serine is one of the proteinogenic amino acids and participates in several essential processes in all organisms. In plants, the light-dependent photorespiratory and the light-independent phosphoserine pathways contribute to serine biosynthesis. In cyanobacteria, the light-dependent photorespiratory pathway for serine synthesis is well characterized, but the phosphoserine pathway has not been identified. Here, we investigated three candidate genes for enzymes of the phosphoserine pathway in *Synechocystis* sp. PCC 6803. Only the gene for the D-3-phosphoglycerate dehydrogenase is correctly annotated in the genome database, whereas the 3-phosphoserine transaminase and 3-phosphoserine phosphatase (PSP) proteins are incorrectly annotated and were identified here. All enzymes were obtained as recombinant proteins and showed the activities necessary to catalyse the three-step phosphoserine pathway. The genes coding for the phosphoserine pathway were found in most cyanobacterial genomes listed in CyanoBase. The pathway seems to be essential for cyanobacteria, because it was impossible to mutate the gene coding for PSP in *Synechocystis* sp. PCC 6803 or in *Synechococcus elongatus* PCC 7942. A model approach indicates a 30–60 % contribution of the phosphoserine pathway to the overall serine pool. Hence, this study verified that cyanobacteria, similar to plants, use the phosphoserine pathway in addition to photorespiration for serine biosynthesis.

Received 9 December 2014
Accepted 17 February 2015

INTRODUCTION

The amino acid L-serine (hereafter serine) belongs to the building blocks of proteins and is a key intermediate of central carbon/nitrogen metabolism. Serine is involved in the biosynthesis of purines and pyrimidines, and serves as an important precursor for other essential compounds, including the amino acids glycine and cysteine or phospholipids (Walton & Woolhouse, 1986). Recently, it has been shown that serine also acts as a metabolic signal for the transcriptional regulation of photorespiratory genes in the model plant *Arabidopsis thaliana* (Timm *et al.*, 2013).

In plants, animals and heterotrophic bacteria, serine is synthesized via the so-called phosphorylated or phosphoserine pathway, with phosphoserine as a key intermediate (Umbarger *et al.*, 1963; Ros *et al.*, 2014) (KEGG database: http://www.genome.jp/kegg-bin/show_pathway?map=map00260&show_description=show). The pathway comprises three enzymatic reactions and starts with the precursor 3-phosphoglycerate (3PGA) (Fig. 1). 3PGA can be synthesized via multiple metabolic routes, such as glycolysis, gluconeogenesis and, in oxygenic phototrophic organisms, the photosynthetic Calvin–Benson cycle. The first enzyme of the phosphoserine pathway, D-3-phosphoglycerate dehydrogenase (PGDH, EC 1.1.1.95), catalyses the oxidation of 3PGA to 3-phosphohydroxypyruvate using NAD^+ or

Abbreviations: GST, glutathione *S*-transferase; 2PG, 2-phosphoglycolate; 3PGA, 3-phosphoglycerate; PGDH, D-3-phosphoglycerate dehydrogenase; PSP, phosphoserine phosphatase; PSTA, phosphoserine transaminase.

Supplementary material is available with the online Supplementary Material.

 000055 © 2015 The Authors *Printed in Great Britain*

$NADP^+$ as cofactor. Then, phosphoserine transaminase (PSTA, EC 2.6.1.52), a pyridoxal-5′-phosphate-dependent enzyme, converts 3-phosphohydroxypyruvate into 3-phosphoserine using glutamate as an amino donor that is converted into 2-oxoglutarate. In the final step, 3-phosphoserine is hydrolysed by the enzyme 3-phosphoserine phosphatase (PSP, EC 3.1.3.3) to serine and orthophosphate (Greenberg & Ichihara, 1957).

In addition to this ubiquitous serine synthesis pathway, organisms performing oxygenic photosynthesis, such as cyanobacteria, algae and plants, use the photorespiratory 2-phosphoglycolate (2PG) metabolism as an alternative, light-dependent pathway to generate serine (Fig. 1). Photorespiration (often also called the C2 cycle) is responsible for removing toxic 2PG. In this metabolic cycle, two molecules of 2PG are converted into one molecule of 3PGA (reviewed by Bauwe *et al.*, 2010). In the entrance reaction, 2PG is dephosphorylated to glycolate that is then oxidized to glyoxylate, which is subsequently aminated to yield glycine. The glycine is used by the glycine cleavage system that splits glycine into CO_2, NH_3, $NADH_2$ and an active C1-unit, i.e. methylenetetrahydrofolate. The active C1-unit is then used by serine hydroxymethyltransferase to convert another glycine molecule into serine, regenerating the tetrahydrofolate carrier. To close the C2 cycle, serine is converted into hydroxypyruvate that is then oxidized to glycerate, which is finally phosphorylated by glycerate 3-kinase to 3PGA. It has been shown that intermediates of the cycle can be used for diverse biochemical purposes (Bauwe *et al.*, 2010). In particular, photorespiratory glycine and serine serve in illuminated plant leaves for protein synthesis. Thus, plants utilize two routes for serine biosynthesis: the light-dependent photorespiratory cycle, which is the main source of serine during the daytime in photosynthetic cells, and the light-independent phosphoserine pathway, which is used in heterotrophic cells and during the night.

Cyanobacteria evolved oxygenic photosynthesis ~3 billion years ago and served as ancestors for plant plastids (e.g. Ochoa de Alda *et al.*, 2014). It has been shown that not only are proteins necessary for oxygenic photosynthesis, but also that many enzymes for plant primary metabolism evolved from ancestral cyanobacterial proteins (Martin & Schnarrenberger, 1997). Therefore, cyanobacteria often serve as models to study plant primary metabolism. The cyanobacterium *Synechocystis* sp. PCC 6803 (hereafter *Synechocystis*) is one of the most popular cyanobacterial model strains. *Synechocystis* is naturally competent for transformation and performs site-specific recombination, which made it possible to obtain targeted mutants (Grigorieva & Shestakov, 1982). Due to its capability of heterotrophic growth, many photosynthetic mutants could be isolated (Anderson & McIntosh, 1991). The complete genome sequence of *Synechocystis* was published in 1996 (Kaneko *et al.*, 1996). The available complete genome allows us to search for the metabolic capabilities of this model strain at the well-curated database CyanoBase (http://genome.microbedb.jp/cyanobase/Synechocystis). Genes for the plant-like C2 cycle that includes the light-dependent pathway of serine

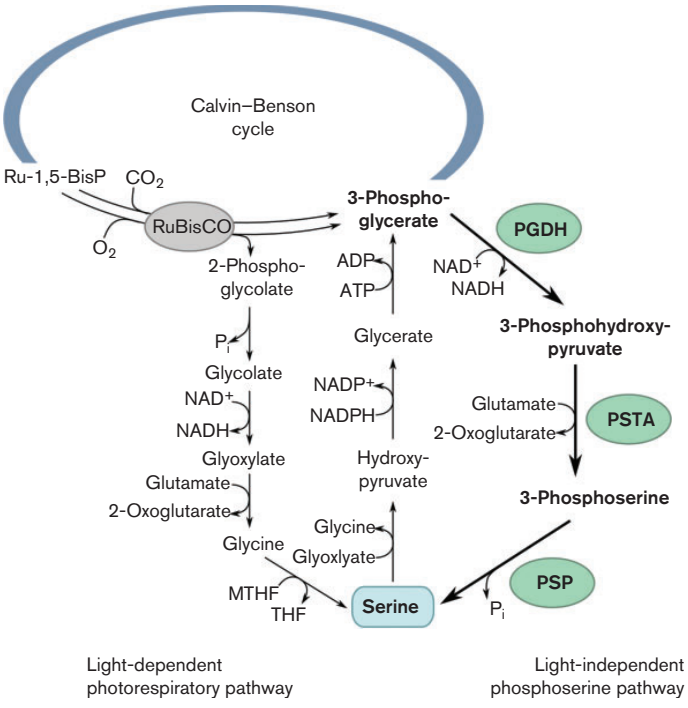

Fig. 1. Known pathways of serine biosynthesis in organisms performing oxygenic photosynthesis. The light-dependent photorespiratory pathway of serine biosynthesis (left-hand side) uses 2PG that is produced in equimolar amounts with 3PGA from ribulose 1,5-bisphosphate (Ru-1,5-BisP) in the oxygenase reaction of ribulose 1,5-bisphosphate carboxylase/oxygenase (RuBisCO). The light-independent or phosphoserine pathway (right-hand side) of serine biosynthesis includes three enzymatic reactions. It starts with 3PGA that is converted via PGDH (EC 1.1.1.95) and PSTA (EC 2.6.1.52) into phosphoserine. Serine is finally obtained via dephosphorylation of the intermediate by PSP (EC 3.1.3.3). MTHF, Methylenetetrahydrofolate; THF, tetrahydrofolate.

biosynthesis were found in *Synechocystis* and were subsequently experimentally verified (Eisenhut *et al.*, 2008).

Surprisingly, not all enzymes for the light-independent synthesis of serine are annotated in the *Synechocystis* genome nor in any other cyanobacterial genome. However, enzyme activities related to the phosphoserine pathway were detected in crude extracts of cyanobacteria (Colman & Norman, 1997). Recent serine and glycine labelling experiments showed a ^{13}C enrichment of serine in *Synechocystis* that was substantially higher than that of glycine (Huege *et al.*, 2011; Young *et al.*, 2011), indicating that serine was synthesized even in the light directly from 3PGA rather than by photorespiration via glycine. These experiments suggested that the phosphoserine pathway was not only active in *Synechocystis*, but contributed substantially to serine production. Another hint for the existence of an alternative serine synthesis route came from the observation that *Synechocystis* mutants blocked in the C2 cycle were dependent on high CO_2, but not on serine supplementation (Eisenhut *et al.*, 2008). However, genome-scale metabolic modelling showed that light-dependent serine biosynthesis via the photorespiratory cycle could meet the demand for serine of *Synechocystis* (Knoop *et al.*, 2010). This controversial situation initiated our study to identify the genes coding for the light-independent, phosphoserine pathway in *Synechocystis*. Here, we present bioinformatic, biochemical and genetic data showing that the phosphoserine pathway is present in *Synechocystis*, and perhaps all cyanobacteria, where it cooperates with the photorespiratory cycle in serine synthesis.

METHODS

Sequence analysis. Amino acid sequences were aligned using CLUSTAL W version 2.1 (Larkin *et al.*, 2007) and formatted using GeneDoc. (http://www.nrbsc.org/gfx/genedoc/gddl.htm). Sequence similarities were determined using EMBOSS Needle software (http://www.ebi.ac.uk/Tools/psa/emboss_needle/). Conserved motifs in amino acid sequences were detected using the PROSITE database (http://prosite.expasy.org/) (Sigrist *et al.*, 2013).

Bacterial strains and culture conditions. *Synechocystis* and *Synechococcus elongatus* PCC 7942 (hereafter *Synechococcus*) and their mutants were grown photoautotrophically under continuous illumination as described previously (Baier *et al.*, 2004). Briefly, the cells were cultivated under light (60 μmol photons m^{-2} s^{-1}; cool-white fluorescent lamps) and 30 °C in BG11 medium buffered with 10 mM TES at pH 8.0 (Rippka *et al.*, 1979). Cells were grown on plates using agar-solidified BG11 medium. Mutant clones were first selected on media containing 10 μg kanamycin ml^{-1}. To enforce segregation, the mutant clones were then cultivated in the presence of 300 μg kanamycin ml^{-1}.

Escherichia coli strains DH5α, BL21 and BL21(DE3) (Novagen; Merck Chemicals) were grown at 37 °C in Luria–Bertani (LB) medium supplemented with 100 μg ampicillin ml^{-1} or 50 μg kanamycin ml^{-1} when appropriate. Cells were grown in Erlenmeyer flasks with shaking at 300 r.p.m.

Mutant construction. To obtain the *Synechocystis* deletion PSP mutant, the gene *slr1124* was replaced by a kanamycin resistance cartridge. The up- and downstream regions of *slr1124* were amplified by PCR using chromosomal DNA from *Synechocystis* as template and specific primers (Table S1, available in the online Supplementary Material) containing added restriction sites for cloning (*Sac*I and *Spe*I) and for insertion of the antibiotic resistance cartridge C.K3 (*Xba*I). After restriction, these PCR fragments were ligated into the pBluescript SKII+ vector (Stratagene). The kanamycin resistance cartridge C.K3 was obtained from plasmid pRL448 (Elhai & Wolk, 1988) by *Xba*I restriction and was ligated into the *Xba*I site created inside *slr1124*, generating plasmid pSKII_KO-PSP6803 (Fig. S1).

To obtain the *Synechococcus* PSP deletion mutant, the Synpcc7942_0485 gene was replaced by the kanamycin resistance cartridge. The amplified PCR product of the upstream region of the gene was cut with *Sac*I and *Xba*I (for primers see Table S1) and the PCR product of the downstream region was cut with *Xba*I and *Apa*I. These fragments were ligated into the pBluescript SKII+ vector. The C.K3 cartridge was obtained as a *Xba*I fragment and ligated into the plasmid, yielding plasmid pSKII+_KO-PSP7942 (Fig. S2).

The final plasmids were checked by DNA sequencing and transferred to *Synechocystis* or *Synechococcus* by transformation (Grigorieva & Shestakov, 1982). Recombinant clones were initially selected on media containing kanamycin and 0.5 mM serine. To achieve complete segregation, kanamycin-resistant *Synechocystis* clones were cultivated under the following conditions: (i) continuous light of 60 or 120 μmol photons m^{-2} s^{-1} with and without addition of 0.5 or 1 mM serine; (ii) 5 days' incubation in the dark with 5 mM glucose; and (iii) 5 days' incubation in the dark with 5 mM glucose and 1 mM serine. Kanamycin-resistant *Synechococcus* clones were incubated in the presence of 2 mM serine under continuous light of 60 μmol photons m^{-2} s^{-1} or in a 12 h/12 h light/dark cycle for up to 4 weeks. The genotype of the mutants was confirmed by PCR using genomic DNA acquired from mutant cells and specific primers (up-fw*slr1124* and down-PCR for *Synechocystis*; up-PCR and down-PCR for *Synechococcus*; Table S1).

Construction of expression plasmids. For the expression of *sll1908* in the *E. coli* vector pET28a (Novagen), the coding sequence of the gene was amplified by PCR using DNA of *Synechocystis* and gene-specific primers with added restriction sites for cloning (Table S1). The resulting fragment was first cloned into pGemT (Promega). After sequence confirmation, *sll1908* was cloned into pET28a using the enzymes *Nde*I and *Eco*RI, resulting in plasmid pET28a_*sll1908*.

For the expression of *sll1559* in the *E. coli* vector pGEX-6P1 (GE Healthcare), the PCR product was cloned into pJET1.2 (ThermoScientific, Fermentas). After cleavage by *Bam*HI and *Not*I, the resulting fragment was inserted into pGEX-6P1, resulting in pGEX_*sll1559*. For the expression of *slr1124* in the *E. coli* vector pGEX-6P1, the PCR product was blunt-end-ligated into pJET1.2. After restriction by the corresponding endonucleases, the resulting fragment was cloned into pGEX-6P1, resulting in plasmid pGEX_*slr1124*.

Protein expression and purification of Sll1908, Sll1559 and Slr1124. To express *sll1908*, chemically competent cells of *E. coli* strain BL21(DE3) were transformed with pET28a_*sll1908*. After growth of the cells at 30 °C in LB medium supplemented with 50 μg kanamycin ml^{-1} for 6 h, protein production was induced by the addition of 1 mM IPTG. *E. coli* cells were then cultured overnight at 30 °C. Cell extract was obtained by sonication with homogenization buffer (20 mM sodium phosphate, pH 7.4, 500 mM NaCl). The His-tagged fusion protein was purified by affinity chromatography on Ni-NTA columns (Macherey-Nagel) and eluted using increased imidazol concentrations. Finally, the enzyme was desalted using PD10 columns (GE Healthcare) and stored in 20 mM sodium phosphate buffer, pH 7.4.

Chemically competent cells of *E. coli* strain BL21 were transformed with pGEX_*sll1559* and pGEX_*slr1124*. The cells were cultured in LB medium supplemented with 100 μg ampicillin ml^{-1} at 37 °C. Protein expression was induced by the addition of 1 mM IPTG. Cells were subsequently cultivated overnight at 18 °C and then harvested by centrifugation (15 min, 3800 ***g***). Total protein of *E. coli* was extracted by sonication. Cell debris was removed by centrifugation (15 min, 20 000 ***g***) to obtain the cell lysates. The glutathione *S*-transferase (GST)-tagged proteins were purified by affinity chromatography using Glutathione Sepharose 4B (GE Healthcare) performed in batch mode according to the manufacturer's instructions. The GST-tag was cleaved off the purified proteins by PreScission Protease (GE Healthcare) overnight at 4 °C. The resulting proteins Sll1559 and Slr1124 were stored in a buffer containing 50 mM Tris/HCl, pH 8.0, 10 mM NaCl and 1 mM $MgCl_2$.

Electrophoresis and protein quantification. The purity of the recombinant enzymes was checked by SDS-PAGE (12 %, w/v, acrylamide, 0.41 %, w/v, methylene bisacrylamide) in the buffer system of Laemmli (1970). The gels were stained with Coomassie blue R250. A Fermentas PageRuler Prestained Protein Ladder (10–170 kDa; Thermo Scientific) was used as molecular mass standard. Protein concentrations of the purified enzymes were determined according to Lowry *et al.* (1951).

Size-exclusion chromatography. The purity and the molecular mass of the native enzymes were validated by size-exclusion chromatography on a calibrated column (TricornSuperdex 200 10/300 GL; GE Healthcare) using 50 mM sodium phosphate buffer, pH 7.4, containing 300 mM NaCl and 50 mM KCl as running buffer. The flow rate was 0.5 ml min^{-1}. Elution of the enzymes was monitored by continuous absorption measurement (A_{280}). Ferritin (440 kDa) combined with standard protein marker (Gel Filtration Standard; Bio-Rad) was used for column calibration.

Enzyme assays and kinetic analyses

PGDH assay. The activity of the purified PGDH (Sll1908) was determined according to Ho *et al.* (1999). The 3PGA oxidation rate was measured in a standard reaction mixture containing 200 mM Tris/HCl, pH 9.0, 2.5 mM EDTA, 2.0 mM DTT, 2.0 mM NAD^+, 2.0 mM 3PGA and 10 μg Sll1908 in a final volume of 1 ml. Rates of NAD^+ reduction were monitored at 340 nm (ε=6.22 mM^{-1} cm^{-1}) and 30 °C. One unit of activity was defined as the amount of Sll1908 forming 1.0 μmol NADH min^{-1} under standard assay conditions. To check the effect of NADH, 0.1 mM NADH was added to the standard reaction mixture. For substrate specification, 5 mM of each potential substrate was added to the reaction mixture with 0.375 mM NAD^+ or NADH.

PGDH kinetics were analysed in the presence of different amounts of the two substrates, NAD^+ and 3PGA. 3PGA was varied in the range 0.1–4.0 mM in the presence of 2.0 mM NAD^+, whereas NAD^+ was used in the range 0.1–2.0 mM with 2.0 mM 3PGA. The reactions were performed with saturating enzyme amounts. To determine K_m and V_{max} for each substrate, kinetic parameters were fit to the Michaelis–Menten equation by SigmaPlot 2006 Enzyme Kinetics Module 1.3. The optimal pH was determined at 28 °C in activity assays containing 4 mM NAD^+, 25 mM EDTA, 2 mM DTT, 2 mM 3PGA and 20 μg enzyme ml^{-1} in 200 mM Tris/HCl buffer in the range pH 7.0–9.0.

PSTA assay. PSTA catalyses the transamination of 3-phosphohydroxypyruvate to 3-phosphoserine with glutamate as amino donor. None of these substrates or reactions could be detected directly. Therefore, PSTA (Sll1559) activity was detected via the reduction of NAD^+ to NADH by PGDH. It is known that PGDH becomes increasingly inhibited by its own product, 3-phosphohydroxypyruvate, as shown for the enzyme of *A. thaliana* (Ho & Saito, 2001). Thus, only consumption of 3-phosphohydroxypyruvate via its transamination to 3-phosphoserine catalysed by PSTA leads to continuous activity of the PGDH measured as synthesis of NADH. PSTA activity was measured in a final volume of 1 ml by carrying out the PGDH standard assay and adding 7.4 μg PSTA (Sll1908) to form the substrate 3-phosphohydroxypyruvate. The co-substrate of PSTA, glutamate, was supplemented to 2 mM. The reaction was started at a constant rate of NADH development by addition of 4.4 μg PGDH (Sll1559). Rates of enhanced NAD^+ reduction were monitored at 340 nm at 30 °C. One unit of activity was defined as the amount of Sll1559 producing 1.0 μmol NADH min^{-1}. To determine PSTA kinetics, the substrate glutamate was varied in the range of 0–8 mM.

PSP assay. The activity of PSP (Slr1124) was measured using a colorimetric method to follow the release of phosphate via the malachite green assay at 650 nm (Lanzetta *et al.*, 1979). The PSP reaction was performed in standard buffer of 50 mM HEPES, pH 7.5, containing 10 mM NaCl, 1 mM $MgCl_2$, 1 mM DTT and 1 or 2 mM 3-phosphoserine at 30 °C. To determine the substrate specificity of PSP, several substrates such as 3-phosphoserine, *sn*-glycerol 3-phosphate, D(+)-3PGA and D(+)-2-phosphoglycerate (Sigma-Aldrich) were used in a final concentration of 1 mM. To test the effect of the end-product serine on PSP activity, 5 or 10 mM serine was added to the standard reaction mixture.

For kinetic analyses, the PSP phosphatase reaction was performed in the presence of 0–2.5 mM 3-phosphoserine. The reaction was started by addition of PSP (Slr1124) and was performed for 8 min at 30 °C. Aliquots of the reaction mixture were applied to the colorimetric malachite green assay. One unit of activity was defined as the amount of PSP producing 1.0 μmol phosphate min^{-1}.

Reconstruction of the phosphoserine pathway *in vitro*. The purified enzymes PGDH (9.0 μg) and PSTA (11.0 μg) were added to 1 ml PSTA standard assay containing PSP (11.0 μg). The reaction was started by addition of PGDH. NADH formation was monitored at 340 nm. At different time points, 25 μl aliquots of reaction mixture were transferred to 75 μl ice-cold water. Enzymes were inactivated by heating for 1 min at 95 °C. After cooling, aliquots were applied to the malachite green assay.

RESULTS AND DISCUSSION

Identification of putative enzymes of the phosphoserine pathway

Three enzymes are necessary to synthesize serine from 3PGA: PGDH, PSTA and PSP (Fig. 1). First, we searched for possible candidate genes coding for PGDH in the genome of *Synechocystis*. There was one putative PGDH homologue annotated as *serA* (*sll1908*) in CyanoBase (http://genome.microbedb.jp/cyanobase/Synechocystis/genes/sll1908). Hence, the protein Sll1908 was our prime candidate for PGDH.

The identification of a candidate gene coding for PSTA turned out to be more difficult, because multiple forms of transaminases exist and the substrate specificity of these enzymes is more difficult to predict from sequence features. PSTA belongs to proteins of the aminotransferase class V family (Interpro; http://prosite.expasy.org/PDOC00514). These proteins require pyridoxal 5′-phosphate as cofactor (Ouzounis & Sander, 1993), which is covalently bound by Lys197 in SerC of *Bacillus circulans* (Fig. 2) forming an

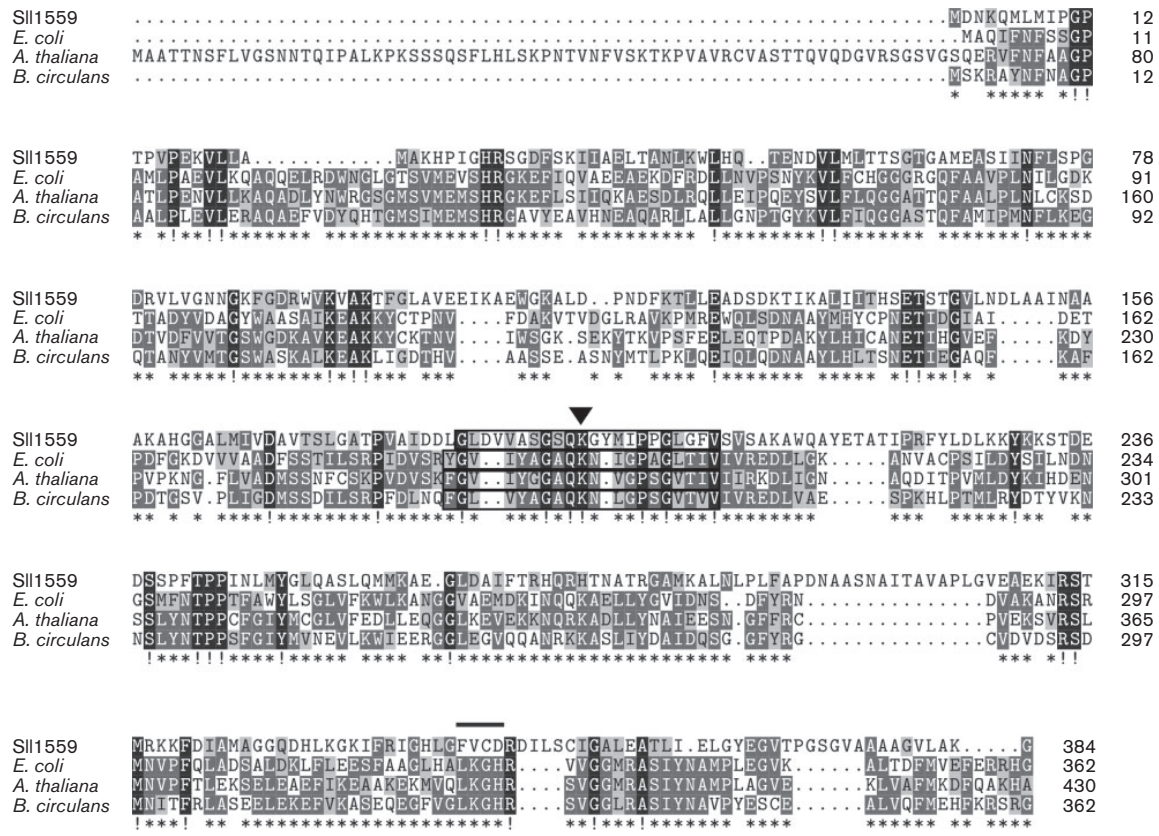

Fig. 2. Identification of conserved features in the primary structure of PSTAs from *Synechocystis* and other organisms. Multiple sequence alignment of amino acid sequences of PSTA of *Synechocystis* (Sll1559), *E. coli* (GenBank accession number C3TGD2) (Duncan & Coggins, 1986), *A. thaliana* (GenBank accession number Q96255) (Ho *et al.*, 1998) and *B. circulans* (GenBank accession number Q59196) (Battchikova *et al.*, 1996) using CLUSTAL W (Larkin *et al.*, 2007). The conserved motif that is characteristic for aminotransferase class V (surrounded by a frame) was determined by the PROSITE database (Sigrist *et al.*, 2013). The catalytic lysine forming an aldimine bond with pyridoxal 5′-phosphate is indicated by a triangle. The signature sequence for PSTA (LKG) is marked by a line (Belhumeur *et al.*, 1994). White letters on black, 100 % conserved; white letters on grey, 80 % conserved; black letters on grey, 60 % conserved.

aldimine bond (Belhumeur *et al.*, 1994). The corresponding domain can be found in aminotransferases and other enzymes including cysteine desulfurases (EC 4.4.1.-). PSTAs with aminotransferase class V domains are also known for *A. thaliana* (At4g35630) and *E. coli* (SerC).

To identify possible genes for PSTA in the genome of *Synechocystis*, a genome-wide Interpro search was performed using aminotransferase class V as a query. The scan revealed six candidates: *sll0704*, *sll1559*, *slr0077*, *slr0387*, *slr2143* and *slr5022*. Only the gene products of *sll1559* and *slr5022* show considerable similarities to aminotransferases, whereas the proteins coded by the other four genes are annotated as cysteine-specific enzymes. *sll1559* has previously been assumed to code for the photorespiratory serine-glyoxylate aminotransferase in *Synechocystis* (Eisenhut *et al.*, 2008). Interestingly, the Sll1559 protein showed sequence similarities to biochemically verified PSTAs, including the enzymes of *E. coli* (Duncan & Coggins, 1986), *A. thaliana* (Ho *et al.*, 1998), *B. circulans* (Battchikova *et al.*, 1996) and two Archaea (Helgadottir *et al.*, 2007). The amino acid sequence alignment displayed highly conserved regions (Fig. 2). The conserved amino acid sequence holding the motif of the aminotransferases class V is around position 200 of Sll1559 (Fig. 2, boxed). Presently, *sll1559* is wrongly annotated in CyanoBase as a gene coding for a soluble hydrogenase subunit (http://genome.microbedb.jp/cyanobase/Synechocystis/genes/sll1559). The four cysteine-dependent enzymes were excluded from further analyses and only the two genes coding for putative aminotransferases (*sll1559* and *slr5022*) were taken into further consideration.

Initially, the bioinformatic search for a putative PSP remained unsuccessful, because none of the biochemically

characterized PSPs from other organisms showed significant sequence similarities to any protein coded in the *Synechocystis* genome. Thus, we started attempts to enrich the PSP from soluble cell extracts of *Synechocystis* by classical protein purification and testing the fractions for PSP activity using the substrate phosphoserine. The application of ammonium sulfate precipitation, hydrophobic interaction chromatography and anion-exchange chromatography led to ~500-fold enrichment of PSP activity (data not shown). The proteins of this fraction were separated by SDS-PAGE and selected bands were used for protein identification via MS (Supplementary data set). Amongst the proteins of this fraction, none showed similarities to phosphatases. However, Slr1124 was identified in several SDS-gel bands of this fraction. It is annotated as phosphoglycerate mutase in CyanoBase (http://genome.microbedb.jp/cyanobase/Synechocystis/genes/slr1124). It turned out that this putative phosphoglycerate mutase might be a promising PSP candidate. Chiba *et al.* (2012) reported that a non-typical phosphoglycerate mutase of the bacterium *Hydrogenobacter thermophilus* displayed only PSP activity instead of the expected mutase activity. Hence, this enzyme was described as the first example for a new class of PSP enzymes, which have close relatives in many other organisms, including *Arabidopsis*. Using the PSP sequence of *H. thermophilus* it was possible to identify a similar protein in the *Synechocystis* genome: the possibly wrongly annotated phosphoglycerate mutase Slr1124. Thus, two lines of evidence qualified the product of *slr1124* as the most likely PSP candidate: its occurrence in a protein fraction highly enriched in PSP activity and its sequence similarity to the new PSP class identified in *H. thermophilus*.

Verification of enzymatic activities of the phosphoserine pathway

To verify the proposed biochemical functions of the candidate proteins, we expressed the genes in *E. coli* and purified the corresponding recombinant proteins for biochemical characterization. Fig. 3 shows that all three recombinant proteins, i.e. Sll1908, Sll1559 and Slr1124, were obtained as soluble proteins. Due to the fused tags, it was possible to isolate considerable amounts of rather pure proteins for the subsequent biochemical assays. All three recombinant enzymes were active and followed Michaelis–Menten kinetics (Fig. 4).

PGDH (Sll1908). The starting enzyme PGDH was obtained as a His-tagged fusion protein with a calculated molecular mass of 58.0 kDa (Fig. 3a). To determine whether Sll1908 could perform the oxidation of 3PGA towards phosphohydroxypyruvate using NAD^+ as cofactor, the reduction of NAD^+ to NADH with 3PGA as substrate was followed at 340 nm. The recombinant enzyme showed clear PGDH activity. However, when $NADP^+$ instead of NAD^+ was used as coenzyme, only ~5 % of the PGDH activity remained visible. The use of related substrates revealed that the highest activity was obtained with 3PGA and NAD^+,

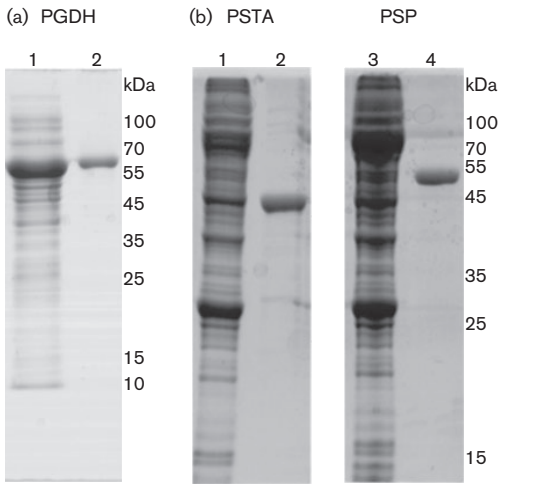

Fig. 3. Purity of recombinant PGDH, PSTA and PSP used in the enzyme assays. (a) SDS-PAGE analysis of His-tagged PGDH. Lane 1, cell-free extract of *E. coli* containing His-tagged PGDH, 20 μg protein; lane 2, purified PGDH, 2 μg protein. (b) SDS-PAGE analysis of PSTA and PSP. Lane 1, cell-free extract of *E. coli* containing GST-tagged PSTA, 21 μg protein; lane 2, purified PSTA, 2 μg protein; lane 3, cell-free extract of *E. coli* containing GST-tagged PSP, 49 μg protein; lane 4, purified PSP, 2 μg protein.

whereas only low activities were observed with D-lactate and glycolate (Table 1). These data support the notion that *sll1908* was correctly annotated as *serA* coding for the PGDH in CyanoBase.

In subsequent biochemical assays we estimated the biochemical features of PGDH. In the presence of 3PGA and NAD^+ the maximum specific activity of Sll1908 reached 2.3 U mg^{-1} at the enzyme's pH optimum of 9.0 with a turnover number of 2.25 s^{-1} (Table 2). A decrease of the pH to 7.5 led to a loss of enzymatic activity of ~67 %. Addition of the final product NADH to 0.1 mM inhibited the reaction rate to 16 % (data not shown). A double-reciprocal plot of the kinetic data was used to calculate the K_m values for 3PGA and NAD^+ of 0.63 and 0.13 mM, respectively, at pH 9.0 (Fig. 4a, Table 2). The K_m value for 3PGA (1.19 mM) of the recombinant PGDH of *Arabidopsis* at pH 9.0 was in the same range, whereas the plant enzyme exhibited a much higher affinity towards NAD^+ (K_m=0.01 mM) than the cyanobacterial PGDH. Finally, the native molecular mass of the recombinant PGDH was estimated via gel-filtration chromatography. The Sll1908 protein eluted at a molecular mass of ~234 kDa, indicating that the enzyme forms a homotetramer. A similar homotetrameric structure was reported for PGDHs of the Gram-positive bacterium *Corynebacterium glutamicum* and of the plant *A. thaliana* (Ho & Saito, 2001).

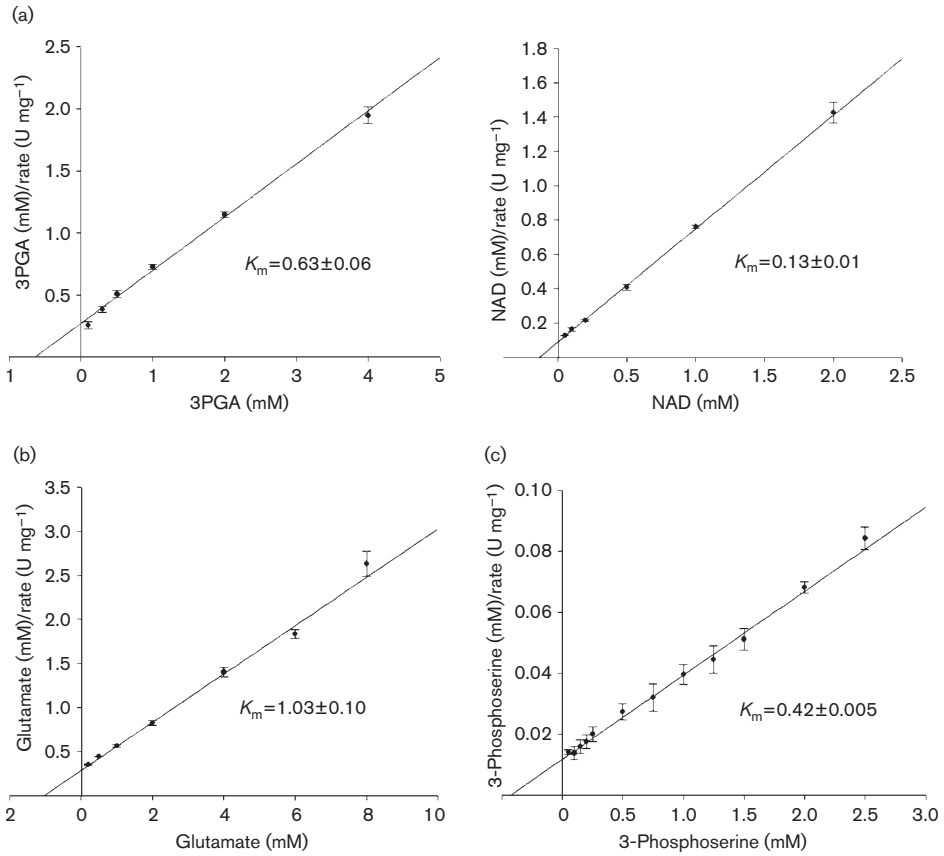

Fig. 4. Enzyme kinetics of recombinant PGDH, PSTA and PSP from *Synechocystis*. (a) Hanes–Woolf plot conversions of kinetic data from PGDH for the substrates 3PGA (left, $n=4$) and NAD^+ (right, $n=3$). (b) Data from PSTA for glutamate ($n=4$). (c) Data from PSP for 3-phosphoserine ($n=2$). Values represent mean ± SE; *n*, number of technical replicates.

PSTA (Sll1559). The bioinformatic searches (described above) identified two candidate PSTA proteins in the *Synechocystis* genome that are coded by *sll1559* and *slr5022*, respectively. These two genes were expressed in *E. coli*, but only the recombinant Sll1559 showed PSTA activity (Table 2), whereas the Slr5022 was not active (data not shown). The purified PSTA has an apparent molecular mass of 41 kDa in SDS-PAGE (Fig. 3b). However, a molecular mass of 84 kDa was determined for Sll1559 by size-exclusion chromatography, indicating a dimeric structure of the native enzyme. A homodimeric structure was also reported for PSTA of *B. circulans* (Battchikova *et al.*, 1996).

Table 1. Substrate specificity [enzyme activity; mean ± SD ($n=3$)] of recombinant PGDH (Sll1908)

Substrate	V_{max} [U (mg protein)$^{-1}$]
3PGA + NAD^+	1.878 ± 0.316
3PGA + $NADP^+$	0.091 ± 0.054
D-Lactate + NAD^+	0.091 ± 0.044
Glycolate + NAD^+	0.063 ± 0.053
3-Hydroxypyruvate + NADH	0
3-Hydroxypyruvate + NADPH	0
Pyruvate + NADH	0
Pyruvate + NADPH	0
Glyoxylate + NADH	0
Glyoxylate + NADPH	0

The purified PSTA of *Synechocystis* catalysed the amino group transfer from glutamate towards 3-phosphohydroxypyruvate *in vitro*. The initial rate of Sll1559 was determined by an enzymatic assay coupled to PGDH to follow the NADH production of this enzyme, because a direct detection of the substrates or products of PSTA was not possible (see Methods). The kinetic parameters of Sll1559 are listed in Table 2. The K_m value for glutamate was 1.03 mM (Fig. 4b) and the maximum specific activity was 3.64 U mg^{-1} for the PSTA from *Synechocystis*. For the recombinant PSTA of *A. thaliana*, different K_m values for

Table 2. Biochemical and kinetic parameters of recombinant PGDH (Sll1908), PSTA (Sll1559) and PSP (Slr1124) from *Synechocystis*

The parameters were determined in standard reaction mixtures.

Parameter	PGDH	PSTA	PSP
Molecular mass (kDa)			
Determined mass of the native complex*	234.0	84.0	50.0
Theoretical mass of the monomer	58.0†	41.0‡	49.8‡
Kinetic parameter	pH 9.0	pH 9.0	pH 7.5
	NAD^+, 3PGA	Glutamate	3-Phosphoserine
K_m (mM)	0.13, 0.63	1.03	0.42
V_{max} [U (mg protein)$^{-1}$]	2.33	3.64	36.2
k_{cat} (s^{-1})	2.25	2.49	30.2
k_{cat}/K_m (s^{-1} mM^{-1})	17.3, 3.6	2.41	71.8

*Molecular mass determined by gel filtration (n=2).
†Including His-tag.
‡Including peptide linker of the GST-tag.

glutamate were reported, ranging from 70 μM (Ho *et al.*, 1998) to 5.05 mM (Ali & Nozaki, 2006).

PSP (Slr1124). The recombinant putative PSP protein with a calculated molecular mass of 49.8 kDa was purified from *E. coli* (Fig. 3b) and was subsequently used for enzymatic assays. The Slr1124 protein of *Synechocystis* showed clear PSP activity, because it catalysed the hydrolysis of the phosphoric acid ester of the substrate 3-phosphoserine, releasing serine and orthophosphate. The PSP was found to be highly specific for its substrate phosphoserine, because enzyme assays with related substrates that contained phosphoric acid esters showed only low enzyme activities (Table 3). The K_m value of Slr1124 for 3-phosphoserine was 0.42 mM (Fig. 4c) and the constant k_{cat} was 30.2 s^{-1} at 28 °C and pH 7.5, which resulted in a high catalytic efficiency of 71.8 s^{-1} mM^{-1} (Table 2). These data revealed that *slr1124* really codes for PSP and is wrongly annotated as mutase in CyanoBase. The recombinant PSP of *Arabidopsis* showed a K_m value of 3.5 mM on 3-phosphoserine at pH 7.5 and a turnover number of 1.8 s^{-1}, resulting in a catalytic efficiency of 0.51 s^{-1} mM^{-1}. Hence, the plant enzyme exhibited ~10-fold lower affinity for the substrate phosphoserine and a lower catalytic efficiency than the enzyme from *Synechocystis*. The enzyme activity of PSP (Slr1124) was also checked in 200 mM Tris/HCl buffer, pH 9.0, because this pH was used in the experiments to reconstitute the phosphoserine pathway by mixing the three recombinant proteins. The PSP activity decreased to 44±14 % at pH 9 in comparison with the rate at pH 7.5. Further experiments showed that the end-product serine caused a distinct inhibition of the *Synechocystis* PSP, because the activity dropped to 46±6.8 % of the initial rate after addition of 5 mM serine to the standard enzyme assay, whilst only 31±4.1 % of the rate remained visible after addition of 10 mM serine. The native molecular mass of Slr1124 was determined by size-exclusion chromatography, where it eluted as one symmetrical peak of 50 kDa, indicating that the PSP is an active monomer (Table 2).

***In vitro* reconstruction of the phosphoserine pathway.** Next, we tried to reconstitute *in vitro* the light-independent phosphoserine pathway of *Synechocystis*. To this end, we performed an *in vitro* assay combining the three recombinant proteins Sll1908, Sll1559 and Slr1124 in the presence of the substrates 3PGA, glutamate and NAD^+. The whole pathway activity was monitored indirectly by measuring the release of inorganic phosphate and NAD^+ reduction over the time (Fig. 5). After 10 min of the enzymatic reaction, 8.8±1.5 μmol phosphate (mg protein)$^{-1}$ was determined. The phosphate release corresponds well with the independently measured NAD^+ reduction of 8.9± 0.6 μmol (mg protein)$^{-1}$ during the same time. As control, an assay containing active PGDH and PSTA, but heat-inactivated PSP, was performed, resulting in no phosphate release (Fig. 5). The rate of NADH generation was not altered in this control reaction, as expected because of the active PGDH. This experiment revealed that the three isolated enzymes are sufficient to perform serine synthesis from the substrates of the phosphoserine pathway *in vitro*.

Table 3. Substrate specificity of recombinant PSP (Slr1124)

Enzyme activity with phosphoserine was normalized to 100 % and the relative activities with other substrates are given (n=2).

Substrate	Rate (%)
3-Phosphoserine	100
sn-Glycerol 3-phosphate	8
D(+)-3PGA	4
D(+)-2-Phosphoglycerate	2

Attempts to delete the phosphoserine pathway in cyanobacteria

The biochemical results clearly indicate that *Synechocystis* is capable of performing serine biosynthesis via the phosphoserine pathway in addition to the light-dependent photorespiratory 2PG pathway. To determine the physiological role of the pathway and to verify the biochemical results in intact cells, we aimed to inactivate the *psp* genes in *Synechocystis* and *Synechococcus*. These cyanobacterial strains are amenable to targeted mutagenesis. To mutate the corresponding genes, the kanamycin resistance cartridge was fused to sequences neighbouring the PSP coding sequences. However, despite cultivation of kanamycin-resistant clones under various conditions, such as different light conditions and serine supplementation to favour the use of the photorespiratory pathway for serine biosynthesis and to complement serine auxotrophy, respectively, homozygous mutants of *Synechocystis* and *Synechococcus* were not obtained. In addition to the mutated fragment, a second fragment of size similar to the WT gene remained visible in PCRs with mutant DNA as template (Figs S1 and S2). These results indicate that the *psp* genes are essential for viability of these two cyanobacterial strains. It has been previously shown that the knockout of *sll1559* coding for PSTA was also not possible in *Synechocystis*, as also in this case only partly segregated clones could be obtained (Eisenhut *et al.*, 2006).

These results point to an essential role of the light-independent serine biosynthesis pathway, at least under the tested conditions. Similar results were reported for the model plant *Arabidopsis*, where a knockout of the *psp1* gene resulted in an embryo-lethal phenotype (Muñoz-Bertomeu *et al.*, 2013) and PGDH was also found to be essential for plant viability (Benstein *et al.*, 2013). Thus, at least in plants, the phosphoserine pathway is responsible for functions additional to serine biosynthesis, such as the involvement in protein/lipid phosphorylation or modulation of cell signalling pathways. Such a broader importance of the phosphoserine pathway could also apply for cyanobacteria, and could explain why even feeding with serine and exposure to light to promote light-dependent serine synthesis did not allow the complete knockout of the genes for the light-independent phosphoserine pathway. At least for *Synechocystis*, the presence of a serine uptake system has been proven (Labarre *et al.*, 1987; Quintero *et al.*, 2001), ruling out the possibility that external serine cannot taken up by the transformants.

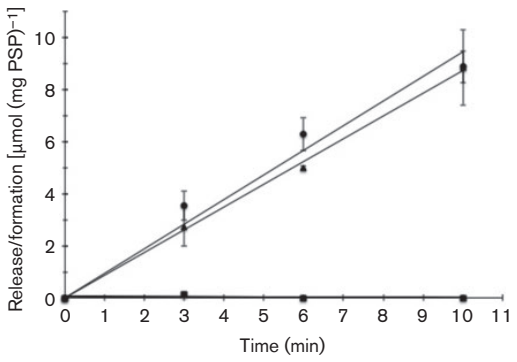

Fig. 5. Reconstruction of the phosphoserine pathways by the combined action of the recombinant PGDH, PSTA and PSP proteins. The three recombinant enzymes PGDH, PSTA and PSP from *Synechocystis* were applied in an *in vitro* assay using the substrate 3PGA. Phosphate release (▲, $n=3$) and NADH formation (●, $n=3$) were monitored over 10 min. An enzyme assay in which intact PGDH and PSTA but heat-inactivated PSP were combined and the release of inorganic phosphate was measured (■, $n=2$) served as a negative control.

Another indication of the important function of the phosphoserine pathway amongst cyanobacteria was obtained from the finding that close homologues of all three enzymes exist in genomes of almost all cyanobacteria listed in CyanoBase despite the universal occurrence of light-dependent serine synthesis via photorespiration amongst cyanobacteria (Hagemann *et al.*, 2013). For PGDH, the related cyanobacterial enzymes show >70 % sequence similarity. Furthermore, the PGDH protein from *Arabidopsis* is closely related to cyanobacterial enzymes (60 % sequence similarity). In the phylogenetic tree of PGDHs from plants, cyanobacteria and heterotrophic bacteria, the proteins from plants and cyanobacteria are sister clades, supporting the cyanobacterial origin of PGDH in plants (Fig. S3). For PSTA, which is coded by the wrongly annotated *sll1559*, the related proteins share >75 % similarity amongst cyanobacteria. However, clear homologues of PSTA from *Synechocystis* are missing in the genomes of some filamentous cyanobacteria, such as *Anabaena* sp. ATCC 29413, *Nostoc* sp. PCC 7120, *Nostoc* sp. PCC 7524 and *Rivularia* sp. PCC 7116, whereas clear PSTA proteins exist in *Nostoc punctiforme* ATCC 29133 and *Nodularia spumigena* CCY 9414. Another class V aminotransferase probably participates in the phosphoserine pathway in strains missing Sll1559 homologues. Proteins closely resembling the identified PSP (coded by *slr1124* in *Synechocystis*) exist in all cyanobacterial genomes with >65 % similarity. It should be noted that probable homologues for the three enzymes of the phosphoserine pathway are also present in the genomes of picoplanktonic cyanobacteria. These strains are characterized by the smallest genomes amongst cyanobacteria. It has been proposed that they have eliminated all unnecessary genes during genome streamlining (Scanlan *et al.*, 2009). Nevertheless, these strains also retain genes for photorespiration (Hagemann *et al.*, 2013) as a light-dependent route for serine biosynthesis as well as the genes identified here for the light-independent route, i.e. the phosphoserine pathway.

CONCLUSIONS

Our results provide clear evidence that the light-independent phosphorylated pathway of serine biosynthesis is active

in cyanobacterial cells (displayed in Fig. 1). Previously, only the light-dependent photorespiratory pathway for serine biosynthesis was annotated and thought to be the source of serine in *Synechocystis* (Knoop *et al.*, 2010). However, there was some doubt that this pathway represents the only source of serine, because the enzyme activities necessary for the phosphoserine pathway were found in crude extracts of six different cyanobacteria (Colman & Norman, 1997) and the complete block of photorespiration at the glycolate conversion step did not result in serine auxotrophy (Eisenhut *et al.*, 2008). However, identification of the phosphoserine pathway enzymes in the cyanobacterial genomes was hampered by its missing or wrong annotation. Only the gene for PGDH was correctly annotated and was functionally verified here. The PSTA gene *sll1559* is wrongly annotated in *Synechocystis* and some other cyanobacteria, despite the clear similarities of the protein to type V aminotransferase. Here, we verified its specific action as PSTA using the pure recombinant protein Sll1559. The last enzyme PSP was initially identified by enzyme purification and protein identification via MS. However, the final recognition of the wrongly annotated Slr1124 as PSP was supported by the report on a new PSP class showing some sequence similarities to phosphoglycerate mutases (Chiba *et al.*, 2012). Finally, using the three verified protein sequences from *Synechocystis*, we found homologous proteins in the majority of cyanobacterial genomes. Thus, we conclude that the light-independent phosphoserine pathway exists at least in most cyanobacteria and contributes to the biosynthesis of serine in addition to photorespiration. It has been shown that some of the enzymes (e.g. PGDH) are potentially sensitive to thiol oxidation (Chardonnet *et al.*, 2014). It could be possible that the redox state of these enzymes regulates the relative contribution of the two pathways to serine biosynthesis depending on the growth conditions, such as light/dark transitions.

Moreover, our results indicate that the pathway is essential in *Synechocystis* and *Synechococcus*. The attempts made here to mutate the gene for the PSP and those previously made to mutate the gene for PSTA (Eisenhut *et al.*, 2006) resulted in only partly segregated mutants, i.e. the WT gene copy was always retained even in the presence of external serine. Obviously, the pathway contributes significantly to total serine synthesis or is involved in additional functions essential for cell viability. The lack of mutants made it difficult to measure the relative importance of the two pathways. Thus, we tried to estimate it using an existing multi-scale kinetic model of *Synechococcus* that took into account existing metabolome and transcriptome data (Jablonsky *et al.*, 2014). According to this model, we predict that in cells grown at 5 % CO_2 the phosphoserine pathway contributes to 66.4 % of serine synthesis, whereas due to the increased photorespiration it delivers only 28–37.6 % of serine under ambient CO_2 conditions (assuming 3–4.5 % oxygenation reaction of ribulose 1,5-bisphosphate carboxylase/oxygenase in cells grown at ambient air with 0.04 % CO_2). The relative contribution of the phosphoserine pathway will further increase if we include night phases and if we assume that not all of the photorespiratory serine is taken off from the cycle. The complete use of photorespiratory glycine and serine for biosynthetic purposes was suggested to occur in diatoms that have an open photorespiratory pathway (Allen *et al.*, 2011).

ACKNOWLEDGEMENTS

We thank Sabine Nicklisch for excellent technical assistance. Peter Jungblut and Monika Schmid (Proteome Facility of Max Planck Institute of Infection Biology, Berlin, Germany) are acknowledged for the MS-based identification of proteins. The work of J. J. was supported by Postdok JU (CZ.1.07/2.3.00/30.0006) and CENAKVA II (LO1205). The work in the group of M. H. (University Rostock) was supported by a grant from the Deutsche Forschungsgemeinschaft in the frame of the Forschergruppe FOR 1186 – Promics. The experiments at Humboldt University were supported by the BMBF (Federal Ministry for Education and Research) (CYANOSYS grant).

REFERENCES

Ali, V. & Nozaki, T. (2006). Biochemical and functional characterization of phosphoserine aminotransferase from *Entamoeba histolytica*, which possesses both phosphorylated and non-phosphorylated serine metabolic pathways. *Mol Biochem Parasitol* **145**, 71–83.

Allen, A. E., Dupont, C. L., Oborník, M., Horák, A., Nunes-Nesi, A., McCrow, J. P., Zheng, H., Johnson, D. A., Hu, H. & other authors (2011). Evolution and metabolic significance of the urea cycle in photosynthetic diatoms. *Nature* **473**, 203–207.

Anderson, S. L. & McIntosh, L. (1991). Light-activated heterotrophic growth of the cyanobacterium *Synechocystis* sp. strain PCC 6803: a blue-light-requiring process. *J Bacteriol* **173**, 2761–2767.

Baier, K., Lehmann, H., Stephan, D. P. & Lockau, W. (2004). NblA is essential for phycobilisome degradation in *Anabaena* sp. strain PCC 7120 but not for development of functional heterocysts. *Microbiology* **150**, 2739–2749.

Battchikova, N., Himanen, J. P., Ahjolahti, M. & Korpela, T. (1996). Phosphoserine aminotransferase from *Bacillus circulans* subsp. *alkalophilus*: purification, gene cloning and sequencing. *Biochim Biophys Acta* **1295**, 187–194.

Bauwe, H., Hagemann, M. & Fernie, A. R. (2010). Photorespiration: players, partners and origin. *Trends Plant Sci* **15**, 330–336.

Belhumeur, P., Fortin, N. & Clark, M. W. (1994). A gene from *Saccharomyces cerevisiae* which codes for a protein with significant homology to the bacterial 3-phosphoserine aminotransferase. *Yeast* **10**, 385–389.

Benstein, R. M., Ludewig, K., Wulfert, S., Wittek, S., Gigolashvili, T., Frerigmann, H., Gierth, M., Flügge, U. I. & Krueger, S. (2013). Arabidopsis phosphoglycerate dehydrogenase1 of the phosphoserine pathway is essential for development and required for ammonium assimilation and tryptophan biosynthesis. *Plant Cell* **25**, 5011–5029.

Chardonnet, S., Sakr, S., Cassier-Chauvat, C., Le Maréchal, P., Chauvat, F., Lemaire, S. D. & Decottignies, P. (2014). First proteomic study of *S*-glutathionylation in cyanobacteria. *J Proteome Res* **14**, 59–71.

Chiba, Y., Oshima, K., Arai, H., Ishii, M. & Igarashi, Y. (2012). Discovery and analysis of cofactor-dependent phosphoglycerate mutase homologs as novel phosphoserine phosphatases in *Hydrogenobacter thermophilus*. *J Biol Chem* **287**, 11934–11941.

Colman, B. & Norman, E. G. (1997). Serine synthesis in cyanobacteria by a nonphotorespiratory pathway. *Physiol Plant* **100**, 133–136.

Duncan, K. & Coggins, J. R. (1986). The *serC–aro A* operon of *Escherichia coli*. A mixed function operon encoding enzymes from two different amino acid biosynthetic pathways. *Biochem J* **234**, 49–57.

Eisenhut, M., Kahlon, S., Hasse, D., Ewald, R., Lieman-Hurwitz, J., Ogawa, T., Ruth, W., Bauwe, H., Kaplan, A. & Hagemann, M. (2006). The plant-like C2 glycolate cycle and the bacterial-like glycerate pathway cooperate in phosphoglycolate metabolism in cyanobacteria. *Plant Physiol* **142**, 333–342.

Eisenhut, M., Ruth, W., Haimovich, M., Bauwe, H., Kaplan, A. & Hagemann, M. (2008). The photorespiratory glycolate metabolism is essential for cyanobacteria and might have been conveyed endosymbiontically to plants. *Proc Natl Acad Sci U S A* **105**, 17199–17204.

Elhai, J. & Wolk, C. P. (1988). Conjugal transfer of DNA to cyanobacteria. *Methods Enzymol* **167**, 747–754.

Greenberg, D. M. & Ichihara, A. (1957). Further studies on the pathway of serine formation from carbohydrate. *J Biol Chem* **224**, 331–340.

Grigorieva, G. & Shestakov, S. (1982). Transformation in the cyanobacterium *Synechocystis* sp. 6803. *FEMS Microbiol Lett* **13**, 367–370.

Hagemann, M., Fernie, A. R., Espie, G. S., Kern, R., Eisenhut, M., Reumann, S., Bauwe, H. & Weber, A. P. (2013). Evolution of the biochemistry of the photorespiratory C2 cycle. *Plant Biol (Stuttg)* **15**, 639–647.

Helgadottir, A., Thorleifsson, G., Manolescu, A., Gretarsdottir, S., Blondal, T., Jonasdottir, A., Jonasdottir, A., Sigurdsson, A., Baker, A. & other authors (2007). A common variant on chromosome 9p21 affects the risk of myocardial infarction. *Science* **316**, 1491–1493.

Ho, C. L. & Saito, K. (2001). Molecular biology of the plastidic phosphorylated serine biosynthetic pathway in *Arabidopsis thaliana*. *Amino Acids* **20**, 243–259.

Ho, C.-L., Noji, M., Saito, M., Yamazaki, M. & Saito, K. (1998). Molecular characterization of plastidic phosphoserine aminotransferase in serine biosynthesis from *Arabidopsis*. *Plant J* **16**, 443–452.

Ho, C. L., Noji, M., Saito, M. & Saito, K. (1999). Regulation of serine biosynthesis in *Arabidopsis*. Crucial role of plastidic 3-phosphoglycerate dehydrogenase in non-photosynthetic tissues. *J Biol Chem* **274**, 397–402.

Huege, J., Goetze, J., Schwarz, D., Bauwe, H., Hagemann, M. & Kopka, J. (2011). Modulation of the major paths of carbon in photorespiratory mutants of *Synechocystis*. *PLoS One* **6**, e16278.

Jablonsky, J., Schwarz, D. & Hagemann, M. (2014). Multi-level kinetic model explaining diverse roles of isozymes in prokaryotes. *PLoS One* **9**, e105292.

Kaneko, T., Sato, S., Kotani, H., Tanaka, A., Asamizu, E., Nakamura, Y., Miyajima, N., Hirosawa, M., Sugiura, M. & other authors (1996). Sequence analysis of the genome of the unicellular cyanobacterium *Synechocystis* sp. strain PCC6803. II. Sequence determination of the entire genome and assignment of potential protein-coding regions (supplement). *DNA Res* **3**, 185–209.

Knoop, H., Zilliges, Y., Lockau, W. & Steuer, R. (2010). The metabolic network of *Synechocystis* sp. PCC 6803: systemic properties of autotrophic growth. *Plant Physiol* **154**, 410–422.

Labarre, J., Thuriaux, P. & Chauvat, F. (1987). Genetic analysis of amino acid transport in the facultatively heterotrophic cyanobacterium *Synechocystis* sp. strain 6803. *J Bacteriol* **169**, 4668–4673.

Laemmli, U. K. (1970). Cleavage of structural proteins during the assembly of the head of bacteriophage T4. *Nature* **227**, 680–685.

Lanzetta, P. A., Alvarez, L. J., Reinach, P. S. & Candia, O. A. (1979). An improved assay for nanomole amounts of inorganic phosphate. *Anal Biochem* **100**, 95–97.

Larkin, M. A., Blackshields, G., Brown, N. P., Chenna, R., McGettigan, P. A., McWilliam, H., Valentin, F., Wallace, I. M., Wilm, A. & other authors (2007). Clustal W and Clustal_X version 2.0. *Bioinformatics* **23**, 2947–2948.

Lowry, O. H., Rosebrough, N. J., Farr, A. L. & Randall, R. J. (1951). Protein measurement with the Folin phenol reagent. *J Biol Chem* **193**, 265–275.

Martin, W. & Schnarrenberger, C. (1997). The evolution of the Calvin cycle from prokaryotic to eukaryotic chromosomes: a case study of functional redundancy in ancient pathways through endosymbiosis. *Curr Genet* **32**, 1–18.

Muñoz-Bertomeu, J., Anoman, A., Flores-Tornero, M., Toujani, W., Rosa-Téllez, S., Fernie, A. R., Roje, S., Segura, J. & Ros, R. (2013). The essential role of the phosphorylated pathway of serine biosynthesis in *Arabidopsis*. *Plant Signal Behav* **8**, e27104.

Ochoa de Alda, J. A., Esteban, R., Diago, M. L. & Houmard, J. (2014). The plastid ancestor originated among one of the major cyanobacterial lineages. *Nat Commun* **5**, 4937.

Ouzounis, C. & Sander, C. (1993). Homology of the NifS family of proteins to a new class of pyridoxal phosphate-dependent enzymes. *FEBS Lett* **322**, 159–164.

Quintero, M. J., Montesinos, M. L., Herrero, A. & Flores, E. (2001). Identification of genes encoding amino acid permeases by inactivation of selected ORFs from the *Synechocystis* genomic sequence. *Genome Res* **11**, 2034–2040.

Rippka, R., Deruelles, J., Waterbury, J. B., Herdman, M. & Stanier, R. Y. (1979). Generic assignments, strain histories and properties of pure cultures of cyanobacteria. *J Gen Microbiol* **111**, 1–61.

Ros, R., Muñoz-Bertomeu, J. & Krueger, S. (2014). Serine in plants: biosynthesis, metabolism, and functions. *Trends Plant Sci* **19**, 564–569.

Scanlan, D. J., Ostrowski, M., Mazard, S., Dufresne, A., Garczarek, L., Hess, W. R., Post, A. F., Hagemann, M., Paulsen, I. & Partensky, F. (2009). Ecological genomics of marine picocyanobacteria. *Microbiol Mol Biol Rev* **73**, 249–299.

Sigrist, C. J. A., de Castro, E., Cerutti, L., Cuche, B. A., Hulo, N., Bridge, A., Bougueleret, L. & Xenarios, I. (2013). New and continuing developments at PROSITE. *Nucleic Acids Res* **41** (Database issue), D344–D347.

Timm, S., Florian, A., Wittmiss, M., Jahnke, K., Hagemann, M., Fernie, A. R. & Bauwe, H. (2013). Serine acts as a metabolic signal for the transcriptional control of photorespiration-related genes in *Arabidopsis*. *Plant Physiol* **162**, 379–389.

Umbarger, H. E., Umbarger, M. A. & Siu, P. M. (1963). Biosynthesis of serine in *Escherichia coli* and *Salmonella typhimurium*. *J Bacteriol* **85**, 1431–1439.

Walton, N. J. & Woolhouse, H. W. (1986). Enzymes of serine and glycine metabolism in leaves and non-photosynthetic tissues of *Pisum sativum* L. *Planta* **167**, 119–128.

Young, J. D., Shastri, A. A., Stephanopoulos, G. & Morgan, J. A. (2011). Mapping photoautotrophic metabolism with isotopically nonstationary ^{13}C flux analysis. *Metab Eng* **13**, 656–665.

Edited by: T. Gavin

Supplemental Table

Supplemental Table S1: Primers that were used for the construction of expression plasmids, knockout mutants and segregation checks in this study. Added restriction sites are underlined.

ORF	Primer
sll1908	fw 5'- CATATGGCTAAAGTTTTAGTTTCTG-3'
	rev 5'- GAATTCTTAGAGCTTAACGGTGTAG -3'
sll1559	fw 5'-GGGATCCATGGATAATAAGCAAATGTTGATG-3'
	rev 5'-GCGGCCGCTTAACCTTTAGCCAAAACC-3'
slr1124	fw 5'-GCAGGATCCTTGGCTACTCGGGTCATC-3'
	rev 5'-ATAATTGGCTAGCGGCCGCACTATAGGG-3'
slr1124	
up region	fw 5'-CCGAGCTCCAGTAAAAGGACAATTAATTGTGC-3'
	rev 5'-CCCTGCCTCTAGAACGATAAAATCAGACC-3'
down region	fw 5'-GTCCTGTCTAGAGCCAATT-3'
	rev 5'-CATTGGGACTAGTTTGGGCG-3'
down-PCR	rev 5'-GTTTGCCCAACTTAGCCATAAATT-3'
Synpcc79420485	
up region:	fw 5`-GGTCAAGCGCCAAAATCGGGGAGCTCGG-3`
	rev 5`-GGTTTTCTCCGCTGAGTCGGTCTAGAGGAC-3`
down region:	fw 5`-ATATCTAGACAGTCATGGCCGATCTGTTGCATC-3`
	rev 5`-AGTATTCTCGAGCAAATGCAACCAAGTGACGCTG-3`
up-PCR	fw 5`-GGAGTTGTTCAACTCTTTGG-3`
down-PCR	rev 5`-CGGTTGGGGATCGAGGTGAT-3`

Supplemental Figures

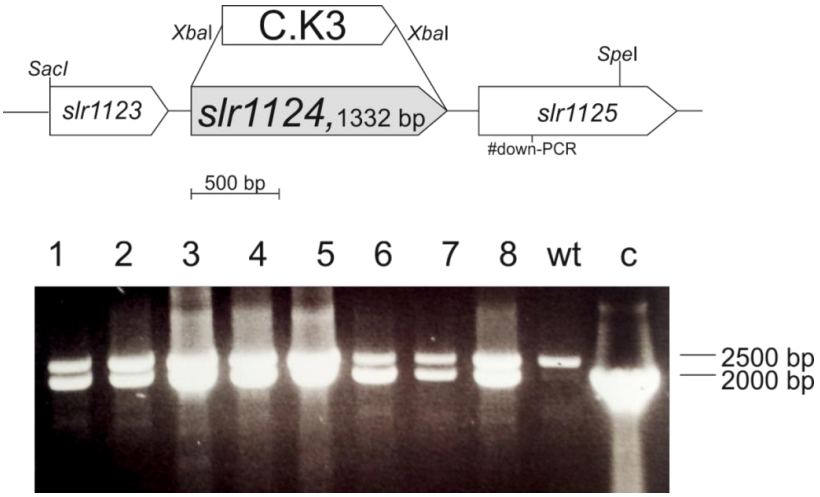

Figure S1: Attempts to mutate the gene *slr1124* coding for the phosphoserine phosphatase (PSP) in *Synechocystis* sp. PCC 6803.

Upper panel: Schematic overview on the genomic region surrounding *slr1124* and the gene knockout strategy. The 1.3-kb gene coding for PSP was replaced by a kanamycin resistance cassette C.K3 of about 1 kb (depiction above). Thus, the mutation construct, in which the deleted *psp* gene became replaced by C.K3, is about 0.3 kb smaller than the wild-type fragment.

Lower panel: The segregation of the mutants was checked by PCR) using specific oligonucleotides (#fw-*slr1124*-SacI, #down-PCR) and genomic DNA. The lanes 1-8 of the gel show the DNA fragment pattern of eight kanamycin-resistant putative mutant clones. As controls, PCR was performed with wild-type DNA (wt) and the plasmid pSKII+_KO-PSP6803, which was used for conjugation, as positive control (c). The expected size of PCR product from wild type is 2246 bp, whereas the mutant fragment is 1974 bp. All 8 mutants showed two PCR products indicating an incomplete segregation. The independent mutant clones were grown in the dark on BG11 agar plates including 150 µg/ml kanamycin, 1 mM serine and 5 mM glucose.

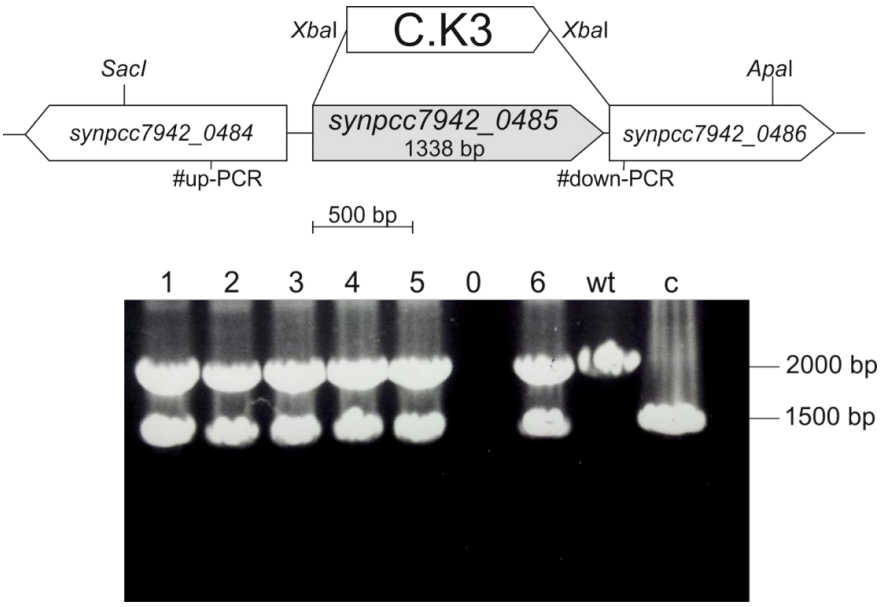

Figure S2: Attempts to mutate the gene *synpcc7942_0485* coding for the phosphoserine phosphatase (PSP) in *Synechococcus elongatus* PCC 7942.

Upper panel: Schematic overview on the genomic region surrounding *synpcc7942_0485* and the gene knockout strategy. The 1.5-kb fragment comprising the gene coding for PSP and flanking DNA was replaced by a kanamycin resistance cassette C.K3 of about 1 kb (depiction above). Thus, the mutation construct, in which the deleted *psp* gene became replaced by C.K3, is about 0.5 kb smaller than the wild-type fragment.

Lower panel: The segregation of the mutants was checked by PCR) using specific oligonucleotides (#up-PCR, #down-PCR) and genomic DNA. The lanes 1-6 of the gel show the DNA fragment pattern of six kanamycin-resistant putative mutant clones. As controls, PCR was performed with wild-type DNA (wt) and the plasmid pSKII+_KO-PSP7942, which was used for conjugation, as positive control (c). The expected size of PCR product from wild type is 1900 bp, whereas the mutant fragment is 1400 bp. All 6 mutants showed two PCR products indicating an incomplete segregation. The independent mutant clones were grown under continuous light on BG11 agar plates including 200 µg/ml kanamycin and 2 mM serine.

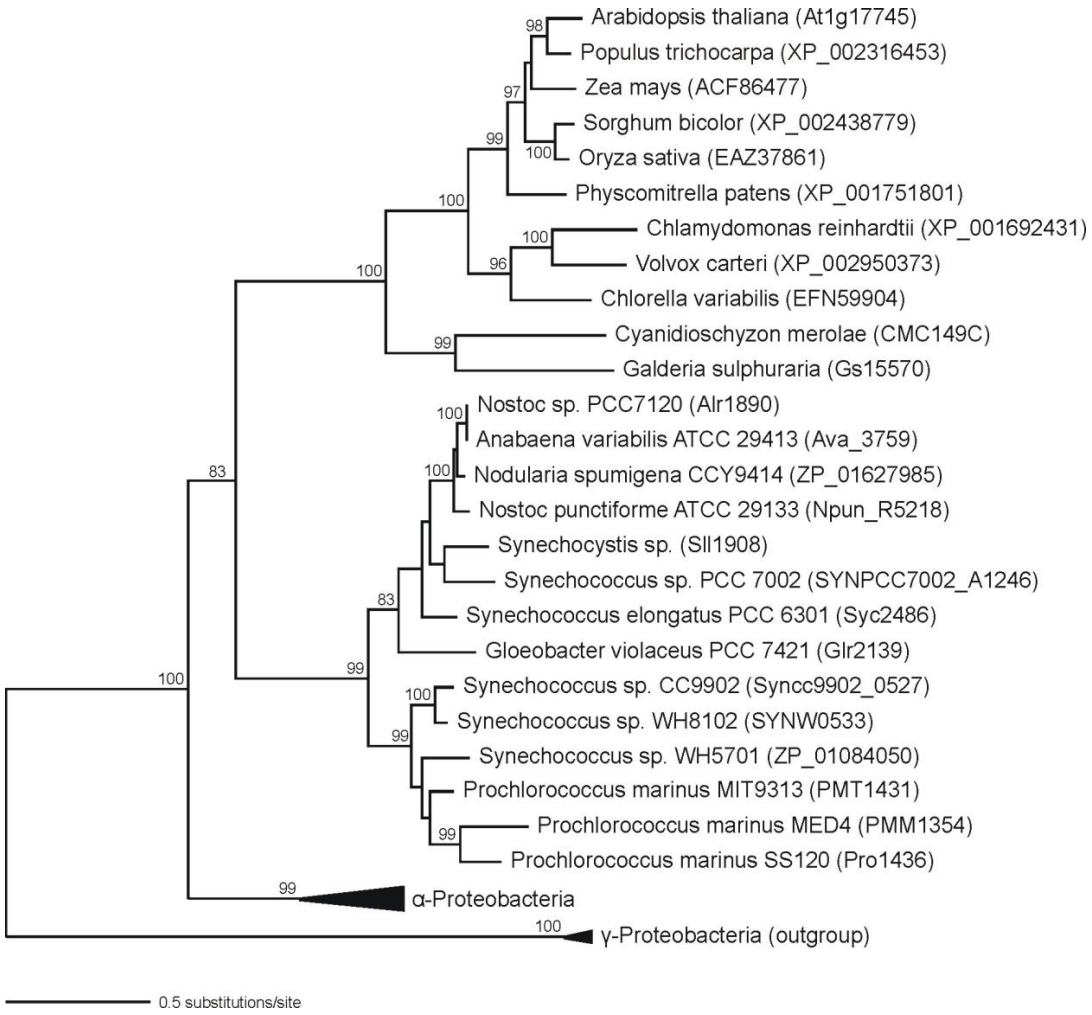

Figure S3: Phylogenetic tree of 3-phosphoglycerate dehydrogenases (PGDHs) from heterotrophic bacteria, cyanobacteria and plants grouping cyanobacterial as sister-branch to plant PGDHs. Accession numbers (NCBI) are displayed in brackets right of the species name.

For most cyanobacteria except *Nodularia spumigena* CCY9414 and *Synechococcus* sp. WH5701, the protein names are extracted from CyanoBase (http://genome.microbedb.jp/cyanobase/). For *Arabidopsis* PGDH the accession number from the TAIR database is shown (http://www.arabidopsis.org/). The group of α-proteobacteria consists of the PGDH from *Rhizobium leguminosarum* WSM1325 (YP_002977271), *Rhizobium etli* CFN 42 (YP_470937), *Agrobacterium fabrum* str. C58 (NP_356914), *Maritimibacter alkaliphilus* HTCC2654 (ZP_01015661), *Xanthobacter autotrophicus* Py2 (YP_001416108), *Methylobacterium* sp. 4-46 (YP_001773092), *Caulobacter crescentus* CB15 (NP_422009), and *Rhodopseudomonas palustris* CGA009 (NP_949644). PGDHs form γ-proteobacteria are represented by *Citrobacter rodentium* ICC168 (YP_003368296), *Serratia proteamaculans* 568 (YP_001480146), *Yersinia enterocolitica* 8081 (YP_001007569), and *Escherichia coli* O157:H7 str. EDL933 (NP_289481).

Supplemental data set – protein identification via mass-spectroscopy

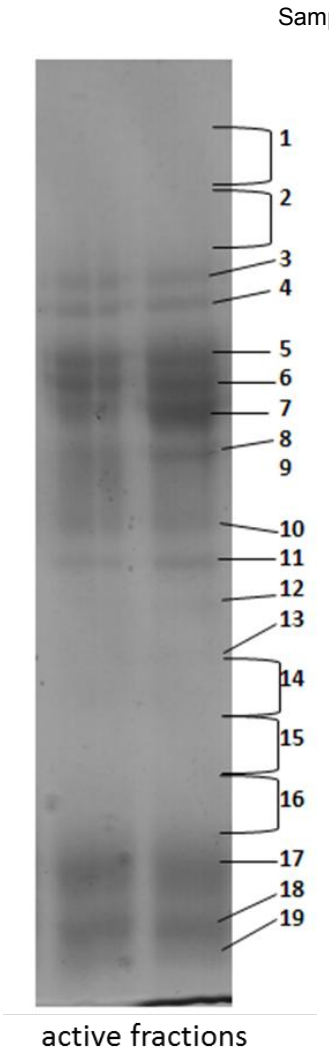

SDS-gel separation of the PSP-enriched protein fraction, which was obtained after ammonium sulfate precipitation, hydrophobic interaction chromatography and anion exchange chromatography of crude *Synechocystis* extracts.

The numbers represent bands, which were excised and then analysed via MALDI-TOF to identify the proteins.

Protein identification via MALDI TOF

Sample	Accession No	*ORF*	MW	PI	Mascot Score	Sequence Coverage %	Status	Protein Name
1	gi|16331785	*sll0480*	45060	5,41	182	40	ident	L,L-diaminopimelate aminotransferase [Synechocystis sp. PCC 6803]
1	a|15912		46183	5,62	183	42	ident	CDS2917545:2918810reverseMW:46212
2	gi|7331218		65978		238			keratin 1 [Homo sapiens]
2	gi|1651723	***slr1124***	38857	5,42	107	12	candidate	phosphoglycerate mutase [Synechocystis sp. PCC 6803]
2	gi|16331785	*sll0480*	45060	5,41	102	28	ident	L,L-diaminopimelate aminotransferase [Synechocystis sp. PCC 6803]
2	a|15912		46183	5,62	109	32	ident	CDS2917545:2918810reverseMW:46212
2	a|25227		50599	5,8	105	9	candidate	CDS84740:86107forwardMW:50631
3	gi|16329869	*sll1913*	66559	5,52	471	43	ident	hypothetical protein sll1913 [Synechocystis sp. PCC 6803]
3	a|24595		67186	5,59	479	44	ident	CDS773831:775645reverseMW:67228
4	gi|16330760	*slr1349*	58320	5,48	585	67	ident	glucose-6-phosphate isomerase [Synechocystis sp. PCC 6803]
4	gi|1651723	***slr1124***	38857	5,42	116	40	ident	phosphoglycerate mutase [Synechocystis sp. PCC 6803]
4	a|6148		60005	5,76	571	63	ident	CDS1744453:1746093forwardMW:60042
4	a|25227		50599	5,8	106	31	ident	CDS84740:86107forwardMW:50631
5	gi|1651723	***slr1124***	38857	5,42	555	69	ident	phosphoglycerate mutase [Synechocystis sp. PCC 6803]
5	a|25227		50599	5,8	561	61	ident	CDS84740:86107forwardMW:50631
6	gi|1651723	***slr1124***	38857	5,42	527	67	ident	phosphoglycerate mutase [Synechocystis sp. PCC 6803]
6	gi|16331785	*sll0480*	45060	5,41	277	45	ident	L,L-diaminopimelate aminotransferase [Synechocystis sp. PCC 6803]
6	a|25227		50599	5,8	553	65	ident	CDS84740:86107forwardMW:50631
6	a|15912		46183	5,62	276	44	ident	CDS2917545:2918810reverseMW:46212
7	gi|16331785	*sll0480*	45060	5,41	793	67	ident	L,L-diaminopimelate aminotransferase [Synechocystis sp. PCC 6803]
7	gi|304569539	***slr1124***	49313	5,97	189	53	ident	phosphoglycerate mutase [Synechocystis sp. PCC 6803]
7	a|15912		46183	5,62	77	63	ident	CDS2917545:2918810reverseMW:46212
7	a|25227		50599	5,8	187	52	ident	CDS84740:86107forwardMW:50631
8	gi|16331785	*sll0480*	45060	5,41	661	53	ident	L,L-diaminopimelate aminotransferase [Synechocystis sp. PCC 6803]
8	gi|16329756	*sll0990*	39186	6,05	260	35	ident	formaldehyde dehydrogenase (glutathione) [Synechocystis sp. PCC 6803]
8	a|15912		46183	5,62	661	54	ident	CDS2917545:2918810reverseMW:46212
8	a|23543		39401	6,06	260	34	ident	CDS644393:645511reverseMW:39426

9	gi|16329756	*sll0990*	39186	6,05	559	48	ident	formaldehyde dehydrogenase (glutathione) [Synechocystis sp. PCC 6803]
9	a|23543		39401	6,06	558	47	ident	CDS644393:645511reverseMW:39426
10	gi|16329756	*sll0990*	39186	6,05	359	44	ident	formaldehyde dehydrogenase (glutathione) [Synechocystis sp. PCC 6803]
10	gi|16332332	*slr0605*	36515	6,1	294	59	ident	hypothetical protein slr0605 [Synechocystis sp. PCC 6803]
10	a|23543		39401	6,06	358	44	ident	CDS644393:645511reverseMW:39426
10	a|21199		37883	6,11	281	50	ident	CDS3566741:3567733forwardMW:37907
11	gi|16329493	*slr0983*	28774	6,07	279	45	ident	alpha-D-glucose-1-phosphate cytidylyltransferase [Synechocystis sp. PCC 6
11	gi|16332332	*slr0605*	36515	6,1	62	45	candidate	hypothetical protein slr0605 [Synechocystis sp. PCC 6803]
11	a|20924		29523	5,78	278	44	ident	CDS353532:354323forwardMW:29542
11	a|21199		37883	6,11	51	37	candidate	CDS3566741:3567733forwardMW:37907
12	gi|339272481	*slr1783*	25751	4,94	224	43	ident	NarL subfamily protein Rre1 [Synechocystis sp. PCC 6803]
12	gi|16329756	*sll0990*	39186	6,05	216	23	ident	formaldehyde dehydrogenase (glutathione) [Synechocystis sp. PCC 6803]
12	gi|16330405	*sll0838*	24689	5,38	144	38	ident	orotidine 5'-phosphate decarboxylase [Synechocystis sp. PCC 6803]
12	a|23543		39401	6,06	215	23	ident	CDS644393:645511reverseMW:39426
12	a|3019		25247	5,38	135	30	ident	CDS1363841:1364551reverseMW:25263
12	a|11759		33958	5,82	91	27	ident	CDS242171:243094forwardMW:33979
12	a|7431		26648	5,58	58	41	candidate	CDS1896872:1897570reverseMW:26665
13	gi|16330405	*sll0838*	24689	5,38	328	47	ident	orotidine 5'-phosphate decarboxylase [Synechocystis sp. PCC 6803]
13	gi|16329756	*sll0990*	39186	6,05	253	31	ident	formaldehyde dehydrogenase (glutathione) [Synechocystis sp. PCC 6803]
13	gi|339272481	*slr1783*	25751	4,94	81	33	ident	NarL subfamily protein Rre1 [Synechocystis sp. PCC 6803]
13	a|3019		25247	5,38	318	39	ident	CDS1363841:1364551reverseMW:25263
13	a|23543		39401	6,06	253	30	ident	CDS644393:645511reverseMW:39426
13	a|11759		33958	5,82	71	20	ident	CDS242171:243094forwardMW:33979
13	a|7431		26648	5,58	50	40	candidate	CDS1896872:1897570reverseMW:26665
14	gi|16329824	*sll1577*	18115	4,98	475	71	ident	phycocyanin subunit B [Synechocystis sp. PCC 6803]
14	gi|16329821	*sll1580*	32501	9,35	120	29	ident	phycocyanin associated linker protein [Synechocystis sp. PCC 6803]
14	a|24175		18558	4,87	425	66	ident	CDS726953:727483reverseMW:18570
14	a|24150		33257	9,32	118	33	ident	CDS724497:725393reverseMW:33277
15	gi|16330466	*slr2067*	17401	4,86	516	78	ident	allophycocyanin a chain [Synechocystis sp. PCC 6803]
15	gi|20151051		18172	5,12	118	15	candidate	Chain B, Crystal Structure Of C-Phycocyanin Of Synechococcus Vulcanus /

								Angstroms
15	gi|16329824	*sll1577*	18115	4,98	98	73	ident	phycocyanin subunit B [Synechocystis sp. PCC 6803]
15	a|3562		18642	5,65	508	73	ident	CDS1430392:1430907forwardMW:18654
15	a|24175		18558	4,87	86	74	ident	CDS726953:727483reverseMW:18570
16	gi|16330466	*slr2067*	17401	4,86	628	85	ident	allophycocyanin a chain [Synechocystis sp. PCC 6803]
16	a|3562		18642	5,65	619	80	ident	CDS1430392:1430907forwardMW:18654
17	gi|16330466	*slr2067*	17401	4,86	514	73	ident	allophycocyanin a chain [Synechocystis sp. PCC 6803]
17	a|3562		18642	5,65	509	69	ident	CDS1430389:1430904forwardMW:18654
18	gi|16330467	*slr1986*	17205	5,43	327	72	ident	allophycocyanin b chain [Synechocystis sp. PCC 6803]
18	gi|16330466	*slr2067*	17401	4,86	247	67	ident	allophycocyanin a chain [Synechocystis sp. PCC 6803]
18	a|3568		18194	7,85	307	58	ident	CDS1430979:1431488forwardMW:18205
18	a|3562		18642	5,65	243	63	ident	CDS1430392:1430907forwardMW:18654
19	gi|16330467	*slr1986*	17205	5,43	325	86	ident	allophycocyanin b chain [Synechocystis sp. PCC 6803]
19	a|3568		18194	7,85	304	72	ident	CDS1430979:1431488forwardMW:18205

black	Identification via *NCBI*
blue	Identification via *SHE_KAZ*

Microbiology (2014), **160**, 2807–2819 DOI 10.1099/mic.0.081836-0

All1371 is a polyphosphate-dependent glucokinase in *Anabaena* sp. PCC 7120

Friederike Klemke,[1] Gabriele Beyer,[1] Linda Sawade,[1] Ali Saitov,[1] Thomas Korte,[2] Iris Maldener,[3] Wolfgang Lockau,[1] Dennis J. Nürnberg[4] and Thomas Volkmer[1]

Correspondence
T. Volkmer
thomas.volkmer@rz.hu-berlin.de

[1]Plant Biochemistry, Humboldt-Universität zu Berlin, Berlin, Germany

[2]Molecular Biophysics, Humboldt-Universität zu Berlin, Berlin, Germany

[3]Institute of Microbiology and Infection Medicine/Organismic Interactions, University of Tübingen, Tübingen, Germany

[4]School of Biological and Chemical Sciences, Queen Mary University of London, London, UK

The polyphosphate glucokinases can phosphorylate glucose to glucose 6-phosphate using polyphosphate as the substrate. ORF *all1371* encodes a putative polyphosphate glucokinase in the filamentous heterocyst-forming cyanobacterium *Anabaena* sp. PCC 7120. Here, ORF *all1371* was heterologously expressed in *Escherichia coli*, and its purified product was characterized. Enzyme activity assays revealed that All1371 is an active polyphosphate glucokinase that can phosphorylate both glucose and mannose in the presence of divalent cations *in vitro*. Unlike many other polyphosphate glucokinases, for which nucleoside triphosphates (e.g. ATP or GTP) act as phosphoryl group donors, All1371 required polyphosphate to confer its enzymic activity. The enzymic reaction catalysed by All1371 followed classical Michaelis–Menten kinetics, with k_{cat}=48.2 s^{-1} at pH 7.5 and 28 °C and K_M=1.76 μM and 0.118 mM for polyphosphate and glucose, respectively. Its reaction mechanism was identified as a particular multi-substrate mechanism called the 'bi-bi ping-pong mechanism'. Bioinformatic analyses revealed numerous polyphosphate-dependent glucokinases in heterocyst-forming cyanobacteria. Viability of an *Anabaena* sp. PCC 7120 mutant strain lacking *all1371* was impaired under nitrogen-fixing conditions. GFP promoter studies indicate expression of *all1371* under combined nitrogen deprivation. All1371 might play a substantial role in *Anabaena* sp. PCC 7120 under these conditions.

Received 19 June 2014
Accepted 9 October 2014

INTRODUCTION

Inorganic polyphosphate, which is a linear polymer of 10–1000 orthophosphates linked by phosphoanhydride bonds, has been found in all representative living cells, including bacteria, fungi, plants, animals and archaea (Achbergerová & Nahálka, 2011; Rao *et al.*, 2009; Remonsellez *et al.*, 2006; Scherer & Bochem, 1983). Polyphosphate is stored in the cytoplasm, where it can be visualized as metachromic inclusions (Meyer, 1902) or electron-dense granules (Jensen, 1968). Evolutionarily, polyphosphate stands as one of the earliest polymers produced in cells. Polyphosphate is considered to be the ancestor of ATP as an energy source (Resnick & Zehnder, 2000), given that hydrolysis of the phosphoanhydride bond between each orthophosphate yields free energy comparable to that generated by cleavage of ATP. In a bacterial cell, polyphosphate functions mainly as a dynamic storage compound for phosphate and energy (Harold, 1966; Kornberg *et al.*, 1956). However, many other functions have been proposed for the polymer, including those in stress responses, complexation of heavy metals, biofilm formation and virulence (Kornberg, 1995; Rashid & Kornberg, 2000; Rashid *et al.*, 2000; Tsutsumi *et al.*, 2000). In bacteria, polyphosphate metabolism is driven by two kinds of enzymes: kinases and phosphatases. Polyphosphate is synthesized by polyphosphate kinase type 1 (Ahn & Kornberg, 1990; Kornberg *et al.*, 1956), which catalyses the formation of the phosphoanhydride bonds between the growing polymer and the γ-phosphoryl residues of ATP or another nucleotide triphosphate. Conversely, polyphosphate is degraded mainly by exopolyphosphatases (Akiyama *et al.*, 1993; Kornberg *et al.*, 1999) and endopolyphosphatases (Lichko *et al.*, 2010).

Abbreviations: *Anabaena*, *Anabaena* sp. PCC 7120; GST, glutathione-*S*-transferase; PPGK, polyphosphate glucokinase; TSS, transcription start site.

Two supplementary tables and five supplementary figures are available with the online Supplementary Material.

081836 © 2014 The Authors *Printed in Great Britain*
This is an Open Access article distributed under the terms of the Creative Commons Attribution License (http://creativecommons.org/licenses/by/3.0/).

Polyphosphate glucokinase (PPGK; EC 2.7.1.63), a paralogue of the ATP-dependent glucokinase (Hsieh *et al.*, 1993), catalyses the transfer of the terminal phosphoryl residue of polyphosphate to glucose in order to generate glucose 6-phosphate. The first ATP/polyphosphate-dependent glucokinase was discovered in *Mycobacterium phlei* (Szymona & Ostrowski, 1964). Since then, such enzymes have been found in many non-eukaryotic organisms (Liao *et al.*, 2012; Lindner *et al.*, 2010; Pepin & Wood, 1986; Phillips *et al.*, 1993; Szymona & Widomski, 1974; Tanaka *et al.*, 2003). All but one of the known PPGKs are bifunctional, in that they are able to utilize both ATP and polyphosphate as phosphoryl donors. The sole known exception to that is the PPGK of the polyphosphate-accumulating bacterium *Microlunatus phosphovorus* (Tanaka *et al.*, 2003), which is a strictly polyphosphate-dependent enzyme.

The potential role of PPGKs in the complex metabolism of cyanobacteria has not yet been investigated. Cyanobacteria are a widespread group of oxygenic photosynthetic prokaryotes. During photosynthesis, energy is transiently stored in the energy-rich phosphoanhydride bonds of ATP molecules. Several genera of cyanobacteria perform both photosynthesis and N_2 fixation; however, these two physiological processes are incompatible, because the oxygen-sensitive nitrogenase complex (Hill *et al.*, 1981) is the key enzyme in N_2 fixation. The diazotrophic cyanobacteria have developed special mechanisms to allow N_2 fixation to take place under aerobic conditions (Berman-Frank *et al.*, 2003). Some filamentous cyanobacteria, such as *Anabaena* sp. PCC 7120 (also called *Nostoc* sp. PCC 7120; hereafter *Anabaena*), form highly specialized cells called 'heterocysts', which fix N_2 in a micro-oxic environment (Adams *et al.*, 1981). The heterocysts are semi-regularly distributed along the filaments and rely on vegetative cells to supply them with photosynthetic products. In return, the heterocysts provide the filament with reduced nitrogen compounds (Flores & Herrero, 2010; Maldener & Muro-Pastor, 2010). In contrast, some unicellular diazotrophic cyanobacteria use a diurnal rhythm to separate N_2 fixation and photosynthesis, protecting the nitrogenase from oxygen by employing it in the dark, when photosynthesis is quiescent (Mitsui *et al.*, 1986; Toepel *et al.*, 2008).

The purpose of this study was to characterize All1371, the PPGK from *Anabaena*, *in vitro* and to explore its biological function *in vivo*.

METHODS

Sequence analysis. A BLASTP search (Altschul *et al.*, 1997) was performed against all cyanobacterial sequences available from the Integrated Microbial Genomes database (Markowitz *et al.*, 2012) and against the sequences of Section V cyanobacteria identified by Dagan *et al.* (2013). The amino acid sequence of the PPGK from *Anabaena* (*all1371*: 637231738, gene ID Integrated Microbial Genomes database) was used as query. Similar amino acid sequences of proteins with known 3D structures were identified using the structure database PDBsum (http://www.ebi.ac.uk/pdbsum/). Sequences were aligned using CLUSTALW2 (Larkin *et al.*, 2007), and formatted with ESPript (Gouet *et al.*, 1999). Sequence similarities were determined using the EMBOSS needle software (http://www.ebi.ac.uk/Tools/psa/emboss_needle/).

Bacterial strains and culture conditions. *Anabaena* was grown in fourfold diluted medium of Allen & Arnon (1955) (AA/4 medium) with or without 10 mM KNO_3. Liquid cultures of *Anabaena* were grown under permanent illumination with white light of 70 µmol photons m^{-2} s^{-1} at 30 °C. Cultures were grown in air lift flasks (Ø 6 cm), bubbled with air enriched with 2 % (v/v) CO_2. Mutants were grown in the presence of 50 µg neomycin ml^{-1} or 4 µg spectinomycin ml^{-1} and 1 µg streptomycin ml^{-1}. *Synechocystis* sp. PCC 6803 (hereafter *Synechocystis*) was grown on BG11 agar plates (Rippka *et al.*, 1979) additionally containing 20 mM HEPES. Liquid cultures were grown at 28 °C and under continuous illumination as described above. Liquid cultures of *Mastigocladus laminosus* SAG 4.84 and *Fischerella muscicola* PCC 7414 were grown in Castenholz medium D (8.24 mM $NaNO_3$, 0.99 mM KNO_3) or medium ND (without nitrate) (Castenholz, 1988) at 42 °C and under continuous illumination of 100 µmol photons m^{-2} s^{-1}.

Chlorophyll *a* content was determined as described by de Marsac & Houmard (1988). For nitrogen starvation, exponentially grown cultures were harvested by centrifugation, washed twice with nitrate-free medium and resuspended to a final concentration of 7 µg chlorophyll ml^{-1} for further growth. *Escherichia coli* strains DH5α and BL21 (DE3) (Novagen; Merck Chemicals) were grown at 37 °C as batch culture in Erlenmeyer flasks with shaking at 300 r.p.m. in Luria–Bertani (LB) medium (Bertani, 1951) supplemented with 10 µg ampicillin ml^{-1}, 150 µg neomycin ml^{-1} or 50 µg spectinomycin ml^{-1} when appropriate.

Construction of expression plasmid. The *all1371* gene was amplified by PCR using genomic *Anabaena* DNA as template and oligonucleotides 5′-A**GGATCC**TACTCAATGGTGGAAGATAACGG-3′ and 5′-**GCGGCCGC**TTCTATAGTGTTTTTTCATCTC-3′ (*Bam*HI and *Not*I restriction sides highlighted in bold, stop codon underlined). The PCR product was ligated into the cloning vector pJET1.2 (Thermo Scientific) to ensure efficient restriction digests. After restriction digest of the resulting pJET-*all1371* by *Bam*HI and *Not*I, *all1371* was inserted into the vector pGEX-6P-1 (GE Healthcare), leading to pGEX_*all1371*. The manipulations were checked by restriction analysis and DNA sequencing.

Protein expression and purification. *E. coli* BL21(DE3) cells were transformed with pGEX_*all1371*. The recombinant strain was grown in LB medium containing 100 µg ampicillin ml^{-1} and 1 % (w/v) glucose. The expression was induced with 1 mM IPTG at an OD_{600} of 0.6. Cells were harvested 3 h after induction by centrifugation (15 min, 3800 ***g***), resuspended in buffer containing 200 mM Tris/HCl (pH 8.5), 300 mM NaCl and 50 mM KCl, and disrupted by sonication. The debris was removed by centrifugation (15 min, 20 000 ***g***). The glutathione-*S*-transferase (GST)–PPGK fusion was purified by affinity chromatography using Glutathion-Sepharose 4B (GE Healthcare) performed in a batch technique according to the manufacturer's instructions. To elute All1371 the GST-tagged PPGK was cleaved on the column by PreScission protease (Walker *et al.*, 1994) (GE Healthcare) overnight at 4 °C. The purity of the enzyme was verified by SDS-PAGE.

Preparation of cell-free cyanobacterial extract, electrophoresis and protein quantification. Cyanobacterial cells were collected from liquid cultures (grown with or without nitrogen for 4 or 6 days) by centrifugation (6500 ***g***). Sedimented cells were washed twice with 50 mM Tris/HCl buffer (pH 8.0) and stored at −20 °C. Thawed filaments of *Mastigocladus laminosus* and *F. muscicola* were pretreated

by sonication. Cells were disrupted in a swing mill (Retsch MM 301) for 30 min at 30 Hz using glass beads (Ø 0.1 mm). Beads and crude extracts were separated by two sequential centrifugations at 10 000 ***g*** and 4 °C for 10 and 30 min. To remove small molecules the supernatants were purified using DextraSEC PRO2 columns (Applichem). The elution was performed by the original buffer. Protein concentrations were estimated according to Lowry *et al.* (1951) using BSA as reference. SDS-PAGE was performed on slab gels [15 % (w/v) acrylamide, 0.41 % (w/v) methylene-bisacrylamide] (Laemmli, 1970). The gels were stained with Coomassie brilliant blue R250.

Determination of molecular mass. The molecular mass of native All1371 was determined by size exclusion chromatography on a Tricorn Superdex 200 10/300 GL column (GE Healthcare) calibrated with the gel filtration standards purchased from Bio-Rad (γ-globulin, 158 kDa; ovalbumin, 44 kDa; myoglobin, 17 kDa; cytochrome, *ca.* 12.4 kDa). As running buffer 100 mM Tris/HCl (pH 7.5), 200 mM NaCl, 6 mM $MgCl_2$ (hereafter basic buffer) and 0.5 mM DTT were used at a flow rate of 0.8 ml min^{-1}. Pure All1371 (100 µg) was loaded onto the column. The elution was monitored by measuring A_{280}. Fractions of 0.5 ml were collected. Aliquots from these fractions were tested for PPGK activity. Precipitated fractions (Bensadoun & Weinstein, 1976) were analysed by SDS-PAGE. Two biological replicates were performed.

Activity assays and kinetic analyses. Glucokinase activity and kinetics of the isolated All1371 were determined *in vitro* by coupling glucose 6-phosphate formation to the glucose-6-phosphate dehydrogenase reaction (Hsieh *et al.*, 1993). Glucose 6-phosphate formation was monitored indirectly by measuring NADH development spectrophotometrically at 340 nm (ε_{340}=6220 M^{-1} cm^{-1}). Measurements were done in basic buffer with 0.6 mM NAD, 0.8 mM glucose, 0.01 mM $polyP_{45}$ (phosphate glass type 45; Sigma-Aldrich; hereafter polyphosphate), 5.7 units glucose-6-phosphate dehydrogenase ml^{-1} and 0.26 µg All1371 ml^{-1} at 28 °C. To verify the cation dependency, $MgCl_2$ was replaced by $MnCl_2$ or water. One unit of PPGK activity was defined as the amount of enzyme which catalyses the formation of 1 µmol glucose 6-phosphate min^{-1}. The reaction was started with All1371. All rates were determined from the linear region of the curves. To check the substrate specificity, the following substrates were applied to the assay at final concentrations of 10 µM, 100 µM and 1 mM: $polyP_{45}$, ATP, ADP, AMP, GTP, UTP, CTP and pyrophosphate. Additionally ATP was tested as a substrate at final concentrations of 5 and 10 mM. Polyphosphate was used to check enzyme activity if no activity was detected *in vitro*. To determine the kinetics of All1371, both substrates (glucose, polyphosphate) were varied. The values of K_M and k_{cat} were calculated from the initial rate. Three biological replicates were performed. Kinetic parameters were analysed by Sigma Plot 2006 Enzyme Kinetics Module 1.3 (Systat software). The initial rate was measured for several glucose concentrations at different non-saturating $polyP_{45}$ concentrations. Measurements were also taken for several polyphosphate concentrations at different non-saturating glucose concentrations.

Mannokinase activity was determined by monitoring the formation of NADH spectrophotometrically at 340 nm. Activity was measured in basic buffer including 0.6 mM NAD, 5–70 mM mannose, 0.02 mM $polyP_{45}$, 5.7 units glucose-6-phosphate dehydrogenase ml^{-1}, 1.0 units mannose-6-phosphate isomerase ml^{-1}, 4.0 units glucose-6-phosphate isomerase ml^{-1} and 23–42 µg All1371 ml^{-1} at 28–30 °C.

When measuring PPGK activities in cell-free extracts, the extracts instead of the pure enzyme were used in standard assays as described above (glucokinase activity). The reaction was started with glucose. To confirm the linearity of the reaction different amounts of the extracts with 23–480 µg protein were added to the reaction mixture. All1371 was applied to the assay as a positive control.

Deletion of *all1371* in *Anabaena*. An *Anabaena* Δ*all1371* mutant was generated by replacing 771 nt including *all1371* [720 nt, genomic region 1625 095–1625 814 (Nakao *et al.*, 2010)] with an antibiotic resistance cassette, not affecting other ORFs.

Upstream and downstream regions of *all1371* were amplified by PCR using genomic *Anabaena* DNA as template. Restriction sites introduced by the primers below are highlighted in the sequence in bold type and termed in parentheses. The upstream region (position 1625 815–1626 817) was amplified using the primers 5′-ATT**GAGCTC**AAGGACGGAAAAAATTACAC-3′ (*Sac*I) and 5′-GAGTATTTACCTTTTTT**TCTAGA**GACTGG-3′ (*Xba*I) yielding a PCR product of 973 nt after restriction. The downstream region was amplified using the primer pair 5′-CCCGAAAC**TCTAGA**TGTGACTGGGTATGGGG-3′ (*Xba*I) and 5′-AATG**CTCGAG**AACCAACCTATACCTGTGC-3′ (*Xho*I). The restricted product yielded a 943 nt fragment. The fragments were successively inserted into the pBluescript KSII+ vector (Stratagene) resulting in pKSII+_up_down. The resistance cassette C.K3 containing the neomycin phosphotransferase II gene was received from pRL448 (Elhai & Wolk, 1988a) and inserted into pKSII+_up_down via the *Xba*I site, yielding pKSII+_up-C.K3-down. The C.K3 cassette was inserted in the same direction as *all1371*. The correctness of the sequence was validated by DNA sequencing. To construct pRL271_up-C.K3-down used for deletion, the *Sac*I/*Xho*I fragment excised from the prior plasmid was cloned into plasmid pRL271 (Black *et al.*, 1993). This plasmid was conjugationally transferred to *Anabaena* by triparental mating using *E. coli* strain J53[RP4] and cargo strain *E. coli* HB101[pRL528] (Elhai & Wolk, 1988b). Neomycin-resistant double recombinants were identified by PCR and *sacB* selection (Cai & Wolk, 1990).

Viability tests. Viability tests of *Anabaena* and the Δ*all1371* mutant were carried out as a spot assay on AA-plates (Allen & Arnon, 1955) with or without 10 mM KNO_3 as a nitrogen source. A 10 µl volume of liquid cultures was applied per spot. These agar plates were exposed to continuous light of 60–70 µmol photons m^{-2} s^{-1} for 6 days. Three biological replicates were tested separately.

Generation of a GFP promoter fusion strain. The *gfp* gene was amplified by PCR using the primer pair 5′-GATGGCTC**TCTAGA**ATGAGTAAAGGAGAAG-3′ and 5′-CT**TCTAGA**TTAATGTTTGTATAGTTCATC-3′ (*Xba*I in bold type, stop codon underlined) and plasmid pJET1.2-GFP as template (Baier, 2013). The *gfp* gene was obtained by *Xba*I digest and inserted in plasmid pKSII+_up_down (see above) via the *Xba*I site, leading to pKSII+_up-gfp-down. By this means, the *gfp* gene was integrated in this plasmid into the upstream region of *all1371* 32 nt after the transcription start site. This plasmid was used as template in a PCR performed with oligonucleotides 5′-CTATAGGGC**GAATTC**GAGCTCAAGGACGG-3′ and 5′-GTGTTCTTCTCC**GAATTC**CCATAC-3′ (*Eco*RI sites in bold type). Finally, the PCR product was inserted into pRL1049 (Black & Wolk, 1994) via the *Eco*RI sites, resulting in vector pRL1049-up-gfp-down, which was validated by DNA sequencing. To generate *Anabaena all1371* GFP promoter fusion strains, pRL1049-up-gfp-down_*all1371* was introduced in the *Anabaena* wild-type and Δ*all1371*. Conjugation was performed as described above. Positive exconjugants selected on AA-agar plates (Allen & Arnon, 1955) containing 4 µg spectinomycin ml^{-1} and 1 µg streptomycin ml^{-1} were checked by PCR using primers 5′-GCCTGCATTTGGTGCTGGACTGG-3′ and 5′-GGTCTGCTAGTTGAACGCTTCC-3′. The plasmid pRL1049-up-gfp-down_*all1371* was self-replicating in these exconjugants.

Confocal microscopy. For confocal microscopy *Anabaena* and mutant strains (Δ*all1371*, promoter fusion) were grown as liquid cultures with and without nitrate for 4 days. Fluorescence in cells of the *Anabaena* Δ*all1371* promoter fusion strain was visualized with a laser-scanning confocal microscope (Olympus FV-1000MPE). GFP

was excited by an argon ion laser (488 nm irradiation). Fluorescence emission was recorded at 500–545 nm (for GFP) and 570–670 nm (for chlorophyll fluorescence) using a 60 × water-immersion objective (Olympus IX-81 60 × /1.2 Water UPlanSApo, DIC, fourfold zoom). All confocal images for each experiment were acquired using identical adjustments. The GFP fluorescence was quantified using Olympus Fluoview version 3.1. The fluorescence of a heterocyst was compared with that of the two adjacent vegetative cells. The Δ*all1371* mutant strain without GFP was used as control. Background fluorescence was subtracted.

RESULTS

All1371 as putative PPGK

The ORF *all1371* from *Anabaena* was assumed to encode a putative PPGK (EC 2.7.1.63), as its amino acid sequence has sequence similarity to several well-characterized bacterial PPGKs, including the polyphosphate/ATP-glucomannokinase from *Arthrobacter* sp. strain KM (Mukai *et al.*, 2003, 2004) (53.1 % similarity), the polyphosphate-dependent PPGK from *Microlunatus phosphovorus* (Tanaka *et al.*, 2003) (46.0 % similarity) and the polyphosphate/ATP-dependent glucokinase from *Mycobacterium tuberculosis* (Hsieh *et al.*, 1993, 1996a, b) (47.4 % similarity). Comparison of these sequences, including secondary structures extrapolated from the crystal structure of the polyphosphate/ATP-glucomannokinase of *Arthrobacter* sp. strain KM (1WOQ) (Mukai *et al.*, 2003, 2004), revealed the presence of some highly conserved common motifs (Fig. 1). Seven structural and functional motifs (Fig. 1, boxed) were found in all of the sequences including All1371.

Purification of All1371 and molecular mass determination

The N-terminal GST-fusion protein of All1371 was expressed for 3 h in *E. coli* BL21(DE3) carrying pGEX_*all1371*. After on-column cleavage with the PreScission protease, the 246 aa

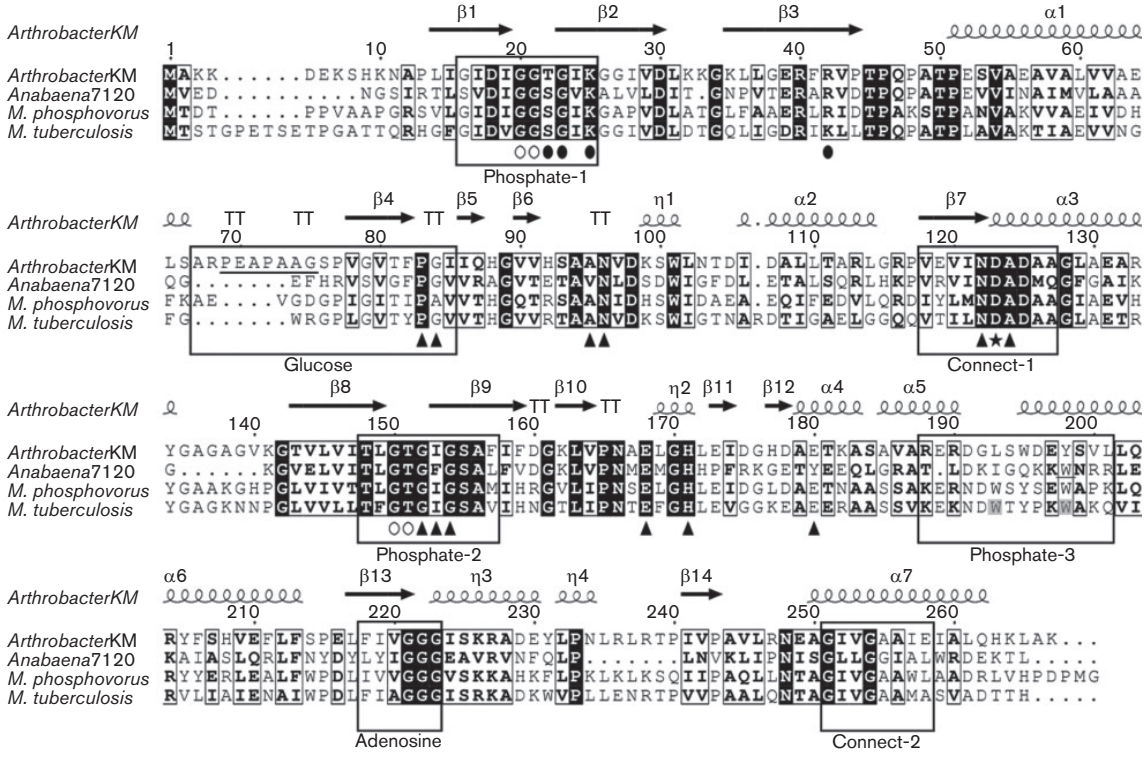

Fig. 1. Primary structural alignments of different PPGKs. Aligned primary structures from *Arthrobacter* sp. strain KM, *Microlunatus phosphovorus* (Tanaka *et al.*, 2003), *Mycobacterium tuberculosis* (Hsieh *et al.*, 1993; Phillips *et al.*, 1999) and *Anabaena* sp. PCC 7120. Strictly conserved residues are shaded in black; similar residues are framed in black. Putative structural and functional domains are enclosed in boxes. Secondary structural elements [e.g. α helices, β sheets, turn-turns (TT)] of the polyP/ATP-glucomannokinase from *Arthrobacter* sp. strain KM are depicted above the alignment. Residues associated with β-D-glucose binding are marked with filled triangles. The heptapeptide is underlined. The catalytic aspartate (D) is highlighted with a star. Residues involved in the binding of both phosphate molecules used as ligands (open, phosphate A; filled, phosphate B) are marked with ovals (Mukai *et al.*, 2004).

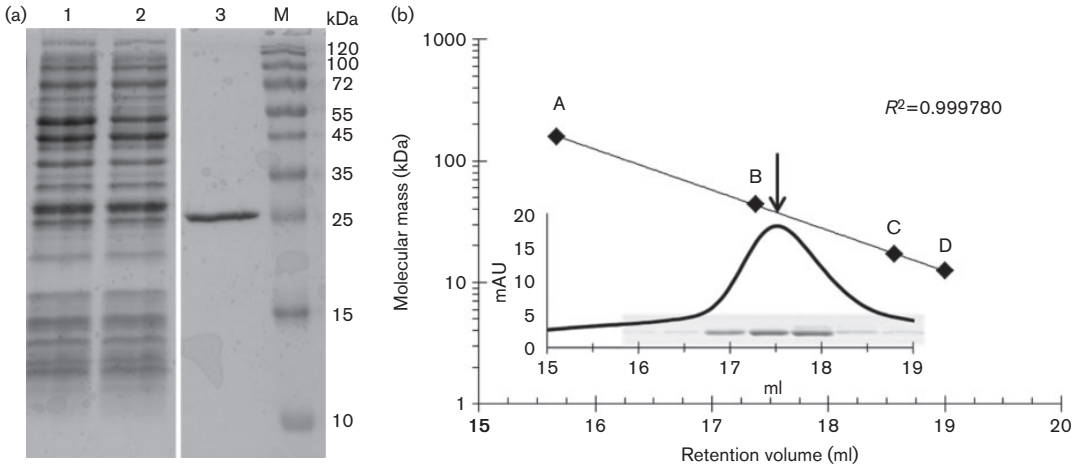

Fig. 2. Purification of recombinant All1371 and gel filtration. (a) SDS-PAGE (15 %) analysis of samples from the various purification steps performed after affinity chromatography. Lane 1, cell-free extract of recombinant *E. coli*, 15 μg protein; lane 2, flow-through, 15 μg protein; lane 3, All1371 after elution, 2 μg; lane M, protein standard. (b) All1371 was subjected to gel filtration calibrated with protein standards (filled diamonds; see Methods for details). The elution profile (indicating the elution position of All1371, arrow) and SDS-PAGE results of the obtained fractions are shown in the inset.

enzyme was eluted and analysed by SDS-PAGE (Fig. 2a). The enzyme appeared as a single band of 26 kDa (Fig. 2a, lane 3; apparent molecular mass). To investigate the oligomeric state of All1371, the recombinant PPGK was analysed by size-exclusion chromatography. A single symmetrical peak (Fig. 2b, inset) of approximately 39.0 kDa was obtained. Fractions corresponding to the protein elution peak showed a single protein band of 26 kDa on SDS-PAGE (Fig. 2b, inset), and exhibited polyphosphate-dependent activity *in vitro* (data not shown). The biochemical and kinetic properties of All1371 are summarized in Table 1.

Table 1. Biochemical and kinetic properties of All1371

Measurements were performed at 28 °C, pH 7.5; $n \geqslant 3$; 100 %=107.1 U mg^{-1}.

Property		Value (mean ± SD)
Molecular mass (kDa)	Native complex*	39
	Monomer, apparent†	26.0
	Monomer, calculated‡	26.6
Oligomeric structure		Monomer or homodimer
K_M (mM)	Glucose	0.118 ± 0.01
K_M (μM)	Polyphosphate	1.76 ± 0.26
v_{max} (U mg^{-1})	Glucose, polyphosphate	107.1 ± 15.3
k_{cat} (s^{-1})	Glucose, polyphosphate	48.2 ± 6.9
$K_{0.5}$ (mM)	Mannose	24.3 ± 2.36
v_{max} (U mg^{-1})	Mannose	0.43 ± 0.04
k_{cat} (s^{-1})	Mannose	0.21 ± 0.017
Phosphoryl donor specificity (% v_{max})	Polyphosphate	100
	ATP, GTP, UTP, CTP, ADP, AMP	0
	Pyrophosphate	0
	Without polyphosphate	0

*Determined by size exclusion chromatography.
†Determined by SDS-PAGE.
‡Calculated according to the primary structure, including the linker peptide of the GST tag.

Biochemical properties of All1371

Our enzyme activity assays indicated that purified All1371 uses polyphosphate to phosphorylate glucose and mannose, with a higher preference for glucose (Table 1). All1371 activity was strictly dependent on the presence of Mg^{2+} or Mn^{2+} (data not shown). All1371 had high substrate specificity and acted as a strict polyphosphate-dependent enzyme. No other phosphoryl group donor was accepted. Kinetic analysis indicated that the reactions of All1371 with polyphosphate and glucose followed Michaelis–Menten kinetics. The K_M values for polyphosphate and glucose were 1.76 μM and 0.118 mM, respectively (at 28 °C and pH 7.5). The maximum rate of All1371-mediated catalysis was 107 U mg^{-1}, yielding a k_{cat} of 48.2 s^{-1} (Table 1). Furthermore, our kinetic analysis revealed that All1371 had a k_{cat} of 0.19 s^{-1} and a $K_{0.5}$ of 24.3 mM for mannose (Table 1).

To characterize the enzymic mechanism of All1371, additional kinetic analyses with glucose and polyphosphate were performed. The initial rate of All1371 activity was determined with varying concentrations of glucose and fixed concentrations of polyphosphate. We obtained a linear double reciprocal plot with parallel lines (Fig. 3a). When polyphosphate was varied, we obtained a similar graph with parallel lines (data not shown).

Distribution of putative PPGKs in cyanobacteria and PPGK activity in cell-free cyanobacterial extracts

To examine the distribution of PPGKs among cyanobacteria, we performed a BLASTP search (Altschul *et al.*, 1997) against all sequenced cyanobacterial genomes (September 2013; 141 genomes) using the amino acid sequence of All1371 as the query. Our analysis revealed that in 34 % of all sequenced cyanobacteria a putative PPGK is present. PPGKs were found in all five sections of cyanobacteria (Table 2) with the highest frequency in the heterocyst-forming species of Section IV (85 %) and Section V (54.5 %), followed by the non-heterocystous species of Section III (52.9 %), Section II (50 %) and Section I (5.7 %). More complete data are presented in Table S1

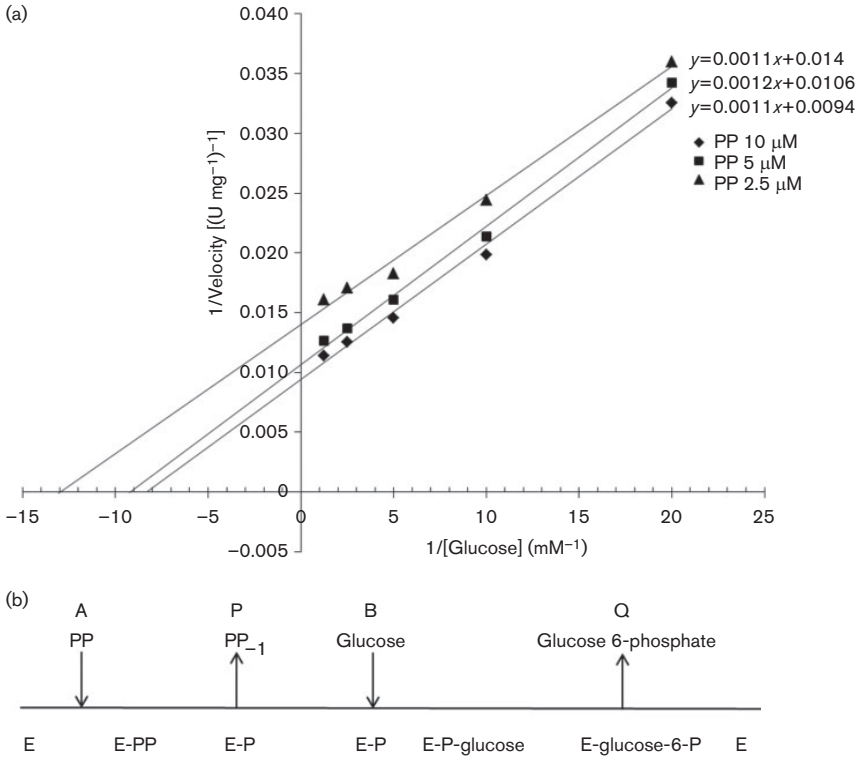

Fig. 3. Kinetics of the All1371 reaction. (a) Activity of All1371. Primary double-reciprocal plot of initial velocity with glucose as the variable substrate and different concentrations of $polyP_{45}$ (PP) as the fixed substrate (pH 7.5; $n=3$). (b) Schematic of the bi-bi ping-pong mechanism. Polyphosphate (PP) acts as the first substrate (A) by covalently binding to PPGK (E). The first product (P), polyphosphate reduced at one phosphate (PP_{-1}), is released, and binding of the second substrate, glucose (B), occurs on the phosphorylated enzyme (E-P). Finally, the second product, glucose 6-phosphate (Q), is released and the enzyme is restored (E).

Table 2. Distribution of PPGKs among cyanobacteria

	Section				
	I	II	III	IV	V
No. of PPGKs	4	3	18	17	6
No. of cyanobacteria	70	6	34	20	11
Percentage	5.7	50.0	52.9	85.0	54.5

(available in the online Supplementary Material). Cell-free extracts of some of these cyanobacteria were tested for specific PPGK activity under different nitrogen conditions, including *Anabaena* (Section V), *Mastigocladus laminosus* (Section V) (Nürnberg *et al.*, 2014), *F. muscicola* (Section V) and *Synechocystis* (Section I), the last lacking a predicted PPGK (negative control). As expected, cell-free extracts of *Synechocystis* did not show any PPGK activity, whereas those of *Anabaena*, *Mastigocladus laminosus* and *F. muscicola* exhibited detectable PPGK activity (Table 3). In *Anabaena*, PPGK activity was increased slightly under nitrogen depletion. PPGK activity in cell-free extracts from the two diazotrophic, branched filamentous cyanobacterial strains of Section V was three- to fourfold higher than in non-branched *Anabaena* cells (Table 3). Interestingly, we found a decrease of PPGK activity in extracts of Section V cells grown without combined nitrogen (Table 3).

Viability of Δ*all1371*

To confirm a function of All1371 *in vivo*, we generated a mutant strain in which ORF *all1371* was replaced with the neomycin-resistance cassette, C.K3 (Fig. 4a). Complete segregation of the mutant was validated by PCR (Fig. S1), and no PPGK activity was detected in cell-free extracts of Δ*all1371* (Table 3). Using light and fluorescence microscopy, we monitored the shape and autofluorescence of cells. When the Δ*all1371* mutant was deprived of combined nitrogen, the filaments showed both vegetative cells and morphologically mature heterocysts. Analysis of Δ*all1371* mutant and WT cells under different light and nitrogen conditions revealed that viability of the mutant was distinctly decreased under combined nitrogen-limiting conditions (Fig. 4b, Fig. S2). This effect was increased under light–dark cycle conditions, but in this case we also noted a reduced viability of the mutant in the presence of nitrate (Fig. S3b).

Expression analysis using a GFP promoter fusion

The transcriptional changes experienced by *Anabaena* during nitrogen-depletion-induced cell differentiation were recently analysed by Mitschke *et al.* (2011). They identified numerous transcription start sites (TSSs) in *Anabaena*, including a TSS of *all1371* at position 1625 874. The organization of the predicted *all1371* promoter region is depicted in Fig. 5(a). We identified a putative palindromic motif that is likely to be a (DIF)+ motif (Mitschke *et al.*, 2011). This putative (DIF)+ motif displays an inverse orientation and one mismatch [Fig. 5a; (DIF)+ in bold type, mismatch in red, AGCCCT].

To investigate the expression of *all1371* along the filaments, the *gfp* gene was transcriptionally fused to the *all1371* promoter and transformed into the Δ*all1371* mutant strain. In the absence of combined nitrogen, we noted distinct GFP fluorescence in the mature heterocysts of 4-day-old filaments of the promoter fusion strain (Fig. 5b). An overview of fluorescence (GFP, autofluorescence) of the promoter fusion strain is given in Fig. S4. No distinct GFP fluorescence was observed in the filaments of the promoter fusion strain when combined nitrogen was supplied (Fig. 5b) compared with Δ*all1371* (Fig. S5). GFP fluorescence in heterocysts was first detected 24 h after nitrogen step down, and persisted until the filaments were harvested 4 days later (data not shown). Quantification of GFP fluorescence of numerous cells in the promoter–*gfp* fusion strain in comparison with cells of the parent strain Δ*all1371* confirmed our microscopic observations: the

Table 3. PPGK activities in cell-free extracts of cyanobacteria

Measurements were performed at 28–30 °C and pH 7.5; $n \geqslant 3$; ND, not detectable ($\leqslant 1$ nmol min^{-1} mg^{-1}).

Strain	Section	Growth conditions	PPGK activity (nmol min^{-1} mg^{-1}) (mean ± SD)
Anabaena	IV	+N	4.3 ± 1.3
		−N	5.8 ± 1.3
Anabaena Δ*all1371*	IV	+N	ND
		−N	ND
F. muscicola	V	+N	15.3 ± 2.3
		−N	13.1 ± 2.1
Mastigocladus laminosus	V	+N	23.6 ± 0.7
		−N	13.9 ± 3.2
Synechocystis	I	+N	ND
		−N	ND

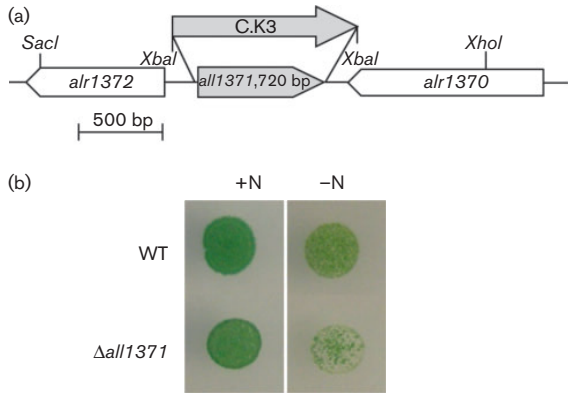

Fig. 4. The Δ*all1371* mutant. (a) Schematic of the chromosomal region surrounding *all1371* and the gene inactivation strategy, in which *all1371* was replaced with the C.K3 cassette. (b) Viability analyses of *Anabaena* wild-type (WT) and the *all1371* knockout mutant strain (Δ*all1371*) on AA-agar plates containing 10 mM KNO_3 (+N) or lacking combined nitrogen (−N). In total, 4.8 ng chlorophyll *a* per spot was plated. The plates were incubated under continuous light for 6 days.

fluorescence intensity in heterocysts (n=42) of the promoter fusion strain was ~2.1-fold higher than in vegetative cells (n=71). The ratio of fluorescence intensity from heterocysts (n=18) to vegetative cells (n=34) in filaments of the parent strain Δ*all1371* was 1 : 0.9 (Table S2).

DISCUSSION

Identification of the putative PPGK, All1371

The structural and functional motifs found in all the aligned amino acid sequences (Fig. 1, boxed) are predicted to interact with the substrates glucose, mannose, ATP and polyphosphate (Liao *et al.*, 2012; Mukai *et al.*, 2003). Five of the identified domains have been proposed to interact with the ATP molecule: phosphate-1 and phosphate-2 are involved in binding β-phosphates and γ-phosphates, while connect-1, connect-2 and the adenosine motif interact with the adenine ring of ATP (Mukai *et al.*, 2003). The conserved aspartate residue in the connect-1 region (Fig. 1, star) is believed to be essential for catalytic activity (Arora *et al.*, 1991; Mukai *et al.*, 2004). The glucose motif has been suggested to participate in glucose binding. The heptapeptide PEAPAAG (Fig. 1, underlined) was proposed to be responsible for mannose phosphorylation in the sequence

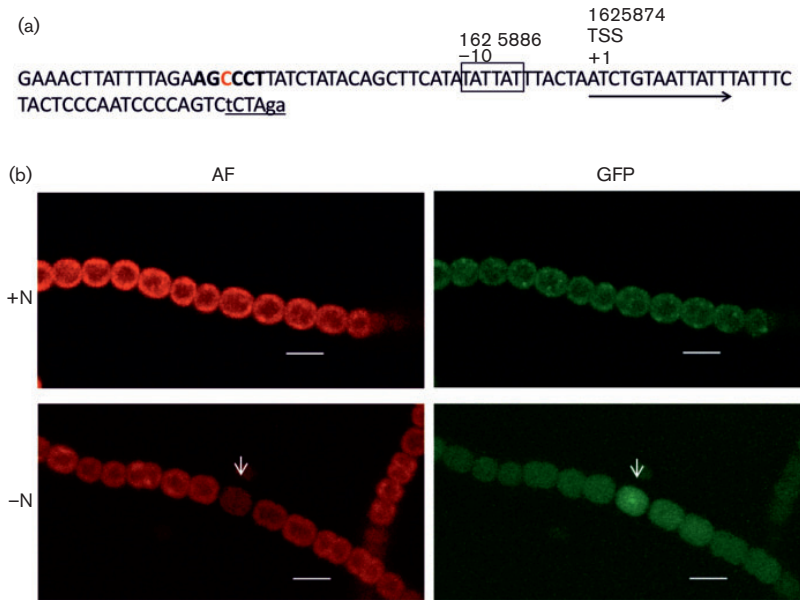

Fig. 5. *All1371* promoter activity in heterocysts. (a) The promoter region of *all1371*, including the TSS and the −10 region (boxed) (Mitschke *et al.*, 2011), was integrated into a self-replicating plasmid. A promoter-less *gfp* gene was integrated via the underlined *Xba*I site (altered bases are depicted in lower case); the presumed DIF+ domain (AGCCCT) is shown in bold. (b) Fluorescence in the *Anabaena* Δ*all1371* promoter fusion strain grown under N_2-fixing conditions (−N) and grown with combined nitrogen (+N). A heterocyst is indicated with an arrow. Bars, 5 μm. AF, auto-fluorescence (red); GFP, GFP fluorescence (green).

of *Arthrobacter* sp. strain KM (Mukai *et al.*, 2003). The phosphate-3 motif was predicted to be a binding region for polyphosphate (Liao *et al.*, 2012). Residues Trp193 and Trp198 (Fig. 1, grey shading) were proposed to be essential for catalytic activity in *Mycobacterium tuberculosis* (Phillips *et al.*, 1999). A residue equivalent to Trp198 is present in the amino acid sequence of *Anabaena* (Fig. 1, underlined W). Furthermore, the phosphate-1 domain is likely to contain a putative polyphosphate-binding site, as both the anionic phosphates used as ligands in a crystallographic study (Mukai *et al.*, 2004) bound at highly conserved amino acid residues similar to Lys25. It was proposed that there may be shared ATP- and polyphosphate-binding sites in the phosphate-1 and phosphate-2 regions (Mukai *et al.*, 2004). Thus, the present amino acid sequence analysis of All1371 (Fig. 1) and the previous findings in similar proteins collectively suggest that All1371 functions as a PPGK.

Purification of All1371, and molecular mass determination

The purified All1371 appeared as a single protein band of 26 kDa in SDS-PAGE analysis (Fig. 2a, lane 3). This result is consistent with the expected molecular mass of 26.6 kDa calculated with the ProtParam tool (http://web.expasy.org/protparam/) (Wilkins *et al.*, 1999) for one monomer of the recombinant All1371.

The protein peak of 39 kDa obtained in size-exclusion chromatography (Fig. 2b) indicates that the native enzyme may exist as either a monomer or a homodimer. PPGK homodimers have also been reported in *Mycobacterium tuberculosis*, *Propionibacterium shermanii* and *Propionibacterium arabinosum* (Phillips *et al.*, 1999), whereas the polyphosphate/ATP-dependent glucomannokinase of *Arthrobacter* sp. strain KM was determined to exist as a monomer (Mukai *et al.*, 2003).

Biochemical properties of All1371

All1371 uses polyphosphate exclusively to phosphorylate glucose and mannose (Table 1) and is strictly dependent on the presence of divalent cations. This requirement for divalent cations is shared with the PPGKs of *Microlunatus phosphovorus* (Tanaka *et al.*, 2003), *Arthrobacter* sp. (Mukai *et al.*, 2003), *Mycobacterium tuberculosis* and *Mycobacterium phlei* (Szymona & Ostrowski, 1964; Szymona & Widomski, 1974). Recently, Mg^{2+} was found to be an indispensable cofactor for the PPGK of *Thermobifida fusca* (Liao *et al.*, 2012). Here, we report that All1371 showed high substrate specificity and acted as a strict polyphosphate-dependent enzyme. This result is a notable feature, as most of the previously described glucokinases utilized either ATP alone, or ATP and polyphosphate. The previous *in vitro* studies on PPGKs revealed that these enzymes were often bi-functional and not restricted to polyphosphate. For example, the PPGKs from *Mycobacterium tuberculosis* (Hsieh *et al.*, 1996a), *Propionibacterium shermanii* (Phillips *et al.*, 1993) and *Corynebacterium glutamicum* (Lindner *et al.*, 2010) were also able to use ATP or GTP. The present work showed that, along with the PPGK of *Microlunatus phosphovorus* (Tanaka *et al.*, 2003), All1371 is one of only two known PPGKs that uses only polyphosphate as its phosphate donor.

Kinetic analyses of All1371 (Table 1) revealed a relatively low K_M value obtained for polyphosphate (1.76 μM), suggesting that All1371 has a high affinity for its sole substrate. In comparison with the K_M values for polyphosphate and glucose (Table 1), the polyphosphate- and ATP-dependent PPGK from *Corynebacterium glutamicum* yielded K_M values of 0.2 mM for $polyP_{45}$ and 1 mM for glucose (Lindner *et al.*, 2010); the PPGK of *Propionibacterium shermanii* yielded a K_M value of 1.2 μM for $polyP_{35}$ (Phillips *et al.*, 1993); the PPGK of *Mycobacterium tuberculosis* yielded a K_M value of 4.6 μM for $polyP_{35}$ (Phillips *et al.*, 1999); and the PPGK of *Microlunatus phosphovorus* yielded a K_M of 3.8 mM for $polyP_{30}$ (Tanaka *et al.*, 2003). The turnover number of All1371 of 48.2 s^{-1} (Table 1) is comparable with the k_{cat} value of 57.0 s^{-1} determined for the PPGK from *Propionibacterium shermanii* against $polyP_{35}$ (Phillips *et al.*, 1999).

According to our analyses, All1371 is a polyphosphate-dependent glucomannokinase. Interestingly, the heptapeptide in the sequence of *Arthrobacter* sp. strain KM (Fig. 1, underlined), which is assumed to be responsible for mannose phosphorylation (Mukai *et al.*, 2004), is not present in the corresponding *Anabaena* sequence. The results of additional kinetic analyses (Fig. 3a) were consistent with the so-called 'bi-bi ping-pong' mechanism (Cleland, 1963). As illustrated in Fig. 3(b), this mechanism is a particular multi-substrate reaction that includes two substrates and two products (bi-bi) and is characterized by alternating processes of substrate binding and product release (ping-pong) for the two substrates. In a first step, polyphosphate is covalently bound to All1371, which is then phosphorylated. Approximately one orthophosphate-reduced polyphosphate is released from the enzyme as the first product. In a second step, glucose is bound to the phosphorylated enzyme, and the second substrate is phosphorylated. Glucose 6-phosphate is released as a second product, and the enzyme returns to its initial state (Fig. 3b). In contrast, the ATP/polyphosphate-dependent PPGK of *Mycobacterium tuberculosis* (Hsieh *et al.*, 1996a) and the ATP-dependent glucokinase from *Streptomyces coelicolor* (Imriskova *et al.*, 2005) were both found to display ordered bi-bi sequential mechanisms. The ordered bi-bi sequential mechanism differs from the bi-bi ping-pong mechanism in that both substrates (glucose and ATP or polyphosphate) bind to the enzyme first before the two products are released.

Putative PPGKs in cyanobacteria

Cyanobacteria may be grouped into five sections according to their morphology (Rippka *et al.*, 1979). While species of Sections I and II are unicellular forms, those of Sections III, IV and V show filamentous forms. Cyanobacteria of

Sections IV and V are additionally able to form heterocysts. The highest level of complexity is seen among Section V strains, which form true branches within their filaments (Golubic *et al.*, 1996). Diazotrophic growth has been observed in both unicellular and filamentous strains (reviewed by Stal, 1995). Our BLASTP search revealed that PPGKs were found very frequently in cyanobacteria of Sections IV and V, which are all diazotrophic strains forming heterocysts. All genomes of the analysed Section IV and Section V strains contained PPGK genes. In about half of the analysed genomes of Section III we found putative PPGK genes (52.9 %). In 11 of these 18 PPGK gene-containing genomes (61 %) we also found nifH genes encoding the key enzyme of N_2 fixation (Table S1). Some of these Section III organisms are known to fix N_2 under micro-oxic conditions, such as *Pseudanabaena* sp. ATCC 27183 (Rippka & Waterbury, 1977) (synonymous with *Pseudanabaena* sp. PCC 6802). Among cyanobacteria of Section II, 50 % of sequenced unicellular strains were also predicted to contain a PPGK. All are known to fix N_2 under anaerobic conditions (Rippka *et al.*, 1979) or to have a nitrogenase complex (Rippka & Waterbury, 1977), or a putative dinitrogenase has been annotated in the genome (Markowitz *et al.*, 2012). Furthermore, strains belonging to *Chroococcidiopsis* are closely related to the heterocyst-forming cyanobacteria (Fewer *et al.*, 2002). These facts may suggest a possible correlation between PPGK appearance and the ability to fix N_2 under anoxic/micro-oxic conditions provided by either heterocysts or the environment. This presumption is supported by the results obtained by analysing Section I organisms. Only four (5.7 %) of the unicellular strains of Section I were found to contain a putative PPGK. *Synechococcus* sp. PCC 7335 and *Synechococcus* sp. PCC 7502 arose through morphological transition events (Robertson *et al.*, 2001; Shih *et al.*, 2013). Interestingly, putative PPGKs were not found in the genomes of *Cyanothece* strains that are able to grow diazotrophically in diurnal rhythm. Based on the present findings, we hypothesized that the presence of a PPGK in cyanobacterial genomes is strongly related to the organism's ability to fix N_2 in heterocysts. A correlation between PPGK appearance and an organism's ability to fix N_2 under anoxic conditions is possible but has to be analysed further, especially from a phylogenetic point of view.

To determine whether PPGK activity was present *in vivo*, PPGK activity in cell-free extracts of some heterocyst-forming cyanobacteria with putative PPGKs was determined. As summarized in Table 3, PPGK activity in *Anabaena* is increased after 4 days of nitrogen depletion. An increase of PPGK activity under this condition is in line with the results of Flaherty *et al.* (2011). Using deep sequencing analyses performed 21 h after nitrogen deprivation, they found a 4.8-fold increase in the mRNA expression level of *all1371*. Furthermore, the increased PPGK activity is in line with a previous report (Thompson *et al.*, 1994), showing that in *Anabaena flos-aquae*, phosphate is stored as sugar phosphate under N_2-fixing conditions, but as polyphosphate in the presence of combined nitrogen. We found that PPGK activity was higher in cell-free extracts from thermophilic Section V strains of *F. muscicola* and *Mastigocladus laminosus* than in *Anabaena* (Table 3). A higher *in vitro* activity might be the result of a higher robustness of the PPGK due to its thermophilic origin (Beadle *et al.*, 1999). Interestingly, we observed an increased PPGK activity in cell-free extracts obtained from these strains grown in the presence of nitrate than under diazotrophic conditions. The higher complexity of Section V strains differing in the regulation of diazotrophic growth (Nürnberg *et al.*, 2014) might explain this observation.

Viability of Δ*all1371*

The impaired viability of the mutant implies that All1371 plays an important role in providing glucose-6-phosphate in *Anabaena*, supporting the canonical hexokinase. This is supported by the PPGK activity measured in cell-free extracts of *Anabaena* obtained from nitrate-supplemented cultures (Table 3). Under diazotrophic conditions heterocysts are not able to fix carbon dioxide. Carbon compounds, probably in the form of sucrose (Curatti *et al.*, 2002), are imported from vegetative cells. NAD(P)H, needed as a reducing equivalent, is generated in heterocysts (Maldener & Muro-Pastor, 2010). There, glucose 6-phosphate is used as substrate for glucose-6-phosphate dehydrogenase, a main enzyme of the oxidative pentose phosphate pathway. Because of the decreased viability of the mutant observed under diazotrophic conditions, we conclude that All1371 may represent an alternative enzyme completing the hexokinase under ATP-consuming (diazotrophic) growth conditions.

Expression analysis using a GFP promoter fusion

In cyanobacteria, the nitrogen-regulated genes are mainly controlled by the transcriptional regulators NtcA and HetR (Kumar *et al.*, 2010). Recently, chromatin immunoprecipitation analysis followed by high-throughput sequencing was used to identify all of the NtcA-binding sites of *Anabaena* at 3 h after a nitrogen step down (Picossi *et al.*, 2014). Interestingly, they detected an internal NtcA-binding site in *all1371* whereas the impact of binding of NtcA remains unclear. Further HetR-controlled promoters characterized by an differentiation-related change (DIF) + motif (TCCGGA, a palindrome at or close to position −35) were identified by comparing results found in *Anabaena* with a Δ*hetR* mutant 8 h after a nitrogen step down (Mitschke *et al.*, 2011). The putative (DIF) + motif with an inverse orientation located in the promoter region of *all1371* (Fig. 5 a) additionally indicates that the promoter might be HetR-dependent. In fact, the promoter of *all1371* responded to nitrogen depletion in WT but not in the Δ*hetR* mutant, indicating a HetR dependency (W. Hess, personal communication). Our results obtained with a GFP promoter fusion strain show that the *all1371* promoter activity is particularly enhanced under nitrogen

starvation in mature heterocysts. N_2 fixation in heterocysts is an energy-intensive process requiring 16 molecules of ATP to reduce one molecule of N_2 (Hill *et al.*, 1981; Howard & Rees, 1996). The ability of PPGKs to utilize polyphosphate instead of ATP for glucose phosphorylation might allow the heterocysts to save ATP for the essential process of N_2 fixation.

ACKNOWLEDGEMENTS

We thank Thomas Zielke for his valuable support with fluorescence microscopy. We are also grateful to Faranak Fassihianifard for performing the initial enzymic analysis.

REFERENCES

Achbergerová, L. & Nahálka, J. (2011). Polyphosphate – an ancient energy source and active metabolic regulator. *Microb Cell Fact* **10**, 63.

Adams, D. G., Carr, N. G. & Wilcox, M. (1981). The developmental biology of heterocyst and akinete formation in cyanobacteria. *Crit Rev Microbiol* **9**, 45–100.

Ahn, K. & Kornberg, A. (1990). Polyphosphate kinase from *Escherichia coli*. Purification and demonstration of a phosphoenzyme intermediate. *J Biol Chem* **265**, 11734–11739.

Akiyama, M., Crooke, E. & Kornberg, A. (1993). An exopolyphosphatase of *Escherichia coli*. The enzyme and its *ppx* gene in a polyphosphate operon. *J Biol Chem* **268**, 633–639.

Allen, M. B. & Arnon, D. I. (1955). Studies on nitrogen-fixing blue-green algae. I. Growth and nitrogen fixation by *Anabaena cylindrica* Lemm. *Plant Physiol* **30**, 366–372.

Altschul, S. F., Madden, T. L., Schäffer, A. A., Zhang, J., Zhang, Z., Miller, W. & Lipman, D. J. (1997). Gapped BLAST and PSI-BLAST: a new generation of protein database search programs. *Nucleic Acids Res* **25**, 3389–3402.

Arora, K. K., Filburn, C. R. & Pedersen, P. L. (1991). Glucose phosphorylation. Site-directed mutations which impair the catalytic function of hexokinase. *J Biol Chem* **266**, 5359–5362.

Baier, A. (2013). *Untersuchungen zum stickstoffinduzierten Phycobilisomenabbau - NblA, ein kleines Protein mit großer Wirkung*. Doctoral thesis, Humboldt-Universität zu Berlin..

Beadle, B. M., Baase, W. A., Wilson, D. B., Gilkes, N. R. & Shoichet, B. K. (1999). Comparing the thermodynamic stabilities of a related thermophilic and mesophilic enzyme. *Biochemistry* **38**, 2570–2576.

Bensadoun, A. & Weinstein, D. (1976). Assay of proteins in the presence of interfering materials. *Anal Biochem* **70**, 241–250.

Berman-Frank, I., Lundgren, P. & Falkowski, P. (2003). Nitrogen fixation and photosynthetic oxygen evolution in cyanobacteria. *Res Microbiol* **154**, 157–164.

Bertani, G. (1951). Studies on lysogenesis. I. The mode of phage liberation by lysogenic *Escherichia coli*. *J Bacteriol* **62**, 293–300.

Black, T. A. & Wolk, C. P. (1994). Analysis of a Het- mutation in *Anabaena* sp. strain PCC 7120 implicates a secondary metabolite in the regulation of heterocyst spacing. *J Bacteriol* **176**, 2282–2292.

Black, T. A., Cai, Y. & Wolk, C. P. (1993). Spatial expression and autoregulation of *hetR*, a gene involved in the control of heterocyst development in *Anabaena*. *Mol Microbiol* **9**, 77–84.

Cai, Y. P. & Wolk, C. P. (1990). Use of a conditionally lethal gene in *Anabaena* sp. strain PCC 7120 to select for double recombinants and to entrap insertion sequences. *J Bacteriol* **172**, 3138–3145.

Castenholz, R. W. (1988). Culturing methods for cyanobacteria. *Methods Enzymol* **167**, 68–93.

Cleland, W. W. (1963). The kinetics of enzyme-catalyzed reactions with two or more substrates or products. III. Prediction of initial velocity and inhibition patterns by inspection. *Biochim Biophys Acta* **67**, 188–196.

Curatti, L., Flores, E. & Salerno, G. (2002). Sucrose is involved in the diazotrophic metabolism of the heterocyst-forming cyanobacterium *Anabaena* sp. *FEBS Lett* **513**, 175–178.

Dagan, T., Roettger, M., Stucken, K., Landan, G., Koch, R., Major, P., Gould, S. B., Goremykin, V. V., Rippka, R. & other authors (2013). Genomes of Stigonematalean cyanobacteria (subsection V) and the evolution of oxygenic photosynthesis from prokaryotes to plastids. *Genome Biol Evol* **5**, 31–44.

de Marsac, N. T. & Houmard, J. (1988). Complementary chromatic adaptation: physiological conditions and action spectra. *Methods Enzymol* 167, 318–328.

Elhai, J. & Wolk, C. P. (1988a). Conjugal transfer of DNA to cyanobacteria. *Methods Enzymol* **167**, 747–754.

Elhai, J. & Wolk, C. P. (1988b). A versatile class of positive-selection vectors based on the nonviability of palindrome-containing plasmids that allows cloning into long polylinkers. *Gene* **68**, 119–138.

Fewer, D., Friedl, T. & Büdel, B. (2002). *Chroococcidiopsis* and heterocyst-differentiating cyanobacteria are each other's closest living relatives. *Mol Phylogenet Evol* **23**, 82–90.

Flaherty, B. L., Van Nieuwerburgh, F., Head, S. R. & Golden, J. W. (2011). Directional RNA deep sequencing sheds new light on the transcriptional response of *Anabaena* sp strain PCC 7120 to combined-nitrogen deprivation. *BMC Genomics* **12**, 332.

Flores, E. & Herrero, A. (2010). Compartmentalized function through cell differentiation in filamentous cyanobacteria. *Nat Rev Microbiol* **8**, 39–50.

Golubic, S., Hernandez-Marine, M. & Hoffmann, L. (1996). Developmental aspects of branching in filamentous *Cyanophyta/Cyanobacteria*. *Arch Hydrobiol Suppl Algol Stud* **83**, 303–329.

Gouet, P., Courcelle, E., Stuart, D. I. & Métoz, F. (1999). ESPript: analysis of multiple sequence alignments in PostScript. *Bioinformatics* **15**, 305–308.

Harold, F. M. (1966). Inorganic polyphosphates in biology: structure, metabolism, and function. *Bacteriol Rev* **30**, 772–794.

Hill, S., Kennedy, C., Kavanagh, E., Goldberg, R. B. & Hanau, R. (1981). Nitrogen fixation gene (*nifL*) involved in oxygen regulation of nitrogenase synthesis in *K. pneumoniae*. *Nature* **290**, 424–426.

Howard, J. B. & Rees, D. C. (1996). Structural basis of biological nitrogen fixation. *Chem Rev* **96**, 2965–2982.

Hsieh, P. C., Shenoy, B. C., Jentoft, J. E. & Phillips, N. F. (1993). Purification of polyphosphate and ATP glucose phosphotransferase from *Mycobacterium tuberculosis* H37Ra: evidence that poly(P) and ATP glucokinase activities are catalyzed by the same enzyme. *Protein Expr Purif* **4**, 76–84.

Hsieh, P. C., Kowalczyk, T. H. & Phillips, N. F. (1996a). Kinetic mechanisms of polyphosphate glucokinase from *Mycobacterium tuberculosis*. *Biochemistry* **35**, 9772–9781.

Hsieh, P. C., Shenoy, B. C., Samols, D. & Phillips, N. F. (1996b). Cloning, expression, and characterization of polyphosphate glucokinase from *Mycobacterium tuberculosis*. *J Biol Chem* **271**, 4909–4915.

Imriskova, I., Arreguín-Espinosa, R., Guzmán, S., Rodriguez-Sanoja, R., Langley, E. & Sanchez, S. (2005). Biochemical characterization of the glucose kinase from *Streptomyces coelicolor* compared to *Streptomyces peucetius* var. *caesius*. *Res Microbiol* **156**, 361–366.

Jensen, T. E. (1968). Electron microscopy of polyphosphate bodies in a blue-green alga *Nostoc pruniforme*. *Arch Mikrobiol* **62**, 144–152.

Kornberg, A. (1995). Inorganic polyphosphate: toward making a forgotten polymer unforgettable. *J Bacteriol* **177**, 491–496.

Kornberg, A., Kornberg, S. R. & Simms, E. S. (1956). Metaphosphate synthesis by an enzyme from *Escherichia coli*. *Biochim Biophys Acta* **20**, 215–227.

Kornberg, A., Rao, N. N. & Ault-Riché, D. (1999). Inorganic polyphosphate: a molecule of many functions. *Annu Rev Biochem* **68**, 89–125.

Kumar, K., Mella-Herrera, R. A. & Golden, J. W. (2010). Cyanobacterial heterocysts. *Cold Spring Harb Perspect Biol* **2**, a000315.

Laemmli, U. K. (1970). Cleavage of structural proteins during the assembly of the head of bacteriophage T4. *Nature* **227**, 680–685.

Larkin, M. A., Blackshields, G., Brown, N. P., Chenna, R., McGettigan, P. A., McWilliam, H., Valentin, F., Wallace, I. M., Wilm, A. & other authors (2007). CLUSTAL W and CLUSTAL_X version 2.0. *Bioinformatics* **23**, 2947–2948.

Liao, H., Myung, S. & Zhang, Y. H. (2012). One-step purification and immobilization of thermophilic polyphosphate glucokinase from *Thermobifida fusca* YX: glucose-6-phosphate generation without ATP. *Appl Microbiol Biotechnol* **93**, 1109–1117.

Lichko, L. P., Kulakovskaya, T. V. & Kulaev, I. S. (2010). Properties of partially purified endopolyphosphatase of the yeast *Saccharomyces cerevisiae*. *Biochemistry (Mosc)* **75**, 1404–1407.

Lindner, S. N., Knebel, S., Pallerla, S. R., Schoberth, S. M. & Wendisch, V. F. (2010). Cg2091 encodes a polyphosphate/ATP-dependent glucokinase of *Corynebacterium glutamicum*. *Appl Microbiol Biotechnol* **87**, 703–713.

Lowry, O. H., Rosebrough, N. J., Farr, A. L. & Randall, R. J. (1951). Protein measurement with the Folin phenol reagent. *J Biol Chem* **193**, 265–275.

Maldener, I. & Muro-Pastor, A. M. (2010). Cyanobacterial heterocysts. In *eLS*. Chichester: Wiley. [doi:10.1002/9780470015902.a0000306.pub2]

Markowitz, V. M., Chen, I. M., Palaniappan, K., Chu, K., Szeto, E., Grechkin, Y., Ratner, A., Jacob, B., Huang, J. & other authors (2012). IMG: the Integrated Microbial Genomes database and comparative analysis system. *Nucleic Acids Res* **40** (Database issue), D115–D122.

Meyer, A. (1902). Orientierende Untersuchungen über Verbreitung, Morphologie, und Chemie des Volutins. *Bot Zeitschr* **62**, 113–152.

Mitschke, J., Vioque, A., Haas, F., Hess, W. R. & Muro-Pastor, A. M. (2011). Dynamics of transcriptional start site selection during nitrogen stress-induced cell differentiation in *Anabaena* sp. PCC7120. *Proc Natl Acad Sci U S A* **108**, 20130–20135.

Mitsui, A., Kumazawa, S., Takahashi, A., Ikemoto, H., Cao, S. & Arai, T. (1986). Strategy by which nitrogen-fixing unicellular cyanobacteria grow photoautotrophically. *Nature* **323**, 720–722.

Mukai, T., Kawai, S., Matsukawa, H., Matuo, Y. & Murata, K. (2003). Characterization and molecular cloning of a novel enzyme, inorganic polyphosphate/ATP-glucomannokinase, of *Arthrobacter* sp. strain KM. *Appl Environ Microbiol* **69**, 3849–3857.

Mukai, T., Kawai, S., Mori, S., Mikami, B. & Murata, K. (2004). Crystal structure of bacterial inorganic polyphosphate/ATP-glucomannokinase. Insights into kinase evolution. *J Biol Chem* **279**, 50591–50600.

Nakao, M., Okamoto, S., Kohara, M., Fujishiro, T., Fujisawa, T., Sato, S., Tabata, S., Kaneko, T. & Nakamura, Y. (2010). CyanoBase: the cyanobacteria genome database update 2010. *Nucleic Acids Res* **38** (Database issue), D379–D381.

Nürnberg, D. J., Mariscal, V., Parker, J., Mastroianni, G., Flores, E. & Mullineaux, C. W. (2014). Branching and intercellular communication in the Section V cyanobacterium *Mastigocladus laminosus*, a complex multicellular prokaryote. *Mol Microbiol* **91**, 935–949.

Pepin, C. A. & Wood, H. G. (1986). Polyphosphate glucokinase from *Propionibacterium shermanii*. Kinetics and demonstration that the mechanism involves both processive and nonprocessive type reactions. *J Biol Chem* **261**, 4476–4480.

Phillips, N. F., Horn, P. J. & Wood, H. G. (1993). The polyphosphate- and ATP-dependent glucokinase from *Propionibacterium shermanii*: both activities are catalyzed by the same protein. *Arch Biochem Biophys* **300**, 309–319.

Phillips, N. F., Hsieh, P. C. & Kowalczyk, T. H. (1999). Polyphosphate glucokinase. *Prog Mol Subcell Biol* **23**, 101–125.

Picossi, S., Flores, E. & Herrero, A. (2014). ChIP analysis unravels an exceptionally wide distribution of DNA binding sites for the NtcA transcription factor in a heterocyst-forming cyanobacterium. *BMC Genomics* **15**, 22.

Rao, N. N., Gómez-García, M. R. & Kornberg, A. (2009). Inorganic polyphosphate: essential for growth and survival. *Annu Rev Biochem* **78**, 605–647.

Rashid, M. H. & Kornberg, A. (2000). Inorganic polyphosphate is needed for swimming, swarming, and twitching motilities of *Pseudomonas aeruginosa*. *Proc Natl Acad Sci U S A* **97**, 4885–4890.

Rashid, M. H., Rao, N. N. & Kornberg, A. (2000). Inorganic polyphosphate is required for motility of bacterial pathogens. *J Bacteriol* **182**, 225–227.

Remonsellez, F., Orell, A. & Jerez, C. A. (2006). Copper tolerance of the thermoacidophilic archaeon *Sulfolobus metallicus*: possible role of polyphosphate metabolism. *Microbiology* **152**, 59–66.

Resnick, S. M. & Zehnder, A. J. (2000). *In vitro* ATP regeneration from polyphosphate and AMP by polyphosphate : AMP phosphotransferase and adenylate kinase from *Acinetobacter johnsonii* 210A. *Appl Environ Microbiol* **66**, 2045–2051.

Rippka, R. & Waterbury, J. B. (1977). Synthesis of nitrogenase by non-heterocystous cyanobacteria. *FEMS Microbiol Lett* **2**, 83–86.

Rippka, R., Deruelles, J., Waterbury, J. B., Herdman, M. & Stanier, R. Y. (1979). Generic assignments, strain histories and properties of pure cultures of cyanobacteria. *J Gen Microbiol* **111**, 1–61.

Robertson, B. R., Tezuka, N. & Watanabe, M. M. (2001). Phylogenetic analyses of *Synechococcus* strains (cyanobacteria) using sequences of 16S rDNA and part of the phycocyanin operon reveal multiple evolutionary lines and reflect phycobilin content. *Int J Syst Evol Microbiol* **51**, 861–871.

Scherer, P. A. & Bochem, H. P. (1983). Ultrastructural investigation of 12 *Methanosarcinae* and related species grown on methanol for occurrence of polyphosphatelike inclusions. *Can J Microbiol* **29**, 1190–1199.

Shih, P. M., Wu, D., Latifi, A., Axen, S. D., Fewer, D. P., Talla, E., Calteau, A., Cai, F., Tandeau de Marsac, N. & other authors (2013). Improving the coverage of the cyanobacterial phylum using diversity-driven genome sequencing. *Proc Natl Acad Sci U S A* **110**, 1053–1058.

Stal, L. J. (1995). Physiological ecology of cyanobacteria in microbial mats and other communities. *New Phytol* **131**, 1–32.

Szymona, M. & Ostrowski, W. (1964). Inorganic polyphosphate glucokinase of *Mycobacterium phlei*. *Biochim Biophys Acta* **85**, 283–295.

Szymona, M. & Widomski, J. (1974). A kinetic study on inorganic polyphosphate glucokinase from *Mycobacterium tuberculosis* H37RA. *Physiol Chem Phys* **6**, 393–404.

Tanaka, S., Lee, S. O., Hamaoka, K., Kato, J., Takiguchi, N., Nakamura, K., Ohtake, H. & Kuroda, A. (2003). Strictly polyphosphate-dependent glucokinase in a polyphosphate-accumulating bacterium, *Microlunatus phosphovorus*. *J Bacteriol* **185**, 5654–5656.

Thompson, P. A., Oh, H. M. & Rhee, G. Y. (1994). Storage of phosphorus in nitrogen-fixing *Anabaena flos-aquae* (Cyanophyceae). *J Phycol* **30**, 267–273.

Toepel, J., Welsh, E., Summerfield, T. C., Pakrasi, H. B. & Sherman, L. A. (2008). Differential transcriptional analysis of the cyanobacterium *Cyanothece* sp. strain ATCC 51142 during light-dark and continuous-light growth. *J Bacteriol* **190**, 3904–3913.

Tsutsumi, K., Munekata, M. & Shiba, T. (2000). Involvement of inorganic polyphosphate in expression of SOS genes. *Biochim Biophys Acta* **1493**, 73–81.

Walker, P. A., Leong, L. E., Ng, P. W., Tan, S. H., Waller, S., Murphy, D. & Porter, A. G. (1994). Efficient and rapid affinity purification of proteins using recombinant fusion proteases. *Biotechnology (N Y)* **12**, 601–605.

Wilkins, M. R., Gasteiger, E., Bairoch, A., Sanchez, J. C., Williams, K. L., Appel, R. D. & Hochstrasser, D. F. (1999). Protein identification and analysis tools in the ExPASy server. *Methods Mol Biol* **112**, 531–552.

Edited by: A. Wilde

All1371 is a polyphosphate dependent glucokinase in *Anabaena* sp. PCC 7120

Friederike Klemke[1], Gabriele Beyer[1], Linda Sawade[1], Ali Saitov[1], Thomas Korte[2], Iris Maldener[4], Wolfgang Lockau[1], Dennis J. Nürnberg[3] and Thomas Volkmer[1*]

[1]Plant Biochemistry, Humboldt-Universität zu Berlin, Germany
[2]Molecular Biophysics, Humboldt-Universität zu Berlin, Germany
[3]School of Biological and Chemical Sciences, Queen Mary University of London, United Kingdom
[4]Institute of Microbiology and Infection Medicine/Organismic Interactions, University of Tübingen, Germany

Supplement

Distribution of PPGK among cyanobacteria

Organisms whose genomes were analyzed according to genes encoding putative PPGK proteins are scheduled in Table S1. Gene ID, sequence length of the identified PPGKs and the ability to fix N_2 (e.g. by the presence of *nifH*) of these organisms are indicated.

Table S1: Distribution of PPGK among cyanobacteria

	organism	gene ID	sequence length (aa)	*nifH* or N_2-fixation
Section I	*Acaryochloris marina* MBIC11017^T	641252899	238	–
	Acaryochloris sp CCMEE 5410	2514738042	238	–
	Chamaesiphon minutus PCC 6605			
	Crocosphaera watsonii WH 0003			
	Crocosphaera watsonii WH 8501			
	Cyanobacterium stanieri PCC 7202^T			
	Cyanobecterium aponimum PCC 10605^T			
	Cyanobium gracile PCC 6307^T			
	Cyanobium sp. PCC 7001			
	Cyanothece sp. ATCC 51142			
	Cyanothece sp. ATCC 51472			
	Cyanothece sp. CCY 0110			
	Cyanothece sp. PCC 7424			
	Cyanothece sp. PCC 7425			
	Cyanothece sp. PCC 7822			
	Cyanothece sp. PCC 8801			
	Cyanothece sp. PCC 8802			
	Dactylococcopsis salina PCC 8305			
	Geminocystis herdmanii PCC 6308^T			
	Gloeobacter violaceus PCC 7421^T			
	Gloeocapsa sp. PCC 73106			
	Gloeocapsa sp. PCC 7428			
	Halothece sp. PCC 7418			
	Microcystis aeruginosa NIES-843			
	Microcystis aeruginosa PCC 7806			
	Prochlorococcus marinus AS 9601			
	Prochlorococcus marinus MIT 9202			
	Prochlorococcus marinus MIT 9211			

	Prochlorococcus marinus MIT 9215			
	Prochlorococcus marinus MIT 9301			
	Prochlorococcus marinus MIT 9303			
	Prochlorococcus marinus MIT 9312			
	Prochlorococcus marinus MIT 9313			
	Prochlorococcus marinus MIT 9515			
	Prochlorococcus marinus NATL 1A			
	Prochlorococcus marinus NATL 2A			
	Prochlorococcus marinus, subsp. *marinus* CCMP 1375^{T}			
	Prochlorococcus marinus, subsp. *pastoris* CCMP 1986			
	Prochloron didemni^{T} P1			
	Synechococcus elongatus PCC 6301			
	Synechococcus elongatus PCC 7942			
	Synechococcus sp. BL 107			
	Synechococcus sp. CB 0101			
	Synechococcus sp. CB 0205			
	Synechococcus sp. CC 9311			
	Synechococcus sp. CC 9605			
	Synechococcus sp. CC 9902			
	Synechococcus sp. JA-2-3B			
	Synechococcus sp. JA-3-3Ab			
	Synechococcus sp. PCC 6312			
	Synechococcus sp. PCC 7002			
	Synechococcus sp. PCC 7335	647579639	228	+
	Synechococcus sp. PCC 7336			
	Synechococcus sp. PCC 7502	2508687249	238	–
	Synechococcus sp. RCC307			
	Synechococcus sp. RS 9916			
	Synechococcus sp. RS 9917			
	Synechococcus sp. WH 5701			
	Synechococcus sp. WH 7803			
	Synechococcus sp. WH 7805			
	Synechococcus sp. WH 8016			
	Synechococcus sp. WH 8102			
	Synechococcus sp. WH 8109			
	Synechocystis sp. GT-S, PCC 6803			
	Synechocystis sp. PCC 6803			
	Synechocystis sp. PCC 6803, GT-I			
	Synechocystis sp. PCC 6803, PCC-N			
	Synechocystis sp. PCC 7509			
	Thermosynechococcus elongatus BP-1			
	unidetified cyanobacterium UCYN-A			

Section II	*Chroococcidiopsis* sp. PCC 6712	2505788827	242	+
	Chroococcidiopsis thermalis PCC 7203			
	Pleurocapsa sp. PCC 7319	2509711744	235	+
	Pleurocapsa sp. PCC 7327			
	Stanieria cyanosphaera PCC 7437	2503800427	237	+
	Xenococcus sp. PCC 7305			
Section III	*Arthrospira maxima* CS-328			
	Arthrospira platensis C1			
	Arthrospira platensis NIES-39			
	Arthrospira platensis Paraca			
	Arthrospira sp. PCC 8005			
	Crinalium epipsammum PCC 9333	2504685141	235	–
	Cyanobacterium sp. ESFC-1			
	Geitlerinema sp. PCC 7105			
	Geitlerinema sp. PCC 7407			
	Leptolyngbya boryana PCC 6306			
	Leptolyngbya sp. PCC 6406			
	Leptolyngbya sp. PCC 7375	2509847651	251	+
	Leptolyngbya sp. PCC 7376			
	Lyngbya sp. CCY 8106	640015231	238	+
	Lyngbya sp. CCY 9616			
	Microcoleus chthonoplastes PCC 7420	647572171	235	+
	Microcoleus sp. PCC 7113	2509437012	235	–
	Microcoleus vaginatus FGP-2	2506349591	235	–
	Moorea producta 3L^{T}	495465535	235	–
	Nodosilinea nodulosa PCC 7104	2509776486	137*	
		2509776488	97*	–
	Oscillatoria acuminata PCC 6304	2509419241	236	–
	Oscillatoria formosa PCC 6407	2508875670	235	+
	Oscillatoria nigro-viridis PCC 7112	2504089037	235	–
	Oscillatoria sp. PCC 10802	2509508264	239	+
	Oscillatoria sp. PCC 6506	648856634	235	+
	Oscillatoriales sp. JSC-1	2502185146	244	+
	Oscillatoriales sp. JSC-12	2510096246	230	+
	Prochlorothrix hollandica PCC 9006			
	Pseudanabaena sp. PCC 6802	2507090369	235	+
	Pseudanabaena sp. PCC 7367	2504680807	237	+
	Pseudanabaena sp. PCC 7429	2504585200	234	+
	Spirulina major PCC 6313			
	Spirulina subsalsa PCC 9445			
	Trichodesmium erythraeum IMS101			
Section IV	*Anabaena cylindrica* PCC 7122	2504134473	235	+
	Anabaena sp. PCC 7108	2506493476	235	+
	Anabaena variabilis ATCC 29413	646569517	239	+
	Calothrix desertica PCC 7102	2510030452	235	+
	Calothrix sp. PCC 6303	2504096916	234	+

	Calothrix sp. PCC 7103	2507473794	235	+
	Calothrix sp. PCC 7507	2505802227	235	+
	Cylindrospermopsis raciborskii CS-505			
	Cylindrospermum stagnale PCC 7417	2509768489	235	+
	Microchaete sp. PCC 7126	2509783891	235	+
	Nodularia spumigena CCY9414	640025553	235	+
	Nostoc azollae 0708	648051402	235	+
	Nostoc punctiforme PCC 73102	642601093	238	+
	Nostoc sp. PCC 7107	2503739016	235	+
	Nostoc sp. PCC 7120	637231738	239	+
	Nostoc sp. PCC 7524	2509810004	237	+
	Raphidiopsis brookii D9			
	Rivularia sp. PCC 7116			
	Scytonema hofmanni PCC 7110		236	+
	Scytonema hofmanni UTEX 2349	2507333765	234	+
Section V	*Chlorogloeopsis fritschii* PCC 6912			
	Chlorogloeopsis fritschii PCC 9212			
	Fischerella muscicola PCC 73103		234	+
	Fischerella muscicola PCC 7414		234	+
	Fischerella sp. JSC-11	2505767484	43*	+
	Fischerella sp. PCC 9339			
	Fischerella sp. PCC 9431	2512980592	234	+
	Fischerella sp. PCC 9605	2516145320	234	+
	Fischerella thermalis PCC 7521			
	Mastigocladopsis repens PCC 10914	2517243485	235	+
	unidetified cyanobacterium PCC 7702			

* stop codon in sequence; +, *nifH* in the genome or known to fix N_2, number of PPGK present: 48, number of cyanobacteria: 141, percentage of PPGK among cyanobacteria: 34.04 %

Generating an *Anabaena* Δ*all1371* strain

Deletion of *all1371* occurred in Anabaena sp PCC 7120. The seggregation of the deletion strain was determined by PCR analysis.
In Figure S1 the seggregation of two clone are illustrated. For details see figure legend.

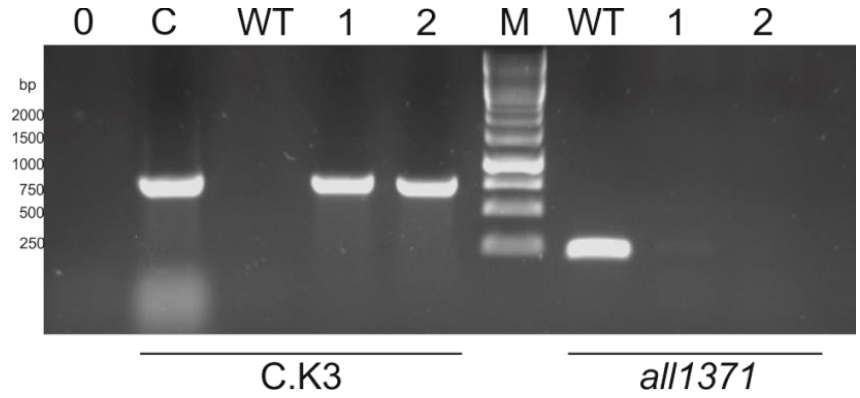

Figure S1: PCR-analysis of Δ*all1371* mutants. Left: C.K3 verification for 0, negative control without DNA; C, plasmid pRL271-up-C.K3-down as positive control (C.K3, 773 bp); WT, wild type-DNA as negative control; 1 and 2, DNA of two deletion mutants; right: verification for *all1371* (300 bp, part of *all1371*) in wild type (WT) and deletion mutant 1 and 2; M, DNA standard

Viability tests

Viability tests were performed with *Anabaena* and the Δ*all1371* mutant. The tests were carried out on AA-plates with or without 10 mM KNO_3 as a nitrogen source. Cultures were normalized to the chlorophyll *a* content and diluted accordingly. 10 µl of culture dilutions were applied per spot. These agar plates were exposed to continuous light or illuminated in a light/dark cycle. Three biological replicates were tested separately. Images of viability test are arranged in Figure S4 and S5. The detailed conditions are explained in the figure legends.

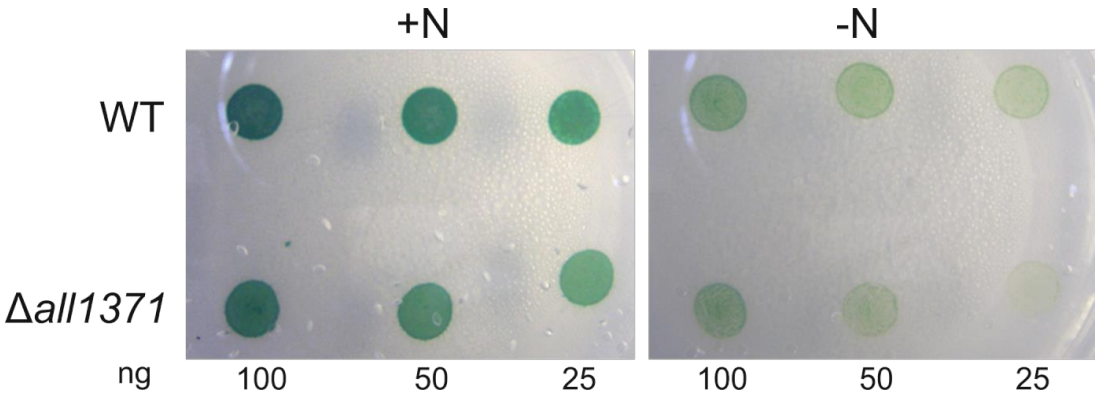

Figure S2**:** Viability analyses of *Anabaena* wild type) and *Δall1371* in continuous light. Culture dilutions of *Anabaena* wild type (WT) and the *all1371* knock-out mutant strain (Δ*all1371*) spotted on AA-agar plates containing 10 mM KNO_3 (+N) or lacking combined nitrogen (-N). Various amounts of chlorophyll *a*; indicated in the bottom panel (ng) were applied. The plates were incubated under continuous light (60 µmol photons m^{-2} s^{-1}, bottom light) for 6 days.

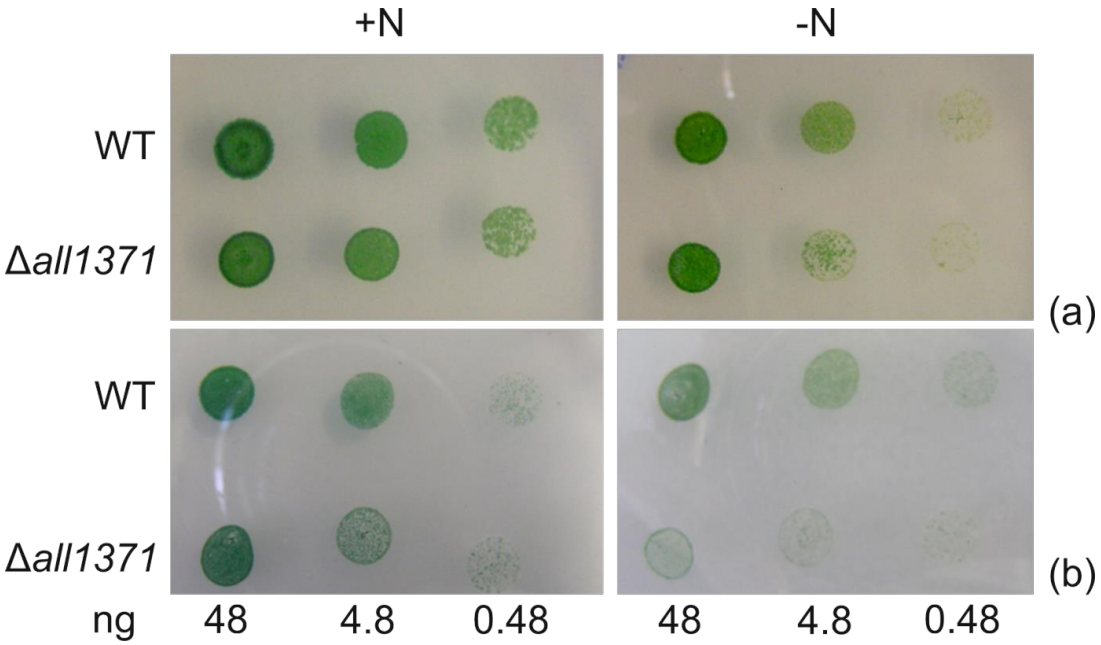

Figure S3**:** Viability analyses of *Anabaena* wild type and *Δall1371* in different light conditions. Culture dilutions of *Anabaena* wild type (WT) and the *all1371* knock-out mutant strain (Δ*all1371*) spotted on AA-agar plates containing 10 mM KNO_3 (+N) or lacking combined nitrogen (-N). Various amounts of chlorophyll a; indicated in the bottom panel (ng) were applied. The plates were illuminated continuously for 6 days (a) or under a light/dark cycle (12 hours each) for 14 days (b) with 70 µmol photons m^{-2} s^{-1} (top light).

Investigation of *all1371* expression conditions

The *Anabaena* promoter fusion and the Δ*all1371* strain were grown as liquid cultures with and without nitrate. Visualization of GFP fluorescence was performed as descripted in section Material and Methods. As summarized in Figure S2 GFP fluorescence events in the *Anabaena* promoter fusion strain occurred only under combined nitrogen depleting conditions (Fig. S2, lower panel, right). For details see figure legend. The parental strain *Anabaena* Δ*all1371* was used as negative control. Supplementing regular Figure 5 the Figure S3 displayed fluorescence events appearing in the *Anabaena* Δ*all1371* indicating the background fluorescence (right image).

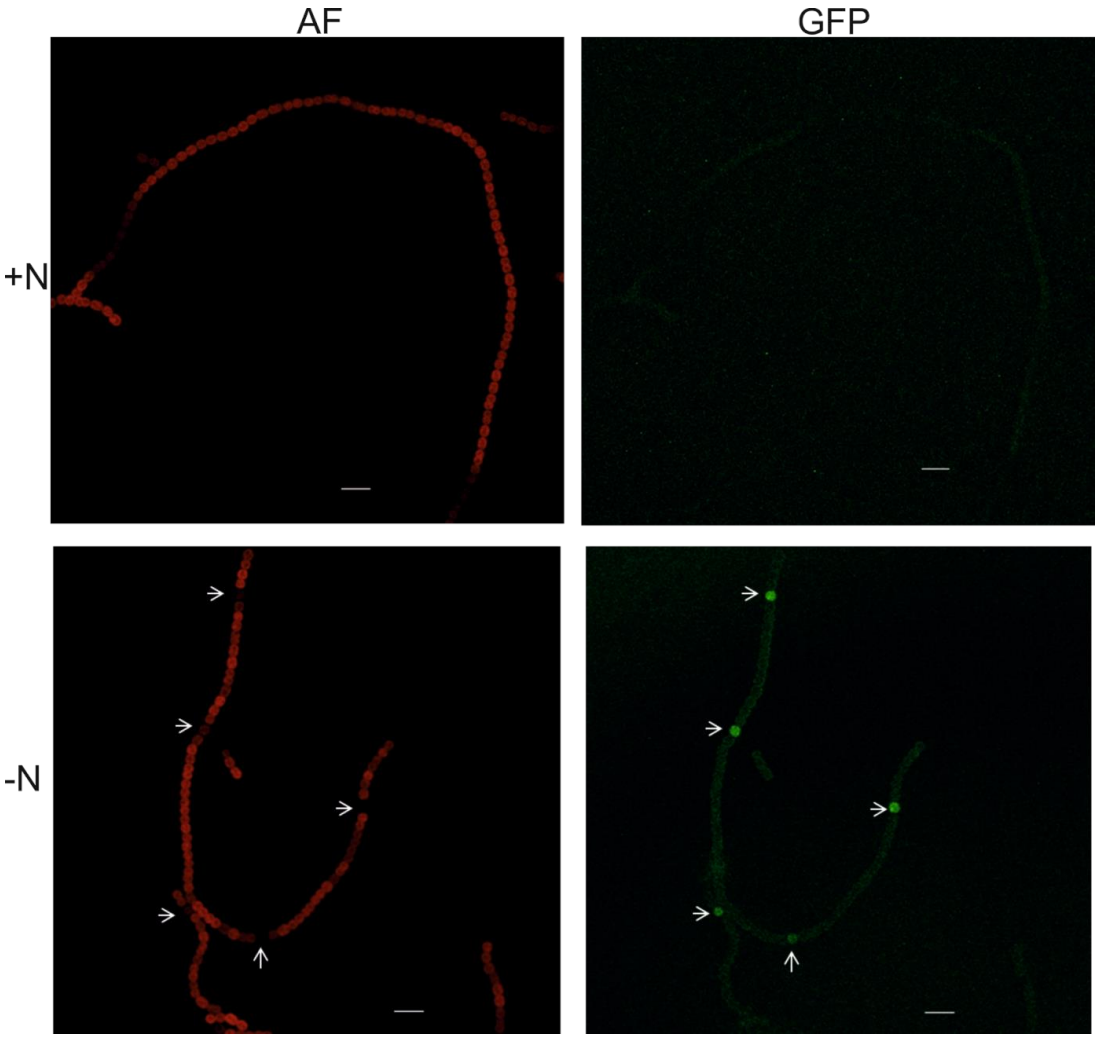

Figure S4: All1371 promoter activity in heterocysts as overview. Fluorescence in the *Anabaena* Δ*all1371* promoter fusion strain grown with combined nitrogen (+N) and after 48 hours under N_2 fixing conditions (-N). Heterocysts are indicated by arrows. Scale bars, 10 µm; AF, auto-fluorescence (red); GFP, GFP fluorescence (green).

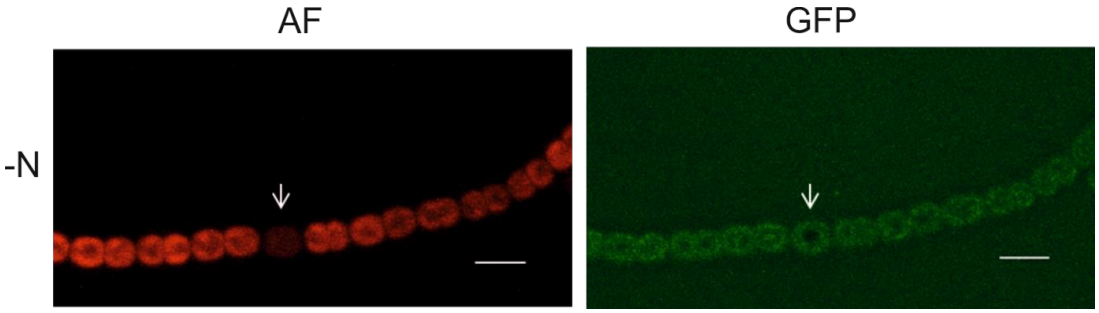

Figure S5: No GFP fluorescence in Δ*all1371* as negative control : Fluorescence in *Anabaena* Δ*all1371* grown in the absence of combined nitrogen (-N). Filaments were visualized by confocal microscopy. A heterocyst is indicated by an arrow. Scale bars, 5 µm; AF, auto-fluorescence (red); GFP, GFP fluorescence (green).

Estimating GFP fluorescence:

To estimate the GFP fluorescence in heterocysts 24 filaments from the Δ*all1371* promoter fusion strain grown without combined nitrogen were analysed as decripted in Material and Methods. We analysed 17 filaments from the Δ*all1371* strain as negative control, also. The fluorescence measured in vegetative cells next to the heterocysts were normalized to value 1. The fluorescence of the according heterocysts were quantified and correlated with the fluorescence of the vegetative cells next to. The determined values are composed in Table S2.

Table S2: Quantification of GFP fluorescence in *Anabaena* Δ*all1371* promoter fusion strain The fluorescence was quantified from each heterocyst and two adjacent vegetative cells in a filament or one for terminal heterocysts, the vegetative cell/heterocyst ratio was determined.

Anabaena strain*	Number of quantified heterocysts	Number of quantified vegetative cells	Mean ratio vegetative cells/heterocysts ± SD
promoter fusion	42	71	1: 2.1 ± 0.8
Δ*all1371*(neg. control)	18	34	1: 0.9 ± 0.2

* grown for 4 day under N_2 fixing conditions